GENERATION AND FUNCTIONAL ANALYSIS OF AN OCTAMERIC C3d CONSTRUCT TO ACT AS A MOLECULAR ADJUVANT IN VACCINE DESIGN

by

Andreas Michael Rossbach

A thesis submitted in candidature for the degree of Philosophiæ Doctor

Department of Medical Biochemistry & Immunology

School of Medicine

Cardiff University

August 2007

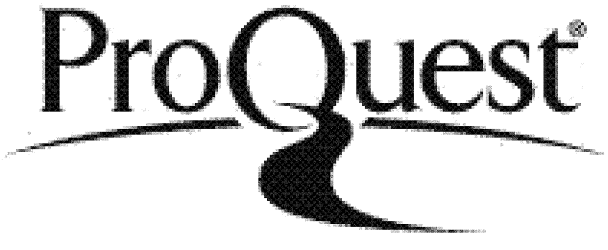

ProQuest LLC
789 East Eisenhower Parkway
P.O. Box 1346
Ann Arbor, MI 48106-1346

Schüler. Ich wünschte recht gelehrt zu werden,
Und möchte gern, was auf der Erden
Und in dem Himmel ist, erfassen,
Die Wissenschaft und die Natur.

Mephistopheles. Da seid Ihr auf der rechten Spur;
Doch müßt Ihr Euch nicht zerstreuen lassen.

Faust, Johann Wolfgang von Goethe

Acknowledgements

I am deeply indebted to every member of Professor B. Paul Morgan's Complement Biology Group of at the Department of Medical Biochemistry and Immunology.

First and foremost I would like to thank my supervisors Dr Kevin J. Marchbank and Dr O. Brad Spiller for their supervision, support, technical advice and in particular for their help with writing this thesis. I am especially grateful to Professor B. Paul Morgan for giving me the opportunity to carry out my project in his world-class laboratory.

I would like to thank Drs Claire Harris, Natalie Hepburn, Timothy Hughes, Sivsankar Baalasubramanian, Rossen Donev, Jason Twohig, Gilda Pino-Chavez and Sarah Clarke. Each of these excellent researchers provided invaluable expertise, help and their time to keep my work and me on track. I am grateful to my fellow PhD students Gareth, Paula and Hannah for many helpful tips and to our technicians Miriam, Andrew, Kate and Sion for keeping the laboratory running.

Special thanks goes to those near and dear to me: Kathryn for her love, emotional support, accepting long working hours and being there for me; my family for their unconditional support and giving me confidence; my friends for being more than just friends.

Finally, I would like to thank Barbara Rexhausen whose dedication to her mission and her patients was an inspiration for me. Sadly, she succumbed to the very diseases she gave everything to treat. She will be sorely missed.

Abstracts submitted to Meetings

Andreas M. Rossbach, O. Brad Spiller and Kevin J. Marchbank: *Boosting Vaccines - C3d as Molecular Adjuvant*. Proc. 19th Annual Postgraduate Research Day, School of Medicine, Cardiff University 2004

Andreas M. Rossbach, O. Brad Spiller and Kevin J. Marchbank: *DNA Vaccines and Complement C3d – Bridging the Gap*. Proc. 20th Annual Postgraduate Research Day, School of Medicine, Cardiff University 2005

Andreas M. Rossbach, O. Brad Spiller and Kevin J. Marchbank: *Generation and Functional Analysis of an Octameric C3d Construct to Act As a Molecular Adjuvant in Vaccine Design*. Molecular Immunology 2007; 44 (1-3): 233

Publications:

Jason Twohig, Liudmila Kulik, Catherine Haluszczak, Jason Reuter, **Andreas Rossbach**, Melanie Bull, V. Michael Holers and Kevin J. Marchbank: Defective B cell ontogeny and immune response in human complement receptor 2 (CR2, CD21) transgenic mice is partially recovered in the absence of C3. Molecular Immunology 2007,44(13): 3434-3444

Abbreviations

α2M	α2-macroglobulin
aa	Amino acid
Ab	Antibody
Ag	Antigen
ANOVA	One way analysis of variance
AP	Alternative Pathway
APC	Antigen presenting cell
APS	Ammonium persulfate
b	Biotinylated
BCR	B-cell receptor
bp	Base pair
C	Complement
C4BP	C4b binding protein
CD	Cluster of differentiation
CFA	Complete Freund's adjuvant
CHO	Chinese hamster ovary
CMV	Cytomegalovirus
CP	Classical Pathway
CpG	Deoxycytidylate-phosphate-deoxyguanylate
CR	Complement receptor
C-terminal	Carboxyl/COOH-terminal
CTL	Cytotoxic T-lymphocytes
CV	Column volume
DAF	Decay accelerating factor, CD55
DAPI	4',6-diamidino-2-phenylindole
DC	Dendritic cell
dH_2O	Distilled water
Dk	Donkey
DMSO	Dimethylsulphoxide
DNA	Deoxyribonucleic acid
DTT	DL-dithiothreitol
EBV	Epstein Barr Virus

ECACC	European Collection of Cell Cultures
EDTA	Ethylenediamine tetraacetic acid
EF1α	Human elongation factor 1 α
ELISA	Enzyme-linked immunosorbent assay
EtBr	Ethidium bromide
evc	Empty vector control
FACS	Fluorescence-activated cell sorting
fB	Factor B
FC	Flow cell
FCS	Foetal calf serum
fD	Factor D
FDC	Follicular dendritic cell
fH	Factor H
fI	Factor I
FITC	Fluorescein isothiocyanate
FPLC	Fast liquid protein chromatography
GC	Germinal centre
Gt	Goat
hC3d	Human C3d
HEL	Hen egg lysozyme
HRPO	Horse radish peroxidase
Hu	Human
i.m.	Intramuscular
IC	Immune-complex
IFA	Incomplete Freund's adjuvant
IFN	Interferon
Ig	Immunoglobulin
IL	Interleukin
kb	Kilobase
K_D	Affinity constant (dissociation constant)
kDa	Kilodalton
L	Litre
LC	Langerhans Cell

LHR	Long homologous region/repeat
LN_2	Liquid nitrogen
LP	Lectin pathway
mAb	Monoclonal Antibody
MAC	Membrane attack complex
MASP	Membrane associated serine protease
MBL	Mannose binding lectin
mC3d	Murine C3d
MCP	Membrane co-factor protein, CD46
MCS	Multiple cloning site
MHC	Major histocompatibility complex
min	Minute
MO	Microorganism
MPa	Mega pascal
Ms	Mouse
MWCO	Molecular weight cut off
MZ	Marginal zone
ns	Not significant
N-terminal	Amino/NH_3-terminal
ODN	Oligodeoxynucleotide
PBS	Phosphate buffered saline
PCR	Polymerase chain reaction
PE	Phycoerythrin
PMSF	Phenylmethanesulfonyl fluoride
Rb	Rabbit
RCA	Regulators of complement activation
RPE	Recombinant phycoerythrin
rpm	Revolutions per minute
RT	Room temperature
Rt	Rat
s	Second
s.c.	Subcutaneous
SA	Streptavidin

SAP	Shrimp alkaline phosphatase
SCR	Short consensus repeat
SDM	Site-directed mutagenesis
SDS-PAGE	Sodium dodecyl sulphate polyacrylamide gel electrophoresis
SEM	Standard error of the mean
Sh	Sheep
sIg	Surface immunoglobulin
SPN	Spleen
SU	Sub-unit
SV40	Simian virus 40
t.d.	Transdermal
TAE	Tris-acetate EDTA
TBS	Tris-buffered saline
TD	T-dependent
TEMED	*N*,*N*,*N'*,*N'*-tetramethyleethylenediamine
T_H	Helper T-cell
Th1	Helper T cell response type 1
Th2	Helper T cell response type 2
TLR	Toll-like receptor
TNF	Tumour necrosis factor
Tris	Tris(hydroxymethyl)methylamine
U	Unit
v/v	Volume per volume
w/v	Weight per volume
YFP	Yellow fluorescent protein

Abstract

This thesis investigated two separate theoretical advancements for vaccine design: (1) present antigen in a self-forming natural C4b binding protein-based octameric array (to engage multiple adjacent B-cell receptors or BCR) and (2) combined with fusion to a molecular adjuvant C3d or C3dg, to cross-link C3d-receptor (complement receptor 2 (CR2); CD21). Initially, yellow fluorescent protein test antigen was evaluated, but only to monitor intracellular and extracellular protein levels for a range of C3 forms: C3dg (smallest covalently bound CR1/factor I processed form of activated C3) or C3d (non-complement enzyme processed C3), as well as consequence of mutating the internal thioester bond (C988S, "C3d^{S}g"/ C3d^{S}) that may confound recombinant production of C3dg/C3d fragments. The test antigen was then switched to hen egg lysozyme (HEL), with the hope that spider-like HEL octamer arrays would be expressed with the C3dg/C3d fused proteins at the outermost reach. Mutating the thioester bond increased expression for both C3 forms, and C3d^{S}g-fusion octamers expressed at the highest levels, although C3d^{S} had the highest binding for human CR2. Receptor binding was considered more important for vaccine function, leading to the prototype vaccine, hC3d^{S}-HEL-Oct. Further dissection of the CR2-C3d interaction utilised cell-based assays and surface plasmon resonance (SPR) analysis, using dimeric immunoglobulin Fc-fusion recombinant forms of human C3d, C3dg and murine C3d. All C3dg/C3d Fc proteins bound strongly, although cross-species murine C3d Fc binding to human CR2 was 2-3 times higher than human counterparts. *In vivo* production of total immunoglobulin G (IgG) and IgM levels was measured, following injection of hC3d^{S}-HEL-Oct, either as DNA or purified protein, and showed successful initiation of a HEL-specific immune response. Data suggested that CpG sequences may have a detrimental impact on vaccine function. These results highlight the power and flexibility of the octamer approach as well as C3d and their applications *in vivo* and *in vitro*.

Contents

Chapter 1

General Introduction

1.1 The First Vaccine

In 1796 Edward Jenner (1749 – 1823) attempted the first controlled immunisation against smallpox (1). Jenner had noticed through keen observation that milk maidens infected with cowpox did not contract smallpox, even years later. The cowpox virus was commonly known in the late 18th century as a relatively harmless relative of smallpox, which caused only minor discomfort in humans (2). Jenner decided to put this close relationship to the test to protect from the disfiguring human virus. He utilised a technique called variolation already known and in use in various parts of the world (e.g. China) and also rural England (3). Pus excreted from pustules on the hands of the milk maidens was injected into healthy individuals followed by observation of their reaction upon smallpox challenge (1, 4). The experiment was a success. The injected patients, including Jenner's own children and relations, were protected against smallpox infection within a matter of weeks. These vaccinations (*vacca*/*vaccinus*, lat. cow/from cows) – highly controversial then and now due to their set-up – were the first controlled experiments to prove cross-protection and the principle of vaccination. Smallpox vaccinations continued to be a success story, possibly the greatest to date, being the first to be officially eradicated in 1979/1980 (4). Poliomyelitis could be next thanks to promising figures showing a 99% reduction in worldwide cases since 1988 (Figure 1.1, (5)).

1.2 Second Generation Vaccines

Almost exactly 100 years passed until a number of scientists caught on to the idea that vaccinations provided an efficient and economical means of protecting against disease. Louis Pasteur developed a method of inactivating ("attenuating") rabies virus by heat or chemical treatments prior to injection (6, 7). Thanks to this approach a number of viral diseases such as measles, rubella, mumps, varicella, and adenovirus have been fought successfully in the past. Attenuated live vaccines were also developed against bacterial diseases such as cholera, anthrax and the most widely known antibacterial vaccine against tuberculosis, bacilli Calmette-Guerin (BCG) (Figure 1.1 (2)).

1.3 How Vaccines Work

1.3.1 Aims of Vaccination

Vaccination or immunisation aims to equip the immune system with the armoury to fend off a harmful pathogen or agent it has not yet encountered. This is accomplished by initiating an appropriate immune response via cytotoxic T-cells and antibody production through the injection of a non-infectious antigen or toxin that results in the induction of long-lived memory B- and/or T-lymphocytes to that antigen (Ag, **1047** (8)). The choice of this specific target is crucial but if vaccination is successful the pathogen will be dealt with quickly and efficiently as the infectious agent is met by an organised, primed or secondary adaptive immune response compared with a slow primary immune response that would be seen if vaccination had not occurred.

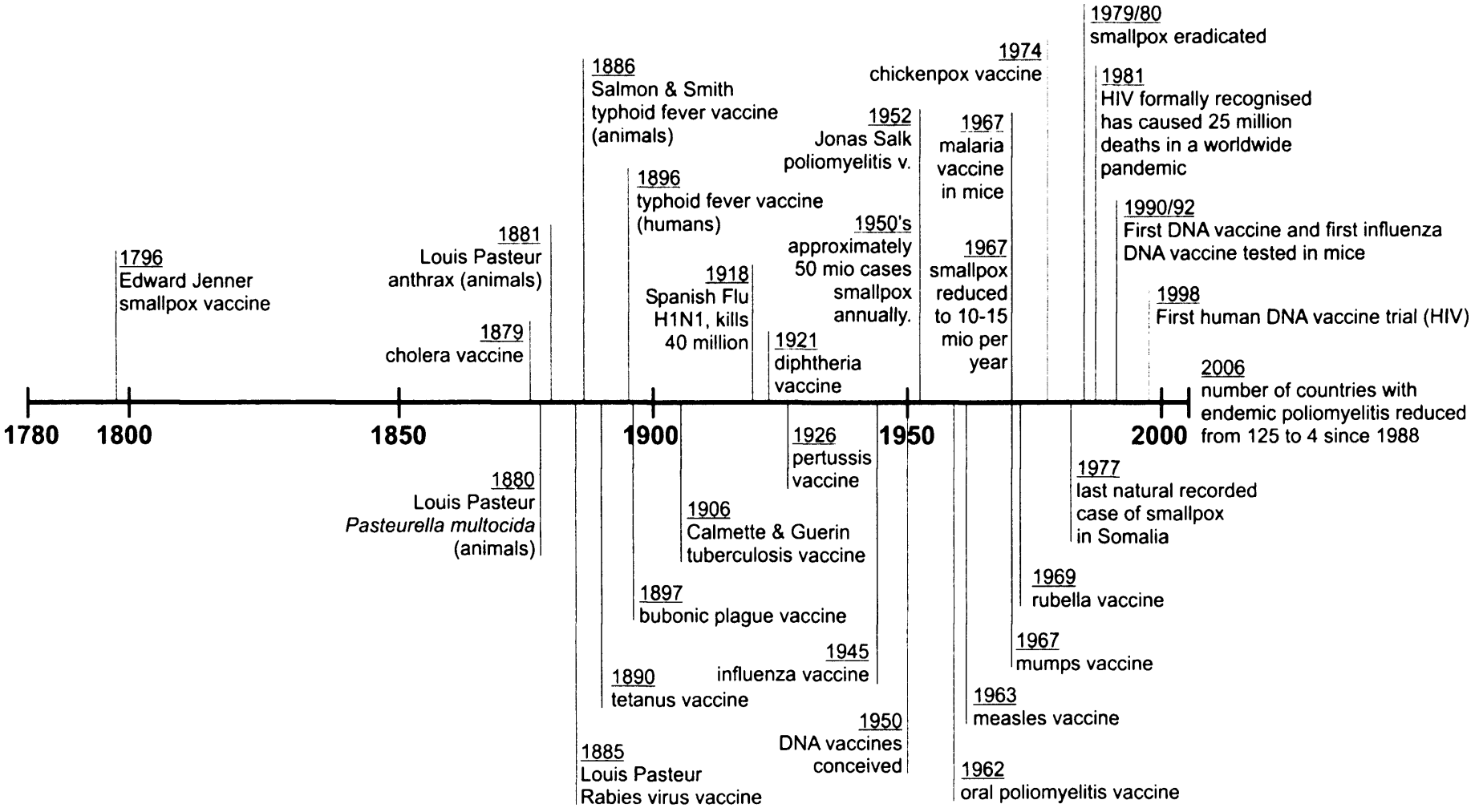

Figure 1.1. Important dates in the history of vaccine development. Data collated from: 1, 3-5

1.3.2 Antigen Administration, Processing and Induction of the Adaptive Immune Response

Antigens are generally introduced into the body in one of two ways. An infection is generally considered as a breach of the body's natural outer defences (e.g. skin, mucosal surfaces, (9)) enabling a pathogen (bacteria, viruses, parasites) to invade the host's tissue and cells. Having arrived at its target location, the foreign organism initiates its specific pathogenic life cycle of replication and preparation for transmission to new hosts. In contrast, vaccination introduces an antigen intentionally, most commonly by parenteral or oral administration. Despite accidental or intentional introduction into the host, both vaccine and pathogen are – theoretically – handled in the same fashion by the host's immune system.

Upon entry, a foreign body first encounters the body's first line of immune defence, the innate immune system (9, 10). It is characterised by a rapid/instant response, but also the inability to develop any memory. The humoral proteins of the innate immune system and a specialised set of immune cells interact with and initiate the inflammatory response against the pathogen at the point and from the moment of entry. The cellular and humoral parts are intertwined in the induction of inflammation caused by the pathogen. Most of the proteins are produced in the liver (complement) and by most lymphocytes (antibodies, chemokines etc.). The components of the complement cascade (discussed in section 1.5) are the first proteins of the humoral immune system to interact with the invader. Sequential activation of the cascade proteins by cleavage on the pathogenic surface releases the anaphylotoxins C4a, C3a and C5a. These small chemotaxins cause localised vasodilatation, an increase in blood flow and increased capillary permeability indicated by redness, heat and

swelling at the site of inflammation (9, 11). Fluid leaks into the site and chemotactic phagocytic cells, which follow the concentration gradient of anaphylotoxins, migrate into the area over a period of three to four hours post infection (figure 1.2; (11)). Equally as important as attracting immune effector cells to the site of infection, complement proteins and immunoglobulins (Ig) opsonise (*opsōnein*, from *opson*, Greek: condiment, delicacy) the foreign bodies. Opsonisation greatly enhances phagocytosis but can also induce direct lysis via the terminal pathway.

Leukocytes of the innate immune system develop from a single common progenitor, the pluripotent haematopoietic stem cell in the bone marrow. Neutrophils, which are polymorphonucleocytes and the most common white blood cell, become activated during injury, trauma or infection (12). They attach to the blood vessel endothelium and – following the chemotactic gradient – enter the affected tissues through extravasation. Neutrophils are the first to arrive at the site of inflammation (13) followed by eosinophils (mostly found in the tissue), basophils and mast cells. Alternatively, resident immune cells (e.g. monocytes, dendritic cells) can be activated directly by pathogen-associated molecular pattern receptors, e.g. Toll-like receptor (TLR) 4, which recognises lipopolysaccharide or TLR9, which activates immune cells following binding of bacterial DNA (see section 1.11.5). Engulfment and subsequent digestion of pathogens induces secretion of more chemotactic factors (cytokines and chemokines) into the surrounding medium. More phagocytes (monocytes/ macrophages, neutrophils) are thus attracted to the site of infection by chemical signals produced *in situ*. Most polymorphonucleocytes exclusively ingest and destroy invading pathogens. However, macrophages belong to a group of immune cells

Figure 1.2. Induction of Inflammation and kinetics of the immune response at the site of infection. Panel A: Pathogens invading the tissue through the epithelial barrier (1) first encounter the opsonins of the innate immune system (e.g. antibodies, complement), which trigger the release of anaphylotoxins (2). These signalling molecules cause vasodilation and attract phagocytic cells, during the early inflammatory response mainly neutrophils (3). Ingestion of pathogens (5) induces these neutrophils to release cytokines, chemokines and interferons alongside the anaphylotoxins (6). More phagocytes, in particular monocytes, which develop into macrophages, are attracted by chemokines (7), extravasate into the area and continue to ingest pathogens. Following uptake, phagocytes migrate to the secondary lymphoid tissue (8). During migration the pathogen is broken down into antigenic fragments and presented on the surface for maturation of the adaptive immune response (see figure 1.3). NK cells also migrate into the tissue to attack virus-infected cells (7). They kill cells with downregulated MHC class I directly (9). Panel B shows the chronological sequence of events starting at the moment of infection (T = 0). Pathogenic invaders are cleared from the site of infection during the first three to four days post infection. Professional APC (e.g. macrophages) migrate to the secondary lymphoid tissue to activate the cells of the adaptive immune system. Antigens are delivered to and retained on follicular dendritic cells (FDC) throughout the germinal centre reaction, clonal expansion and up to 12 months later (see text). B-cells and T-cells subsequently leave the secondary lymphoid tissue to settle in the bone marrow or return into circulation to patrol the host tissues respectively. APC: antigen presenting cell; FDC: follicular dendritic cell; NK cell: natural killer cell. Figure adapted from (11-13).

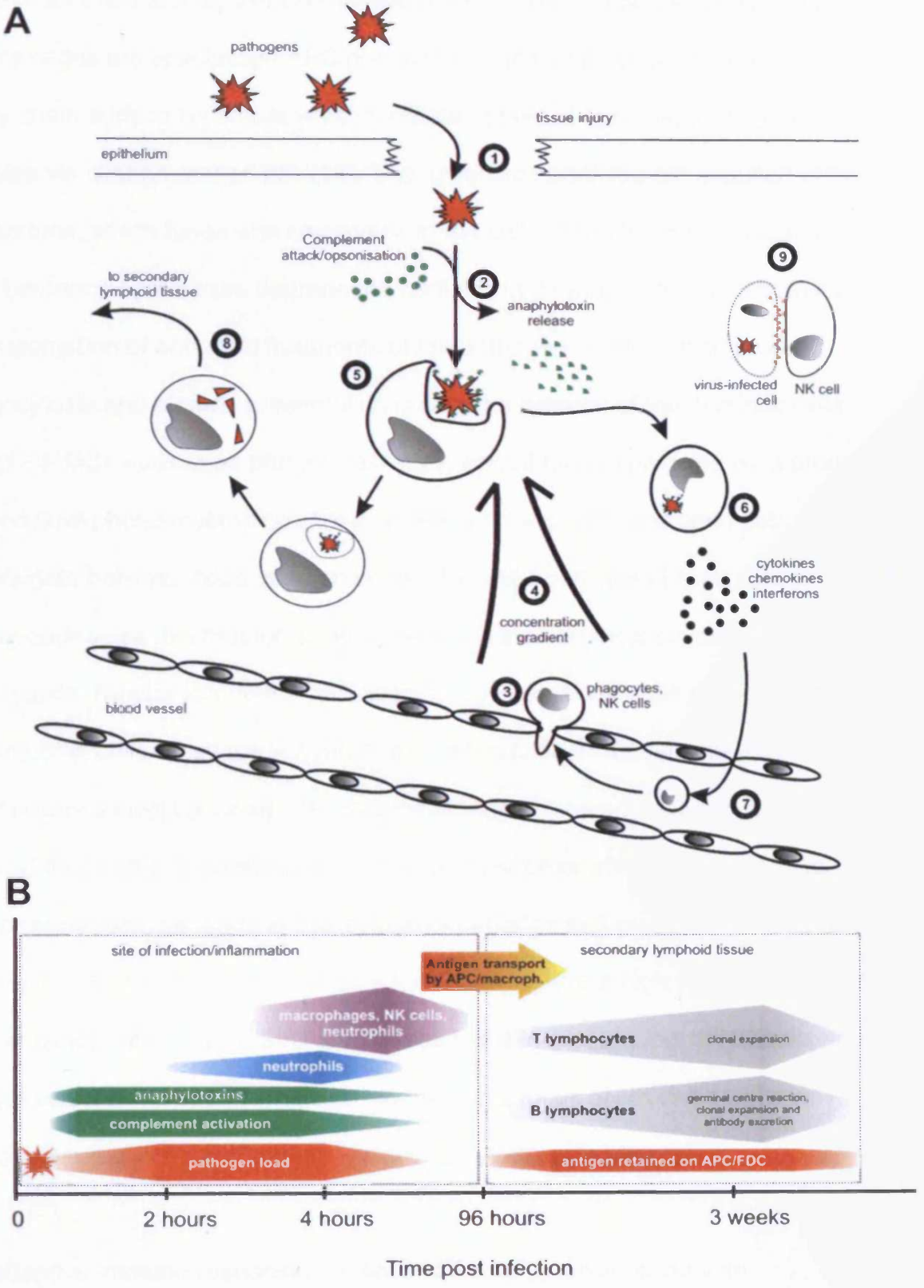
A
pathogens
tissue injury
epithelium
1
Complement
attack/opsonisation
2
anaphylotoxin
release
9
virus-infected
cell
NK cell
to secondary
lymphoid tissue
8
5
6
cytokines
chemokines
interferons
4
concentration
gradient
blood vessel
3
phagocytes,
NK cells
7
B
site of infection/inflammation
Antigen transport
by APC/macroph.
secondary lymphoid tissue
macrophages, NK cells,
neutrophils
T lymphocytes
clonal expansion
neutrophils
anaphylotoxins
B lymphocytes
germinal centre reaction,
clonal expansion and
antibody excretion
complement activation
pathogen load
antigen retained on APC/FDC
0
2 hours
4 hours
96 hours
3 weeks
Time post infection

called professional antigen presenting cells (APC). They represent the link between innate and adaptive immunity and are the most important APC *in vivo*. Macrophages are specialised APC due to their additional complement and Ig heavy chain surface receptors which facilitate uptake of opsonised antigenic particles via clathrin-coated pits (14). The opsonised particles are engulfed in the phagosome, which fuses with lysosomes in the cell to form the phagolysosome (15). Lysosomal proteases degrade the particles in an acidic environment followed by presentation of antigenic fragments of the pathogen on the cell surface. Phagocytosis and surface presentation is also the function of the dendritic cells (DC,(13)). DCs – same as phagocytes – only engulf foreign particles via a process dubbed fluid-phase macropinocytosis, which is non-specific and does not discriminate between opsonised and non-opsonised particles (14, 16, 17). Macrophages use this method of uptake but rely also on receptor-mediated endocytosis. Natural killer (NK) cells specifically interact with and destroy virus infected host cells. They are activated upon interaction with host cells exhibiting much reduced levels or complete absence of major histocompatibility complex class I (MHC I, (9)). In combination with a range of other stimulating and inhibitory surface receptors this leads to the release of perforins and granzymes, which lyse the target cell ((12), figure 1.2). Virus-infected cells excrete high levels of interferon into the surrounding tissue. Similar to phagocytes, large numbers of NK cells are thus attracted to the site of infection, turning into a focus of NK cell activity while the adaptive response and pathogen-specific cytotoxic T cells mature.

The adaptive immune response, the second line of defence, is induced simultaneously with the innate response and the two work hand in hand (9). Onset

and maturation are much slower and immunological memory is developed over the next three to four weeks. The cells and molecules are highly specific for the inducing pathogen and are able to create a memory cell pool in preparation for subsequent infections (8). Chemical messenger release (i.e. anaphylotoxins, cytokines and chemokines) caused by opsonisation and phagocytosis during the initial innate response as well as efficient antigen presentation provides essential signals for humoral and/or cellular immunity. The innate proteins of the complement cascade can also contribute to adaptive immune response activation directly by facilitating uptake not only by macrophages but also B-cells. The antigen is opsonised by C3b, which is quickly broken down to C3d (discussed in detail below) and subsequently processed in the secondary lymphoid organs (e.g. spleen, draining lymph nodes). These immune complexes (IC), Ag opsonised by complement or antibodies, are transported by the blood stream (18). They subsequently bind to B-cells or follicular dendritic cells (FDC) via immunoglobulin heavy chain (Fc) or complement-specific receptors. Otherwise, antigen internalised by professional APC (macrophages, dendritic cells, DC or Langerhans cells, LC, figure 1.3) is broken down and combined with major histocompatibility complex class II (MHC II). In case of viral infections or DNA vaccination, the exogenous DNA is transcribed and translated by the cell and is thus – like any other protein – expressed inside the cell. The target protein is assembled and peptide fragments combined with MHC I and subsequently presented on the surface. MHC I/II bound to antigenic peptide is transported to the surface where it co-localises with the adhesion molecules CD80 (B7.1) and CD86 (B7.2, (19)). The MHC-peptide complexes can be recognised by T-cell receptor on T-cell precursors in co-operation with CD28 binding to CD80/86. MHC I-bound antigens interact with $CD8^+$

T-cells inducing a cellular response (figure 1.2). MHC II-bound antigens interact with $CD4^+$ T cells. B-cells also act as antigen presenting cells. They are able to bind soluble IC arriving at secondary lymphoid organs, internalise it via their surface IgM (B-cell receptor, BCR) and complement receptor (CR) 2 and present it on the surface before entering the T cell zone (19). B-cells lacking Ag specificity can act as APC, especially if the antigen is present in low concentrations (discussed further below; (20-23)). During migration through the T-cell zone antigen presenting B-cells receive a number of activation and accessory signals from antigen-activated T helper ($CD4^+$ T_H) cells. Naive B-cells do not respond to Ag-stimulation alone, therefore MHC II/TCR binding to CD4 requires support by APC CD40 ligand (CD40L, CD154, (22)) binding to CD40 on B-cells, essential for B-cell activation and germinal centre (GC) formation (24). The surface interactions and the release of the cytokines interleukin (IL) 4, IL-5 and IL-6 (19, 25) ultimately lead to the formation of foci of B-cell proliferation (13). B-cells activated in this way either differentiate into short-lived plasma cells (see section 1.4) to provide an early source of circulating antibody, or express the surface marker GL7 and migrate into the B-cell areas to enter primary follicles (26, 27). The resulting germinal centres are a complex organised network of cells and provide a microenvironment for B-cell proliferation, affinity maturation, somatic hypermutation of the V-region Ig genes (discussed below) and B-cell clone selection (27-31). GCs first appear 2 – 4 days post antigen stimulation (32), although development is delayed by 3 – 5 days in the spleen. The follicles consist of a "dark zone" densely packed with rapidly proliferating centroblasts and long protruding FDC processes (30).

Figure 1.3 Innate and adaptive immune response following vaccination or infection. The development of a specific response to a pathogen or vaccine is a multi-step process. Antigen may be present in the circulation or produced by virus-infected somatic cells, which may excrete some of the antigen extracellularly. Following uptake into professional APC (e.g. DC) and degradation within the cell, the antigen is combined with MHC I/II (depending on the type of infection or vaccination) and deposited on the surface of the APC. The mature APC migrates to the secondary lymphoid organs to present the antigen on MHC together with several co-receptors (see text) to T-cells. Dependent on the MHC class, $CD8^+$ cytotoxic T-lymphocytes (CTL) or $CD4^+$ helper T-lymphocytes (T_H) are activated. CTL leave the secondary lymphoid tissue to destroy cells presenting MHC I + Ag on their surface. $T_{H,}$ on the other hand, interact with B-cells and induce affinity maturation in conjunction with IC trapped on FDC in the B-cell follicle. Following this germinal centre reaction, highly antigen-specific antibody-producing plasma cells, as well as memory B-cells, exit the GC and settle in the bone marrow. There they remain as long-lived Ag-specific clones ready for re-activation by subsequent infection with the same pathogen. Adapted from (16, 33).

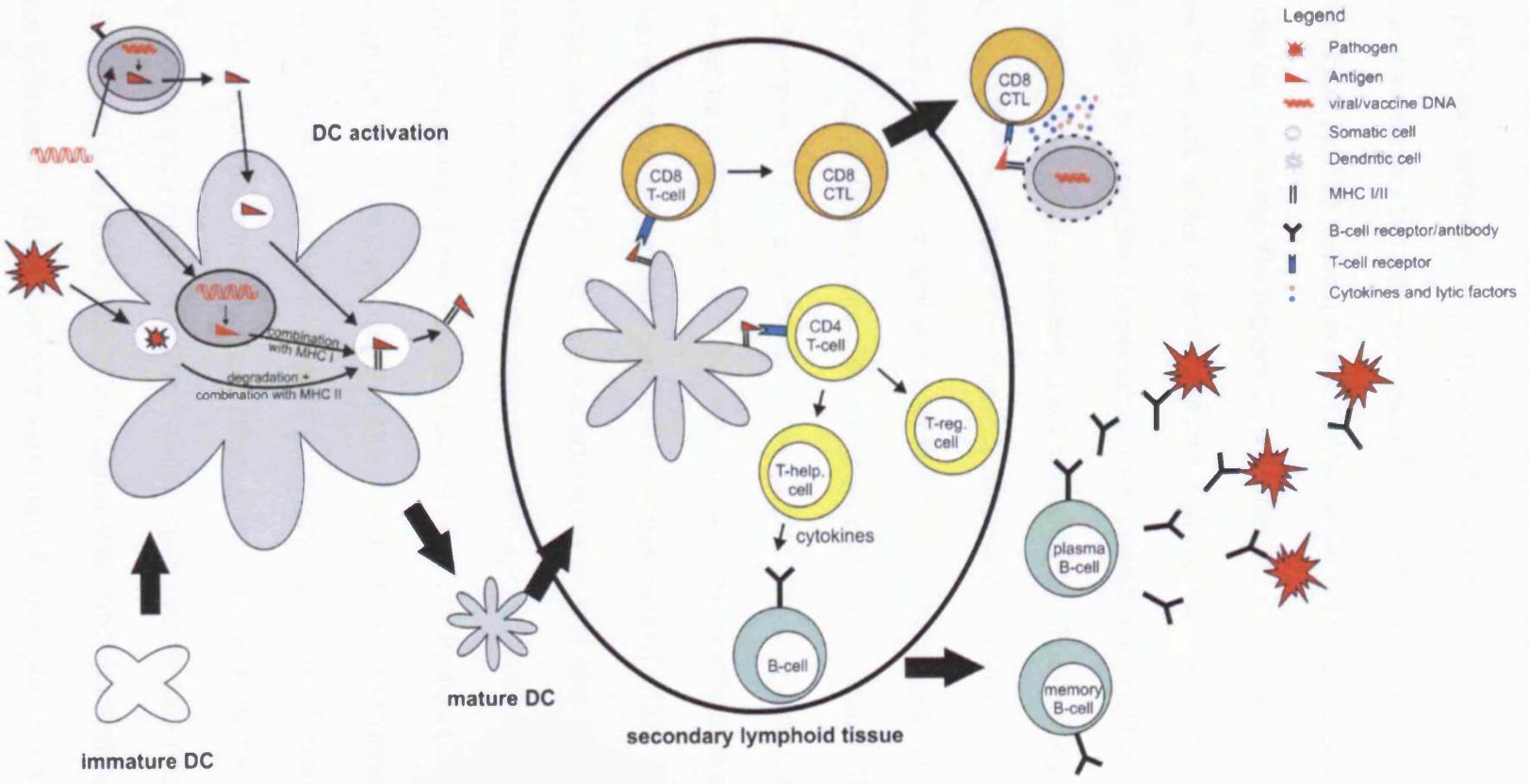
DC activation
combination with MHC I
degradation + combination with MHC II
immature DC
mature DC
CD8 T-cell
CD8 CTL
CD4 T-cell
T-help. cell
T-reg. cell
cytokines
B-cell
secondary lymphoid tissue
plasma B-cell
memory B-cell
Legend
Pathogen
Antigen
viral/vaccine DNA
Somatic cell
Dendritic cell
MHC I/II
B-cell receptor/antibody
T-cell receptor
Cytokines and lytic factors

As the reaction progresses, numerous circulating antigen-activated B-cells increasingly colonise the dark zone. Hypermutation starts just prior to GC formation, peaks between days 10 and 12 and tails off during the following days (34). Class switching from immunoglobulin (Ig) M to IgG also occurs in the centre. GC cells (IgM^+ IgD^{low}) remain in the centre while primary B-cells (IgD^+ $CD38^-$, (35)) are displaced into a mantle region. Soon after GC induction, the population changes from polyclonal to an oligoclonal cell network. The mature centroblasts ($CD38^+$, (36)) stop dividing to become small centrocytes ($CD38^+$), which migrate into the light zone, a less densely packed area (29). There, they make extensive contact with FDC and their long network of extended cellular processes. FDC represent the only site of antigen retention as they take up the IC carried by APC via their Fc receptors and complement receptors, in particular CR2 (37). This allows provision of a long-term IC reservoir for up to one year (29, 31, 38, 39). *In vitro* assays have shown that FDC are markedly more effective at stimulating B-cells than soluble antigen with particular involvement of CD21 and CD35 on the lymphocyte surface (40, 41). Several adhesion factors also play a role in FDC-B-cell interaction providing proliferation and anti-apoptotic signals. Thus, FDC are an essential component of memory and plasma cell production (27). Therefore, this interaction fulfils a dual purpose, the site of somatic hypermutation and class switching as well as rescue of B-cells from apoptosis (37). Centrocytes cease to proliferate and migrate into the light zone. If they are able to displace antigen from the FDC surface to present it to the T-cells again, some may return to the dark zone for further V-region modification. Otherwise, and depending on interaction between CD40 and CD40L, some differentiate further (29, 42). Death rates are very high in the GC, firstly due to apoptosis of low-affinity clones, but also due to

controlled cell death of cells that have become autoreactive or whose DNA repair is faulty (32). Cell death, as well as proliferation induction, is mediated by T-cells via the death receptor Fas (CD95) and Fas ligand (CD95L) interaction (43). Surviving centrocytes differentiate into plasma cell precursors ($CD138^-$, (44) and plasma cells ($CD138^+$, $CD38^+$; (32, 35)), or memory cells ($CD38^-$, (36)), mainly committed to high specificity IgG production. A small minority of B-cells produce IgA while a minor subset expresses IgM. In the mouse, CD38 expression is reversed (27). CD38 appears on naïve B-cells prior to entry into the GC where expression is downregulated (45, 46). Expression remains low on plasma cells and is conversely displayed on memory cells (42, 47). Differentiation depends on the cytokines excreted by the connected T-cell, which seem to support Th1 and Th2 responses, as well as class switching (30). IL-4 facilitates production of memory cells while IL-10 induces plasma cell production. IL-2 acts in synergy with either interleukin (41). Somatic hypermutation continues into the third week following the primary challenge. The secondary GC reaction, upon recurrent challenge, proceeds much quicker thanks to the memory cells (32). Secondary GC have shorter life spans, are smaller and due to a more rapid and efficient "learned" reaction, centroblast cell death is far reduced (27). This pathway is potentiated by C3d-opsonised Ag and relies on Ag-specific memory B-cells from a previous encounter (18, 48). The hypermutability of B-cells is one of the major contributors of flexibility of the vertebrate immune system. It is thanks to this cell type, the production of highly specific antibody and the generation of long-lived memory cells that the constant onslaught of infectious agents from the environment can be confronted efficiently. This crucial role in the adaptive immune response has focussed much immunological research interest on B-cells.

1.4 B-cell Development and Humoral Immunity

Lymphocytes, and their sites of production and physiology, have been studied since the 1930s (49). Chickens lacking an organ called the Bursa of Fabricius were unable to mount an antibody-mediated immune response. Closer investigation revealed that antibody-producing cells were generated in the bursa, hence termed B-cells (50). Adult mammals do not possess a bursa, but produce their B-cells in the bone marrow. During foetal development, however, B-cells are produced in the blood, liver, placenta and the omentum (51).

B-cells, as all other blood cells, develop from the pluripotent haemopoietic stem cells to multilineage progenitor cells followed by the common lymphoid progenitor stage. Most of the developmental phases take place in the bone marrow and are identifiable through surface expression of a variety of surface markers (52, 53). In mice, B220 (CD45 receptor, CD45R) is expressed at the earliest B-cell stage (pre-pro-B) and remains on the surface throughout the life of the cell. CD19, B-cell specific and a member of the Ig superfamily, appears at the second, pro-B-cell stage (54, 55). CD19 is involved in inducing signalling cascades inside the cell via its highly charged cytoplasmic tail (see below, (52, 56)). During their development, the cells undergo extensive mutation and rearrangement in their diversity (D), variable (V) and joining (J) Ig genes. The products from these genes make up a unique or monoclonal surface-bound Ig also known as the BCR, which is responsible for specific antigen recognition, binding and B-cell activation. This specificity can be revised and improved during an immune response within the germinal centre reaction. BCRs go through three construction phases: V/D/J combination and heavy/light (H/L) chain arrangement, nontemplated nucleotide

insertion and receptor editing (57, 58). During these processes the theoretical potential to recognise different antigens rises from 2 x 10^6 to at least 10^8 to 10^9. Through the processes of clonal selection, anergy and receptor editing fully functional tolerant monoclonal B-cells reach maturity, leave the bone marrow and enter the circulation (57). Mature B-cells are distributed throughout the body and continually patrol the secondary lymphoid organs: lymph nodes, spleen, gut associated lymphoid tissue (peyers patches, tonsils, appendix), but also the lung, peritoneal cavity and blood for pathogens. The main function of a B-cell is to mount an adaptive humoral immune response through the production of high affinity Ig to pathogen or antigen.

Three types of B-cell are present in mice and humans, B1a, B1b and B2. The majority of B1 cells of the peritoneal cavity are $CD5^+$ B1a type cells, B1b on the other hand are $CD5^-$ (51). B2 cells are the peripheral and follicular B-cells constantly developing in the bone marrow. B1 are the dominating cell type populating the newborn spleen although their numbers decrease to 3 – 7% in adult life and are found in peritoneal tissues and at low levels in the spleen and lymph nodes. B1 cells carry intermediate to high levels of BCR (51), are long-lived and undergo self-renewal mediated by enteric bacteria along with CR2-co-receptor signalling and not FDC interaction (59).Therefore these cells – among them marginal zone (MZ) B-cells – are generally seen as more "primitive" B-cells due to a restricted repertoire of natural antibody and an altered repertoire against some but not all self-antigens (60). It is believed that this natural antibody repertoire contributes to innate immunity and B1 as well as MZ B-cells provide a strong and rapid antibody response (61-64). B1-excreted natural circulatory antibodies are

able to opsonise pathogens activating the classical complement pathway and are responsible for intravascular clearance of and protection against high doses of endotoxin (51, 65).

1.5 The Complement System

As well as being one of the oldest components of the immune response, complement was one of the earliest to be described and characterised, mainly by Buchner, Pfeiffer, Bordet, Ehrlich and Morgenroth (66, 67). So far more than 30 proteins have been identified as being part of the complement cascade. They function as effectors of the host defences against microbial infection and as mediators of immunopathological events. There are three activation pathways in which each step is activated in a sequential fashion similar to a relay race ((68, 69), figure 1.4). A significant proportion of the components are proteases that are activated by cleavage, converting the substrate into the new enzyme to activate the next step in the pathway. This ingenious arrangement leads to a massive amplification of activation able to deal with an infection very efficiently.

The influence of the complement cascade is extensive and diverse. Opsonins aid phagocytosis and presentation. Anaphylotoxins are released from three complement components and represent potent promoters of the inflammatory response and attraction of more phagocytic cells. The pathway is regulated tightly by a number of soluble and membrane-bound regulators and inhibitors to limit and prevent damage to the host. All components are highly conserved throughout the animal kingdom, which is evidence for the evolution of the complement system a long time before any more sophisticated mechanisms such as adaptive and

cellular immunity. All higher vertebrates possess the full set of complement proteins and utilise all three activation pathways (70-72).

1.5.1 The Classical Pathway

The classical pathway (CP, figure 1.4) represents the most recently developed of the three activation pathways, though it was the first one to be discovered. Activation is initiated by Ig binding to microorganisms (MOs), viruses or cell debris to form IC in the serum (73, 74). The C1 complex mainly binds to the constant regions of μ- and γ-type Ig, but is also able to bind directly to some pathogenic surfaces (69, 74-76). C1 initiates the classical complement pathway, through autolytic cleavage of the C1s and C1r components, following conformational "squeezing" of the C1q constituents of the C1 complex; a result of binding a single surface bound IgM molecule or a sufficient density of bound IgG molecules (approximately 10^6) to engage multiple C1q arms. Key to localised, specific activation of this pathway is the covalent binding of the C4b fragment by a thoiester bond to the target surface (subsequent to cleavage by C1r/s), followed by docking of C2 (which is also cleaved by C1r/s). This leads to the formation of the CP C3 convertase C4b2a. Surface deposition of these components acts as a focal point for activation of the cascade on the target surface leading to deposition of C3b, the pivotal molecule in all three activation cascades (68, 69, 77).

Figure 1.4. The complement cascade. The pathway is initiated by antibody bound to an antigenic surface (classical pathway), surface carbohydrates (mannose-binding lectin pathway) or by baseline hydrolysis of C3, central component of the pathway. Components are activated in the fashion of a relay race.

Key:

C1 – 9 = Complement component 1 – 9

MBP = Mannose-binding lectin

MASP = MBL-associated serine protease

P = properdin

B = factor B

D = factor D

CXa/CXb = breakdown products of complement component X

C9n = variable numbers of C9 molecules in the membrane attack complex

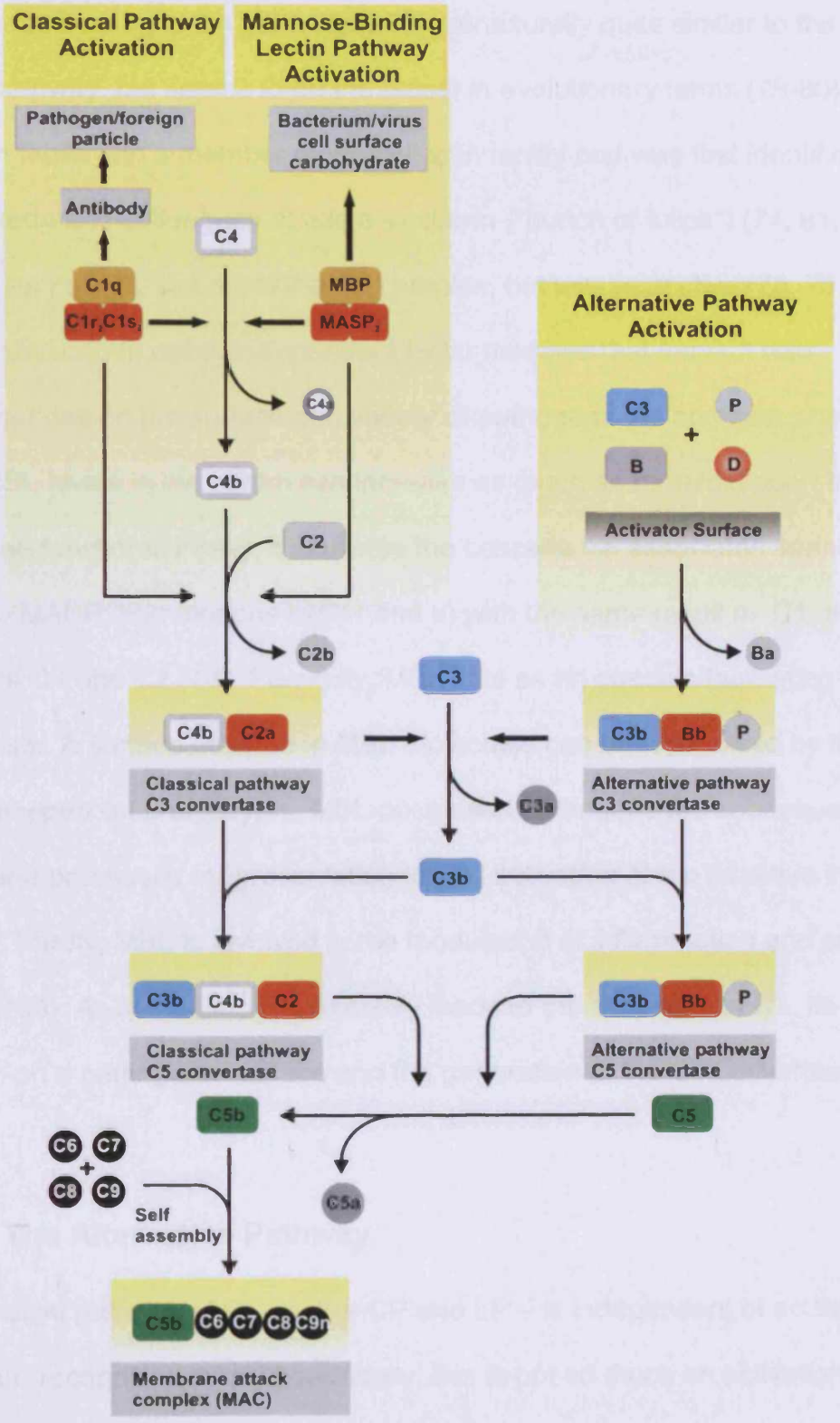
Classical Pathway Activation
Mannose-Binding Lectin Pathway Activation
Pathogen/foreign particle
Bacterium/virus cell surface carbohydrate
Antibody
C4
C1q
C1r2C1s2
MBP
MASP2
C4a
C4b
C2
C2b
Alternative Pathway Activation
C3
P
B
D
Activator Surface
Ba
C3
C4b
C2a
C3b
Bb
P
Classical pathway C3 convertase
C3a
Alternative pathway C3 convertase
C3b
C3b
C4b
C2
C3b
Bb
P
Classical pathway C5 convertase
Alternative pathway C5 convertase
C5b
C5
C6
C7
C8
C9
C5a
Self assembly
C5b
C6
C7
C8
C9n
Membrane attack complex (MAC)

1.5.2 The Mannose-Binding Lectin (MBL) Pathway

The Mannose-binding lectin pathway (LP) is structurally quite similar to the classical pathway, but seems to be the oldest in evolutionary terms (78-80). MBL is a C-type lectin and a member of the collectin family and was first identified in 1987 by Ikeda and colleagues. It has a sertiform ("bunch of tulips") (74, 81, 82) structure, very similar to C1q in the C1 complex, but less restrictive (76, 78, 82). The subunits contain calcium dependent lectin modules that interact with oligosaccharides on the surface of a variety of pathogens. As an acute phase protein, MBL levels in the serum can increase as much as threefold upon infection to fulfil three functions. Firstly, it activates the cascade via associated serine proteases (MASP; homologous to C1r and s) with the same result as C1: the cleavage of C4 and C2 (74). Secondly, MBL acts as an opsonin facilitating phagocytosis. A surface covered in MBL molecules can be recognised by the collectin receptor on phagocytes. MBL-opsonised pathogens are subsequently ingested and processed for presentation to and activation of the adaptive immune response. Thirdly, MBL is involved in the modulation of inflammation and promotes apoptosis (83). As in the CP, LP ultimately leads to the activation of C3, its deposition on a pathogenic surface and the generation of the C5 convertase

1.5.3 The Alternative Pathway

The alternative pathway (AP) – unlike CP and LP – is independent of activation by Ig or pattern recognition. More specifically, this is not so much an activation pathway, but a failure to inhibit the low baseline level of C3 constantly undergoing spontaneous hydrolysis (69). As it circulates, C3 frequently turns into the

metastable C3(H_2O), dubbed the tick-over phenomenon (66, 75). This form is functionally very similar to C3b, with the internal thioester bond exposed. As depicted in figure 1.5, C3(H_2O) can then bind factor B (fB), which in turn is a substrate for the serine protease factor D (fD) (84) that leads to cleavage of serum C3 into the anaphylotoxin C3a and C3b. Unless C3b encounters a surface within a timeframe of milliseconds, it is hydrolysed and destroyed. Otherwise, it covalently binds to surface hydroxyl or amine groups through nucleophilic attack via its exposed thioester bond. The resultant immobilised AP C3 convertase, C3bBb, is stabilised by properdin (85). Properdin protects C3bBb from degradation by factor I, but only if C3b is membrane-bound (also see (86, 87)). In this amplification loop more and more C3 can be deposited and more C3 convertases are formed, and since the other activation pathways deposit C3b, the alternative pathway may also act as a further amplification loop for C1- or MBL-mediated activation. The fate of C3 heavily depends on the competition between several C-inhibitors and fB. These inhibitors are factor I (fI) together with the co-factor, factor H (fH), in the serum or complement receptor (CR) 1 and membrane cofactor protein (MCP) as membrane-bound cofactors. Complement activity is regulated by the presence of inhibitors on the host surface, which are usually absent on pathogens. Thus, presence of regulators can discern between host and pathogen. Finally, the alternative pathway C5 convertase is generated in a similar fashion to the classical pathway C5 convertase. A second molecule of C3b binds to the C3 convertase, giving rise to C3bBb3b, the alternative pathway C5 convertase.

1.5.4 The Terminal Pathway

The cleavage of C5 to C5a, the most powerful anaphylotoxin of the C3-family of proteins, and C5b is the first and only proteolytic event in the formation of the membrane attack complex (MAC). C5b binds to the next protein in the terminal pathway, C6. The C5b6 dimer associates with freely circulating C7, C8 and C9 (75). Subsequent binding of each component increases the hydrophobicity of the complex, allowing deeper insertion into the plasma membrane, until C5b678 is considered a "leaky patch" on the membrane. Spontaneous assembly of multiple units of C9 results in insertion of a highly stable hollow cylinder (hydrophilic in the centre) leading to osmotic leakage and eventual bursting of the target cell.

1.6 The Third Component of Complement – C3

C3 plays a central role in the cascade as all three activation pathways result in its activation. It has been found to interact with more than 20 proteins (69, 88). Müller-Eberhard described C3 in humans first in 1960 following previous publications on guinea pig C3 (89, 90). Through opsonisation of target surfaces it coordinates the immune response by leading to the destruction of the target cell via the membrane attack complex or through phagocytosis. Additionally, opsonisation signals cells of the immune system to respond vigorously to the pathogen by enhancing Ag uptake and presentation on B-cells (18).

C3 is conserved across vertebrate species (88, 91, 92) and is one of the most prominent acute-phase and most abundant plasma proteins (1 – 2 mg/ml (88)). It is part of the α2-macroglobulin (α2M) family, which is characterised by a unique β-cysteinyl-γ-glutamyl thioester motif (75, 93, 94) and emerged about 700 million years ago. C3 is a 187 kDa glycoprotein (95) encoded on chromosome 19. It is

encoded by a 41 kb gene in 41 exons (ranging from 52 – 213 bp), 16 of which encode the β chain and 25 the α chain (91, 96). C3 is produced as a 1663 aa single-chain pre-pro C3 molecule primarily in the liver, but also in macrophages/monocytes, neutrophils and many other cell types (66, 88). Expression is strongly dependent on cytokines and controlled at transcription level and by the stability of mRNA. The life of C3 from translation to degradation to its smallest immunologically significant breakdown products is shown in figure 1.5.

The α and β chains of the mature protein (figure 1.5, (95)) are connected by a single disulphide bond although the remainder of the two chains associates non-covalently (91) in the shape of a flat ellipsoid and a smaller flat domain (66). These are independent of the domain structure but represent the two major fragments C3c and C3d respectively. C3d contains the conserved thioester motif and shares a proportion of its sequence with α2M (92, 97, 98). The structure of human as well as murine C3d has been addressed in a number of studies (99-106). C3d (the final breakdown product of C3) consists of 12 α-helices, arranged in a α6-α6 structure (102) and comprises about 18% of the whole C3 molecule. The surface of one end of the α helix barrel is convex containing the thioester site while the other side has a concave depression with a negatively charged acidic pocket (102). C3 is transported through the Golgi apparatus and glycosylated at residues 917 and 63 in α and β chains, respectively (107). A 22-residue signal peptide is removed from the amino terminal and the thioester is formed by transacetylation of the thiol group of Cys^{988} and the γ-amide group of Gln^{991} (native C3 numbering).

Figure 1.5. The life of C3. C3 is produced as a single amino acid chain pro C3. A furin-like enzyme removes an arginine tetrapeptide to produce mature C3. Activation of C3 is catalysed by enzymatic removal of C3a by C3 convertase (C4b2a for CP + LP and C3bBb for AP) resulting in C3b. The thioester is exposed and is quickly deactivated by hydrolysis or binds to a substrate surface (see figure 1.6). C3b is then quickly degraded by the indicated enzymes and co-factors to iC3b, C3c, C3d and C3g. C3d remains attached to the substrate via the thioester (adapted from (68, 75, 108, 109).

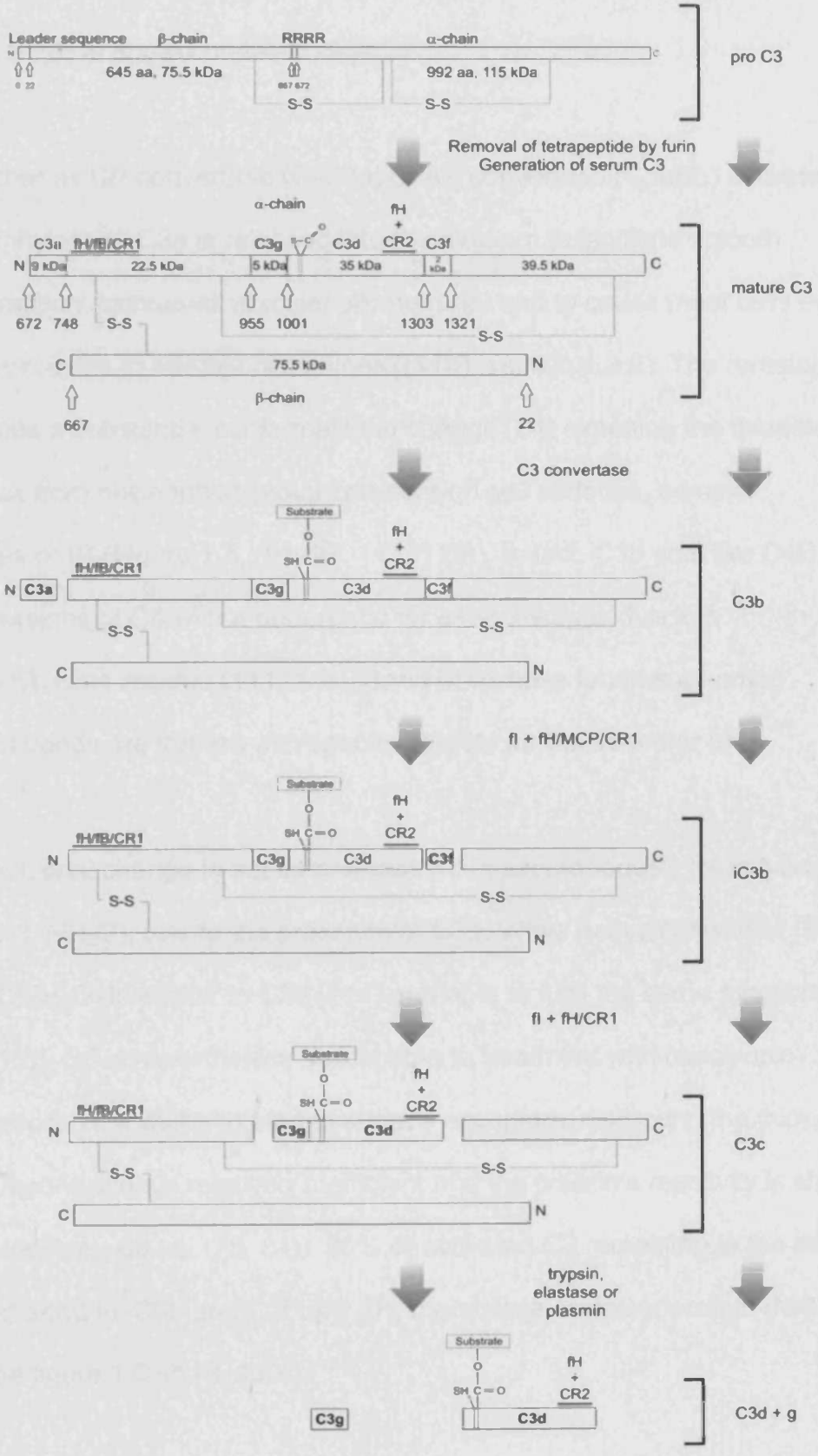
Leader sequence
β-chain
RRRR
α-chain
645 aa, 75.5 kDa
992 aa, 115 kDa
S-S
S-S
pro C3
Removal of tetrapeptide by furin
Generation of serum C3
α-chain
fH
+
CR2
C3a
fH/fB/CR1
C3g
C3d
C3f
9 kDa
22.5 kDa
5 kDa
35 kDa
2 kDa
39.5 kDa
672
748
S-S
955
1001
1303
1321
S-S
75.5 kDa
β-chain
667
22
mature C3
C3 convertase
Substrate
fH/fB/CR1
C3b
fI + fH/MCP/CR1
iC3b
fI + fH/CR1
C3c
trypsin,
elastase or
plasmin
C3g
C3d
C3d + g

The thioester bond is then protected in a hydrophobic pocket (68), which is part of the α2M conserved region (97). The half-life of this protection from water and small nucleophiles is approximately 6 days.

Cleavage either by CP convertase (C4b2a) or AP convertase (C3bBb) activates C3. The anaphylotoxin C3a is released into the medium to facilitate smooth muscle contraction, increased vascular permeability and to cause mast cells and basophilic leukocytes to release histamines ((110), section 1.3.2). The remaining C3b undergoes a substantial conformational change (84) exposing the thioester bond to attack from nucleophilic groups present on cell surfaces, complex carbohydrates or IC (Figure 1.5, (91, 97, 111, 112)). In fact, C3b acts like C4B, one of two versions of C4 with a preference for ester linkages due to a downstream histidine residue (111, 113). Sahu *et al.* have found supporting evidence that bonds are formed with specific targets for the thioester (91).

This conformational change is not as pronounced in spontaneously hydrolytically activated C3, C3(H_2O), due to the presence of C3a. While native C3 is inert (84), metastable C3(H_2O) is similar to C3b (114) and able to fulfil the same functions (see also (115)). C3 is nevertheless susceptible to treatment with chaotropic agents that abolish the ability to bind to surface acceptors, disrupting the thioester (116-118). Opsonisation is relatively inefficient and the protein's reactivity is short ($t_{1/2}$ of the thioester ~ 60 μs, (75, 84)). 90% of activated C3 remaining in the serum is rapidly degraded to iC3b and C3f by fI, fH, membrane co-factor protein (MCP) and CR1 (see figure 1.5, (119, 120)).

Figure 1.6. The thiolactone ring and the thioester binding reaction of C3. The residues Cys^{988}-Gly-Glu-Gln^{991} of C3 form a thiolactone ring. Activation of C3 leads to a conformational change leaving the thioester motif open to nucleophilic attack. In the majority of cases the reaction does not lead to transesterification but deactivation by hydrolysis. Adapted from (111, 121).

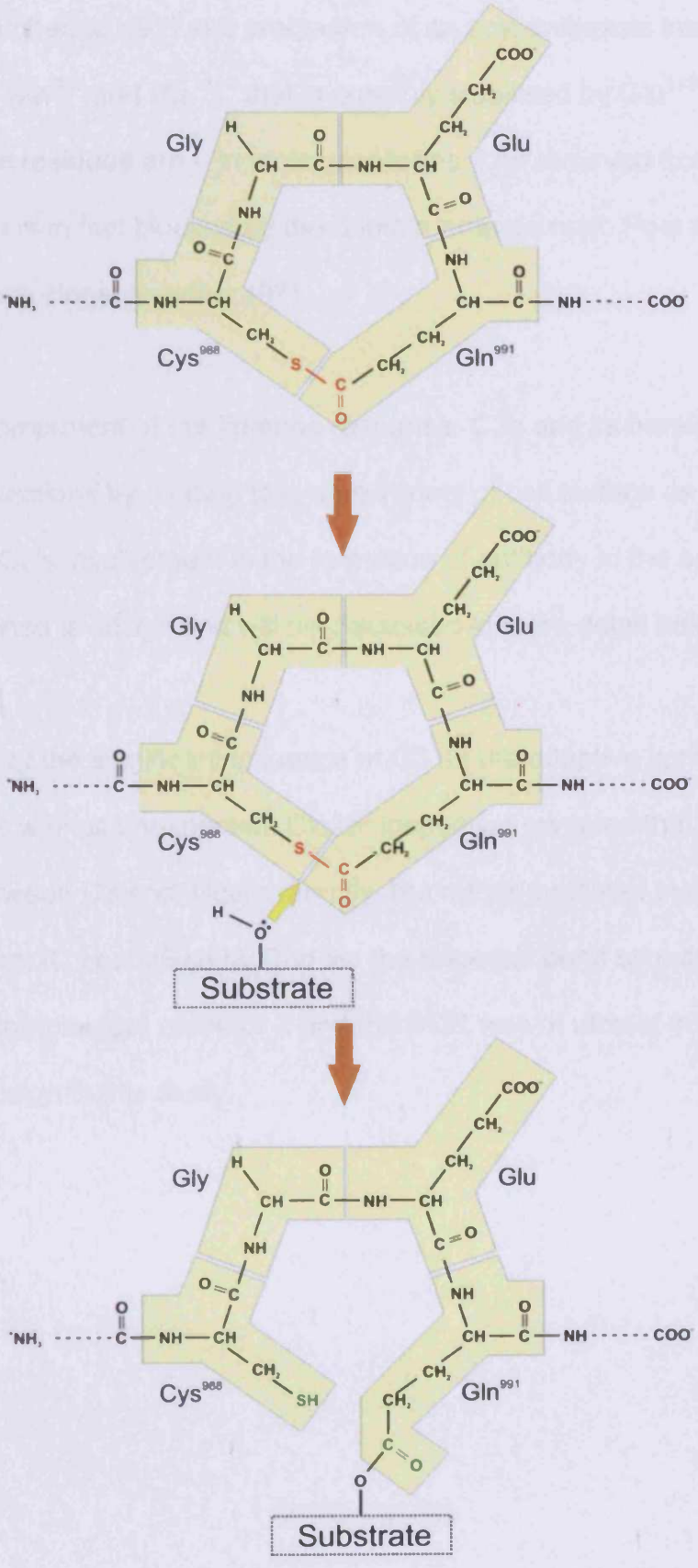
Gly
Glu
Cys968
Gln991
Substrate
Gly
Glu
Cys968
Gln991
Substrate

The breakdown quickly continues to C3c, C3dg, C3d and C3g. The reactivity changes due to a transformation from the thioester to a thiolate anion on Cys^{988} (mature C3 numbering, (91) and production of an acyl-imidazole intermediate ((98) see below) by Gln^{991} and His^{1104} that is possibly stabilised by Glu^{1106}. In the native molecule these residues are – in molecular terms – far removed from each other and interaction is in fact blocked by the domain arrangement. Post activation they are moved much closer together (97).

As a central component of the immune response, C3b and its breakdown products fulfil several functions by binding to a wide variety of cell surface as well as serum proteins (88). C3's involvement in the formation of antibody in the adaptive immune response is critical and will be discussed in more detail below.

The discovery of the significant influence of C3 on the adaptive immune response was striking as well as unexpected. Closer inspection revealed that there was no interaction between C3 and T-cells directly, but rather mediated by B-lymphocytes. This finding, that IC opsonised by C3d via the thioester bond stimulate B-cells by cross-linking complement receptor 2 and the BCR was of utmost importance for the vaccine design in this study.

1.7 Complement Receptors (CR)

Four complement receptors have been identified, all involved in binding of activated complement C3 and C4 breakdown components. CR type 1 (CR1) and CR2 are members of the regulators of complement activation (RCA) gene cluster (reviewed in (122, 123)). RCA proteins are characterised by an ancient repeated motif known as short consensus repeat (SCR), complement control protein (CCP) or sushi domain (from here referred to as SCR). Each SCR is approximately 60 – 65 amino acids in length, 10 – 15 of those are highly conserved among all family members (122). The remaining two receptors, CR3 (CD11b/CD18) and CR4 (CD11c/CD18), are heterodimeric glycoproteins with a shared β-chain (CD18). They are members of the integrin superfamily, however, neither receptor consists of SCRs (68, 124). They appear on a wide range of immune cells and FDC (125) where they are involved in antigen presentation. The primary function of both molecules is the induction of phagocytosis and leukocyte adhesion (69, 124, 125). iC3b, which is outside the scope of this study, is the interaction partner of these two receptors, hence they will not be discussed further. In contrast, complement receptors 1 and 2 have received intensive interest due to their particular involvement in the adaptive immune response. This has prompted further study of a variety of novel uses in vaccination and therapeutic design.

1.7.1 Complement Receptor 1

CR1 (CD35) was first identified in 1973 by Ross *et al.* (126) and described as the C3b receptor by Fearon in 1980 (127). It is expressed on the surface of erythrocytes (in most primates), B-cells (126), polymorphonuclear leukocytes, macrophages/monocytes, neutrophils, eosinophils, basophils, NK cells, follicular dendritic cells, some T-cells, Kupffer cells and glomerular podocytes (123, 124). CR1 is a type I polymorphic single-chain glycoprotein encoded on the long arm of chromosome 1 expressed as one of four allotypes (figure 1.7). The membrane-proximal domains of CR1 consist of a 39 amino acid (aa) cytoplasmic domain, 4 positively charged residues and a 25 aa transmembrane region. The long extracellular domain protrudes into the surrounding medium and consists of two membrane-proximal SCRs and 28 SCRs organised into three to six sub-domains (long homologous regions, LHRs) of 7 SCRs each (123). All LHRs exhibit 70 – 95% homology, indicating gene segment duplication during the evolution of the receptor.

In mice, CR1 is encoded in the *Cr2* gene and expressed on the surface as part of a composite receptor (128, 129). 6 SCRs in the N-terminal segment represent CR1, the remaining 15 SCRs attached to the surface represent CR2 (figure 1.7, (124)). CR1 fulfils several functions however the distribution is slightly different in mouse and human (130). Approximately 6,000 – 12000 receptors can be found on blood leukocytes although receptor numbers can be upregulated by chemotactic agents (124). Human erythrocytes however possess about 25 – 50x less receptor on their surface while mice hardly express any. Its main function however is the interaction with C4b and C3b bound to foreign particles (strength of association

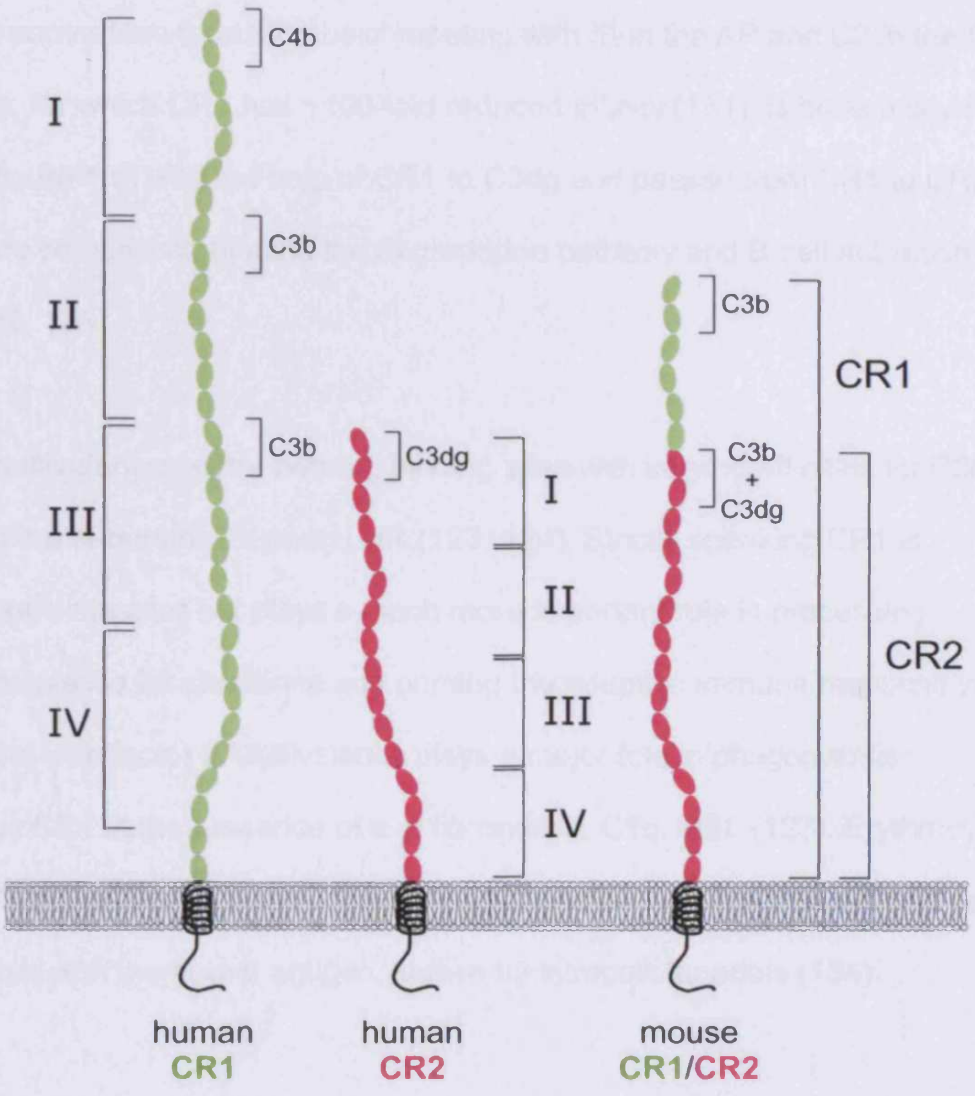

Figure 1.6. Mouse and human complement receptors 1 and 2. Human complement receptors are encoded on different genes while mouse CR1 and CR2 are encoded on a single gene (*Cr2*) and are splice variants of each other. The receptors consist of SCR domains organised into homologous repeat regions in humans (I – VI). Human CR1 binds C3b at multiple sites, as does the mouse receptor. CR2 in both species has only one binding site for C3dg (adapted from 122, 123).

~2 – 5 x 10^7 L mol^{-1}, (124)). On B-cells, CR1 contributes to the degradation of C3b to iC3b/C3c/C3dg and C4b to C4c/C4d in co-operation with factor I (fI). CR1 also inhibits C3 convertase formation by competing with fB in the AP and C2 in the CP (123). iC3b, for which CR1 has ~100-fold reduced affinity (131), is broken down by fI and fH (figure 1.5) with the help of CR1 to C3dg and passed from CR1 to CR2 via a ternary complex continuing the degradation pathway and B-cell activation (37, 51, 132, 133).

CR1 is a multivalent receptor bearing binding sites with varying affinities for C3b and C4b at the N-terminal of each LHR (123, 124). Strictly speaking CR1 is therefore not a receptor but plays a much more important role in processing immune complexes for clearance and priming the adaptive immune response in co-ordination with factor I. Multivalency plays a major role in phagocytosis induction by CR1 in the presence of e.g. fibronectin, C1q, MBL (123). Erythrocytes transport IC to the liver for destruction by Kupffer cells (123, 124), which take up CR1 together with the bound antigen, shown by intracellular pools (134).

1.7.2 Complement Receptor 2

CR2 (CD21, C3d receptor, EBV receptor) is the receptor for the C3 breakdown products iC3b, C3dg and the proteolytic limit fragment C3d (figure 1.7). It is also the only SCR-containing member of the Regulators of Complement Activation (RCA) gene cluster at chromosome1q32 that definitively does not have any complement inhibitory activity. The other binding partners of CR2, Epstein Barr Virus (EBV), CD23 and interferon (IFN) α are outside the scope of this study and will not be discussed further here. CR2 is encoded on chromosome 1 and

expressed as a single chain glycoprotein of 145,000 Da, first identified by Iida (135). CR2 was first detected by Lay in 1968 (136), who observed that 10 – 25% of cells from mouse lymph nodes, but not the thymus, macrophages, monocytes and polymorphonuclear cells bound IC via a specific receptor. CR2 was first described in 1973 by two independent groups (Grey (126) and Nussenzweig (137)). Ross *et al.* (126) were the first to identify CR2 as the C3d-specific receptor, which clearly showed that the complement receptors were distributed differently among lymphocytes and bound different subspecies of C3. The structure and binding specificities were investigated further, namely by Tedder (138) and Weis *et al.* (139). The EBV-immortalised B-cell lymphoma cell line Raji was instrumental and used extensively in CR2 research and its ligands (140, 141). Raji cells do not express CR1 and several other B-cell surface markers and were originally used to isolate the C3d-receptor (135, 142, 143). Thus the mode of action of C3dg/C3d was discovered in conjunction with the B-cell mitogen EBV although they do not share their binding sites ((144); also see (124, 145, 146)). The discovery that the C3dg/C3d and EBV receptor were in fact the same (147) led to the conclusion that C3 could also activate B-cells via this receptor. Iida *et al.* finally assigned CR2 its role of C3d receptor followed by subsequent discovery of C3d's intimate connection with B-lymphocytes via binding, activation, support and induction of further differentiation (135). Experiments using $C3^{-/-}$ mice exhibited very similar responses to $Cr2^{-/-}$ mice confirming that C3d is the chief ligand for CR2 (65, 148, 149).

CR2 is not expressed as ubiquitously as CR1. 80 – 90% of all mature B cells express it on their surface (approx 8000 per cell (57, 124)) as well as FDCs in

lymphoid follicles, pharyngeal and cervical epithelial cells, a subset of thymocytes (21, 66, 150-153), and there is some evidence for CR2 expression on mast cells (154). CR2 appears on the B cell surface later than CR1, at the IgM^{hi} IgD^{lo} stage (138, 150). The promoter is regulated by NF-κB (155) and is not tissue specific. Instead, an intronic silencer determines B-cell specificity. Some of the receptors are shed, but expression ceases as soon as B-cells differentiate into plasma cells (156).

CR2 evolved during several duplication events from a single SCR to a 16-SCR molecule in a variety of heavily N-glycosylated species (104), which also gave rise to a four-module structure called homology groups I – IV (figure 1.7 (146)). Yet there are two forms of CR2, one similar to CR1, organised into the four homologous domains with 16 SCRs, the other with only 15 SCRs. This is due to alternative splicing of the exon expressing SCR 12, however cells express both types and both are also functional (157). The extra SCR appears between SCRs 10 and 11 and is found in CR2 on FDCs in particular (158). The receptor has a highly flexible extracellular domain of 1013 or 954 aa respectively, a 24 aa transmembrane domain and a 34 aa intracellular tail (139). Though the cytoplasmic domain is relatively short and signalling potential into the cell remains to be proven, some studies have reported some interaction with intracellular proteins (159-162). Its main function is the involvement in internalisation of bound IC (146). On B-cells, the membrane proximal portion and the transmembrane domain of CR2 associates with CD19 (95 kDa) and CD81 (TAPA-1, 20 kDa), a member of the tetraspanin family and Leu-13 (CD223; 16 kDa (87, 163, 164)). All components are critical for the shaping of the so-called CR2 signalling complex

and are organised into lipid rafts via their extracellular domains (18, 150, 165-168). CD19 has a 234 aa cytoplasmic domain and is regarded as the most important signalling member of the complex due to its association with many intracellular kinases and that it has been found to be vital for T-dependent (TD) responses (168, 169). By binding C3d-opsonised Ags the CR2 complex and the BCR are brought close together, which leads to high-level localised activation of intracellular kinases (figure 1.8). Thus the threshold for B cell activation is lowered at least hundredfold.

The mouse receptor was seen as a model to examine human CR2, although murine CR2 expression is limited to FDCs and B-cells (170). Marchbank and colleagues (171, 172) designed a transgenic mouse model by replacing mouse CR2 with human CR2. The immune response was restored to near normal levels, confirming the functional and structural similarities of the receptors of the two species. Moreover, and in line with previous findings by Sato *et al.*, human CR2 associated with CD19 on a mouse B-cell line thus proving the close evolutionary relationship between the two species (173).

The function of CR2 in the immune response was mostly determined by manipulating CR2 binding with monoclonal antibodies, soluble CR2 or by using $CR2^{-/-}$ mice (also see section 1.4). However, it should be noted that mouse CR2 expression – as mentioned above – is regulated very differently. Molina (174) and colleagues showed in 1990 that murine CR1 and CR2 are encoded on a single gene dubbed *Cr2* and are splice variants of each other (figure 1.7, also see (129, 175)). The close similarity between mouse and human proteins was demonstrated

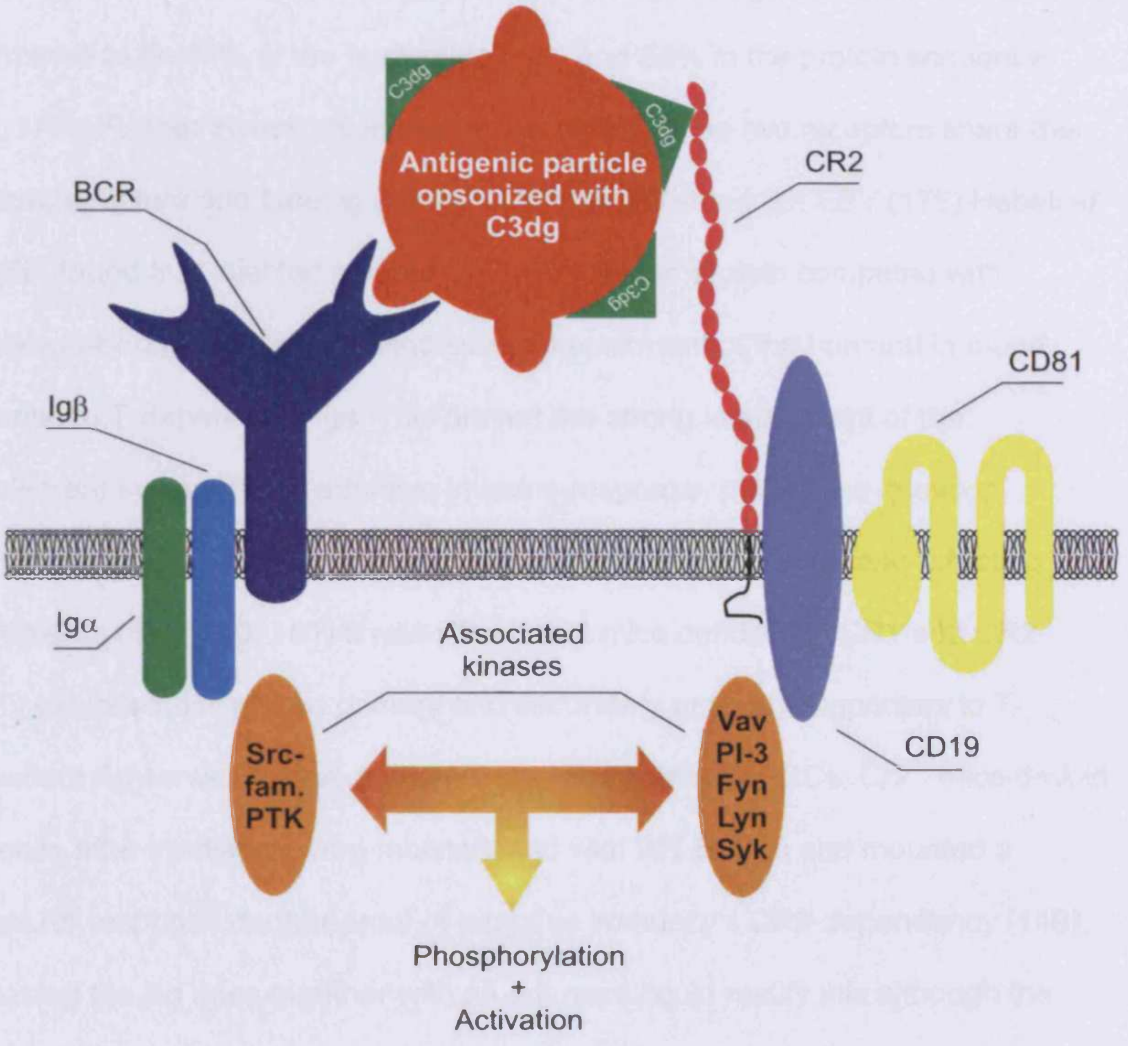

Figure 1.7. Receptor Cross-linking. Both receptor complexes are brought close together by binding the same protein via different determinants. The close proximity co-localises internal kinases into a single lipid raft complex, resulting in increased signalling potential. This cross-linking of receptors by opsonised antigen dramatically reduces the threshold of activation of B-cells. Adapted from 62, 50

by detecting the murine receptor with rabbit antiserum raised against the human counterpart (176, 177). Indeed, comparison of the two receptors' C-terminal sequences revealed 79% homology. Total homology of the two receptors was determined to be 67% at the nucleotide level and 58% in the protein sequence (174, 175). Further investigations have revealed that the two receptors share their function, structure and binding site for iC3b/C3dg/C3d but not EBV (178) Hebell *et al.* (179) found that injected soluble CR2 IgG1 fusion protein competed with membrane-bound CR2 and caused severe impairment of the humoral immune response to T-dependent Ags. This proved the strong involvement of the complement system in the adaptive immune response, but left the question whether B-cells or FDCs were responsible for that effect. Using gene targeting experiments (149, 180, 181) it was shown that mice deficient in CR1 and CR2 ($Cr2^{-/-}$) exhibited diminished primary and secondary antibody responses to T-dependent Ag as well as a reduction in size and number of GCs. $Cr2^{-/-}$ mice devoid of B-cells after irradiation were reconstituted with WT B-cells and mounted a normal Ab response, further proof of adaptive immunity's CR2-dependency (149). Increasing the Ag dose together with an adjuvant could rectify this although the response in the serum was short-lived. In addition, the immune system failed to produce long-lasting plasma cells (182). In an elegant approach, Croix *et al.* were able to complement RAG-2 mice blastocysts with $Cr2^{-/-}$ embryonic stem cells, which allowed them to analyse mice that were exclusively deficient in B-cell CR2 but possessed $CR2^{+}$ FDCs. Immune responses to T-dependent Ag were severely impaired with reduced GC numbers of normal size, and CD19 expression was limited to the periphery, indicating the absence of the germinal centre reaction (183). Chen *et al.* (182) reported similar kinetics of lower Ab titre and faster decline

post immunisation in the same model. Importantly, the experiments focussed on the affinity of the antibody, which was found to be stronger in the deficient animals. Roberts and Snow suggested involvement of CR2 in protection of Ag-activated B-cells from apoptosis by FDC bearing CR2 and C3d-coated Ag ((184), also see (185)). In addition to rescue from cell death, this facilitated somatic hypermutation in the germinal centre (18). This showed that B-cells reacting to C3d-coupled Ag have a selective advantage in the GC and a better chance of entering the memory pool ((40, 150, 186) also see (37) and section 1.3). In summary, these experiments highlighted the importance of CR2 in the immune response. CR2/C3d enhance presentation of antigen to T-cells and their mutual subsequent activation. In contrast, FDC provide a long-lasting Ag depot within the secondary lymphoid tissue, which is heavily involved in affinity maturation. Antigen is thus trapped directly at the site of memory development. A vaccine should therefore aim to target this key site by facilitating opsonisation with C3.

1.8 Interaction Between CR2 and C3d

C3d is the smallest breakdown product that remains attached to the Ag and at the same time the main binding partner of CR2. Native C3 remains inert with active residues and binding sites obscured (69, 187). Residues 1200 – 1274 of iC3b and C3dg/C3d interact with SCRs 1 and 2 of CR2 in a 1:1 fashion (146, 188, 189) via salt-sensitive hydrogen bonds, hydrophobic and van-der-Waals interactions (99, 104). While only SCR2 makes contact with C3d, complementarity is ensured through the V-shaped interaction surface of SCR1 and 2. Six amino acids constitute the CR2-binding sequence in human C3d: Leucine^{1227}-Tyrosine-Asparagine-Valine-Glutamate-Alanine^{1236} (LYNVEA, (151, 189), also see (118)

and (75)). The sequence is similar in mice between residues 1218 and 1236 with three residues replaced at 1222 (human/mouse: D/E), 1224 (G/D) and 1225 (K/Q) (106).

1.9 Cross-Linking the BCR – CR2 Signalling Complexes Strongly Activate B-cells

One of the most striking functions was discovered notably in prolific studies by Pepys and colleagues in the 1970s (115, 190-196). In pioneering work cobra venom factor, a C3 convertase homologue, was injected transiently depleting mice of C3. Subsequent injection of sheep red blood cells showed severe impairment of the humoral response (193). Studies conducted in humans (197), guinea pigs (198), dogs (199) and mice (148, 200) deficient of C3 also showed impaired or defective humoral responses to T-dependent Ag within the immune response.

The C3d-CR2-complex interaction has since been of major interest in complement research, as these experiments had determined the link between innate and adaptive immunity. To date, the interaction site has been mapped using mutagenesis (118, 201), peptides (189), competing antibodies (100, 128, 202, 203), chimeric molecules (128, 178, 179), crystallisation/sequence analysis (99, 102) and SPR (188, 204) all indicating that the C3d binding site lies in SCRs 1 and 2, however whether C3d binds to one or multiple sites is still subject of debate. In conjunction with the studies by Pepys *et al.,* this confirmed that the pivotal step in the immune response is opsonisation of the antigen with CP, LP or AP-derived C3d. The potential of B-cells to act as APC (205) was reinforced by findings from Nemerow and colleagues ((202), also see (206)), who demonstrated that infection

with EBV via CR2 led to subsequent internalisation. This implied that C3d-IC also would be transported into the cell for subsequent breakdown and presentation on the surface revealing a clear role for CR2 in B cell APC function. Experiments with C3dg-coated gold confirmed uptake into Raji cells (23). Full activation of B-cells requires engagement of both CR2 and IgM, otherwise polymeric C3dg was merely able to prime B-cells (207) or facilitate IC uptake (23). These priming functions may have important implications with respect to the B-cell's role as a potent APC and highlight the functional difference between Ag-specific and non-specific B-cells. Non-specific B-cells only interact with the antigen via their complement receptor while specific B-cells utilise both specific BCR as well as CR2. This added CR2-C3d binding event allows cooperative uptake and interaction enhancing subsequent cellular reactions and processes (133). Ag-specific B-cells are therefore active at concentrations 10^3-10^4 times lower than non-specific B-cells, which equal conventional APC in their macropinocytic uptake (14, 208). Conflicting evidence suggests that the CR2 complex is not able to internalise IC independently, but enhance it, thus preventing polyclonal B cell activation (18, 209-211).

Recruitment of T-cells by specific B-cells leads to exchange of reciprocal activation signals, stimulating antibody production by the B-cell. Antigen taken up following CR2/BCR cross-linking is presented with preference by selective trafficking to MHC II vesicles (209). In addition, the interaction between B and T-cells is aided by CR2-induced upregulation of co-stimulatory molecules (CD80/CD86, (18, 212)). C3d IC enhance presentation and thus lower the threshold for T-cell cytokine excretion and synergy between the IL-4 receptor and the BCR/CR2 complex (18,

48, 56, 185, 213). In summary, C3d enhances the T-dependent response by enhancing presentation of antigen via MHC II at much lowered concentrations, causing resting B-cells to enter the G1 phase early (213, 214). C3 also mediates the T-cell independent response (18). Especially B-cells from the splenic marginal zone have been attributed with enhanced activation and proliferation when C3d-opsonised antigen was present. MZ B-cells possess higher levels of CR2, Ag-specific uptake mediated by BCR engagement is therefore augmented by the C3d-CR2 interaction (61, 215).

As well as improving presentation, it was found that antigen in conjunction with C3d could lower the activation threshold by several orders of magnitude. Carter *et al.* discovered that co-ligation of BCR and CR2 at sub-optimal and saturating antibody concentrations, respectively, caused signalling in B-cell enriched tonsillar cells (216). Anti-BCR alone caused activation, whereas exclusive targeting of CR2 did not activate, but primed the B-cell for activation (165, 207, 217). B-cell activation by C3d-Ag IC seems to be particularly advantageous at low antigen concentration ((20) also see (22)). Ca^{2+} release within the B-cell due to this receptor ligation has also been used to study the BCR/CR2 relationship (216, 218-221). The main finding was that both receptors had to be in close proximity to facilitate Ca^{2+} release through CD19 (219), regardless of the method. Carter and Cherukuri *et al.* have conducted extensive research on BCR-CR2 proximity and cross-linking (213, 216). Both groups recorded synergistic effects when BCR and CR2 were ligated with specific antibodies or avidin. Cross-linking leads to recruitment of BCR and CR2 to lipid rafts, where CR2 stabilises the BCR, thus prolonging presentation in addition to enhancing signalling (figure 1.8 (167)).

Lowering the activation threshold (20), enhancement of uptake, presentation and signalling clearly shows that CR2-specific C3 breakdown products, i.e. iC3b, C3dg and C3d, are involved in every step towards generation of an adaptive immune response. The discovery of these immune-enhancing effects of C3d during the course of the immune response had led to some initial vaccination trials of antigen cross-linked with C3 (185, 205, 222). Similar to the history of vaccination, this process was refined and eventually resulted in an elegant study published in 1996 by Dempsey and colleagues (218). A recombinant protein was produced consisting of the model antigen hen egg lysozyme (HEL) and one, two and three copies of murine C3d ($mC3d^S$). As well as confirming complement's crucial role in the shaping of the adaptive immune response, it also highlighted with equal importance three vital and novel properties of such a vaccine. Firstly, more than one copy of mC3d was required as a single molecule fused to HEL acted inhibitory (158, 217, 223, 224). Secondly, HEL-$mC3d^S_2$ and HEL-$mC3d^S_3$ did not require an additional adjuvant formulation. Thirdly and most importantly, the linear C3d dimer and trimer were able to enhance the response up to 10,000 fold. The immune response and B-cell activation were triggered at far lower concentrations than a conventional antigen + adjuvant formulation consisting of HEL and complete Freund's adjuvant (CFA). Most important for this study, the use of C3d as a molecular adjuvant in a linear trimer arrangement offered a novel vaccine design seemingly applicable to almost any antigen.

1.10 A New Generation of Vaccines and Adjuvants – Following Nature's Lead

Why are new approaches to vaccine design required? The first vaccines developed mid-20th century were reasonably successful despite major technical difficulties (lack of animal models, culture systems, purification techniques) and insufficient knowledge of the workings of the immune system. Therefore early tests of prototypes and means and methods of their administration had to be carried out in human subjects with written consent (225).

Vaccinations still carry inherent risks due to possible contaminants such as bacterial toxins (3) or potential but rare anaphylactic reactions in sensitive recipients, yet their benefits far outweigh the risks. New vaccines must, however, anticipate and preclude any detrimental effects during the design phase as required by modern standards. For obvious reasons the pathogen in its natural state cannot be used for immunisation, therefore either a related, non-pathogenic version, attenuated or a sub-unit of the pathogen is injected (7, 225). Attenuation of live organisms or vigorous inactivation of the pathogen by means of heat, enzymatic breakdown and/or chemical treatment, are methods of providing antigen in a normal conformation, but without the risk of inducing associated disease (6). Obviously, inoculation with killed or replication deficient pathogens leads to decreased immunogenicity through loss of antigen propagation and results in a truncated immune response. In fact, for some killed vaccines (e.g. cholera, meningitis (3)) efficacy could not be proven.

Though safer, sub-unit vaccines – as any other vaccine – also require optimisation of the formulation (i.e. adjuvants, discussed below), site and route of administration and dose. The correct subunit targets are often elusive, due to surface factors on the pathogen that evade the immune system or imitate immune proteins. Regular booster immunisations to refresh the immunological memory are required as protection can wane over a period of several years after which the host becomes susceptible again. Problems arise however, if it proves difficult to produce sufficient material, especially if the pathogen cannot be cultured (e.g. hepatitis B virus (HBV) or parasites (7)). Some variants of parasites and viruses vary in their genetic makeup or are subject to constant change, shift and drift due to rearrangements or mutations (e.g. human immune deficiency virus (HIV), influenza). Keeping track of these changes is simply neither technically nor economically possible (7). Alternatively, the subunits can be purified from expression of recombinant DNA, compensating for poor culture capabilities, inherent variation in sequence integrity. This also circumvents the need for the removal of toxins and allows sequence modification, if required. Live-vector based recombinant protein vaccine has combined the two successful approaches enhanced by use of peptide epitope-based vaccines, utilising minimal structure to elicit a reaction. The most recent development, DNA vaccines, is subject of this study.

Currently, most commonly used vaccines are administered by injection with exception of the polio vaccine. The disadvantages are obvious. Sterile syringes and needles are essential, equipment that is difficult to obtain in developing countries (7). Pain and discomfort are minimal, yet improper administration carries

the serious risk of infection despite sterile equipment, which calls for new and safer routes of administration. The poliovirus for example multiplies in the intestinal epithelium, it is therefore sensible to administer the live vaccine orally (7). As many other pathogens enter the body via mucosal surfaces, these routes are investigated for a number of vaccines (226-229).

1.10.1 DNA Vaccination

Nucleic acid or DNA vaccines have emerged within the last 15 years and have the potential to solve the problems encountered with traditional vaccines. By administering the antigen production blueprint directly into the organism, protein purification, pathogen attenuation and the risk of allergic reactions are circumvented (230). Genetic vaccines have been developed for three main uses: pre-empt infection, fight tumours and fight allergies. Some have even found use in monoclonal antibody production (231). DNA vaccines have not been licensed for human use but they are researched heavily promising easy production, storage and efficacy. DNA vaccinations aim to (1) broaden the target strain range, (2) provide a correctly folded and processed target, (3) ensure a constant supply by constitutive expression, (4) induce high quality humoral and cellular responses and (5) utilise multivalent vaccines aimed at protection against different pathogens (231, 232).

DNA vaccines were first conceived in 1950 with the injection of whole chromosomes into rat livers to monitor tumour formation (233). Around 40 years later Will *et al.* and Dubensky *et al.* injected naked DNA into chimpanzees and mouse livers and spleens *in vivo* respectively (234, 235). The chimpanzees

developed typical hepatitis from the cloned HBV DNA, while mice expressed the reporter genes in the treated organs. Wolff and colleagues achieved similar results with injections into mouse muscle, detecting the protein in circulation months later (236). Two years later human growth factor, human α-1 anti-trypsin and influenza virus DNA were administered via a biolistic approach and successfully triggered an immune response (237, 238). Conflicting results have disputed some of these findings, identifying genetic immunisations as transient (239, 240) especially for biolistic transfer, which was subject to skin sloughing and loss of gold particles (240).

Genetic vaccination has since been developed further and optimised, based on crucial design requirements. Two main functions have to be fulfilled: Maintenance and propagation in bacterial culture and protein expression inside mammalian cells. High copy numbers in bacteria can be obtained with an origin of replication such as ColE1 (231, 241, 242). Antibiotic resistance markers allow selection of positive clones harbouring the plasmid. Mammalian promoters (e.g. from cytomegalovirus, CMV or elongation factor 1 α, EF1α), transcription enhancers and terminators (poly-A) facilitate expression of the antigen of interest.

Safety issues are an integral element of any vaccine design (243-246). In general, vaccine vectors do not share high homology with mammalian DNA and lack a mammalian origin of replication or any recombination sequences (243). This minimises the already low likelihood of insertion into chromosomal DNA and thus tumour formation or other disruption of cellular processes (230, 231). Other detrimental effects are autoimmune disease, antigen presenting cells becoming

targets of the immune system and tolerance due to sub-optimal protein concentration in circulation to trigger a response (242). These effects have been questioned (247) and contrary to concerns, autoantibodies to DNA do not develop as readily as presumed. In one study, production of anti-DNA immunoglobulins could only be induced when the double stranded DNA was denatured and injected together with methylated bovine serum albumin and complete Freund's adjuvant (see below, (248)).

Intramuscular (i.m.) injection (236, 238, 249-251) and biolistic transfer/intradermal (i.d.) delivery of DNA vaccines by gene gun into skin (249, 252-257) and mucosal surfaces and organs (227, 229, 258-260) have been the most commonly applied routes of administration. A large variety of other techniques have been discussed and reviewed (238, 241, 261), including electroporation, topical application and micro- and nanoparticles for oral delivery (230, 262).

Generally, DNA vaccines appear to mimic viral infection without being restricted to a cellular response (263). Intramuscular injection seems to have three outcomes (compare figure 1.3). (1) Antigen presenting cells (APC) are transfected directly (MHC I/$CD8^+$ or II/$CD4^+$ T-cell interaction), (2) somatic cells also seem to take up the DNA and mobilise protein fragments to the surface (MHC I) or (3) antigen is produced by somatic cells, presented on MHC I, excreted and presented by APC (MHC II), known as cross-priming (230, 231, 241, 247, 262). Other evidence suggests that APC infiltrate the muscle to take up and process the DNA, as muscle cells are not involved in expression and presentation (263, 264). Dermal immunisation mainly leads to transfer of DNA into LC, which are professional APC.

Therefore the response elicited is different with respect to each immunogen, as well as each route of administration, and each vaccine has to be adjusted according to the pathogen's biology and normal course of infection, if known (265). Intramuscular injections exhibit bias towards Th1 responses, while gene gun immunisations appear to favour initiation of a Th2 response (231). Planning the timing and schedule of the immunisation regimen is crucial. Antibody titres are dependent on the dose of DNA, number of boosts and addition of adjuvants to the formulation (266). The response to the injection can vary greatly between neonatal and aged recipients (267).

Since the development of the first vaccines a major obstacle for mass immunisation has been vaccine formulation availability and storage. Most can only be produced in limited amounts, require cold storage and are affected by limited shelf life. DNA vaccines, in contrast, do not require cooling and can be stored for a long time. The immune response to DNA vaccination in mice points to a requirement of less vaccine to achieve similar results to that of protein injections. Moreover, large amounts of DNA can be manufactured quickly at low cost with relative ease (268). DNA vaccines have a good safety record compared to traditional vaccines so far. The first ever DNA vaccine trial conducted in the USA showed no adverse effects to intramuscular injection of a human immune deficiency virus (HIV) vaccine (269). Several other potential vaccine candidates have also undergone clinical trials. Notoriously evasive pathogens such as influenza, hepatitis B, tuberculosis, malaria and of course HIV have been examined with varying success (270, 271). Use of DNA vaccines in combating

allergies and cancer are also being researched, primarily as a way of changing the bias of an immune response (272) and breaking tolerance respectively (263).

Traditional vaccine formulations have had to rely on addition of adjuvants to trigger an efficient immune response. In most studies mentioned above, DNA was either injected in an aqueous/saline solution or shot into the skin with a gene gun. DNA derived from bacterial vectors possesses an intrinsic adjuvant, known as the CpG motif. Krieg *et al.* first identified this feature and have continued to research and review these motifs intensively (273-276). In 2000, the intracellular receptor Toll-like receptor 9 (TLR9), which binds to bacterial DNA, and stimulates the immune system, was identified (discussed below (277)).

1.11 Adjuvants

1.11.1 Aims and Definition

By definition adjuvants are substances used in combination with a specific antigen that prolong, accelerate and/or enhance the quality of the specific immune response to that antigen compared to the antigen alone (278, 279). Some substances can direct the immune response in a specific direction, i.e. cytotoxic responses, Th1 or Th2 by promoting association of the Ag with MHC I ($CD8^+$ T-cells, cellular response) or MHC II ($CD4^+$ T-cells, humoral response). They also facilitate mucosal delivery and improve the efficacy of the vaccine in patients with weakened immune responses (newborns, aged, immunocompromised).

1.11.2 History

Attenuated or killed sub-unit (SU) vaccines often lose some of the stimulating activity of the infectious agent. A way to restore the activity of vaccines guaranteeing their safety at the same time was found in 1916, when Ag was administered in mineral oil solutions (280). The term adjuvant (lat. *adjuvare* = help) was coined a decade later by Jules Freund who discovered that *Mycobacterium tuberculosis* infected guinea pigs had higher antibody titres than their healthy counterparts (280). Further refinement of a water-in-oil emulsion with metabolisable oils such as squalene (281) led to the development of Freund's complete and incomplete (lacking the bacterial components) adjuvant (CFA and IFA), the most frequently used research adjuvant.

1.11.3 Safety Requirements

Adjuvant safety requirements for human use are strict. Additives must be non-toxic, non-mutagenic, non-carcinogenic, non-teratogenic, non-pyrogenic and non-autoimmunogenic (280). Toxicity is acceptable if levels are negligible at a dose range for effective adjuvanticity. CFA did not fulfil the safety requirements and due to patient discomfort and intense inflammation at the site of injection never passed clinical trials (3). IFA, which lacks the bacterial component, has undergone human testing in vaccine formulations where others failed (e.g. saponin, alum). Aluminium salt (alum) was first added to human vaccine formulations to raise their immunogenicity in 1926 and was for a long time the only approved adjuvant (278, 282). More have been declared safe and have been licensed, e.g. M59 and IFA ((278, 279, 281, 283, 284) also see (285)).

1.11.4 Adjuvant Types and Properties

Grouping adjuvants into distinct classes is problematic as many characteristics and effects overlap. Three types have been suggested: adjuvants *per se*, carriers and vehicles (284). A comprehensive classification, which includes formulations (e.g. CFA), according to five functions was devised by Cox and Coulter (286) (also see (283) and (6)): (1) Modulation of the immune bias (i.e. Th1/Th2), (2) enhanced presentation (maintaining epitope conformation), (3) CTL-response induction, (4) targeting of stabilised antigen to specific immune cells, and (5) depot generation. Economical as well as practical factors such as biodegradability, stability, ease of manufacture, cost and compatibility with a wide range of vaccines also play a major role and have to be taken into account at an early stage in development of adjuvants (279). Adjuvants have to be chosen carefully based on pathogen tropism, life-cycle and disease pathogenesis if known (6). If unknown, adjuvants can be characterised by empirical addition to formulations according to the kind of immune response they generate.

1.11.5 New Generation of Adjuvants – Hypomethylated DNA Sequences and Immune Proteins

Bacterial genetic material contains hypomethylated deoxycytidylate-phosphate-deoxyguanylate (CpG)-DNA sequences (287), in which the cytosine is hypomethylated (288). One in sixteen bases in prokaryotic DNA is non-methylated while this ratio is approximately 1:64 in eukaryotes, thus conferring added antigenicity upon bacterial DNA (274). TLR9, an intracellular pattern recognition receptor of the innate immune system, has been identified as the CpG receptor

thought to provide a danger-signal upon invasion of bacterial pathogens into the cell (277, 289). CpG DNA in the cytoplasm of dendritic cells, B-cells (274, 276) and macrophages (274, 290) causes increased levels of reactive oxygen species. MyD88, a TLR-specific receptor adaptor induces activation of NF-κB and activation of the mitogen-induced protein kinase (MAPK, (291, 292)). In macrophages, this leads to expression of inducible nitric oxide synthase (with IFN-γ). Within the last decade, CpG-oligonucleotides have therefore been devised as a vaccine adjuvant. The first trial using CpG oligodeoxynucleotides (ODN) against a *Leishmania major* infection determined that CpG was able to switch from a normally lethal Th2 response to a protective Th1 response (293). Co-injection of synthetic CpG ODN with the vaccine has led to efficient enhancement of the immune response in several studies (275, 294). Indeed, CpG-rich DNA has been suggested to induce stronger Th1 responses than the gold standard adjuvant, CFA (274, 275, 295). As a safer vaccine adjuvant, clinical trials with human subjects have been carried out in addition to investigations into potential therapeutic use (274, 288). DNA vaccines utilise CpG sequences as an in-built tool to boost the response.

Other adjuvants are based on, or derived from, the immune system itself. Examples include members of the cytokine network, e.g. interferon (IFN) γ (7), IL-1, IL-2, IL-12, GM-CSF (279). The disadvantage of these adjuvants is that they are limited by toxic concentrations exerting detrimental effects on the recipient organism. Within the last ten years C3d of the complement system has been established as a potent and potential molecular adjuvant. As a naturally present protein C3d avoids the typical problems with adjuvant formulations and pre-empts

several steps of the innate immune response. As already discussed above, results with C3d-conjugated protein (218, 296-298) and DNA vaccines (252-256, 299) encoding C3d and a variety of antigens have been very encouraging.

1.12 Vaccine Development Using C3d as a Molecular Adjuvant

The revolutionary approach by Dempsey *et al.* using HEL-mC3d$^{S}_{3}$ generated considerable interest in the field and led to a number of follow-up studies targeting influenza and pneumococcus. Most groups made use of the original linear C3d trimer because of its high reactivity *in vivo* (218, 296, 297). Some adhered to the original schedule while others introduced different means of administration of proteinaceous vaccines such as intranasal administration (296).

With the emergence of DNA vaccines, C3d trimer constructs were soon inserted into vaccine vectors. Injection of the vaccine in DNA format allowed prompt testing without the need to produce sufficient amounts for protein injections. Vaccines against influenza (252, 256, 296), human immune deficiency virus (HIV (253, 255)), measles (254), bovine viral diarrhoea virus (300), bovine rotavirus and herpesvirus (299) and polysaccharide serotype 14 of *Streptococcus pneumoniae* (PPS14 (297)) were developed using mostly the linear trimer configuration. All DNA vaccines were administered in a prime-boost schedule (DNA/DNA (252, 253, 256, 296); DNA/protein (253)) although methods varied between intramuscular (252), transdermal (252-255), intranasal (296), intradermal and intravenous (299) adminstration. C3d DNA vaccine administration led to higher affinity antibody, increased titre, activation of specific T-cell population and – in some – heterosubtypic immunity, i.e. cross-strain protection (252, 253, 255, 256, 296,

297). Others on the contrary (255, 256) reported insufficient amounts of neutralising antibody and a rather slow response, which only developed over a number of weeks and required repeated boosting. One report described inhibitory effects of C3d (299), which was probably due to only one and two copies of the molecular adjuvant present in the construct.

Above results implied considerable potential of the C3d-adjuvanted vaccine design and applicability to almost any antigen. Although these results were impressive, the arrangement is artificial and unlikely to occur in nature. If more copies of the antigen are combined with more CR2 binding sites, i.e. C3d, the amplification potential can be increased significantly. Some attempts have been made to raise the number of C3d in a single multimeric construct using avidin (165, 301) or antigen opsonised *in vitro* (302, 303). So far however they have not been developed further as vaccines due to their strong immunogenicity. Therefore, oligomerisation methods have to be selected carefully to cater for copy numbers or the specific *in vitro* or *in vivo* application. Chatellier *et al.* (304) demonstrated improved activity when two naturally occurring bacterial chaperones, monomeric GroEL and heptameric Gp31 (Cpn10 family), were combined. Heptameric GroEL (MC_7) was able to refold denatured proteins by itself where monomeric GroEL requires co-factors thus highlighting the advantages of avidity effects. The present study specifically required mammalian oligomers. A protein from the complement system itself provided the blueprint for a more natural polymer design. C4b binding protein (C4BP), first described by Nussenzweig *et al.* (305, 306), interferes with the formation of the CP C3-convertase by binding to C4b (307, 308). It has a spider-like appearance (309, 310) with several isoforms in the serum (311-313). Libyh *et*

al. (314, 315) utilised the C-terminal region of the C4BP α chain responsible for octamerisation to design a recombinant multivalent anti-Rhesus(D) and CR1. In 2000, Christiansen *et al.* (316) described the successful generation and *in vivo* application of a recombinant octameric measles virus decoy receptor (CD46/MCP). These studies clearly highlighted the potential use of the C4BP core region for polymerisation of recombinant proteins as the octamer formed inside the cell naturally. The success of the measles decoy receptor *in vivo* prompted us to develop an octamer that could serve a dual role of antigen delivery and cell targeting, i.e. polymerising C3d and the antigen (figure 1.9 A). Thanks to the spider-like shape the octamer presents eight CR2 binding sites as well as eight antigen binding sites to the cell. This potentially cross-links eight of each receptor covering an area on the surface rather than a single dimension as in case of the linear trimer (figure 1.9 B). More receptors in close proximity in the lipid rafts should lower the activation threshold further thanks to the higher number of intracellular kinases able to signal into the cell.

For the present study HEL was chosen as an antigen because it is a well-established model protein of known structure and sequence and easily available (317-322). It is a well-characterised antigen, allowed comparison with the original immunisation studies (218, 323-325) and has been used in autoimmune and tolerance studies (326, 327).

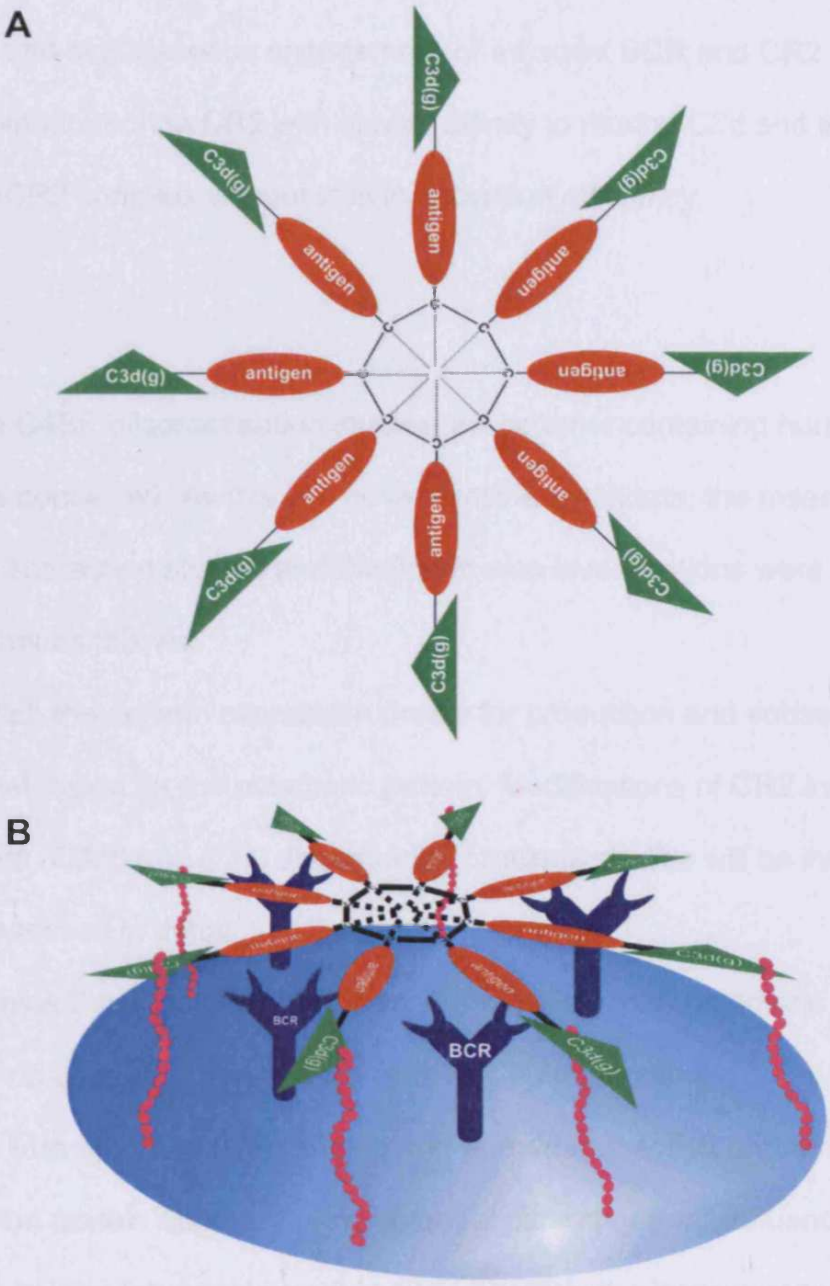

Figure 1.9. The proposed octameric vaccine. The human C3dg/C3d^{S}g/C3d/C3d^{S} – antigen construct forms a protein with eight arms with the help of the C4BP octamerising sequence to form the spider-like protein shown in panel A. The proposed protein could bind to the B-cell surface as shown in panel B and cross-link a larger number of BCR and CR2.

The octameric hC3d-containing vaccine is expected to induce a vastly increased immune response relative to non-adjuvant or monomeric configurations thanks to co-ordinated and simultaneous engagement of adjacent BCR and CR2. Human C3d should bind to murine CR2 with similar affinity to murine C3d and thus cross-link the BCR/CR2 complex without loss in activation efficiency.

1.13 Aims

Based on the C4BP oligomerisation studies, an octamer containing human C3d and HEL was conceived. As this is a novel vaccine candidate, the means of optimisation, interaction studies and the first *in vivo* investigations were devised and set as aims as follows:

- Establish the optimal expression profile for production and subsequent DNA vaccine design for the octameric protein. Modifications of CR2 interaction partners (C3dg and C3d) discussed in previous studies will be incorporated and assessed in detail.
- Determine the best interaction partner for hCR2 in the octameric set-up based on current understanding of CR2-C3d interaction.
- Clarify true affinities of the murine and human interaction partners using an Fc fusion protein approach. Any potential differences will influence the results in later transgenic models and ultimately the human immune system.
- Test functionality of the vaccine *in vivo,* the single most conclusive approach to prove the vaccine is functional.
- Assess traditional protein injections as well as DNA vaccines.
- Correlate a potential humoral response to cellular events in the secondary lymphoid tissue.

Chapter 2

General Materials and Methods

2.1 Reagents

Acros Organics (Geel, Belgium) supplied agar powder, hydrochloric acid (HCl) and N, N' – Methylene bis/acrylamide 37:5.1 40% in water; ECL western blotting detection reagent was obtained from Amersham (Little Chalfont, UK); Autogen Bioclear (Calne, UK) provided G418/geneticin; BOC (Guildford, UK) provided liquid nitrogen (LN_2) and 100% pure Helium; Hyperladder I and IV markers for DNA agarose gel electrophoresis were obtained from Bioline Ltd. (London, UK); Dako UK Ltd. (Cambridge, UK) provided OPD substrate; Fisher (Loughborough, UK) supplied ammonium persulphate (APS), analytical grade ethanol, brilliant blue, bromophenol blue, calcium chloride, citric acid, dimethylsulphoxide (DMSO), di-sodium carbonate (Na_2CO_3), DNA-grade ethanol, ethylenediamine tetraacetic acid (EDTA), ethidium bromide, glycerol, glycine, isopentane, isopropanol, laboratory grade methanol, manganese chloride, potassium acetate, potassium chloride, silver nitrate ($AgNO_3$), sodium acetate, sodium chloride (NaCl), sodium dodecyl sulphate (SDS), sodium hydrogen carbonate ($NaHCO_3$), sodium hydroxide (NaOH), *N,N,N',N'*-tetramethyleethylenediamine (TEMED), tris(hydroxymethyl)methylamine (Tris), tryptone and Tween 20; RPMI-1640, Foetal calf serum (FCS), low bovine Ig foetal calf serum (LBIg), penicillin/streptomycin, sodium pyruvate, L-glutamine, trypsin EDTA were obtained from Gibco (by Invitrogen, Paisley, UK); Agarose electrophoresis grade, Hygromycin B (50 mg/ml in PBS), SeeBluePlus2 protein gel marker, Zeocin were obtained from Invitrogen (Paisley, UK); Oxoid (Basingstoke, UK) supplied Yeast extract and PBS tablets; PolyPlus Transfection SA (Illkirch, France) provided JetPEI; Sigma Aldrich Company Ltd. (Poole, UK) supplied ampicillin, glacial acetic acid, deoxinucleotides (dNTP), DL-dithiothreitol, formaldehyde 37% solution, glutaraldehyde, hydrogen

peroxide (H_2O_2, 35% solution in water), kanamycin, MOPS sodium salt, Phenylmethanesulfonyl fluoride (PMSF), Orange-G, sulphuric acid (H_2SO_4), triton X-100; Vector Laboratories Inc. (Burlingame, USA) provided Vectashield;

2.2 Buffers

Tris-acetic acid ethylenediamine tetraacetic acid (TAE) consisted of 40 mM Tris, 40 mM glacial acetic acid, 10 mM EDTA, pH 7.2; ELISA plate bi-carbonate coating buffer contained 24 mM $NaHCO_3$, 13.5 mM Na_2CO_3, the pH was adjusted to 9.6. Lysis buffer contained 20 mM Tris-HCl pH 8.0, 1 mM EDTA, 2 mM PMSF, 1% v/v triton X-100. Phosphate buffered saline (PBS) was made up with tablets in dH_2O (1 in 100 ml) yielding 160 mM NaCl, 3 mM KCl, 8 mM Na_2HPO_4, 1 mM K_2HPO_4. Agarose gel electrophoresis sample buffer consisted of 50% v/v glycerol, 50% v/v TAE buffer and 0.01% w/v Orange-G. SDS-PAGE stacking gel buffer was 0.5 M Tris pH 6.8, 0.4% w/v SDS in water, separating gel buffer was 1.5 M Tris, 0.4% w/v SDS in water, pH 8.8, 2x non-reducing sample buffer contained 0.008% v/v bromophenol blue, 0.125 M Tris pH 6.8, 4% v/v SDS, 20% v/v glycerol, 2x reducing sample buffer consisted of non-reducing sample buffer and 5% v/v β-2 mercaptoethanol, running buffer was made up as a 5x concentrated stock solution: 0.1% SDS, 1.25 M Tris, 1.9 M glycine. Transfer buffer contained 10 mM $NaHCO_3$, 3mM Na_2CO_3, 20% methanol in dH_2O. Western wash buffer consisted of PBS 0.05% Tween 20. Blocking buffer contained wash buffer with 2% fat free milk. ELISA buffers were the same except 1% v/v low bovine Ig FCS was used instead of milk. Flow buffer consisted of PBS, 1% low bovine Ig FCS, 15mM EDTA, 0.02% sodium azide.

2.3 Enzymes

Amersham (Little Chalfont, UK) provided restriction enzymes including buffers and additives: Bam H1, Bgl II, Eco R I, Eco R V, Hind III, Nhe I, Not I, Spe I, Xba I, Xho I; BIOTaq including buffers was obtained from Bioline Ltd. (London, UK); New England Biolabs (Ipswich, MA, USA) supplied Bts I. Pfu DNA Polymerase (3 U/µl) and T4 DNA ligase (3 U/µl) with the respective buffers were supplied by Promega; Shrimp alkaline phosphatase (SAP) was from USB (Staufen, Germany)

2.4 Antibodies from Commercial Sources

2.4.1 Monoclonal Antibodies

BD Biosciences Pharmingen (San Diego, CA, USA) provided monoclonal antibodies rat (Rt) anti (α) mouse (Ms) CD16/CD32 (FcγIII/II receptor, clone 2.4G2, "Fc block"), Rt α Ms T/B-cell activation antigen ("GL-7", Ly7.7) FITC, Rt α Ms CD19 (clone 1D3) phycoerythrin (PE), biotinylated (b) Rt α Ms CD138, Rt α Ms CD45R/B220 (clone RA3-6B2) FITC, Rt α Ms IgM PercP-Cy5.5 (clone R6-60.2), Rt α Ms CD25 PE (IL-2R α-chain), Rt α Ms CD8a (Ly-2, clone 53-6.7) PercP-Cy5.5, Rt α Ms bT-cell receptor α-β chain (clone H57-597), Ms α human (Hu) CR2/CD21 PE, Ms α Hu CR1/CD35 PE and Ms α Hu CD19 FITC. Caltag α mouse CD4 FITC (clone L3T4) was provided by Invitrogen (Paisley, UK). Quidel (Santa Clara, CA, USA) provided an unconjugated monoclonal Ms α Hu C3d. Southern Biotech (Birmingham, AL, USA) supplied Rt α Ms CD38 RPE (clone NIMR-5) and Rt α Ms bIgD (clone 11-26).

2.4.2 Polyclonal Antibodies and Reagents

DAKO Cytomation UK Ltd. (Ely, UK) supplied unconjugated polyclonal rabbit (Rb) α Hu C3d; Biotinylated antibodies were detected with streptavidin allophycocyanin (SA-APC, BD Pharmingen); Jackson ImmunoResearch Laboratories Inc. (West Grove, PA, USA) supplied affinitypure + minimum cross-reactivity $F(ab)_2$ fragment donkey (Dk) α Hu Fc heavy and light (H+L) chain specific conjugated to recombinant PE (Dk α hFc RPE) and affinitypure goat (Gt) α Ms Fc H+L horse radish peroxidase (Gt α mFc HRPO), streptavidin-phycoerythrin (SA-PE); Novus Biologicals Inc. (Littleton, CO, USA) supplied Rb anti Ms IgM HRPO; Sigma-Aldrich Company Ltd. (Poole, UK) supplied affinity adsorbed Gt anti Hu unconjugated and HRPO-conjugated; The Binding Site Ltd. (Birmingham, UK) supplied a sheep (Sh) anti Hu C3d antibody and two polyclonal secondary HRPO-conjugated antibodies specific for Rb and Sh/Gt, respectively.

2.5 Bacterial Culture Organisms

Aseptic technique was applied in any work involving bacteria or mammalian cells. Work surfaces and equipment were sterilised with 70% v/v ethanol. Chemically competent One Shot DH5α cells were provided by Invitrogen (Paisley, UK). Vector DNA transformations and culture were carried out according to manufacturer's instructions. XL10-Gold cells were supplied with the Strategene (La Jolla, California, USA) Site-directed Mutagenesis (SDM) XL kit and used according to the supplier's instructions. GT115 *Escherichia coli* were supplied by InvivoGen (San Diego, California, USA). Bacteria were supplied lyophilised and prepared for chemical transformation according to the manufacturer's instructions. Electrocompetent bacteria (EasyShock™ 10B Competent Cells, Bio-Rad

Laboratories, Hemel Hampstead, UK) were transformed using a BioRad XCel Plus electroporator following the manufacturer's protocol.

2.6 Media

Pipette tips, containers and media were sterilised in moist heat at 120°C for at least 10 minutes or prepared according to the manufacturer's specifications. Medium was prepared as described below (see Table 2.1).

Nutrient Medium	Ingredients	Organism
LB-Broth (LB agar)	add to dH_2O: 1.0% w/v tryptone 1.0% w/v NaCl 0.5% w/v yeast extract (1.5% w/v agar powder)	DH5α, XL-10 Gold
TB-Broth (TB agar)	add to dH_2O: 1.0% w/v Bacto-tryptone 0.5% w/v NaCl 0.5% w/v yeast extract (1.5% w/v agar powder)	GT115
NZY^+ Broth	add to dH_2O: 1.0% w/v NZ amine 0.5% w/v NaCl 0.5% w/v yeast extract adjust pH to 7.5 with NaOH autoclave, then add filter sterilised 1.25% v/v 1 M $MgCl_2$ 1.25% v/v 1 M $MgSO_4$ 20.00% w/v glucose	XL-10 Gold

Table 2.1. Medium formulations for all bacteria used in this study. Preparations were supplemented with antibiotic according to plasmid requirements.

2.7 Mammalian Cells

Cells were grown in 25, 80 and 175 cm^2 tissue culture flasks, 96, 24, 12, 6-well plates (Nunc, Roskilde, Denmark) and Integra Cell Line Adhere1000 flasks (IBS Integra Biosciences AG, Chur, Switzerland). Flasks were incubated at 37°C in 5% CO_2/95% air. RPMI-1640 was supplemented with 1 mM sodium pyruvate, 2 mM L-glutamine, 50 International Units/ml (IU/ml) penicillin and 50 IU/ml streptomycin as standard. Foetal calf/bovine serum (FCS) was heat-inactivated (56°C for 30 min). FCS was filtered through a 0.45 µm syringe filter (Sartorius, Hannover, Germany) before addition to the medium as required.

2.7.1 Adherent Cells

The Chinese Hamster Ovary (CHO) cell line was originally obtained from European Collection of Cell Cultures (ECACC No. 00102307). CHO cells were grown in RPMI-1640/10% v/v FCS (NUNC flasks) and 5% v/v low bovine Ig FCS (Integra flasks). Cells were split when confluent by washing with sterile saline solution (0.9% w/v or 150 mM NaCl, Fresenius Kabi Ltd., Warrington, UK) followed by treatment with Trypsin EDTA for 5 mins. Cells were then washed off with saline solution and diluted 1:10 into fresh medium before being transferred to new flasks. CHO cells cultured in integra flasks were not trypsinised but received fresh medium once a week and were reseeded once every eight weeks.

2.7.2 Non-Adherent Cells

The human B cell lymphoma cell line Raji, originally isolated and described by Epstein *et al.* (141), was obtained from the ECACC (No. 85011429). Raji cells

were grown in RPMI-1640/15% FCS v/v and 16 μM β-mercaptoethanol. SP2/0 (ECACC No. 85072401) and hybridoma cell lines were grown in RPMI-1640/ 15% v/v FCS. Medium containing the cells was removed from the flask; cells and debris were removed by centrifugation at 350 x *g* for 5 minutes. Fresh medium was added to the culture flask allowing the remaining cells to re-populate the vessel.

2.7.3 Macrophages

Macrophages were isolated from wild type (C57BL/6) mice by injecting the peritoneum of humanely sacrificed animals with 10 ml RPMI-1640/15% v/v FCS. Following a short incubation period, the cell suspension was collected and transferred via syringe into a sterile 30 ml Fisherbrand universal container (UC, Fisher, Loughborough, UK). Cells were washed once in RPMI, resuspended in 15 ml RPMI-1640/15% FCS and divided equally into 24-well plates.

2.8 Cell Culture Methods

2.8.1 Transfection of Vector DNA

DNA was transfected into CHO cells using the JetPEI reagent. Reactions were prepared according to the manufacturer's guidelines and as published by Boussif *et al.* (328) and Lambert *et al.* (329). A nitrogen-to-phosphate (N/P) ratio of 5 was used to calculate DNA/JetPEI ratio.

2.8.2 Clonal Selection of Protein Expressing Cells

Cells were trypsinised, washed with saline solution and counted with a haemocytometer (Neubauer, Marienfeld, Germany). Cells were diluted in selective medium (Hygromycin B or G418/geneticin were added to media at 100 – 400 µg/ml as appropriate) to approximately 30, 10 and 3 cells/ml. The suspensions were transferred into flat-bottomed 96-well plates; single wells contained100 µl each. Single-colony wells were assessed for protein content by dot blot, western blot and ELISA. Clones expressing the protein correctly at high levels were propagated further.

2.8.3 Liquid Nitrogen Storage of Mammalian Cells

Cells were trypsinised, washed twice with saline solution, resuspended in FCS + 10% dimethylsulphoxide (DMSO) and transferred to a screw-top freezer vial. The cells were then frozen at –80°C using a Nalgene Cryo 1° Freezing Container "Mr Frosty" (Nalge Europe Ltd., Hereford, UK). Cells were stored in liquid nitrogen (LN_2). Cells retrieved from LN_2 storage were rapidly thawed and transferred to pre-warmed medium. The cells were washed once in RPMI, re-suspended in the appropriate culture media and transferred into culture containers.

2.8.4 Cell Lysis

Cells were trypsinised, washed twice in saline solution and counted with a haemocytometer. Cell concentration was adjusted to10^7 cells/ml with lysis buffer. Drawing the suspension through a syringe needle disrupted the cell structure. The lysate was then incubated for 30-minutes on ice and transferred to a sterile 1.5 ml

eppendorf. Debris was removed with additional centrifugation at 20,000 x *g* for 10 minutes.

2.9 Flow Cytometry

For flow cytometry or fluorescence-associated cell sorting (FACS) analysis, cells were washed in saline solution, counted with a haemocytometer and diluted in flow buffer. All antibody probes were diluted in flow buffer. The cell concentration was adjusted to $1x10^6$ cells/ml. Murine splenocyte surface Ig-receptors were blocked with 3 µg/ml Rt α Ms CD16/CD32 for 15 minutes on ice. Human Fc receptors were blocked with heat-inactivated goat serum at a concentration of 1:3. Antibody stains were made up at the recommended concentrations and combined with the cells in round-bottom 96-well plates (Nunc, Roskilde, Denmark). Cell stains were incubated for 30 minutes on wet ice, spun at 250 x *g* for 3 minutes at 4°C and washed three times with flow buffer. The above steps were repeated as required with secondary or tertiary fluorescently conjugated antibodies. Finally, cells were resuspended in 200 µl flow buffer containing 1% formaldehyde to fix cells and transferred into round bottom 5 ml tubes (BD Biosciences). Samples were analysed on a BD FACSCalibur (San Diego, CA, USA) within 24 hours of staining.

2.10 Molecular Biology Methods

Work surfaces and equipment were sterilised with 70% analytical grade ethanol. Only autoclaved pipette tips or filter tips (Starlab, Ahrensburg, Germany) were used. All solutions were prepared with de-ionised water and filter sterilised where necessary. DNA concentration was measured using a Gene Quant Pro

(Amersham, Little Chalfont, UK) or UV-1700 double beam spectrophotometer (Shimadzu UK Ltd, Milton Keynes, UK) at 1:20, 1:50 or 1:100 (DNA:dH_2O) dilution.

2.10.1 Plasmid Purification

Bacteria containing the plasmid of interest were streaked out on nutrient agar plates using a sterile loop and incubated at 37°C over night. Single colonies were picked from the plate and propagated in the appropriate liquid cultures in a radial shaker at 37°C and 200 – 220 rpm. Small-scale plasmid purification was carried out with the QIAprep Spin Miniprep kit (Hilden, Germany) according to the manufacturer's instructions. Large-scale plasmid purifications were carried out using the Invitrogen PureLink™ HiPure Plasmid Purification Kit (Maxiprep, Paisley, UK) according to the manufacturer's instructions.

2.10.2 Restriction Digest

DNA digests contained 5 µl enzyme-specific buffer (supplied 10x concentrated), 0.1 µg – 2 µg plasmid DNA, 15 units (U) enzyme and bovine serum albumin (BSA) or triton-X, if required. The volume was adjusted to 50 µl with dH_2O. Reactions were incubated for 2 hours in a 37°C water bath. Double digests were carried out according to the compatibility of the various enzymes and buffers.

2.10.3 DNA Precipitation

DNA was precipitated with 0.1 volumes sterile filtered 3 M sodium acetate and 4 volumes 100% DNA-grade ethanol. The mixture was incubated at –20°C for at

least 30 minutes and centrifuged for 10 minutes at 20,000 x *g*. The pellet was washed and rehydrated during three wash steps with 70% ethanol. Supernatants were discarded, the pellet was air dried and then resuspended in 1/3 of its original volume. DNA from Polymerase Chain reaction (PCR), restriction digests and ligations were extracted with the Qiaquick PCR Cleanup kit (Qiagen, Hilden, Germany) according to the manufacturer's instructions.

2.10.4 Polymerase Chain Reaction

PCR was carried out with a Dynex Dynablock (MJ Research at BioRad, Hemel Hampstead, UK). Reactions were set up as shown in table 2.2

Ingredient	20 µl mix	50 µl mix
10x Taq buffer	2.0 µl	5.0 µl
$MgCl_2$	0.4 µl	1.0 µl
dNTP	0.2 µl	0.5 µl
forward primer	0.2 µl (5 pmol)	0.5 µl (5 pmol)
reverse primer	0.2 µl (5 pmol)	0.5 µl (5 pmol)
BIOTaq	0.1 µl	0.2 µl
dH_2O	16.9 µl	42.0 µl

Table 2.2. Ingredients for 20 µl and 50 µl PCR reactions

Primers were from MWG Biotech AG (Ebersberg, Germany) and reconstituted according to the manufacturer's recommendations. Reaction conditions were as shown in table 2.3:

Step	Temperature	Duration	No of cycles
Dissociation	95°C	5 minutes	1
Dissociation	95°C	1 minute	35
Annealing	55°C	1 minute	
Extension	72°C	BIOTaq: 1 minute/kb Pfu: 1.5 minute/kb	
Extension	72°C	10 minutes	1
Storage	4°C	∞	-

Table 2.3. PCR reactions using Pfu or Taq DNA polymerases

Reactions were processed immediately or stored at –20°C until needed.

2.10.5 Agarose Gel Electrophoresis

Agarose gels were prepared with TAE buffer and 0.8 - 2% w/v electrophoresis grade agarose. The agarose was dissolved by boiling in a microwave, cooled to ~50°C and supplemented with ethidium bromide (final concentration 1 µg/ml) or 0.1% v/v crystal violet (Fisher, Loughborough, UK) solution. Gels were poured into a sealed gel tray, left to set at room temperature (RT) and subsequently submerged in a gel tank filled with TAE buffer. Samples were prepared with 10 – 20% v/v sample buffer and carefully injected into sample wells. 5 µl DNA standards (Hyperladder I or IV) were run on each gel. Gels were run at 120 V for one hour. Ethidium bromide gels were examined using a BioRad ChemiDoc 2000 and the BioRad Quantity One Software Package. Crystal violet gels were used to carry out DNA extraction and were processed on a light table.

2.10.6 Agarose Gel Extraction

DNA was extracted from gels with the QBioGene Geneclean III kit (CMP Biomedicals, Cambridge, UK) according to the manufacturer's instructions and recommendations. However, in the final step pellets were dried to remove residual ethanol, resuspended in 10 – 15 µl dH_2O and incubated for 10 minutes at 55°C mixing occasionally. Glass beads were spun down, supernatant removed and the elution repeated once more with the same volume. The extract was stored at –20°C until needed and quantified by ethidium bromide agarose gel electrophoresis.

2.10.7 Sequencing

Sequencing reactions were run in a Dynex Dynablock using ABI Big Dye 3.1 sequencing mix (Applied Biosystems Applera UK, Warrington, UK). 10 µl reactions were set up with 500 ng DNA, 4 µl Big Dye reagent, 25 pM primer and water. The reaction was run as shown in table 2.4.

Step	Temperature	Time	No. of cycles
Dissociation	95°C	5 minutes	1
Dissociation	95°C	15 seconds	25
Annealing	60°C	10 seconds	
Extension	72°C	3 minutes	

Table 2.4. Sequencing reactions using the BigDye 3.1 system

Following the PCR reaction, 30 µl dH_2O and 60 µl isopropanol were added to the tubes, which were then vortexed briefly and incubated at –20°C for a minimum of 45 minutes. DNA was pelleted by centrifugation at 20,000 x *g* and 4°C for 30

minutes, washed in 80% ethanol and spun again for 10 minutes. The supernatant was discarded and the pellet air-dried. The sequencing reaction was run in an ABI Prism Genetic Analyzer 3100 (Applied Biosystems).

2.10.8 Ligation

Vectors were de-phosphorylated as part of restriction digests using 2 units SAP (sufficient for 1 – 2 µg DNA) in the digest buffer during the final 1 hour in a 37°C water bath. The concentration of vector and insert was determined in an analytical ethidium bromide agarose gel using a molecular weight standard. The quantity of insert required for a 5:1 insert to vector ratio was calculated using the formula:

$$insert[ng] = \frac{vector[ng] \times insert[kb]}{vector[kb]} \times 5$$

Vector and insert were mixed with 10x ligase buffer, 1 mM ATP and 3 – 6 U T4 ligase and dH_2O as required. Ligation reactions were carried out using a Dynex Dynablock Thermal Cycler as shown in table 2.5.

Temperature	Time [min]	Cycles
5°C	2	20
15°C	2	
25°C	2	
16°C	120	1
4°C	∞	-

Table 2.5. Ligation reaction conditions run in a thermocycler (see section PCR)

Ligations were removed from the PCR block and transformed into competent bacteria.

2.10.9 Site-Directed Mutagenesis (SDM).

SDM was carried out with the Stratagene Quikchange XL kit. Thermocycling reaction, digest of parental DNA and transformation were set up according to the manufacturer's instructions.

2.11 Protein Purification Methods

2.11.1 Purification Equipment

Proteins were purified using three automated purification systems, the Äkta Prime, Äkta Purifier and Äkta FPLC (Amersham, Little Chalfont, UK). Additionally, recombinant protein A fast flow (rProteinA FF), Superose 6 and SourceQ columns were also supplied by Amersham. For column specifications please refer to table 2.6. All purifications were run in the cold room at 4°C according to manufacturer's instructions and following set programs. All buffers and samples were filtered and degassed prior to use using a Millipore filter unit (Fisher, Loughborough, UK) and 0.2 µm cellulose acetate (Sartorius, Göttingen, Germany) filters.

Column	Type	Volume	pH range	pressure limit	flow rate
HiTrap rProteinA FF	affinity column	1 ml	2 – 9	0.3 MPa	2.0 ml/min
Source Q	anion exchange	20 ml		1.5 MPa	2.0 ml/min
Superose 6	gel filtration	24 ml	3 – 12	1.5 MPa	0.5 ml/min

Table 2.6. Purification columns

Results were recorded in real time. Fractions collected from the purifications were analysed by dot blot, ELISA, SDS-PAGE and western blotting.

2.11.1.1 Äkta Prime

This machine was used exclusively with the 1 ml rProteinA FF column using pre-programmed methods. Columns were stored in PBS containing 0.02% sodium azide. All lines and pumps were washed with deionised water and primed with their respective buffers. Five lines were prepared, Tris-buffered saline (TBS, running buffer, line A1), 100 mM citrate pH 5 (elution buffer, A2), 500 mM NaOH (wash buffer, A3) and 100 mM glycine pH 2.5 (elution buffer, B). Cell culture supernatant containing the protein of interest was injected via line A8. Prior to loading, samples were centrifuged (10,000 x *g* for 30 minutes) followed by filtration through a 0.2 µm filter (Sartorius, Göttingen, Germany) to remove particulate matter. Purifications were run at 2 ml/min. Each buffer step consisted of 10 column volumes (CV) and TBS was applied between buffer changes. The buffers were applied in the following order: TBS, sample, citrate, glycine and TBS. All elution and wash samples were collected into 5 ml collection tubes (Elkay, Basingstoke, UK) on a fraction collector. Glycine eluate containing the purified protein was collected into tubes containing an appropriate volume of Tris HCl pH 8 to neutralise the pH. The cell culture supernatant was collected post column into a clean container via the waste line. Due to the limited capacity of the column and to reduce the potential that protein would be left over in the medium, the supernatant was re-applied to the column as required, using the same conditions. Positive fractions were pooled and dialysed against PBS.

2.11.1.2 Äkta Purifier and FPLC

The two machines were used interchangeably for the Source Q column but only the Purifier was used with the Superose 6. The buffer lines and columns were stored with 20% ethanol. Prior to sample application, the buffer lines A1 and B1 as well as the columns were subjected to water and buffer washes. Source Q purifications were carried out with 0.1 M Tris pH 9 (A1) as start and 0.1 M Tris 1 M NaCl pH 9 (B1) as elution buffer. Samples were prepared by filtration and adjustment to pH 9 with 5% v/v 1 M Tris pH 12. The samples were loaded onto the column using a 50 ml super loop (Amersham, Little Chalfont, UK). The column was washed with 2 CV 0.1 M Tris pH 9 prior to sample elution with 0.1 M Tris 1 M NaCl pH 9 in a continuous gradient over 20 CV. Fractions of the flow-through and the elution gradient were collected in 5 ml tubes (Elkay). The column and the machine were washed extensively with elution buffer, water and returned to storage in 20% ethanol. The Superose 6 column was prepared and shut down in the same way. Aggregates were removed from samples by spinning at 20,000 x *g* for five minutes followed by loading into a 500 µl loop. The protein was eluted with PBS over 1.5 CV, 0.5 ml fractions were collected into 5 ml tubes (Elkay).

2.11.2 Spin Column

20 ml Vivaspin spin columns (Sartorius, Göttingen, Germany) with 100,000 or 300,000 molecular weight cut off (MWCO) were washed with buffer to remove trace amounts of azide and glycerine. Protein suspensions were forced through the filter in a bench top centrifuge at approximately 2000 x *g*. Concentrations were stopped when approximately 1 ml remained on top of the spin filter. The remaining

supernatant was transferred to a sterile 1.5 ml eppendorf tube with a sterile Pasteur pipette and stored at 4°C.

2.11.3 Dialysis

Dialysis tubing was supplied by Medicell Int. Ltd. (London, UK) and had a 12,000 – 14,000 MWCO. Tubing was prepared by boiling in water and stored in water and 0.02% v/v sodium azide. Prior to use azide was removed by rinsing in water and the appropriate buffer. Dialysis was carried out following Äkta Prime rProteinA FF purification to exchange the glycine elution buffer with PBS. Pooled fractions were transferred with a Pasteur pipette (Fisher) into the tubing, which was subsequently sealed. The tube containing the column eluate was submerged in cold PBS and dialysed overnight at 4°C. The buffer was changed at least once. The protein preparation was removed from the dialysis tubing and stored in 0.5 – 1 ml aliquots at –20°C until needed.

2.11.4 Measurement of Protein Concentration

Protein concentration was measured using the Gene Quant Pro (Amersham) spectrophotometer. The extinction coefficient at 280 nm (A_{280}) was measured against a blank PBS sample.

2.12 Protein Analysis Methods

2.12.1 Sodium Dodecyl Sulphate Polyacrylamide Gel Electrophoresis

2.12.1.1 Gels Prepared from Communal Reagents and Buffers

SDS-PAGE was carried out with freshly prepared gels using the Mighty Small II Gel System (Amersham, Little Chalfont, UK) following the method of Lämmli (330). Plates and spacers were cleaned thoroughly with absolute methanol prior to assembly in the gel caster. The stacking gel and the separating gel were made up as described in table 2.7.

Stacking Gel	2.5%	3.5%
Stacking gel buffer pH 6.8	1.200 ml	1.200 ml
40% bis/acrylamide 37.5:1	0.313 ml	0.438 ml
dH_2O	3.386 ml	3.206 ml
10% APS w/v	0.050 ml	0.050 ml
TEMED*	0.015 ml	0.015 ml

Separating Gel	7.5%	10%
Separating gel buffer pH 8.8	3.750 ml	3.750 ml
40% bis/acrylamide 37.5:1	2.800 ml	3.750 ml
dH_2O	8.210 ml	7.260 ml
10% APS w/v	0.150 ml	0.150 ml
TEMED	0.015 ml	0.015 ml

Table 2.7: sodium dodecyl sulphate polyacrylamide gel constituents; Volumes were sufficient for two gels 80x70x1 mm;

The separating gel was poured between the gel plates leaving 1.5 – 2 cm empty for the stacking gel. The stacking gel was prepared as above and once the separating gel had solidified, approximately 1 ml of stacking gel was poured over the separating gel followed immediately by the gel comb. After the stacking gel

solidified the comb was removed. Gels were transferred into the gel running apparatus and the compartments filled with running buffer. Samples were prepared with 2x non-reducing running buffer or 2x reducing buffer and boiled at 100°C for 3 – 5 minutes. Wells were loaded with a maximum volume of 18 µl using thin-tipped gel loading tips. 5 µl SeeBluePlus2 was loaded as molecular weight standard. Acrylamide gels were run at a maximum voltage of 130 V until the loading dye front reached the bottom of the gel.

2.12.1.2 Precast Gels

Pre-cast NuPage Novex Tris-Acetate gels (Invitrogen, Paisley, UK) were prepared and set up according to the manufacturer's instructions. Samples were prepared according to the guidelines; a 10 µl mix consisting of 2.5 µl 4x NuPage LDS sample buffer and 7.5 µl sample. For reducing conditions the constituents changed to 2.5 µl sample buffer, 1 µl reducing agent (proprietary) and 6.5 µl sample.

2.12.2 Western Blotting

Protein was transferred from SDS-PAGE gels onto nitrocellulose membranes using a water-cooled Jencons (Leighton Buzzard, UK) JB10 transfer apparatus. Gels, nitrocellulose membrane, sponges and Whatman 3MM Chr blotting paper (Brentford, UK) were submerged in sodium bicarbonate transfer buffer (331) and then arranged into transfer cassettes according to the manufacturers guidelines. The tank was filled with transfer buffer until the blotting cassette was submerged. The transfers were run for two hours at 45 V. After electrophoretic transfer nitrocellulose membranes were incubated with blocking buffer for at least 60 minutes. Alternatively, test samples were applied to nitrocellulose using a pipette

tip (dot blotting) or by using the BioRad dot blotting apparatus (Hemel Hampstead, UK) followed by air-drying followed by blocking as above. The nitrocellulose membranes were then incubated with a 1/1000 – 1/5000 dilution of primary antibody (polyclonal and monoclonal) in blocking buffer for 30 – 60 minutes to bind the desired protein. Membranes were washed extensively with washing buffer following each probe. HRPO conjugated secondary or tertiary antibody was used as required to detect the probing antibodies. The nitrocellulose was then incubated with ECL western blotting reagent according to manufacturers guidelines and the reaction visualised with Hyperfilms (Amersham Biosciences, Little Chalfont, UK).

2.12.3 Coomassie Staining

SDS-PAGE gels were transferred to a weighing boat and incubated on a rocker with coomassie blue stain (0.2% w/v brilliant blue, 10% v/v glacial acetic acid, 30% methanol in dH_2O) for 15 – 30 minutes. Gels were destained with 7% v/v glacial acetic acid, 20% methanol in dH_2O (destain solution) and changed at least three times until protein bands were clearly visible.

2.12.4 Silver Staining

Silver staining was carried out following a modified protocol by Morrissey (332). As for coomassie staining, gels were transferred to a weighing boat. The staining procedure was as follows:

1. 50% v/v methanol, 10% v/v glacial acetic acid in dH_2O 20 – 30 min
2. 5% v/v methanol, 7% v/v glacial acetic acid in dH_2O 20 – 30 min
3. Rinse with dH_2O
4. 5% v/v glutaraldehyde in dH_2O 20 – 30 min
5. 3x wash with dH_2O
6. 5 µg/ml DL-dithiothreitol in dH_2O 20 – 30 min
7. 0.1% w/v $AgNO_3$ 20 – 30 min
8. Rinse with dH_2O
9. Brief wash with developer solution
10. Develop with developer solution + 0.05% v/v formaldehyde
11. Stop reaction with solid citric acid.

2.12.5 Drying of SDS-PAGE Gels

Coomassie and silver stained gels were soaked in gel drying buffer consisting of 20% v/v methanol and 4% v/v glycerol and placed between two sheets of pre-soaked gel drying film (Promega, Southampton, UK). The assembly was held in a drying frame (Promega) using paper clamps, left to dry over night and scanned.

2.12.6 Enzyme-Linked Immunosorbent Assay (ELISA)

Enzyme linked immunosorbent assay (ELISA) was carried out using Medisorp plates by NUNC (Roskilde, Denmark). Typically, 100 ng per well of protein was immobilised to microtitre plates in bi-carbonate buffer for one to two hours at 37°C or overnight at 4°C. Unbound protein was removed by washing the plates extensively with ELISA wash buffer. Free binding sites were blocked for at least

one hour at room temperature with ELISA blocking buffer. Samples were diluted in blocking buffer and 50 µl was added in triplicate to microtitre plate wells. Assay-specific positive controls were applied as a standard curve generally starting at 1 µg/ml and diluted 1/2 across the plate (12 steps). Plates were covered and incubated at 37°C for one hour followed by extensive washes. Dependent on the assay the HRPO-conjugated antibody was the secondary or tertiary antibody. Antibody was diluted in blocking buffer and 50 µl was added to each well. Incubation and wash steps were carried out as before. Bound HRPO antibody was detected with substrate solution consisting of 2 tablets OPD, 2.5 µl H_2O_2 in 6 ml dH_2O. 50 µl was added to the wells and incubated for up to 30 minutes. The reaction was stopped by adding an equal volume of 10% H_2SO_4. The absorbance through colour change was measured using the BMG Labtech Ltd. (Aylesbury, UK) plate reader at 490 nm.

2.13 Microscopy

Microscope slides (Surgipath, Peterborough, UK) were prepared by drawing 'wells' with a PAP pen (Sigma-Aldrich Company Ltd, Poole, UK). Cell suspension in saline solution was then added to the 'wells' and left to air-dry for 30 –45 minutes. Cells were fixed with ice-cold acetone for 10 minutes and dried at 37°C for 15 – 30 minutes. After a 5-minute PBS wash, 100 µl 1/1000 4',6-diamidino-2-phenylindole (DAPI) stain (Molecular Probes, Invitrogen, Paisley, UK) was added to each well and incubated in the dark at RT for 45 minutes. Slides were washed with dH_2O for 5 minutes to remove excess stain. The cells were dehydrated with 70%, 90% and 100% ethanol for 1 minute each. The slides were air dried again for 10 minutes, mounted with Vectashield (Vector Laboratories Inc, Burlingame, USA) and stored

in the dark at 4°C until used. Fluorescent cells were examined using a Leica DM LB2 (Leica Microsystems UK Ltd., Milton Keynes, UK) fluorescent microscope and OpenLab software.

2.14 Statistical Analysis

Statistical analyses were carried out using GraphPad Prism version 3.02 for Windows (GraphPad Software, San Diego, California USA). Differences between more than two data sets were calculated using the One Way Analysis of Variance (ANOVA) and Tukey's Multiple Comparison test. Specific differences between two groups were calculated using a standard Students *t*-test. Comparison of more than two groups where a Gaussian distribution did not apply was carried out using the Kruskal Wallis test followed by Dunn's Multiple Comparison test. Statistical differences between two specific sets of data were calculated using the Mann-Whitney test. Differences between data sets in parametric and non-parametric tests were regarded as significant when $p < 0.05$.

Chapter 3

Optimisation of the Molecular Adjuvant C3dg/C3d

3.1 Introduction

A number of multimerisation approaches have been applied to C3dg/C3d, e.g. covalent linkage via the thioester bond (302, 303) or tetramerisation with biotin/streptavidin (165, 301). In the years since the first publication utilisation of the linear C3d-trimer has been developed further for protein vaccines ((218, 296-298) also see (302)) and DNA vaccines (252-256). Throughout this time, the arrangement of the components, i.e. antigen followed by three copies of the adjuvant, has not changed. The present study was inspired by an oligomerisation approach described by Libyh *et al.* C4BP was used to increase valency of a recombinant antibody (314, 315) or as a measles decoy receptor ((316) section 1.12). Contrary to the artificial – and spatially limited – arrangement of the C3d-trimer vaccines, octamerisation produced an array of ligands to engage multiple adjacent receptors. C3dg/C3d was positioned first in the sequence and thus on the outer rim of the octamer. The antigen was inserted nearer the core between the adjuvant and the C4BP octamerising sequence (Oct). Most of the studies mentioned used a mutated form of C3d, which had its thioester moiety at cysteine 988 mutated to serine or alanine to maintain the three-dimensional structure (102, 165, 218, 333). The rationale behind this alteration was not fully reported in detail. Most vaccine designs containing C3d were based on the linear mouse C3d trimer containing the C988S mutation.

During this initial phase of octamer analysis, yellow fluorescent protein (YFP) was used in place of the antigen to aid visualisation of the fully formed octamer protein during the *in vitro* optimisation. The aim was to determine, which version of human hC3dg/hC3d, native or mutated, was expressed to the highest level, correctly

folded and functional (i.e. the candidate vaccine adjuvant that bound strongest to the natural receptor, hCR2). This information was vital in terms of its utility as a DNA vaccine and *in vivo* production.

The aim of this part of the study was therefore to determine the optimal variant of hC3dg/hC3d to be used in this novel vaccine. Following optimisation, the fluorescent tag, used for analytical and optimisation purposes only, was exchanged with the well-established model antigen HEL (section 1.12). Subsequently, sufficient amounts were produced using *in vitro* cell culture and purified for testing *in vivo*.

3.2 Materials & Methods

Methods were carried out as outlined in chapter 2 unless stated otherwise below.

3.2.1 Vectors

3.2.1.1 pDR2EF1α

This vector was chosen because of its ability to drive high levels of protein production in mammalian cells. Expression of the protein of interest was driven by the human elongation factor 1 α (EF1α), a housekeeping gene promoter that inherently operates at high levels irrespective of the cell type. It was originally described by Charreau *et al.* (334) and has been used on a regular basis in our laboratory (e.g. (335), figure 3.1 A). The vector contains both an ampicillin resistance gene and a hygromycin resistance gene for selection in bacteria and mammalian culture, respectively.

3.2.1.2 pEYFP-C1

This vector was from BD Biosciences Clontech (San Jose, CA, USA) and used as the source for the yellow fluorescent protein tag (figure 3.1 B). Besides the tag the vector contained a neomycin/kanamycin resistance gene for selection in bacteria; a cytomegalovirus (CMV) promoter drove expression.

A

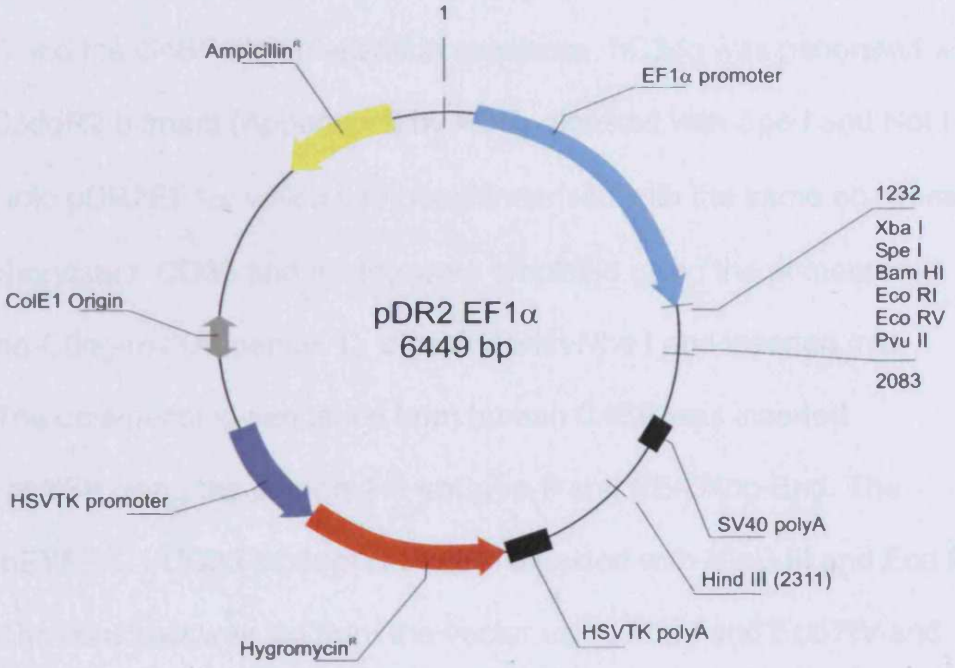
1
Ampicillin^R
EF1α promoter
1232
Xba I
Spe I
Bam HI
Eco RI
Eco RV
Pvu II
2083
ColE1 Origin
pDR2 EF1α
6449 bp
HSVTK promoter
SV40 polyA
Hind III (2311)
HSVTK polyA
Hygromycin^R

B

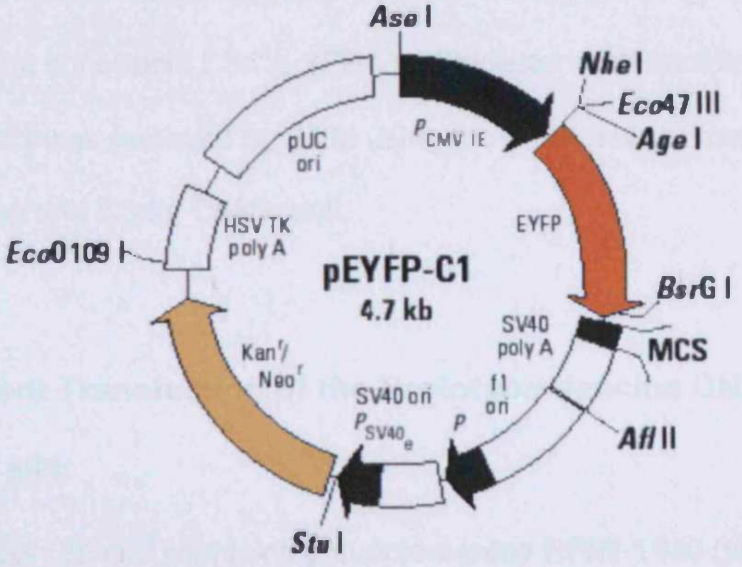
Ase I
Nhe I
Eco47 III
Age I
pUC ori
$P_{CMV\ IE}$
HSV TK poly A
EYFP
Eco0109 I
pEYFP-C1
4.7 kb
BsrG I
SV40 poly A
MCS
Kan^r/ Neo^r
SV40 ori
f1 ori
AflII
P_{SV40}
P
Stu I

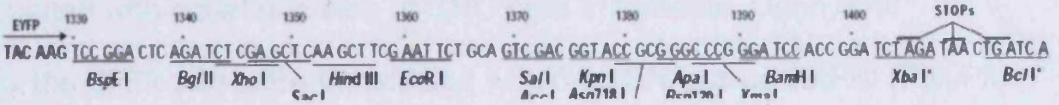
EYFP
1339
1340
1350
1360
1370
1380
1390
1400
STOPs
TAC AAG TCC GGA CTC AGA TCT CGA GCT CAA GCT TCG AAT TCT GCA GTC GAC GGT ACC GCG GGC CCG GGA TCC ACC GGA TCT AGA TAA CTG ATC A
BspE I
Bgl II
Xho I
Sac I
Hind III
EcoR I
Sal I
Acc I
Kpn I
Asp718 I
Apa I
BamH I
Xba I*
Bcl I*

3.2.2 Generation of a Recombinant Octameric C3d Vaccine Prototype

The prototype octamer consisted of the human C3dg wild type, yellow fluorescent protein (YFP) and the C4BP oligomerisation sequence. hC3dg was generated with C3dgF and C3dgR2 primers (Appendix I) by PCR, digested with Spe I and Not I and inserted into pDR2EF1α, which had been linearised with the same enzymes and dephosphorylated. CD33 and hC3dg were amplified using the primers nx-signal and nhe-C3dg-rev (Appendix 1), digested with Nhe I and inserted into pEYFP-C1. The octamerising sequence from human C4BP was inserted downstream of YFP using the primers H3-shC4bp-F and EE-C4bp-End. The product and pEYFP-C1 CD33-hC3dg-YFP were digested with HinD III and Eco RI and ligated. The construct was cut from the vector using Xba I and Eco RV and inserted into pDR2EF1α (figure 3.2 A). This construct will be referred to as hC3dg-YFP-Oct. hC3d-YFP-Oct (shortened, 'g'-deleted wild type) was produced as described in section 2.10.9 with C3g_deletion_F and C3g_deletion_R. The thioester motif in the constructs C3d^{S}g-YFP-Oct (thioester motif mutated C→S) and hC3d^{S}-YFP-Oct was removed by SDM using the mutagenic primers C3dg_C58S_sense and C3dg_C58S_anti.

3.2.3 Transient Transfection of the Prototype Vaccine DNA into CHO Cells

Tissue culture flasks (75 cm^2) containing supplemented RPMI-1640 (section 2.7.) were inoculated with equal numbers of CHO cells in triplicate. Upon 60% confluency the CHO cells were transfected with 6 µg DNA using JetPEI (PolyPlus

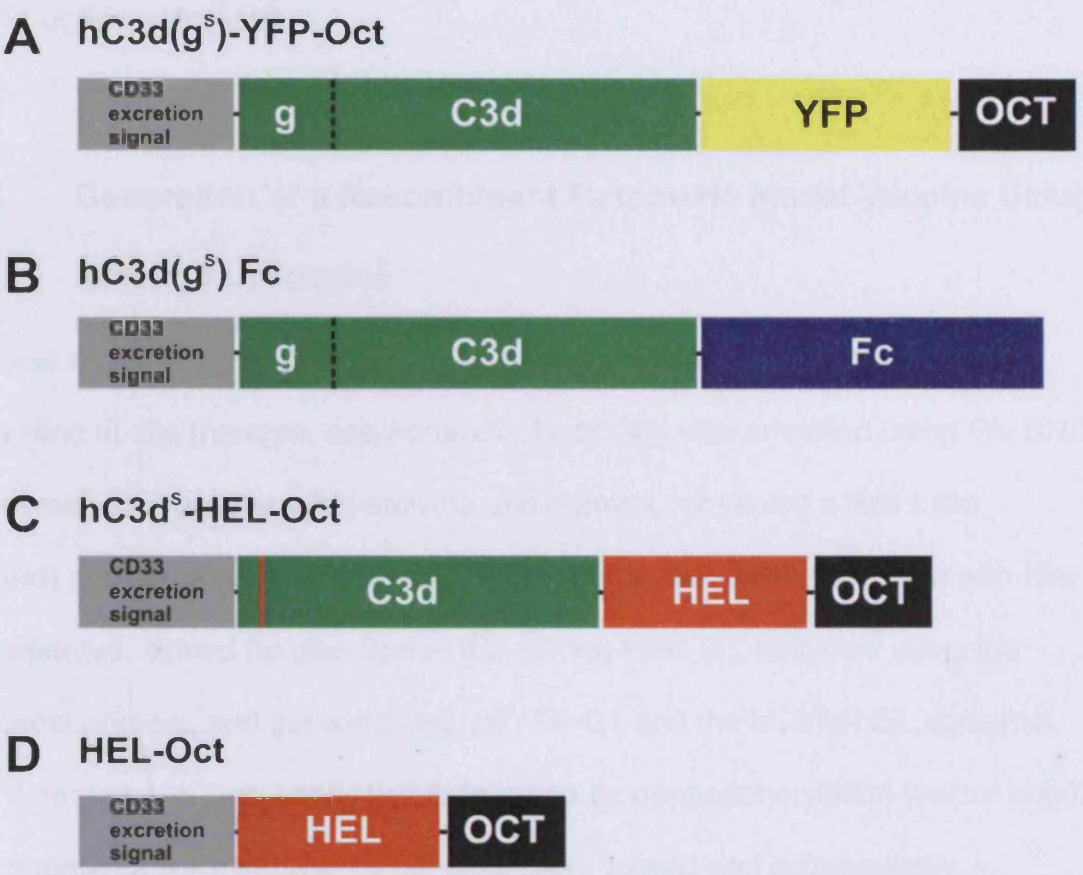

Figure 3.2. Expression constructs. Panel A shows the YFP octamer used for optimisation of expression, excretion and binding (compare figure 3.3). Panel B shows the human immunoglobulin Fc fragment fusion proteins used for further CR2 binding studies (discussed in chapter 4). Panels C and D represent the two octameric HEL vaccine constructs hC3d^S-HEL-Oct and HEL-Oct. The mutated thioester moiety is shown in red (C).

Transfection, Illkirch, France). 72 hours later, medium was removed and stored at –20°C until needed. The cells were divided up for further analysis by lysis, western blotting or flow cytometry.

3.2.4 Generation of a Recombinant Octameric Model Vaccine Using Hen Egg Lysozyme

HEL was amplified from cDNA using primers containing an Nhe I site (forward) and a Hind III site (reverse, see Appendix 1). hC3dg was amplified using *Pfu* DNA polymerase as a proofreading enzyme and primers containing a Spe I site (forward) and an Nhe I site (reverse). Both PCR products were digested with Nhe I, precipitated, ligated (to give Spe I-HEL-hC3dg-Hind III), amplified using the outermost primers, and gel extracted. pEYFP-C1 and the hC3dg-HEL construct were digested with Spe I and Hind III followed by dephosphorylation (vector only). Both fragments were purified by gel-extraction, ligated and subsequently transformed by electroporation. The whole sequence was digested out of pEYFP-C1 with Xba I and Eco RV and inserted into the same sites in pDR2EF1α (figure 3.2 C). hC3dg was mutated to $hC3d^S$ as described before in two separate steps.

A control protein lacking hC3d (HEL-Oct) was generated by amplifying the HEL and C4BP part of the sequence using *Pfu* DNA polymerase with a forward primer containing Spe I and the reverse primer 3' EF1α, which binds downstream of the MCS. The PCR fragment and pDR2 EF1α $hC3d^S$-HEL-Oct were digested with Spe I and Eco RV, dephosphorylated (plasmid only) and isolated by gel extraction followed by ligation and electroporation (figure 3.2 D).

3.3 Results

3.3.1 Four Versions of Octameric Protein Are Generated

To establish what determined ideal vaccine characteristics, site directed mutagenesis was performed in an attempt to improve expression and excretion of the octamer containing hC3dg. In preparation for experiments to be carried out based on Dempsey's work (218, 256) and the subsequent studies on m/hC3d linear trimer vaccines, we designed a fluorescently tagged octamer to aid visualisation in downstream optimisation processes.

The four prototype constructs hC3dg, hC3d, hC3d^{S}g and hC3d^{S} (figure 3.3 A) were verified by restriction digest, first with Spe I and Eco RV. Restriction maps of the constructs are shown in figure 3.3. Bands in each lane from top to bottom (figure 3.3 B) represent the vector backbone (7 kb) and the whole construct sequence of 2163 bp for 'g'-containing and 1962 bp for 'g'-lacking sequences. Figure 3.3 C shows a more detailed map using Spe I, Nhe I, Hind III and Eco RV. The bands in each lane from top to bottom represent hC3dg/hC3d^{S}g/hC3d/hC3d^{S} (0.9 – 1.1 kb), an expected fragment containing SV40 poly A (1 kb), YFP (750 bp) and C4bBP octamer (180 bp). Mutated and unmutated DNA fragments have the same size at 1.1 kb and 0.9 kb as expected. hC3d and hC3d^{S} can be clearly distinguished showing a band 200 bp lower than hC3dg and hC3d^{S}g. This data indicated that the short and long wild type constructs had been generated in the correct orientation.

Figure 3.3. hC3dg variants. Panel A shows the construct sequences of four the YFP-octamers as contained in the expression vector pDR2 EF1α, including relevant restriction enzymes. The thioester-forming residue (cysteine) is indicated in blue, the mutated thioester residue (serine) in red. Panel B shows a 1% TAE agarose gel. 1 µg of Plasmid DNA was digested with Spe I and Eco RV (Marker = Hyperladder I) to give two bands. The lower band relating to the particular cDNA construct inserted and one being the remaining plasmid backbone. Panel C shows a 2% TAE agarose gel. 1 µg of DNA was digested with Spe I, Nhe I, Eco RV and Hind III. Shown are the bands generated from digest of the hC3dg/hC3d variant constructs into their component parts as illustrated in panel A, (hC3dg/hC3d, YFP and Oct, respectively). A 1 kb band is also visible (hC3d,g construct lanes) released from digest of the vector backbone. The rest of the vector backbone (approx. 6Kb) is omitted for the sake of clarity (Marker = Hyperladder IV).

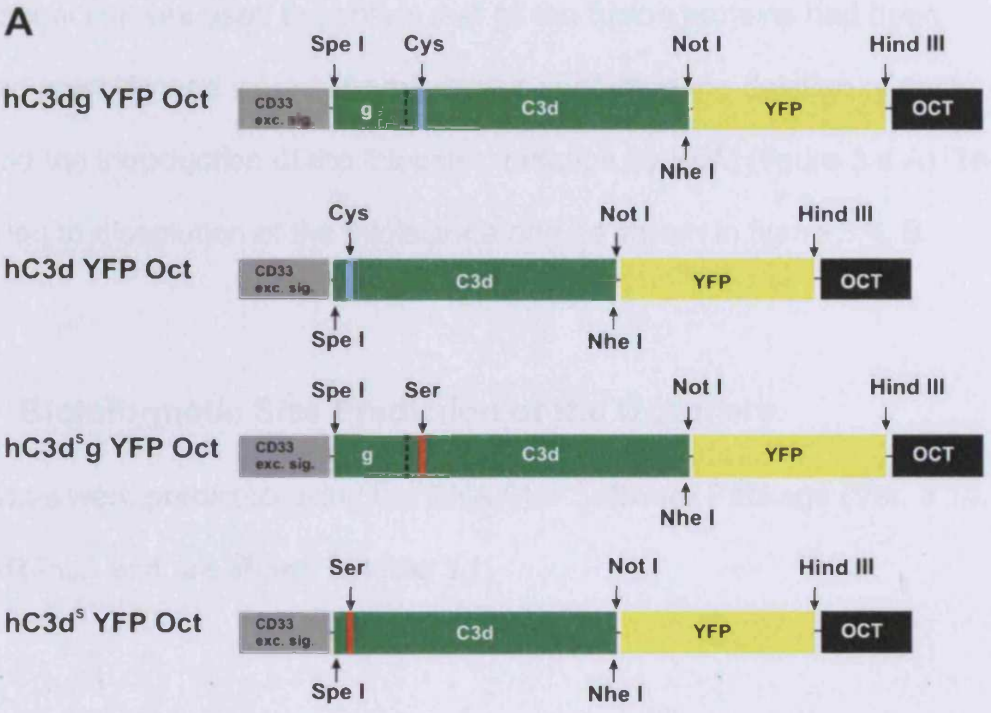
A
hC3dg YFP Oct
Spe I
Cys
Not I
Hind III
CD33 exc. sig.
g
C3d
YFP
OCT
Nhe I
hC3d YFP Oct
Cys
Not I
Hind III
CD33 exc. sig.
C3d
YFP
OCT
Spe I
Nhe I
hC3d^{s}g YFP Oct
Spe I
Ser
Not I
Hind III
CD33 exc. sig.
g
C3d
YFP
OCT
Nhe I
hC3d^{s} YFP Oct
Ser
Not I
Hind III
CD33 exc. sig.
C3d
YFP
OCT
Spe I
Nhe I


B
hC3dg-YFP-Oct
hC3d-YFP-Oct
hC3d^{s}g-YFP-Oct
hC3d^{s}-YFP-Oct
Marker
10 kb
7 kb
2 kb
1.5 kb

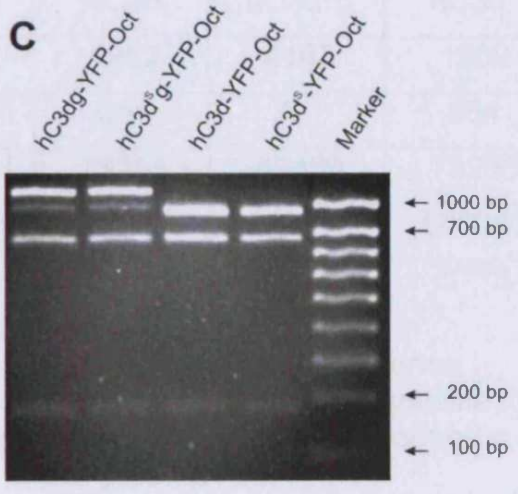
C
hC3dg-YFP-Oct
hC3d^{s}g-YFP-Oct
hC3d-YFP-Oct
hC3d^{s}-YFP-Oct
Marker
1000 bp
700 bp
200 bp
100 bp

The restriction enzyme digest suggested that all vectors were constructed as predicted. However, the two mutated sequences showed the same restriction pattern and were therefore indistinguishable from the wild types on agarose gels. Thus, sequencing was used to confirm that all the fusion proteins had been assembled correctly and were in frame. It also confirmed the deletion of the 'g' portion and the introduction of the thioester mutation by SDM (figure 3.4 A). The mutation led to dissolution of the thiolactone ring as shown in figure 3.4. B.

3.3.2 Bioinformatic Size Prediction of the Octamers

Protein sizes were predicted using the DNA Star Software Package (Ver. 3.14, DNASTAR Inc.) and are shown in table 3.1.

YFP-octamer version	hC3dg	hC3d	$hC3d^{S}g$	$hC3d^{S}$
Length [kb]	2163	1962	2163	1962
Length [aa]	721	654	721	654
M.W. single chain [Da]	80433	73255	80433	73255
M.W. octamer [Da]	643465	586040	643465	586040
Mutations	-	-	$C^{988}S$	$C^{988}S$

Table 3.1. Predicted sizes of the four octamers based on a sequence assembled from dideoxysequencing. Mutated proteins had the cysteine to serine mutation introduced at aa residue 988 (mature hC3 numbering).

Figure 3.4. Confirmation of the thioester mutation by dideoxysequencing. The thioester residue of both long and short wild type variants, hC3dg and hC3d, was mutated by SDM using a whole-plasmid amplification kit (see section 2.10.9 and 3.2.2). Panel A shows sequencing data comparing mutated and unmutated DNA and amino acid sequences. The mutated triplet is shown in red, a single base change tyrosine to adenosine leads to the mutation cysteine to serine. The top panel in B shows the thiolactone ring formed naturally in α2M proteins such as C3 and C4. For the thioester binding reaction please refer to figure 1.5. The lower panel shows the mutated C→S residue and the presumed non-reactive structure.

A

WT	I V T P S G C G E Q N M I
hC3dg/hC3d	ATTGTGACCCCCTCGGGCTGCGGGGAACAGAACATGATC
C→S	ATTGTGACCCCCTCGGGCAGCGGGGAACAGAACATGATC
hC3d^{S}g/hC3d^{S}	I V T P S G S G E Q N M I

B

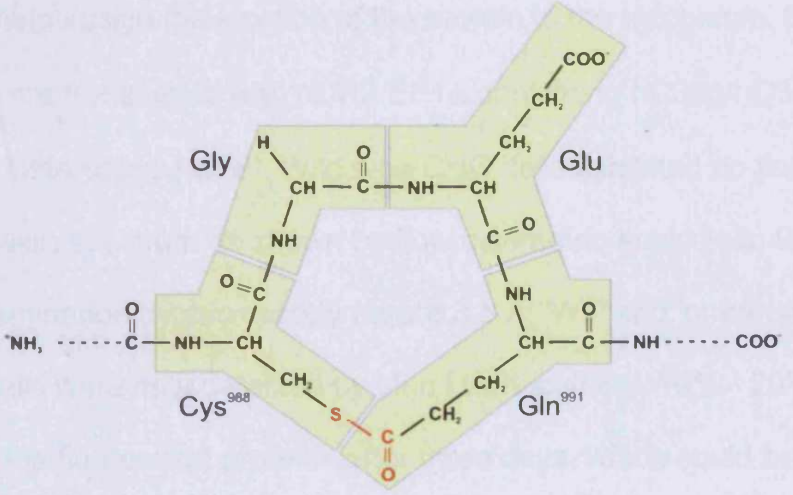

WT thioester motif

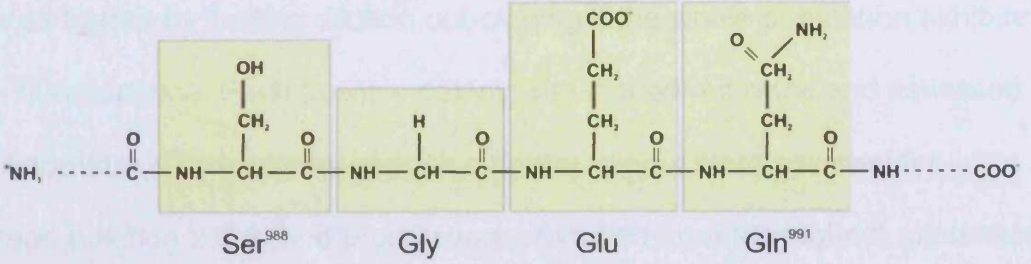

Cys → Ser

3.3.3 Stably Transfected CHO Cells

The overall aim within this chapter was to devise a method to produce protein at high levels and ensure sufficient excretion into the surrounding medium for subsequent purification of the potential vaccine. Stably transfected cell lines circumvent the need for repeated transient transfection and collection of product, a time consuming and costly procedure. For this optimisation multiple clones were assessed by flow cytometry and microscopy (figure 3.5) facilitated by the use of YFP inserted into the octameric construct between hC3d and the octamerising signal in the antigen's stead. The nuclear DNA stain DAPI was employed to help detection of the cells in the field of view. Thus, DAPI provided a useful counterstain to help assign the location of the protein to the cytoplasm. 60 – 70% confluent cells were transfected with pDR2 EF1α containing hC3dg/hC3d^{S}g/hC3d/ hC3d^{S}-YFP-Oct DNA using JetPEI. Wild type CHO cells exhibited no fluorescence in the YFP emission spectrum as shown by flow cytometric analysis in the FL1 channel and examination by microscopy (figure 3.5 A, 'WT' and 'untransfected'). Untransfected cells were only detected by blue DAPI staining. 10% - 20% of the cells expressed the fluorescent proteins after three days, which could be detected in the FL1 channel (FACS) and with the fluorescent microscope. Cells from single-clone colonies in tissue culture plate wells were screened by FACS and propagated further by limiting dilution out-cloning if the whole population exhibited a shift in fluorescence. Each positive colony was cloned out twice and assessed by flow cytometry. Three clones of each octamer variant were selected for cryostorage (section 2.8.3) and protein was produced from the highest expresser (figure 3.5 B).

Figure 3.5. Production of stable transfectants. WT CHO cells were transfected with one variant of hC3dg/hC3d^{S}g/hC3d/hC3d^{S}-YFP-Oct each and cloned out by limiting dilution as outlined in section 2.8.2. Panel A shows on the left a histogram of the mean fluorescence of untransfected wild type CHO cells. Fluorescent microscopy images of cells were taken at the respective emission peaks of 461 nm (nuclear stain DAPI) and 529 nm (YFP) using the appropriate filters and then overlaid. The images next to the histogram represent typical overlays using this process. Three stages in the production of stable transfections are shown: untransfected cells identifiable by blue DAPI staining, 3 days after transfection and stably expressing cell lines, each expressing YFP, shown in green. Panel B shows a representative mean fluorescence histogram measured at three days after transfection or of the stably expressing cells as determined by standard FACS analysis (section 2.9). Results are representative of at least three replicate cell transfections. Each hC3d YFP octamer variant is indicated on the left. Forward and side scatter profiles were used to gate live cell populations and collect 10,000 gated events.

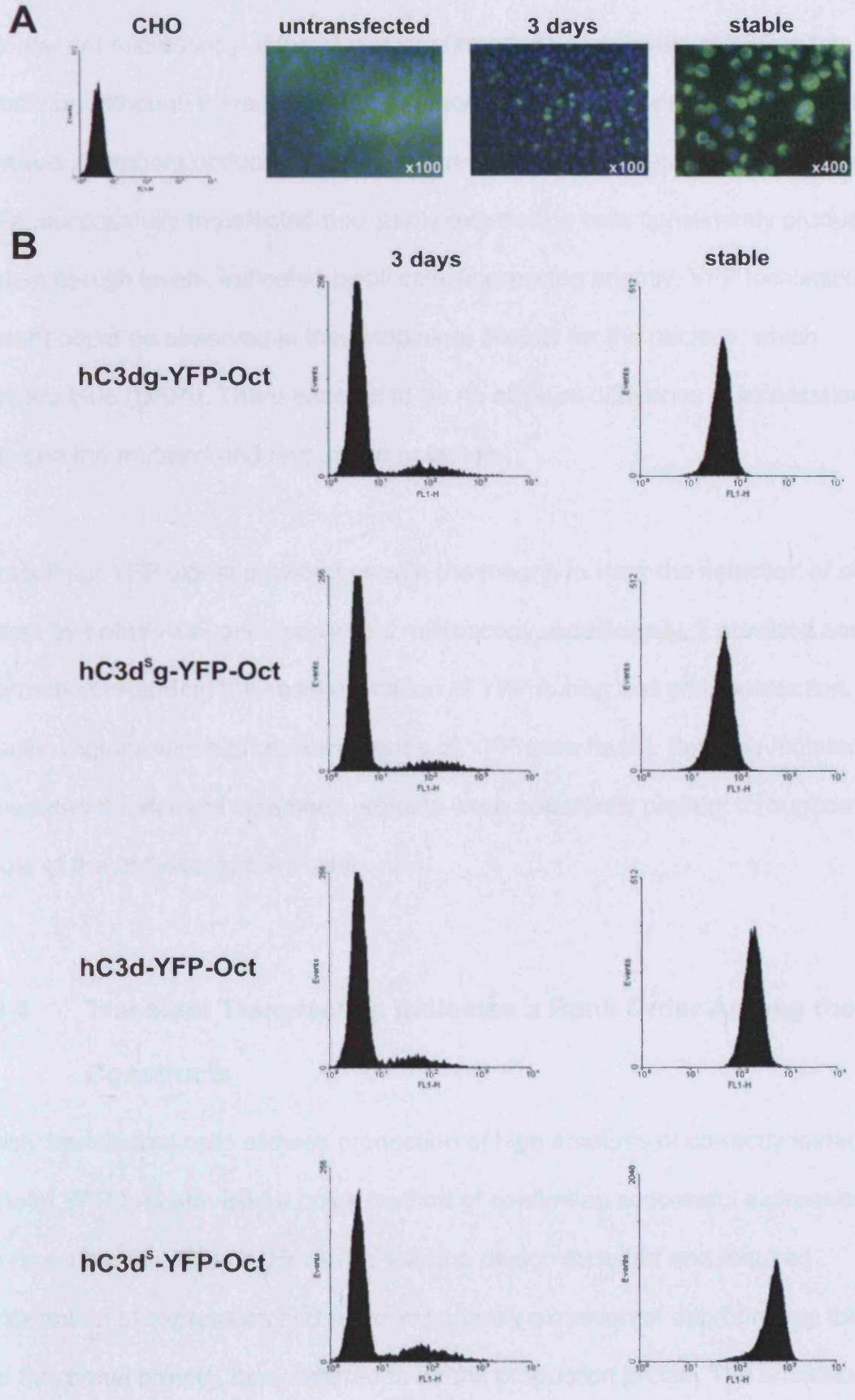
A
CHO
untransfected
3 days
stable
x100
x100
x400
B
3 days
stable
hC3dg-YFP-Oct
hC3d^Sg-YFP-Oct
hC3d-YFP-Oct
hC3d^S-YFP-Oct

Clonal selection achieved shifts in the cell population one (hC3dg and hC3d^{S}g) or two (hC3d and hC3d^{S}) orders of magnitude for the most efficient expressers. Fluorescent microscopy of the clones confirmed the high levels of YFP in the cytoplasm although there were no differences in cellular localisation (figure 3.5 A). However, numbers of fluorescing cells were low after transfection. On the other hand, successfully transfected and stably expressing cells consistently produced protein at high levels, indicated by all cells fluorescing brightly. YFP localisation (green) could be observed in the cytoplasm, distinct for the nucleus, which appears blue (DAPI). There seemed to be no obvious difference in localisation between the mutated and unmutated octamers.

Intracellular YFP signal provided us with the means to track the selection of stable clones by both FACS and fluorescent microscopy. Additionally, it provided some information regarding the cellular location of YFP during and after production. No specific regions with high accumulations of YFP were found. Both the mutated and unmutated fluorescent octameric proteins were apparently present throughout the whole of the cell except the nuclei.

3.3.4 Transient Transfection Indicates a Rank Order Among the Constructs

Stably transfected cells allowed production of high amounts of correctly folded protein. YFP had provided a quick method of confirming successful expression of the recombinant proteins. However, vaccine design included and required confirmation of expression and more importantly excretion of appropriately folded and functional protein, here referred to as the production profile. The amounts of

fusion protein produced, retained in the cytoplasm and excreted into the medium would have a direct impact on the subsequent immune response raised after exposure to DNA vaccines. Genetic vaccination in effect represents *in vivo* transfection, requiring investigation of the fate of the hC3dg/hC3d^{S}g/hC3d/hC3d^{S} octamers after introduction into a somatic cell. To simulate this *in vitro*, cells were transiently transfected with the four octamer-encoding plasmids. Medium from two separate experiments carried out in triplicate were collected 72 hours after transfection for western blotting and ELISA analysis. Cells were also collected for FACS analysis and lysed for immunoblotting by western blotting. The recombinant octamers were larger than C4BP (540 – 570 kDa (66)) with a maximum predicted size of approximately 643.5 kDa (hC3dg and hC3d^{S}g, table 3.1) or 586 kDa (hC3d and hC3d^{S}, table 3.1). Due to their size, separation on SDS-PAGE gels and transfer onto nitrocellulose membranes electrophoretically required thorough optimisation. The use of low-density gels and transfer in bi-carbonate buffer (331) was found to give adequate visualisation of these large proteins.

Pooled replicate samples were analysed by western blotting. A high molecular weight band was clearly identified using anti-hC3d in both the lysate and medium samples (figure 3.6 A and C). This band likely corresponds to the fully formed octamer proteins. Additionally, several lower molecular weight bands were detected in the cell lysate and potentially relate to the single chains and partially generated octameric proteins in the golgi apparatus. The sizes of the component monomeric bands were confirmed by treatment of the lysate samples with reducing agent prior to Western blot analysis. Bands at 80.4 and 73.3 kDa were identified as the long and short wild type as well as mutated monomeric subunits

Figure 3.6. Western blotting of media and cell lysate after transient transfection of hC3dg/hC3d^{S}g/hC3d/hC3d^{S}-YFP-Oct variants. Medium was removed from all cultures 72 hours after transfection. Replicate samples of lysates were pooled and visualised under non-reducing (panel A) and reducing conditions (panel B). Supernatants (panel C) were pooled and analysed only under non-reducing conditions. All gels underwent Western blotting following separation in a 2.5% stacking/7.5% separating SDS-PAGE gel. Western blotting was carried out as described in section 2.12.2. The proteins were detected with Rb α hC3d and anti Rb HRPO. Methylamine treated human C3, a kind gift from Claire Harris, is an artificial homologue to human iC3b and was used as a positive control. An empty transfection (JetPEI), wild type untransfected CHO cells and RPMI-1640 alone served as negative controls. Marker: SeeBlue Plus2.

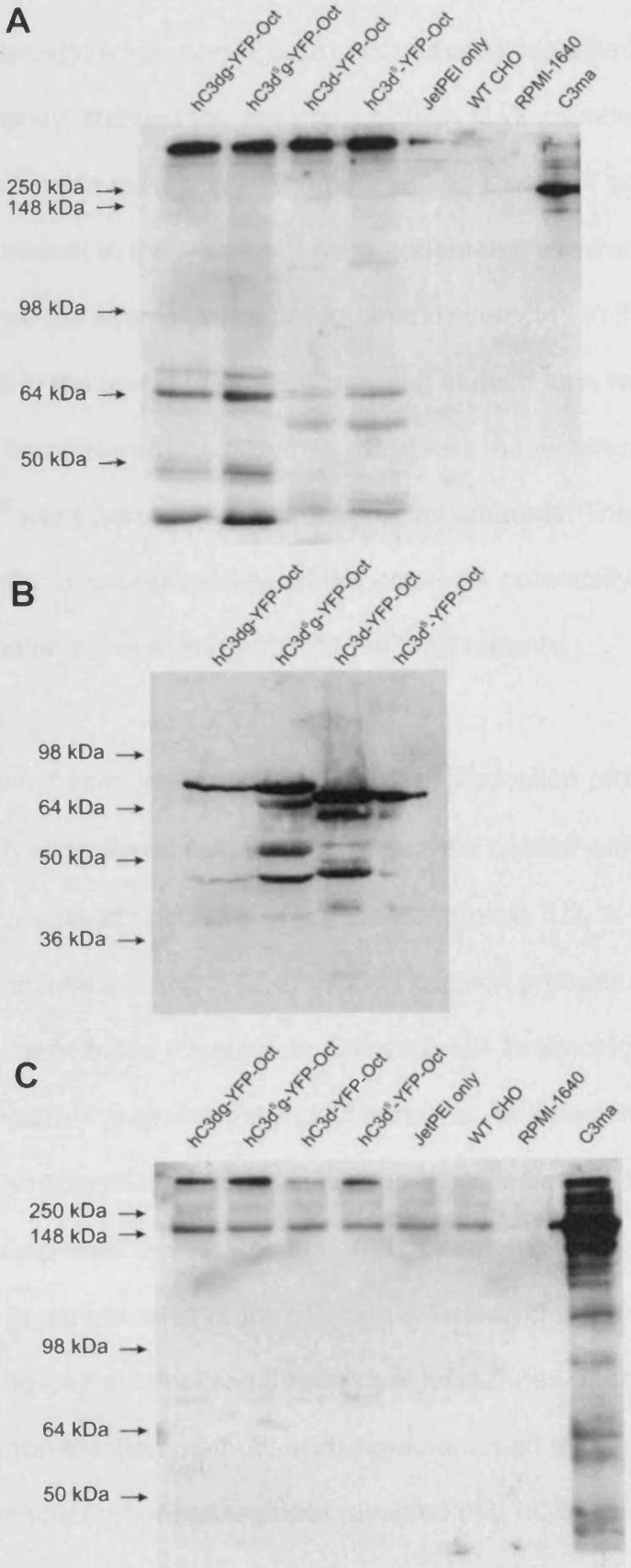
A
hC3dg-YFP-Oct
hC3d®g-YFP-Oct
hC3d-YFP-Oct
hC3d®-YFP-Oct
JetPEI only
WT CHO
RPMI-1640
C3ma
250 kDa
148 kDa
98 kDa
64 kDa
50 kDa
B
hC3dg-YFP-Oct
hC3d®g-YFP-Oct
hC3d-YFP-Oct
hC3d®-YFP-Oct
98 kDa
64 kDa
50 kDa
36 kDa
C
hC3dg-YFP-Oct
hC3d®g-YFP-Oct
hC3d-YFP-Oct
hC3d®-YFP-Oct
JetPEI only
WT CHO
RPMI-1640
C3ma
250 kDa
148 kDa
98 kDa
64 kDa
50 kDa

of the octamer (figure 3.6 B). One irrelevant band at approximately 150 kDa was detected in all sample supernatants and the cell control supernatant. The higher molecular weight bands (under non-reducing conditions), identified by polyclonal Rb anti-hC3d antibody, showed the assembly of high M.W. proteins containing hC3d. These bands were most likely oligomers with at least 8, 7 or 6 arms. Monomers were present in the lysate but were undetectable in the medium. The higher molecular weight species were predominantly detected in the medium. Visible differences in the levels of signal generated in each lane were noted, hC3d^{S}g-YFP-Oct being the strongest, while hC3d was the weakest (figure 3.6 B). hC3dg and hC3d^{S} were present at apparently equal amounts. These data suggested variability in excretion levels of the octamers potentially due to the presence of 'g' and/or the mutation within the hC3dg variants.

In order to establish if there were differences in the production profiles, a quantitative ELISA was carried out. ELISA plates were coated with Rb α hC3d and incubated with four triplicate dilutions of supernatant (neat, 1:2, 1:4, 1:8) in blocking buffer (sections 2.2 and 2.12.6). hC3d Fc fusion proteins (generated in house) and monomeric hC3d (Comptech, Complement Technology Inc, Tyler, USA) served as positive control in the ELISA screens. As a baseline or negative control, comparison supernatant from untransfected cells or cells that only received JetPEI were used. Replicates of samples were included to compensate for any variability in growth rates or transfection efficiency. Furthermore, the risk of variations occurring was minimalised through use of cultures of equal cell density and standardised transfection methods with predetermined amounts of DNA. Analysis of the immunosorbent assay data revealed that hC3d^{S}g-YFP-Oct was

excreted at significantly higher levels than hC3dg ($p < 0.05$), hC3d^S ($p < 0.01$) and hC3d ($p < 0.001$); figure 3.7 A), which confirms the observations from figure 3.6 B. Comparison with hC3dg-YFP-Oct suggests that the thioester mutation facilitated higher levels of octamer in the medium ($p < 0.05$), comparing hC3d to hC3d^S also shows a similar trend. There were no significant difference in excretion of hC3dg, hC3d and hC3d^S when compared with each other. Thus, hC3d^{S}g-YFP-Oct was identified as the variant with the optimal excretion profile.

FACS experiments were designed to measure the mean fluorescence of 10,000 events above baseline thus excluding the proportion of untransfected cells not exhibiting fluoresence. Higher mean fluorescence intensity of the positive population therefore corresponded to higher amounts of protein produced and contained in the cell. Results obtained from FACS analysis did not produce as striking results as the immunosorbent assay but a similar trend was discernible (figure 3.7 B). All variants fluoresced strongly above CHO cell intrinsic baseline levels and there was a tendency to higher fluorescence in cells expressing the mutated proteins, reflecting the results obtained from the western blots (figure 3.6).

The data obtained from ELISA and FACS assays were subsequently compared directly by plotting cell fluorescence against protein in supernatant. Both were defining features of the mentioned production profile, therefore this graphical presentation allowed a simplified means of comparison and provided more conclusive information on performance of the octamers ((336) figure 3.7 C). Expression level of mutants and wild type proteins clearly decreased upon removal

Figure 3.7. Quantitative analysis of octamer production after 72 hours transient transfection. Protein content of the supernatant and the cytoplasm was analysed with an anti-hC3d ELISA (panel A, section 2.12.6) and flow cytometry analysis using a FACSCalibur (panel B, section 2.9), respectively. Data sets are presented in bar graph format plotting the mean and SEM of five independent experiments. The hatched bars represent the two wild type proteins, hC3dg-YFP-Oct and hC3d-YFP-Oct. Bars shown in shades of grey are the mutated variants hC3d^{S}g-YFP-Oct (light grey) and hC3d^{S}-YFP-Oct (dark grey). Panel C shows retained octamer (cell fluorescence) plotted against excreted protein. Round symbols represent versions containing the 'g' portion; square symbols show the short variants. Filled symbols are WT proteins; empty symbols represent proteins containing the thioester mutation. The filled diamond and empty triangle represent JetPEI only and untransfected CHO respectively. * $p < 0.05$, ** $p < 0.01$, *** $p < 0.001$. Data were analysed by One-way ANOVA and Tukey's multiple comparison test.

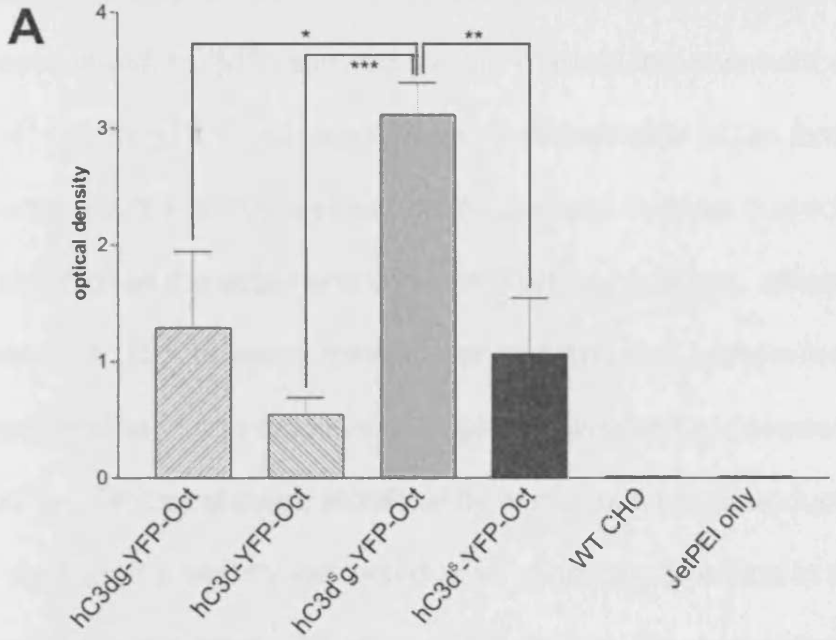
A
optical density
*
**
***
hC3dg-YFP-Oct
hC3d-YFP-Oct
hC3d^{s}g-YFP-Oct
hC3d^{s}-YFP-Oct
WT CHO
JetPEI only

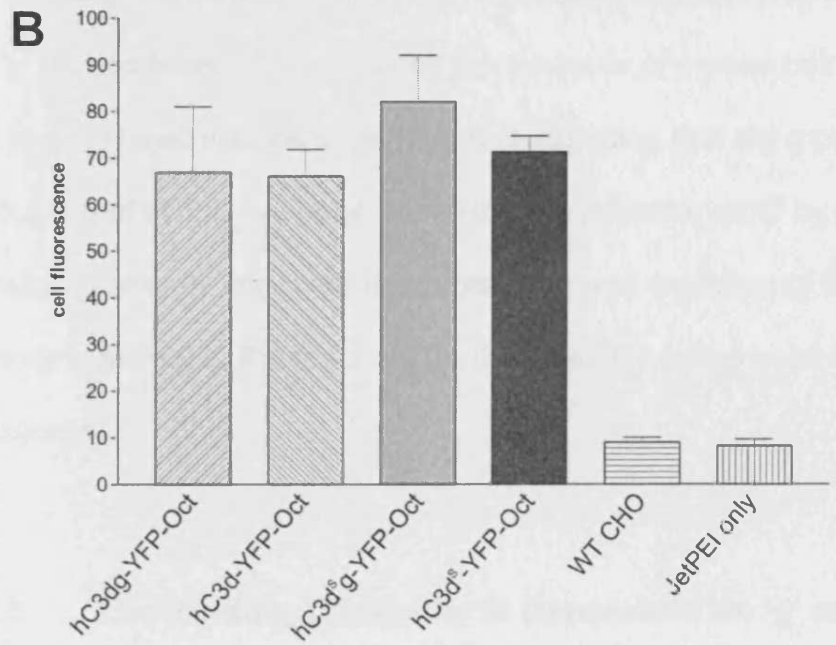
B
cell fluorescence
hC3dg-YFP-Oct
hC3d-YFP-Oct
hC3d^{s}g-YFP-Oct
hC3d^{s}-YFP-Oct
WT CHO
JetPEI only

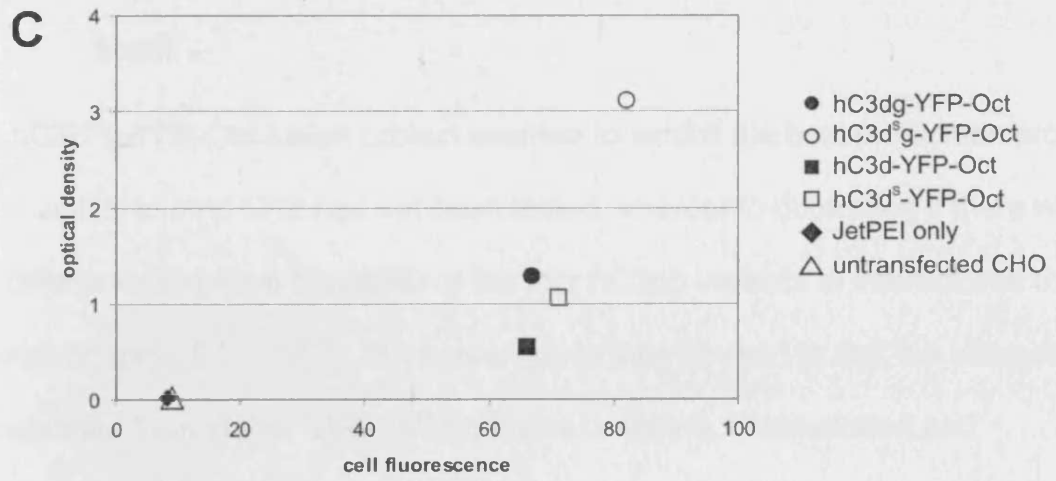
C
optical density
cell fluorescence
hC3dg-YFP-Oct
hC3d^{s}g-YFP-Oct
hC3d-YFP-Oct
hC3d^{s}-YFP-Oct
JetPEI only
untransfected CHO

of 'g', conversely, production of long and short variants benefited from mutating the thioester motif. hC3d^{S}g showed a more marked improvement compared to hC3dg. hC3d^{S} exhibited a similar improvement compared to hC3d, however not as striking. In summary, the above western blotting results indicate correct expression and excretion of all the octameric variants. Further analyses, utilising FACS and sandwich ELISA to assay intracellular and excreted protein respectively, suggested that some differences in production existed between the variants. hC3d^{S}g-YFP-Oct showed significantly higher excretion/production profile but also demonstrated a slightly increased level of protein retention in the cytoplasm when compared to the other variants. In combination, the data showed that removal of the 'g' portion from hC3dg reduced the amounts of protein being produced in the cell and excreted into the supernatant, suggesting that the g portion stabilised production of hC3d. However, removing the thioester motif by cysteine to serine mutation markedly improved the expression and excretion of the respective octamers, providing the rationale for this mutation being used in previous C3d constructs.

3.3.5 The Binding Capability Is Dependent on 'g' and the Thioester Motif

The hC3d^{S}g-YFP-Oct fusion protein seemed to exhibit the best production profile but its ability to bind CR2 had not been tested. In order to determine if there was any difference between the ability of the four hC3dg variants to interact with the natural receptor, CR2, an ELISA-based assay was devised to test the interaction. Supernatant from stable CHO cell lines was collected, concentrated and concentrations of each variant were estimated by anti-hC3d sandwich ELISA (see

previous section). Samples were prepared at 10 ng/ml in blocking buffer and diluted 1:1 in three steps to 1.25 ng/ml. hCR2 (100 ng/well hCR2-Fc SCR1-4, developed in house, see later chapter) was immobilised on 96-well ELISA plates and incubated with the prepared samples for 2 hours at 37°. Bound hC3d was detected with Rb α hC3d and α Rb HRPO. CD59 octamer, a kind gift by Sivsankar Baalasubramanian, as well as WT CHO supernatant and RPMI-1640 served as negative controls, monomeric hC3d was used as positive control. As expected, the negative controls did not interact with the receptor. This showed that there were no secondary interactions dependent on the octamerising sequence (no binding of CD59-Oct), medium constituents (RPMI-1640) or CHO excretions (untransfected CHO supernatant). All variants bound to hCR2 Fc successfully according to the concentrations applied to the wells (figure 3.8). As expected, the octamers did not bind to hCR2 with equal strength. Removal of 'g' significantly increased binding efficiency ($p < 0.001$) although this modification had caused a slight decrease in expression and excretion (see section 3.3.4). It is possible that this mimics the normal physiological situation where B-cell binding to hC3dg/hC3d after the removal of C3g in a final enzymatic step might enhance affinity for CR2 and thus, enhance an immune response. hC3d^{S}-YFP-Oct exhibited strongest binding to hCR2-Fc SCR1-4, significantly higher than all other variants. Surprisingly however, hC3d^{S}g-YFP-Oct, which had outperformed all of the other variants in production, exhibited weakest interaction with hCR2. The mutated hC3d^{S}g construct also had less affinity for hCR2 than wild type hC3dg within this assay. Although this was not found to be significant, it was a notable trend. Taken together the data indicated that mutation of the thioester and removal of the 'g'-portion maximised binding to the natural receptor.

Figure 3.8. Binding capabilities of the four variants to hCR2 vary. hCR2 SCR1-4 Fc was immobilised in wells of an ELISA plate and incubated with a dilution series of the four octameric variants in blocking buffer. Bound hC3dg/ $hC3d^{S}g$/hC3d/$hC3d^{S}$ was detected with Rb α hC3d and anti-Rb HRPO antibodies. CD59-Oct, untransfected CHO supernatant and RPMI-1640 served as negative controls. The bar graph shows optical density at 490 nm measured by spectrophometry (section 2.12.6) plotted against each concentration. High-purity hC3d (CompTech, Tyler, USA) applied at 1 µg/ml exhibited (O.D. 2.57 ±0.04) was used to generate a standard curve (inset). Data was analysed by one-way ANOVA for each concentration. Data were derived from two independent experiments carried out in triplicate. * $p < 0.05$, ** $p < 0.01$, *** $p < 0.001$.

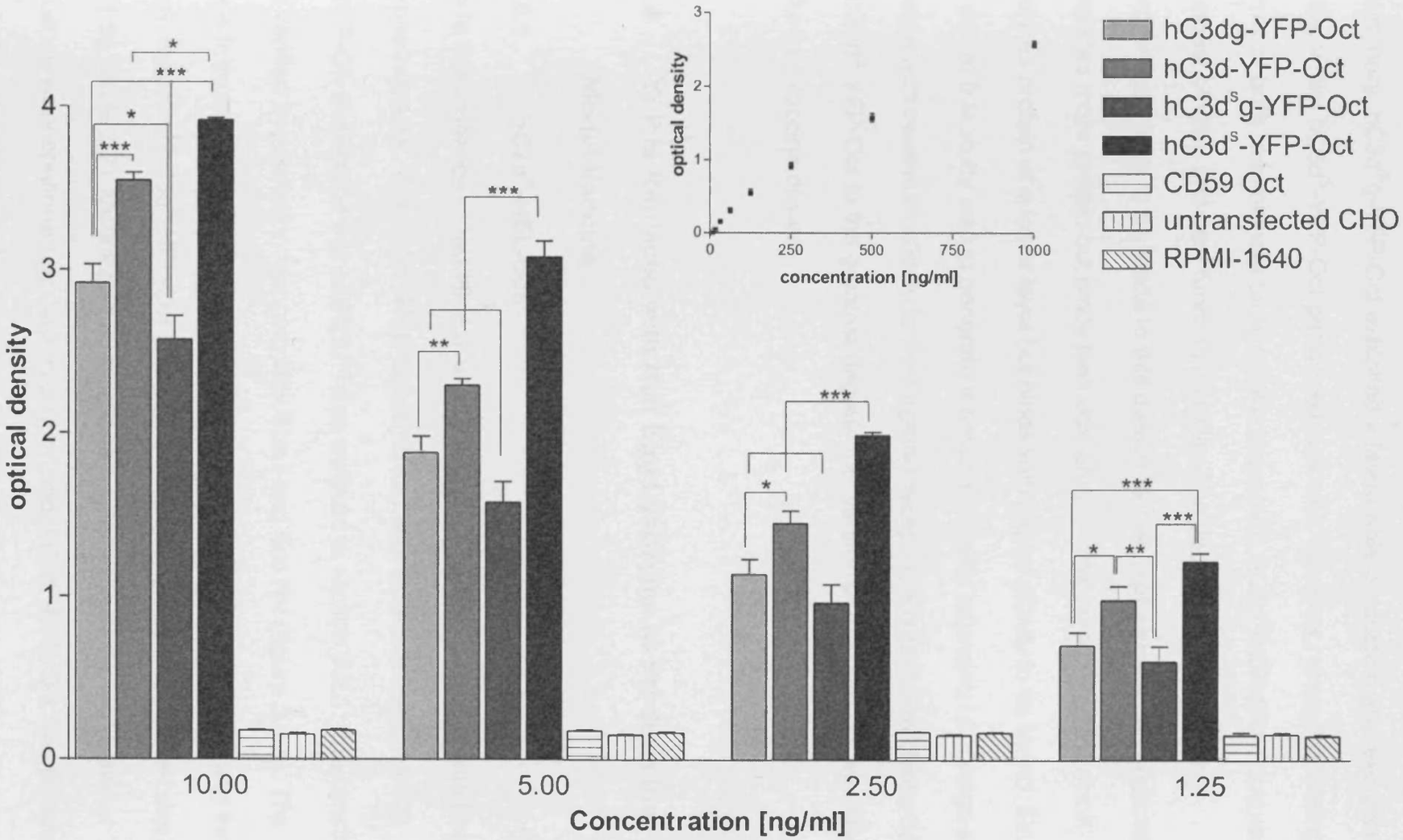
optical density
4
3
2
1
0
10.00
5.00
2.50
1.25
Concentration [ng/ml]
hC3dg-YFP-Oct
hC3d-YFP-Oct
hC3d^{S}g-YFP-Oct
hC3d^{S}-YFP-Oct
CD59 Oct
untransfected CHO
RPMI-1640
optical density
concentration [ng/ml]
0
250
500
750
1000

Figure 3.9. Production of hC3d^S-HEL-Oct and HEL-8. YFP was replaced with HEL and inserted into pDR2 EF1α. Two proteins were produced, one containing hC3d^S and one lacking hC3d^S to control for hC3d^S activity in vaccine studies. Panel A shows a 1% TAE agarose gel. 1 µg of DNA was digested with Spe I and Eco RV (Marker = Hyperladder I). The excised bands indicate the presence of hC3d^S-HEL (~1.6kb) and HEL (~0.7kb) components of the new generated variant constructs, respectively. Panel B shows a western blot of a 7.5% SDS-PAGE gel loaded with unreduced hC3d^S-HEL-Oct from CHO supernatant. Several different species were detected, the octamer is indicated by an arrow. HEL-Oct protein in Panel C was treated the same way as described in B. Antibodies for octamer detection were Rb α Oct (a kind gift from Timothy Hughes) and α Rb HRPO. Molecular weight marker: SeeBlue Plus2. Panels D and E are graphical representations of hC3d^S-HEL-Oct and HEL-Oct respectively.

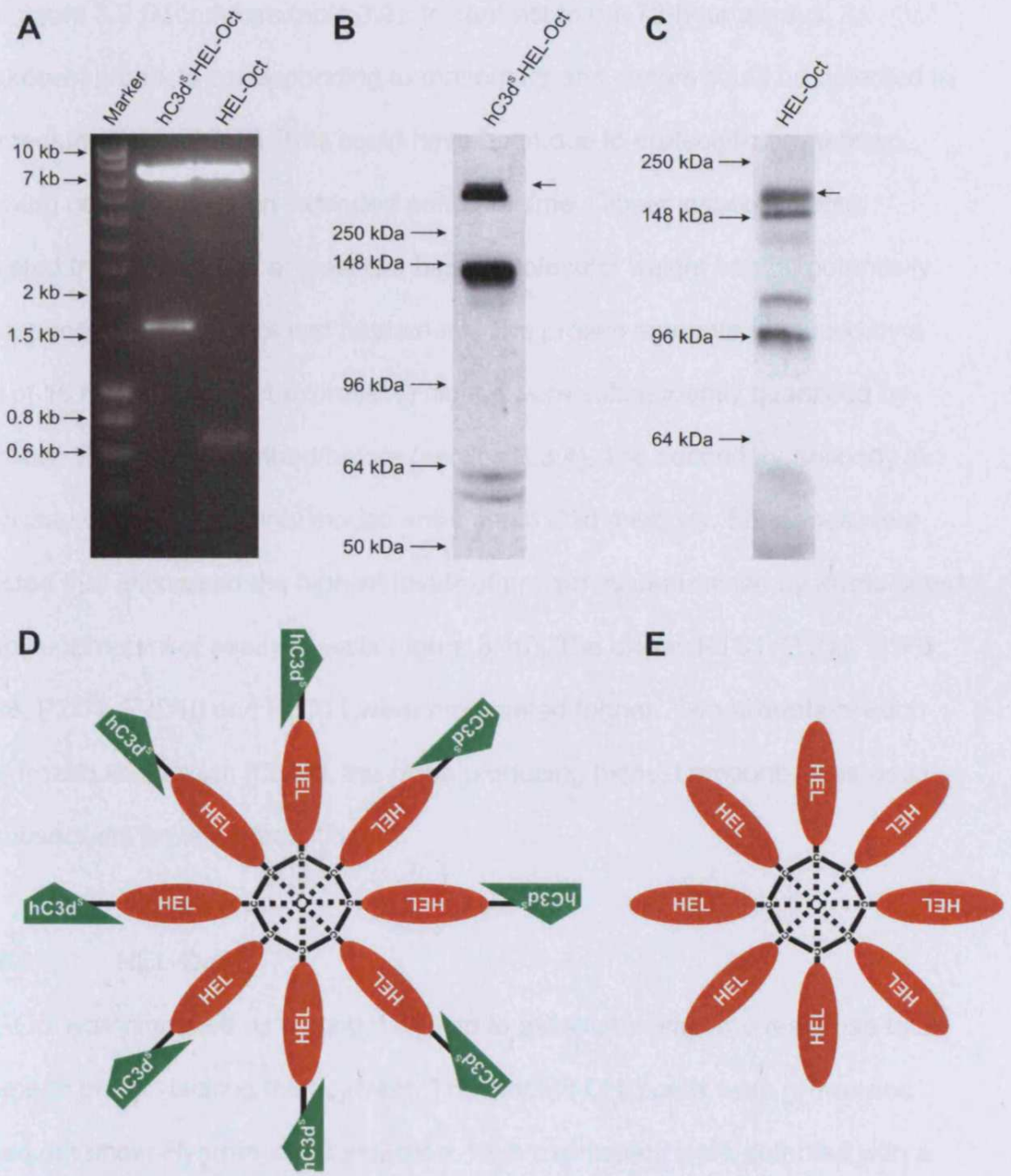
A
Marker
hC3d^s-HEL-Oct
HEL-Oct
10 kb
7 kb
2 kb
1.5 kb
0.8 kb
0.6 kb
B
hC3d^s-HEL-Oct
250 kDa
148 kDa
96 kDa
64 kDa
50 kDa
C
HEL-Oct
250 kDa
148 kDa
96 kDa
64 kDa
D
hC3d^s
HEL
E
HEL

single CHO colonies underwent preliminary screening by dot blotting. Western blot analysis indicated expression and excretion of the octamer at approximately 500 kDa (figure 3.9 D, compare table 3.2). In contrast to the 72-hour assays, breakdown products corresponding to monomers and dimers could be detected in the medium (figure 3.9 B). This could have been due to proteolytic breakdown following cell culture for an extended period of time. Closer inspection also indicated the presence of at least two higher molecular weight bands, potentially corresponding to octamers and heptamers. The protein amounts produced by a total of 16 hC3d^{S}-HEL-Oct-expressing clones were subsequently quantified by sandwich ELISA as described before (section 3.3.4). The secondary antibody in this assay was a monoclonal mouse anti-human C3d antibody. Six clones were selected that expressed the highest levels of protein as determined by levels noted in the supernatant of assayed wells (figure 3.10). The clones P1C1, P1D1, P1F5, P1G8, P2D4, P2D10 and P2D11 were propagated further. Two aliquots of each were frozen as backup; P2D10, the clone producing highest amounts, was used for subsequent protein production.

3.3.6.2 HEL-Oct

HEL-Oct was produced as a control protein to assess the immune response to an octameric protein lacking the adjuvant. Transfected CHO cells were grown and cloned out under Hygromycin B selection. High expressers were detected with a Rb α Oct antibody, a kind gift from Dr Timothy Hughes. Due to the lack of suitable antibodies for selection via ELISA, clones for propagation, protein production and liquid nitrogen storage were selected by dot blot. A western blot of the selected

Figure 3.10. Clonal selection of hC3d^{S}-HEL-Oct. Neat tissue culture supernatant was loaded from individual clonal cultures in triplicate onto the anti-hC3d sandwich ELISA (section 2.12.6). High-purity hC3d served as positive control and standard for quantitative analysis (panel A). The concentration of each individual clone in the supernatant was determined by linear regression analysis (panel B).

A

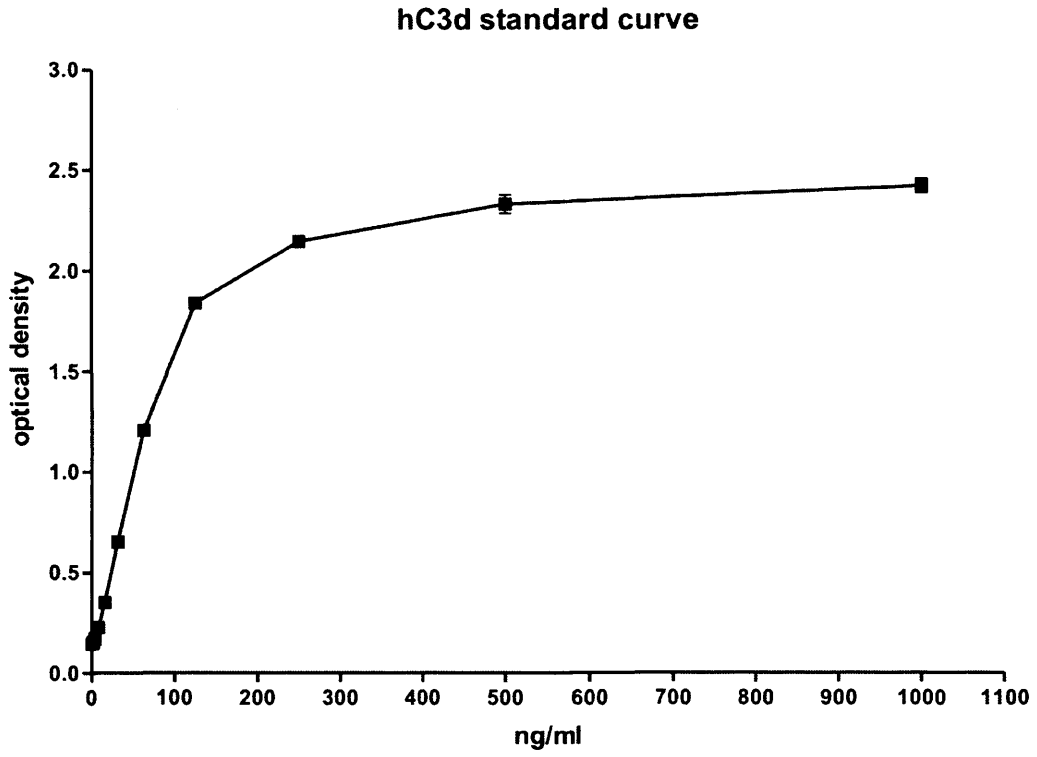
hC3d standard curve
optical density
3.0
2.5
2.0
1.5
1.0
0.5
0.0
0
100
200
300
400
500
600
700
800
900
1000
1100
ng/ml

B

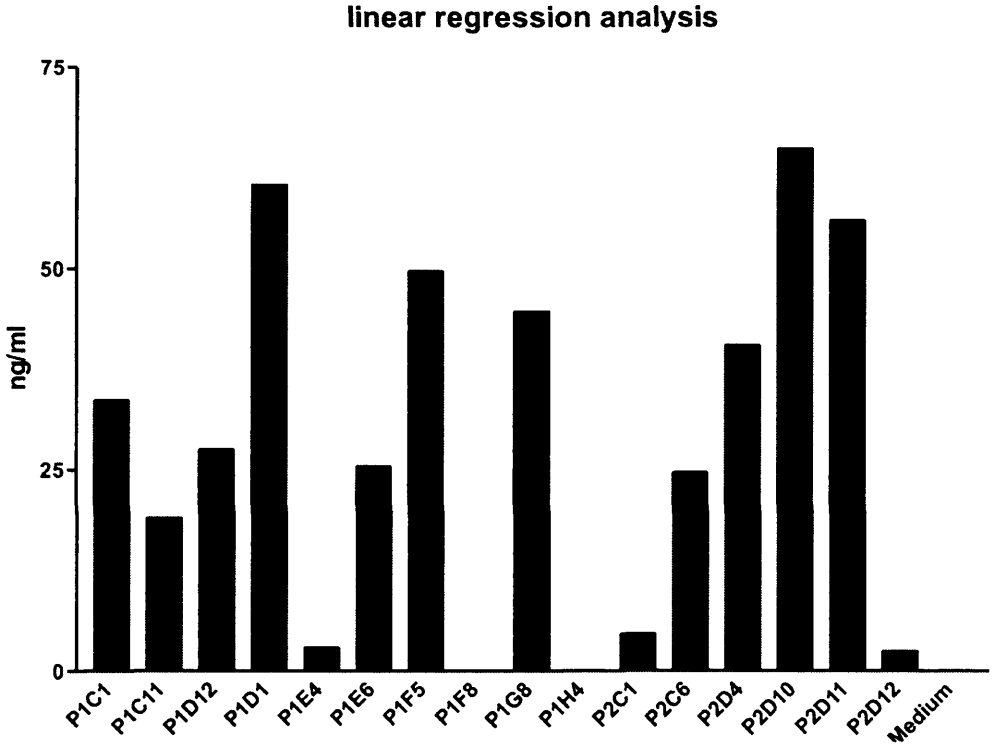
linear regression analysis
ng/ml
75
50
25
0
P1C1
P1C11
P1D12
P1D1
P1E4
P1E6
P1F5
P1F8
P1G8
P1H4
P2C1
P2C6
P2D4
P2D10
P2D11
P2D12
Medium

high-level expressing clone showed expression of a multimeric protein (figure 3.9 C, arrow). Multiple bands detected in the gel however indicated the presence of several breakdown products. The size of the bands in the gel corresponded to M.W. assumed by the octameric protein (figure 3.9 E, compare table 3.2).

	hC3d^S-HEL-Oct	HEL-Oct
Length [kb]	1761	663
Length [aa]	587	221
M.W. single chain [Da]	65432	24674
M.W. octamer [Da]	523456	197392
Isoelectric point	6.67	7.77

Table 3.2. DNA and protein sizes of the vaccine octamers

Two octameric proteins containing the model antigen hen egg lysozyme were produced (figure 3.9 D and E). One included the molecular adjuvant hC3d^S, the other only consisted of HEL and the octamerising sequence. The sequences were verified and CHO cells expressing the proteins at high-levels were selected. In the next step these cell clones were transferred into a cell flask, which supports protein production at optimum yield in small volumes.

3.3.7 High Level Production hC3d^S-HEL-Oct and HEL-Oct

The selected clones were grown in Integra CELLine AD1000 cell culture flasks over a period of three months. The flasks consist of two individually accessible compartments, a 1 L medium compartment and a 20 ml cell compartment separated by a 10 kDa semi-permeable cellulose acetate membrane. This allows small molecules and waste products to diffuse across the membrane whilst higher

M.W. products are retained in the cell compartment. Due to the molecular weight cut off (MWCO) of the membrane, the medium compartment is not supplemented with foetal calf serum. A filter in the medium compartment screw cap and a silicon membrane below the cell compartment facilitate gas transfer, i.e. oxygen supply and carbon dioxide exchange. 15 ml aliquots supernatant were collected each week from the cell compartment and protein concentration established. Medium was replaced in both the cell and medium compartment according to manufacturers instructions. Average protein concentration of hC3d^{S}-HEL-Oct from CELLine AD1000 culture was approximately 3 – 5 fold higher than conventional flask culture. 10 – 20 fold increases were observed with Fc fusion protein production (discussed in a later chapter) when conventional and CELLine culture were compared. The cell compartment was replenished with fresh cells once a month after extensive treatment with trypsin EDTA. Integra flasks proved very useful from an economic point of view, saving the use of large numbers of conventional tissue culture flasks (~90% reduction) and time. Despite the higher cost of the flasks themselves, the benefits of the integra system far outweighed cell culture in normal flasks.

3.3.8 Purification of hC3d^{S}-HEL-Oct and HEL-Oct

Use of the octameric proteins in further experiments required purification from the tissue culture supernatant. A two-step process was developed utilising anion exchange chromatography, which allowed the removal of most medium components, followed by size exclusion chromatography to exclusively purify high molecular weight protein. Figure 3.11 shows the elution traces recorded in real time during Source Q purification on the Äkta FPLC. High M.W. C3d-containing

proteins were detected in the final elution peak. The purifications of both octamers had very similar profiles, illustrated by the fact that the protein concentration traces were nearly identical (figure 3.11 C). Collected fractions containing the octamer were pooled and concentrated using vivaspin columns ($C3d^S$-HEL-Oct: 300,000 MWCO, HEL-Oct: 100,000 MWCO). The filtered samples were spun for 10 minutes at 13,000 rpm to remove aggregates in preparation for the second step in the purification. 500 µl aliquots of concentrate were loaded onto a superose 6 gel filtration column and eluted with 1.5 column volumes (CV) of PBS, to exchange from Tris NaCl (figure 3.12 A). Contrary to expectations, several peaks were observed on the gel filtration elution traces indicating breakdown of the octameric proteins into smaller subspecies. The reason for the instability of the oligomers and whether its causes were physical (filtration and purification conditions) or chemical (proteases, pH, ionic strength) is unknown.

Fractions from each peak contained C3d although oligomers with the highest molecular weight were presumed to be contained in the first peak fractions (figure 3.12 A, arrow). Proteins of larger size percolated through the gel matrix quicker due to the particle pore size, which shortened their path length through the column. For more detailed analysis the fractions from the first peaks from $hC3d^S$-HEL-Oct and HEL-Oct purifications were pooled and analysed using 3-8% Tris-acetate gradient gels. Samples were separated under reducing conditions with the Invitrogen proprietary reducing agent. Gradient gels were used instead of manually prepared gels because they promised higher resolution, better reproducibility and the visualisation of a wider range from very large to smaller M.W. species. Moreover, despite the sensitivity of silver nitrate staining, conventional gels

Figure 3.11. Source Q anion exchange chromatography of C3d^{S}-HEL-Oct and HEL-Oct. Samples were adjusted to pH 9 with 1 M Tris (pH 12) and subjected to Source Q anion exchange chromatography on the Äkta FPLC system at 4°C (section 2.11.1. and 2.11.1.2.). Panel A shows a typical elution trace for hC3d^{S}-HEL-Oct axis plotting absorbance at 280 nm, which is a measure of protein concentration, during fraction collection. Panel B shows a typical trace for HEL-Oct. Both traces have been overlaid in panel C to illustrate the almost identical elution profiles. Arrows indicate peak fractions containing the octameric proteins.

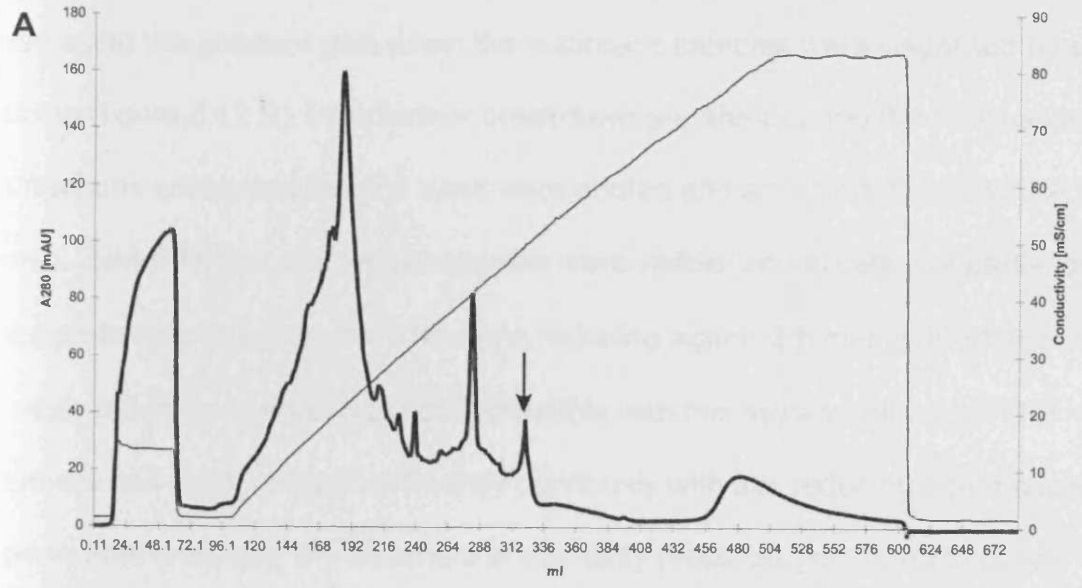
A
A280 [mAU]
Conductivity [mS/cm]
0.11 24.1 48.1 72.1 96.1 120 144 168 192 216 240 264 288 312 336 360 384 408 432 456 480 504 528 552 576 600 624 648 672
ml

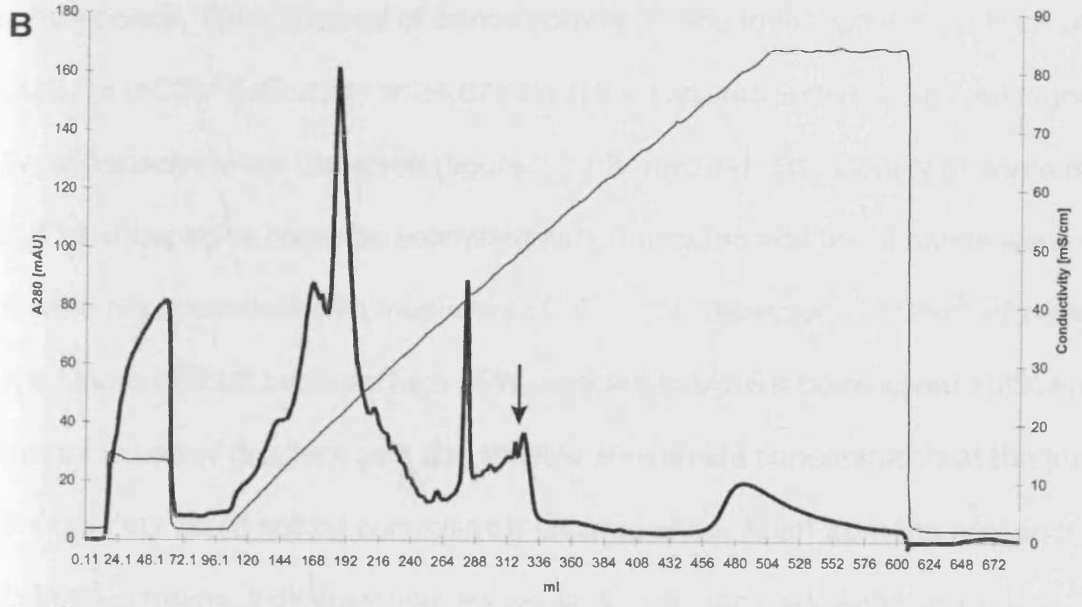
B
A280 [mAU]
Conductivity [mS/cm]
0.11 24.1 48.1 72.1 96.1 120 144 168 192 216 240 264 288 312 336 360 384 408 432 456 480 504 528 552 576 600 624 648 672
ml

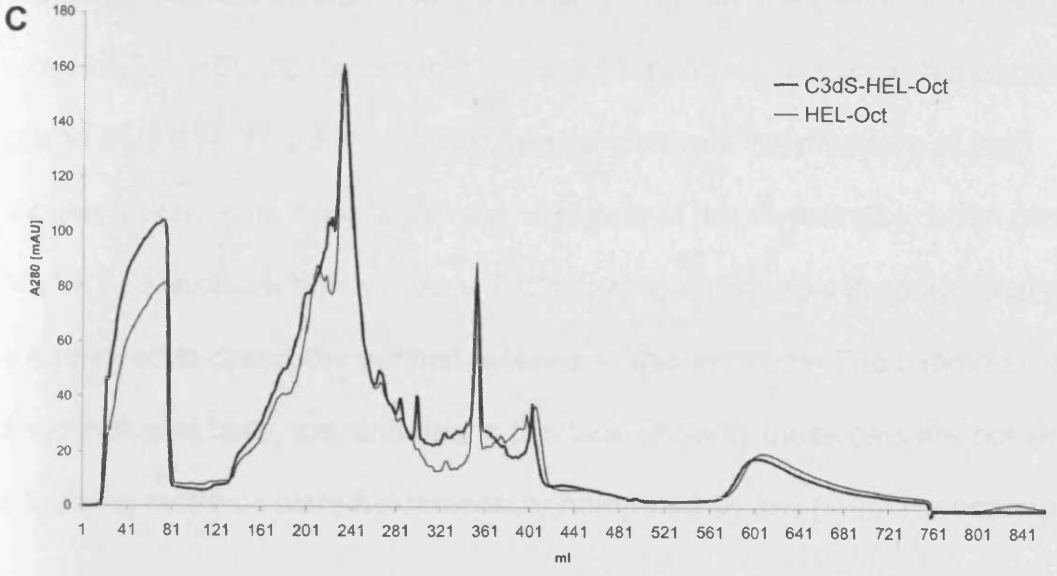
C
C3dS-HEL-Oct
HEL-Oct
A280 [mAU]
1 41 81 121 161 201 241 281 321 361 401 441 481 521 561 601 641 681 721 761 801 841
ml

provided insufficient resolution to distinguish the purified proteins. Similar problems arose using the gradient gels when the octameric samples were visualised by silver staining (figure 3.12 B). With further breakdown apparent during the purification only the fractions containing the first peak were pooled and analysed (figure 3.12 A, arrow). Several molecular weight species were visible, an indication of partial or incomplete reduction with the Invitrogen reducing agent. 2-β mercaptoethanol, as well as other reducing agents, was not compatible with this system. Although YFP octamers had been reduced efficiently previously with this reducing agent several experiments analysing the octamers in manually prepared gels failed to break disulfide bonds. Thus, instead of bands corresponding to monomeric proteins at 65,432 Da (hC3d^{S}-HEL-Oct) or 24,674 Da (HEL-Oct) respectively, several higher M.W. subspecies were observed (figure 3.12 B, arrows). The identity of some of the HEL-Oct subspecies could be estimated although some additional bands were visible that were not consistent with multimers of HEL-Oct. Detection of hC3d^{S}-HEL-Oct proved more difficult because high M.W. species could not be resolved sufficiently. Despite the use of gradient gels and the low acrylamide concentration at the top end of the gel they could not be conclusively distinguished. Apart from the presence of high M.W. proteins, individual species could not be identified. Analysis of non-reduced hC3d^{S}-HEL-Oct by western blotting following separation with manually prepared SDS-PAGE (2.5%/7.5%) proved conclusively the presence of high molecular weight protein, possibly octameric and at the correct size, when probed with a hC3d-specific antibody (figure 3.12 C). An octamer-specific polyclonal antibody was employed to detect the purified proteins in western blots. The banding pattern was inconclusive here, too, and due to this lack of clarity these gels are not shown. The imaging methods were fundamentally hampered by low protein concentration,

Figure 3.12. Size exclusion chromatography and protein analysis. Panel A shows typical elution traces recorded during the gel filtration using the superose 6 column on the Äkta Purifier system. 0.5 ml of concentrated anion exchange eluate in Tris NaCl was loaded and eluted into PBS over 1.5 CV. The graphs show the elution peaks at the volumes shown on the x-axis. The y-axis, as in figure 3.11 shows absorbance at 280 nm. The arrow indicates the elution peak fractions containing the largest M.W. proteins. These fractions were pooled and analysed. Panel B shows 3-8% Tris-acetate gradient gels (Invitrogen) prepared according to the manufacturer's instructions. Samples from the pooled peak fractions were separated under reducing conditions and stained with silver nitrate according to the standard procedure. The samples are indicated above, molecular weight markers on the left of each of the gel images. Arrows on the right indicate protein bands corresponding to the molecular weight of the octameric protein species. Arrows without molecular weight indicate that the specific weight could not be determined with certainty. Panel C shows a western blot of non-reduced hC3d^{S}-HEL-Oct loaded onto a manually prepared 2.5%/7.5% SDS-PAGE gel. hC3d^{S}-HEL-Oct was detected with Rb α hC3d and anti-Rb HRPO. Marker: SeeBlue Plus2; markers relate to different M.W. in Tris-acetate gels.

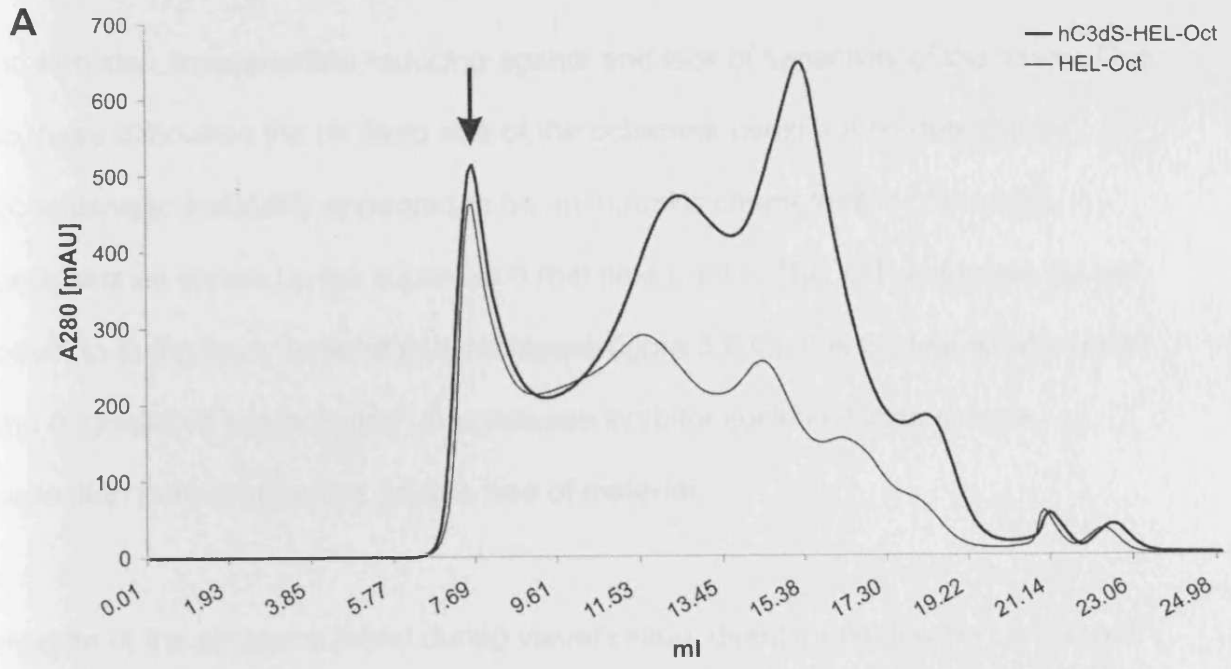
A
hC3dS-HEL-Oct
HEL-Oct
A280 [mAU]
700
600
500
400
300
200
100
0
0.01
1.93
3.85
5.77
7.69
9.61
11.53
13.45
15.38
17.30
19.22
21.14
23.06
24.98
ml

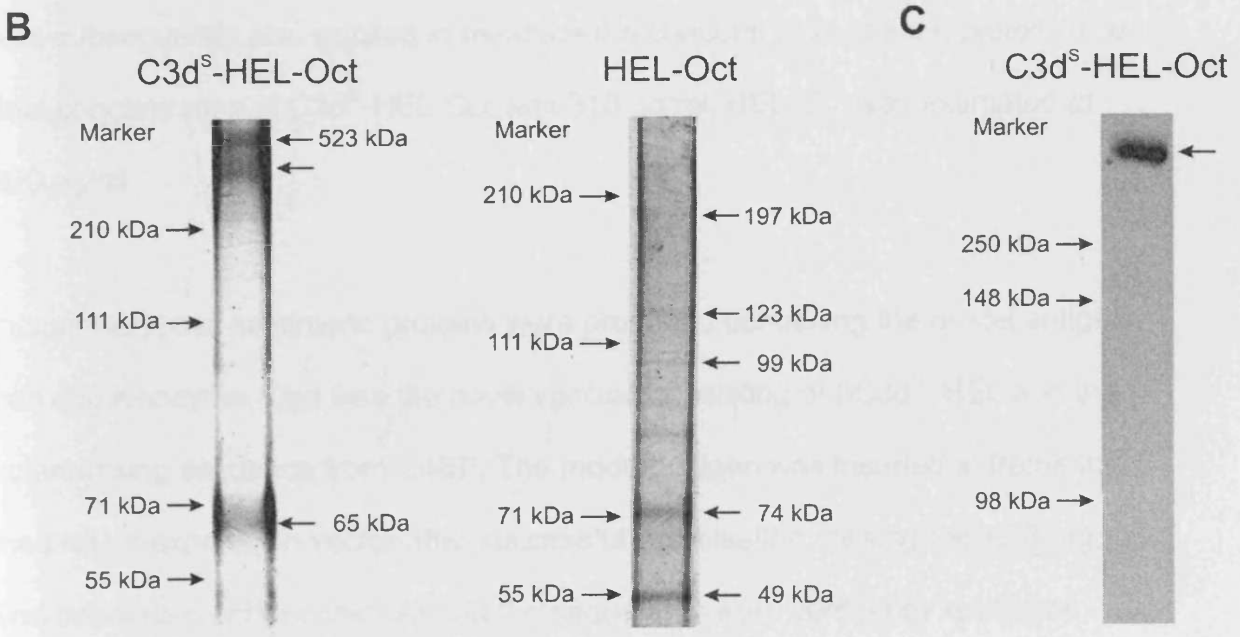
B
C3d^S-HEL-Oct
Marker
523 kDa
210 kDa
111 kDa
71 kDa
65 kDa
55 kDa
HEL-Oct
Marker
210 kDa
197 kDa
123 kDa
111 kDa
99 kDa
71 kDa
74 kDa
55 kDa
49 kDa
C
C3d^S-HEL-Oct
Marker
250 kDa
148 kDa
98 kDa

protein size, inappropriate reducing agents and lack of sensitivity of the assay. Due to these difficulties the *de facto* size of the octamers could not be determined conclusively. Instability appeared to be an intrinisic characteristic of the HEL octamers as shown by the superose 6 real time traces. The YFP octamers did not seem to suffer from these effects (compare figure 3.6 C). It is unclear what caused the degradation but inclusion of a protease inhibitor cocktail during sample collection may counter this severe loss of material.

In spite of the problems faced during visualisation, direct immobilisation in 96 well plates allowed detection of the proteins in an immunosorbent assay. This method was subsequently also applied to measure the concentration of each protein. The final concentration of $C3d^S$-HEL-Oct was 310 µg/ml, HEL-Oct was estimated at 200 µg/ml.

In summary, two multimeric proteins were produced containing the model antigen hen egg lysozyme. One was the novel vaccine consisting of $hC3d^S$, HEL and the octamerising sequence from C4BP. The model antigen was inserted in frame into the protein expression vector after successful optimisation utilising the YFP tag. The orientation of the construct and the sequences were verified by restriction digest and sequencing. Further examination by ELISA confirmed correct expression and excretion into the medium. Following a period of high-level protein production the proteins were purified for subsequent immunisation studies.

3.4 Discussion

The first study of this kind was published in 1996 using $mC3d^S$ as a molecular adjuvant in a linear trimer arrangement, which worked very efficiently (218). This pre-fabricated yet unnatural arrangement provided a protein complex consisting of antigen and C3d thus pre-empting opsonisation inside the body directing IC directly to B-cells and FDC. However, immune complexes do not develop as linear trimers during an immune response. Antigens are rather opsonised in all dimensions, covering the pathogenic surface cross-linking the target receptors BCR and CR2 in more than one dimension. We aimed therefore to design a recombinant immune complex that presented the antigen more naturally and at the centre of the protein. Although an elegant method of multimerising C3d as a tetramer by biotinylation have been described, this design does not easily lend itself to vaccine design (165). Using the self-octamerising signal from the C-terminus of C4BP, other investigators have created soluble oligomeric forms of cell-surface expressed complement receptors and inhibitors (315, 316). C4BP and these two recombinant proteins self-assembled in the cell and were excreted as multi-arm proteins. The present study therefore aimed to develop the molecular adjuvant approach further in this fashion by assembling a multivalent molecule covering a large surface area to recruit more BCR and CR2 to a single site.

The aim of this chapter was to establish an appropriate C3d construct that could be produced in DNA or protein form using our current vector and protein production facilities. The most appropriate choice of the human C3d component for cell binding also had to be confirmed. Most studies to date that used murine C3d had opted for a thioester-deactivated C3d ($mC3d^S$). Our octamer was optimised

according to presence or absence of the thioester moiety and the 'g' segment. YFP aided in the optimisation process in place of an antigen, which allowed visualisation via microscopy and FACS. Anti-hC3d, and later on anti-C4BP antibodies, were used for detection in immunosorbent assays and visualisation on western blots as well as dot blots.

Primarily the question of whether the hC3dg/hC3d octamer constructs could be expressed in mammalian cells was answered. This was vital for subsequent *in vivo* studies where the constructs would be administered both as DNA-based vaccines and as protein after production in cell culture. In previous studies, bacterial cell or insect cell-produced protein had been used for bulk production (165, 337-339). To avoid inappropriate antigenicity caused by misfolding and differences in posttranslational modification it was decided to generate all constructs in eukaryotic cells. This also provided a valuable base for comparison for the purpose of DNA vaccine design. Expression in prokaryotic or lower eukaryotic (such as insect cells) models could not provide adequate information. Eukaryotic cells are routinely utilised to confirm expression of DNA vaccines prior to *in vivo* administration (252, 253, 299, 300). Among them are CHO cells, which are frequently used for protein production prior to vaccine administration (340-342) and as a production system (343). These hardy and reliable cells are renowned for their longevity and robust production of protein (344) and were available in the laboratory. They provided a flexibly and easily applicable system for the experiments carried out in this study and were hence used for transient transfection and protein production. However, cell lines derived from skin (e.g. keratinocytes, see (252, 253, 296)) or muscle (e.g. myocytes) could have provided

more representative results when testing DNA vaccine administered by biolistic transfer or intramuscular injection (described in a later chapter), respectively but using CHO cells avoided optimisation of transfection for each cell line, which was not the aim of this current study. Additionally, each cell line has unique transfection characteristics and excretion of produced protein may vary. Although this approach may have yielded some useful information on the performance of the vaccines, the production profiles of cell lines are not a representation of events *in vivo*. Moreover, the mechanism of uptake of DNA especially following intramuscular injection is still uncertain and under intense investigation (section 1.10.1).

Attempts to transfect the finished constructs into CHO cells and the establishment of cell lines that exclusively produced one octameric variant at high levels were successful. Clones were selected that expressed protein up to two orders of magnitude above baseline indicated by the shift in mean fluorescence (figure 3.5). Together with western blotting experiments (figure 3.6) it was clearly demonstrated that fluorescent protein containing hC3dg, hC3d^{S}g, hC3d or hC3d^{S} was produced in the cell.

The size of the octamers (tables 3.1 and 3.2) proved cumbersome, especially concerning visual detection via SDS-page, throughout the optimisation process. SDS-PAGE gels were prepared at low density to allow entry of the protein into the separating gel from the stacking gel. Transfer onto nitrocellulose membranes was optimised thoroughly by extending the transfer time, changing the buffer system (331) and adjustment of detecting antibody concentration until post-transfer silver stains of the gels confirmed complete transfer of the separated protein.

Visualisation of the octamers by silver staining and Coomassie blue staining was particularly difficult, mainly caused by low concentration of protein making it hard to distinguish it from the background staining. Reduction had been successful following the assessment of cellular content of hC3dg/hC3d^{S}g/hC3d/hC3d^{S}-YFP-Oct. Later experiments with octamers containing HEL only achieved incomplete reduction for reasons that are unknown. This caused "laddering" of hC3d^{S}-HEL-Oct and HEL-Oct, which made identification of specific bands challenging.

The purification process used in this study was optimised following several attempts to make affinity columns. In general, this approach is favourable and used in preference to charge separation or size exclusion. However, affinity columns using a variety of monoclonal and polyclonal antibodies failed to effectively purify the octamers. This was apparently due to insufficient affinity of commercial and in-house produced polyclonal antibodies. Furthermore, production of a monoclonal antibody specific for human C3dg resulted in an antibody, which would function in conjunction with its carrier and not just with hC3dg alone. Additionally, as the purification of HEL-Oct would also require a separate affinity column or a different approach, a purification method was devised that could be applied to both octameric proteins. As no HEL-specific monoclonal antibody was available in the lab it was decided to use column chromatography. A two-step method using ion exchange and size exclusion chromatography was chosen, allowing both octamers to be purified with the same protocol. Although hC3d^{S}-HEL-Oct and HEL-Oct were exposed to several buffer changes, filtration and two columns this method produced sufficient amounts for vaccinations. Visualisation of the purified proteins was particularly challenging. The wells in gradient and conventional gels only

allowed loading of approximately 2 – 3 µg per well. This could also only be attempted a limited number of times to conserve enough reagent for the *in vivo* experiments. Non-reduced protein was relatively simple to detect with a hC3d-specific antibody (figure 3.12 C). The protein detected by silver stain was to undergo mass spectrometry analysis however due to the low amounts in the gel and the limitations discussed above this final identification step was abandoned. Mass spectrometric analysis will in the future provide definite information on the number of arms present in the molecule. The size observed in gels indicates a natural conformation of seven or eight arms, very much similar to C4BP in serum (345-347). The purification method, purification conditions (buffers, temperature, etc.) and ultimately the products, their stability following anion exchange and gel filtration (storage, contamination, etc.) and purity therefore require comprehensive investigation and possibly revision. Protein production may also have to be modified in an attempt to minimise breakdown, e.g. with a protease inhibitor cocktail. Visualisation could have been improved using larger gels, which would be more suitable for the resolution of such large proteins. Such experiments could not be carried out at this point due to the limited availability of material. This could have been resolved partially with proteins of known molecular weight run as standards through the gel filtration column.

The above experiments proved conclusively that fluorescent proteins containing hC3d were expressed. As part of this project and due to the realisation that large-scale production of the protein was cumbersome and time-consuming, the decision was taken to incorporate hC3d^{S}-HEL-Oct in a DNA vaccine. DNA vaccination in essence represents *in vivo* transfection of the recipient, therefore two vital

variables had to be addressed prior to administration: successful expression and excretion from the cell. As the octamer was intended to bind to B-cells and FDC for activation and affinity maturation it was vital the protein was not retained in the cell. The addition of the CD33 signal sequence aided excretion but several factors within the adjuvant could influence expression and potentially cause retention. Although the 'g' segment could play a role, the main focus was on the thioester and behaviour of respective variants that contained the mutated cysteine to serine or the wild type sequence. The results clearly showed that mutation of the thioester motif significantly increased the amounts in the supernatant of transfected cells. Cytoplasmic content was also slightly higher in cells expressing the mutated variants. Interestingly – though not quantitative – the differences in excretion were distinguishable in western blotting analysis. Thus, the data herein showed that there were clear differences between the four variants. Surprisingly, hC3d^{S}, the human equivalent to the mouse protein favoured by most studies in the past (165, 218, 252, 253, 256, 300), did not show the best expression and excretion profile, in fact it performed worse than hC3dg. Compared to each wild type, mutating the thioester moiety improved the production (figure 3.7). It was speculated that there would also be differences in excretion levels. These would be dependent on the presence of the thioester motif, which, from the moment of translation, could allow formation of ester linkages to intracellular structures. This could lead to higher cellular retention of the wild type versions. Surprisingly, the data suggested this was not the case, probably because the thioester motif underwent instant hydrolysis internally before it could interact with internal target sites. Considering all constructs were under the control of the same promoter, were transfected into equal numbers of cells at adjusted plasmid concentrations, these diverse quantities

in the cells do suggest that the modifications of the C3 portion of these fusion proteins had a measurable effect on eventual protein production levels. Of the four, hC3d^{S}g-YFP-Oct performed best in these assays, suggesting that the 'g' portion may act to stabilise this protein and aid its successful excretion. These data indicated that the choice of the minimal C3d form in previous vaccines might have been ill advised, possible based on production in other cell types (i.e. bacteria production).

High expression levels of octamer fusion protein are desirable but functionality of the protein is paramount. An ELISA-based assay using immobilised hCR2 (SCR1-4) Fc fusion protein demonstrated that all these proteins were correctly folded and that octamerisation did not directly affect their function, i.e. they interacted well with their natural ligand. Both hC3d versions bound stronger than their hC3dg counterparts, with hC3d^{S} binding stronger than any of the other variants. hC3d^{S}g-YFP-Oct consistently exhibited weakest binding.

The two degradation products of C3, C3dg and C3d, have been employed in the literature for a number of years and have been treated as equals (23, 165, 189, 207, 217, 223, 348-350). C3d – unless produced as a recombinant protein in DNA vaccination studies – is usually generated by trypsin digestion (297, 351, 352). Two more non-complement enzymes, elastase and plasmin, have also been reported to produce C3d (353) although the sizes of C3d and C3g deviate slightly depending on the respective protease used to cleave C3 (96). The resultant fragment C3g so far has not had a specific function ascribed to it and only two monoclonal antibodies have been identified (353-355). Thus, due to the

interchangeability of the two degradation products the influence of C3g on CR2-binding has not been addressed directly. Indeed, it is because of this that the actual degradation product attached to the antigen and binding CR2 has not been conclusively described. All studies taken into account, C3d, degraded by above-mentioned proteolytic enzymes, may be the physiological cross-linking protein. Hence, C3dg may only have a very short life span. This fact reinforces the rationale behind the arrangement hC3d^{S}-HEL-Oct of the current vaccine design. In the coding sequence C3g is encoded upstream of C3d. This positions C3g outermost in the octamer and exposes it as a target for trypsin cleavage in physiological conditions. Arranging the single-arm sequence as HEL-hC3dg-Oct or HEL-hC3d^{S}g-Oct would have caused destruction of the functional vaccine as HEL-hC3g are released.

The results presented herein explain why hC3d^{S} was previously chosen to be employed as molecular adjuvant and indicate that a small compromise with regards to stability or production profile has been taken with its use thereof. The data would suggest that hC3g, though small (~5 kDa), was influencing binding to CR2. This possibility was addressed in more detail in the following chapter. Interactions between ligand and receptor were analysed with each, C3dg, C3d^{S}g, C3d and C3d^{S}, as Fc fusion protein. These proteins were designed and produced to allow more accurate measurements of the strength binding to human as well as murine CR2 in Biacore analysis, where analysis using the previous octameric proteins would be practically impossible.

Chapter 4

In Depth Analysis of the Functional Interactions Between C3d and CR2 of Human and Murine Origin

4.1 Introduction

The successful production of a mutant version of human C3d fused to the model antigen HEL and the octamerising sequence derived from C4BP was demonstrated in the previous chapter. Further key steps serving its characterisation had to be taken before the C3d octamer construct could be taken from research in the laboratory to immunisation of human subjects. At this stage, function was examined by *in vitro* methods ahead of *in vivo* modelling in mice. Three strains of mice comprise the *in vivo* model, wild type mice, expressing CR2 normally on B-cells and FDC (section 1.7.2), $Cr2^{-/-}$ mice and human CR2 transgenic mice, $Cr2^{-/-}$ $hCR2^{+/-}$. In preparation of the *in vivo* studies the aim was to dissect the interaction between C3d and CR2, specifically between human and murine complement protein species. These analyses relied on established methods such as cell surface binding and detailed single molecule interactions using surface plasmon resonance (SPR).

In this part of the study, cell assays as well as SPR analyses were used to investigate the interaction of C3d with CR2. Fc fusions of all interaction partners were designed and generated to elucidate affinities between the various ligands and receptors. Fc fusions have found wide use in a variety of *in vitro* and *in vivo* methods (179, 356-358). They provide a bivalent recombinant protein that can be purified with relative ease thanks to widely available specific affinity purification columns (e.g. protein A, protein G). As mentioned above, murine and human complement proteins have been used interchangeably in past studies. Nevertheless, specific and detailed data on the ability of hC3d to bind in a physiological manner to mouse CR2 is not available. Therefore, the experiments

described in the following section were designed to assist in making predictions on functionality of the human C3d octamer vaccine in another species (primarily mouse) with closely related complement proteins. Firstly, the ability of the four human C3d variants described in the previous chapter to bind hCR2 was compared in depth via cell-based assays. Secondly, the experiments were broadened to examine the interaction of murine C3d and human CR2. Finally, experiments were carried out to investigate the interaction of hC3d with mouse CR2. To date, the kinetic mechanisms of interactions of this kind have not been clearly defined. Thus, surface plasmon resonance studies were also used to examine the cross-species relationships between these molecules in order to assess their implications in future vaccine designs and their testing *in vivo*.

4.2 Materials and Methods

4.2.1 Preparation of Constructs and Vectors

pDR2 EF1α Fc (figure 4.1) was based on vector pDR2 EF1α (see 3.2.1). The Fc version contained the Fc region of human IgG1 (726 bp) inserted at the Bam H1 and Eco RV site was previously described by Harris *et al.* (356, 359). The protein of interest was inserted in-frame into the multiple cloning site using the Spe I and Not I restriction sites (figure 3.2).

4.2.2 Murine Splenocytes

C57Bl/6 mice were sacrificed humanely according to Home Office guidelines. Isolated spleens were crushed between two frosted glass slides, ground to a single cell suspension and resuspended in 10 ml PBS. After a 10-minute incubation on ice large debris fragments had settled to the bottom of the tube. 8 ml were taken off without disturbing the precipitate and spun at 300 x *g* for 3 minutes. The supernatant was discarded; the cell pellet was resuspended in flow buffer and washed once more. The remaining staining procedure was carried out as described in section 2.9.

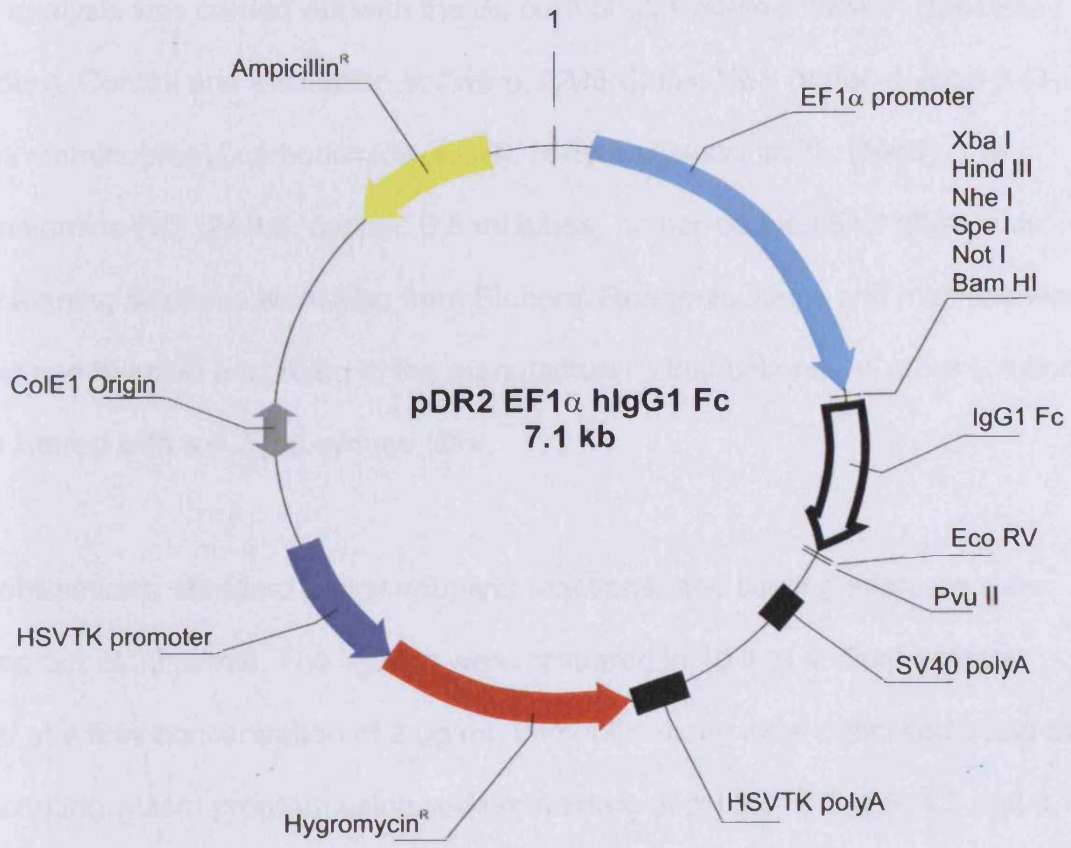

Figure 4.1. pDR2 EF1α hIgG1 Fc

4.2.3 Surface Plasmon Resonance Analysis

SPR analysis was carried out with the Biacore 3000 system (Biacore, Uppsala, Sweden). Control and evaluation software, CM5 Chips, HBS buffer, 1-ethyl-3-(3-dimethylaminopropyl)carbodiimide (EDC), N-hydroxysuccinimide (NHS), 1 M ethanolamine-HCl pH 8.5, capped 0.8 ml tubes, rubber-capped 5 ml glass vials and cleaning solutions were also from Biacore. Reagents, chips and machine were set up and handled according to the manufacturer's instructions. All other solutions were filtered with a 0.2 µm syringe filter.

Immobilisations, standard amine coupling reactions, and binding analyses were carried out at 30 µl/min. The ligands were prepared in 10 mM sodium acetate buffer at a final concentration of 2 µg/ml. Immobilisations were optimised using the pH scouting wizard program using sodium acetate at pH 5.4, 5.0, 4.6, 4.2 and 3.7. The immobilisation wizard controlled the coupling reactions. Solutions were set up as advised using equal volumes of NHS and EDC, the ligand in the appropriate buffer, 1 M ethanolamine-HCl pH 8.5 and 50 mM NaOH. The coupling was automatically terminated when the response unit (RU) target was reached. Typically, flow cell one (FC1) was left blank to act as control flow cell and only received NHS/EDC and 1 M ethanolamine-HCl pH 8.5. The dextran matrix in FC2 was activated with NHS/EDC, followed by ligand. Remaining free binding sites in the matrix were blocked with 1 M ethanolamine-HCl pH 8.5.

Binding analyses were carried out immediately after coupling. Prior to loading of the samples, flow was allowed to stabilise for one minute. Analyte concentrations were 0 nM (blank buffer control), 0.195 nM, 0.39 nM, 0.78 nM, 1.56 nM, 3.125 nM,

6.25 nM 12.5 nM, 25 nM, 50 nM. Analytes were injected in triplicate for 360 seconds. The injection was changed from sample to buffer and dissociation was monitored for 240 seconds. Typically the flow path was FC1 followed by FC2, which allowed subtraction of any secondary interactions with the dextran matrix. Chip surfaces were regenerated with two brief pulses of 0.5 M NaCl for 30 seconds.

Results were analysed using the BIAevaluation Software version 4.1. Single flow cells were analysed following blank flow cell background subtraction (e.g. FC2-FC1). Curves were aligned by y-axis transformation and blank samples (0 nM) were subtracted from the curve to compensate for buffer-surface interactions. Sensogram data was analysed with a steady state affinity model. Good fits were indicated by low residual and χ^2 values (< 5) as calculated by the evaluation software.

4.3 Results

4.3.1 Production of Fc Fusion Proteins

4.3.1.1 Mouse C3d^S, Human CR2 and Mouse CR2

Plasmids containing mouse C3d^S Fc (mC3d^S Fc) or human CR2 Fc SCR 1 – 4 (hCR2 Fc) FC fusions were previously available in the laboratory. The mouse CR2 Fc (mCR2 Fc; based on Crry Fc (357) and later work by Atkinson *et al.* (360) vector DNA was a kind gift from Dr Susan Boackle (University of Colorado at Denver and Health Sciences Centre, USA). These plasmids were transformed in DH5α and transfected into CHO cells as outlined in sections 2.7 and 2.8.1.

4.3.1.2 Construction of hC3dg, hC3d^{S}g, hC3d and hC3d^S Fc Fusions

Fc fusion proteins of the four previously described hC3dg variants (chapter 3.2 and figure 4.2 A) were produced to study the affinities of each with CR2. These recombinant bivalent proteins were intended as the next step in the vaccine optimisation process. The fluorescent C3d octamer approach had covered the production side of the optimisation. The Fc fusions on the other hand served to provide a model to forecast effects *in vivo*, highlighting the vital need to examine cross-species functionality of the novel vaccine. The present experiments were carried out in parallel to the production of the octamer as part of the hC3d selection process; hence all four mutations were examined to provide data on their relative functionality.

Figure 4.2. Fc fusion DNA and protein expression. Panel A is a graphical representation of the fusion protein structure. Fc fusion proteins are homodimers of the protein of interest fused to the human IgG1 Fc region. Panel B is a restriction digest carried out with Eco RV, Spe I and Not I. Shown are two clones of each hC3dg, hC3d and hC3d^{S}g as the final clone, hC3d^{S}, was generated by deletion of 'g' from hC3d^{S}. Bands in each lane refer from top to bottom to pDR2 EF1α Fc vector backbone, hC3dg variant and Fc fragment. Non-reducing (panel C) and reducing (panel D) SDS-PAGE gels/western blots were set up ten days after transfection. Neat supernatant samples were loaded as indicated into wells of 2.5%/7.5% gels and transferred onto nitrocellulose membranes following separation. hC3d-containing proteins were detected with Rb α hC3d and α Rb HRPO at the approximate predicted sizes (see text).

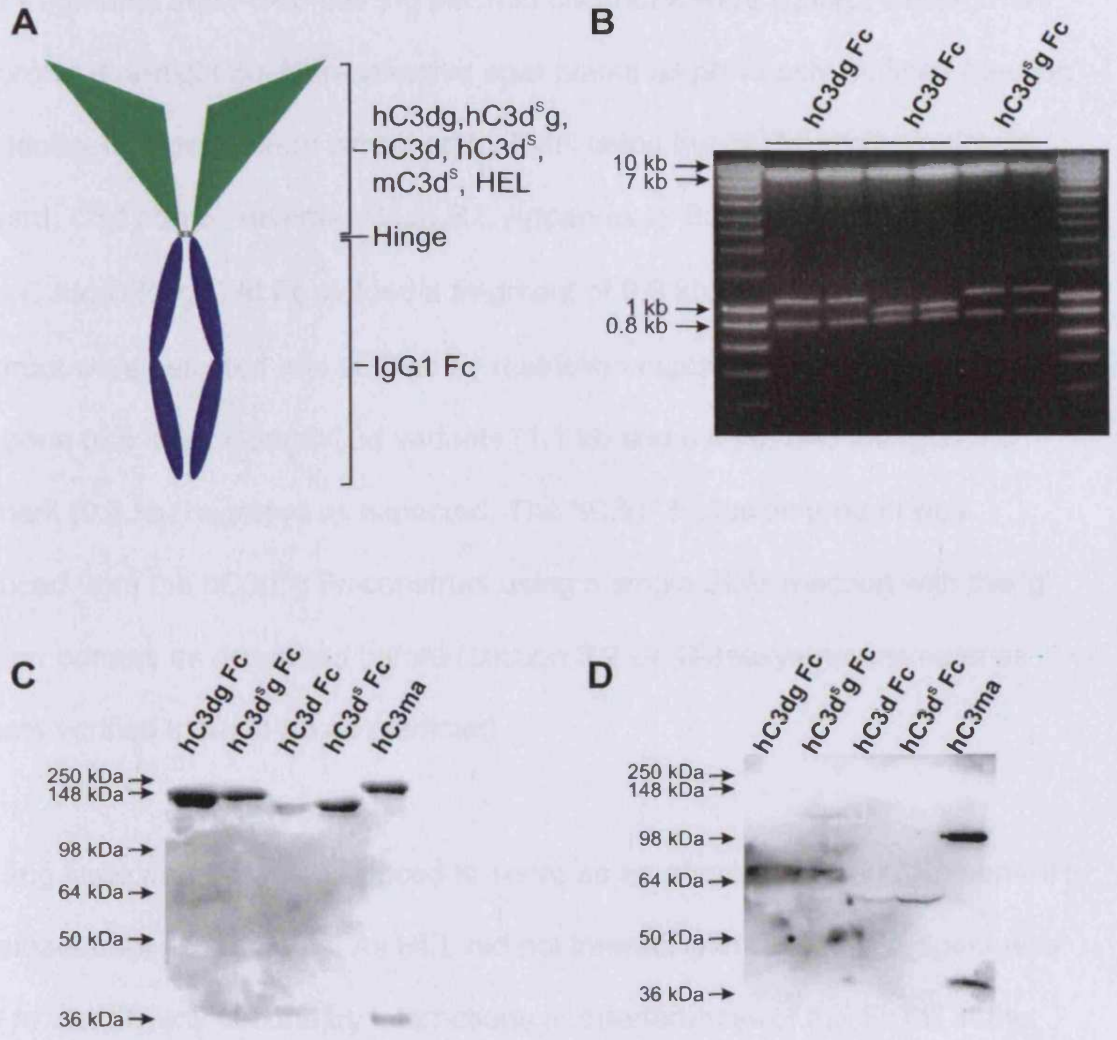
A
hC3dg,hC3d^{S}g,
hC3d, hC3d^{S},
mC3d^{S}, HEL
Hinge
IgG1 Fc
B
hC3dg Fc
hC3d Fc
hC3d^{S}g Fc
10 kb
7 kb
1 kb
0.8 kb
C
hC3dg Fc
hC3d^{S}g Fc
hC3d Fc
hC3d^{S} Fc
hC3ma
250 kDa
148 kDa
98 kDa
64 kDa
50 kDa
36 kDa
D
hC3dg Fc
hC3d^{S}g Fc
hC3d Fc
hC3d^{S} Fc
hC3ma
250 kDa
148 kDa
98 kDa
64 kDa
50 kDa
36 kDa

hC3dg, hC3d and hC3d^{S}g cDNA fragments were cut out of their respective octamer plasmids using Spe I and Not I (compare figure 3.3). pDR2 EF1α Fc was then digested with the same enzymes and dephosphorylated using SAP. The hC3d fragments and Fc-containing plasmid backbone were ligated, transformed and grown overnight on Amp-selective agar plates as previously outlined (section 2.6). Isolated colonies were screened by PCR using two hC3d-internal primers (forward: C3d nog 5', reverse: C3dg R2, Appendix I). Bacteria containing pDR2 EF1α C3dg/C3d^{S}g/C3d Fc yielded a fragment of 0.9 kb. Two clones of each construct were selected and verified by restriction digest (figure 4.2 B). The vector backbone (6.5 kb), hC3dg/hC3d variants (1.1 kb and 0.9 kb) and the IgG1 Fc fragment (0.8 kb) migrated as expected. The hC3d^{S} Fc fusion protein was produced from the hC3d^{S}g Fc construct using a single SDM reaction with the 'g' deletion primers as described before (section 3.2.2). Dideoxysequencing of all variants verified them to be as predicted.

Hen egg lysozyme Fc was produced to serve as an appropriate negative control in the subsequent experiments. As HEL did not interact with CR2, this reagent was used to identify any secondary interactions or interferences of the Fc tail in the assays. HEL Fc was generated in the same way as the above fusions with HEL primers containing Spe I (forward) or Not I (reverse) restriction sites respectively. Clones were identified by PCR, their sequences were verified by sequencing only.

4.3.2 Optimisation of the hC3dg/hC3d Fc Fusions Production and Purification

hC3dg/hC3d Fc fusion plasmid DNA was transfected into CHO cells as described in materials and methods (section 2.8.1). Ten days after transfection, supernatant was collected for western blot analysis. hC3dg/hC3d-containing proteins were expressed at the predicted sizes (figure 4.2 C) i.e. bands corresponding to hC3dg and hC3d^{S}g (approximately 139 kDa) and hC3d and hC3d^{S} Fc fusion proteins (approximately 122 kDa). The positive control, methylamine-treated human hC3 (hC3ma) was detected at the expected size of 185 kDa and smaller bands in that lane are likely to represent the final proteolytic breakdown product of hC3, hC3dg (36 kDa) or hC3d (30 kDa). Western blots carried out under reducing conditions (figure 4.2 D) showed monomeric Fc fusions. The detected bands corresponded to the predicted sizes of hC3dg and hC3d^{S}g (69.5 kDa) and hC3d and hC3d^{S} (66.3 kDa). Again, in the hC3ma control lane the remaining hC3 α-chain could be visualised at approximately 104 kDa as well as the 36 kDa hC3dg band. Only the α-chain was detected because it contained the hC3d portion and this assay was carried out using a hC3d specific antibody.

The Fc fusion protein supernatants were subjected to trial purifications using a protein A column. Fc fusion proteins are usually affinity purified with Ig-specific protein A or protein G affinity columns. Protein A was chosen because the affinity to human IgG1 was higher compared to protein G. Analysis of purified samples by SDS-PAGE and dot blotting revealed contamination with bovine immunoglobulins (figure 4.3 A, top band with asterisk, B). In an attempt to remove bovine Ig from

Figure 4.3. Expression and purification of the human C3dg, C3d^{S}g, hC3d and C3d^S Fc proteins. Panel A shows a 2.5%/7.5% SDS-PAGE stained with silver nitrate (section 2.12.4). Samples were derived from a trial protein A purification. Separate bands detected from top to bottom refer to the different species of fusion protein as indicated to the right of the image. A contaminant band is indicated by an asterisk (*). B: Glycine and citrate eluate samples were screened by dot blot with an α bovine Ig antibody indicating bovine Ig contamination in the 0.1 M glycine pH 2.5 eluates in fractions 1 and 2. rProtein A FF pre-column samples (CHO culture supernatant, S) and column purified samples (P) were analysed by non-reduced (panel C) and reduced (panel D) SDS-PAGE. Samples were visualised by coomassie staining. Molecular weight marker: SeeBlue Plus2

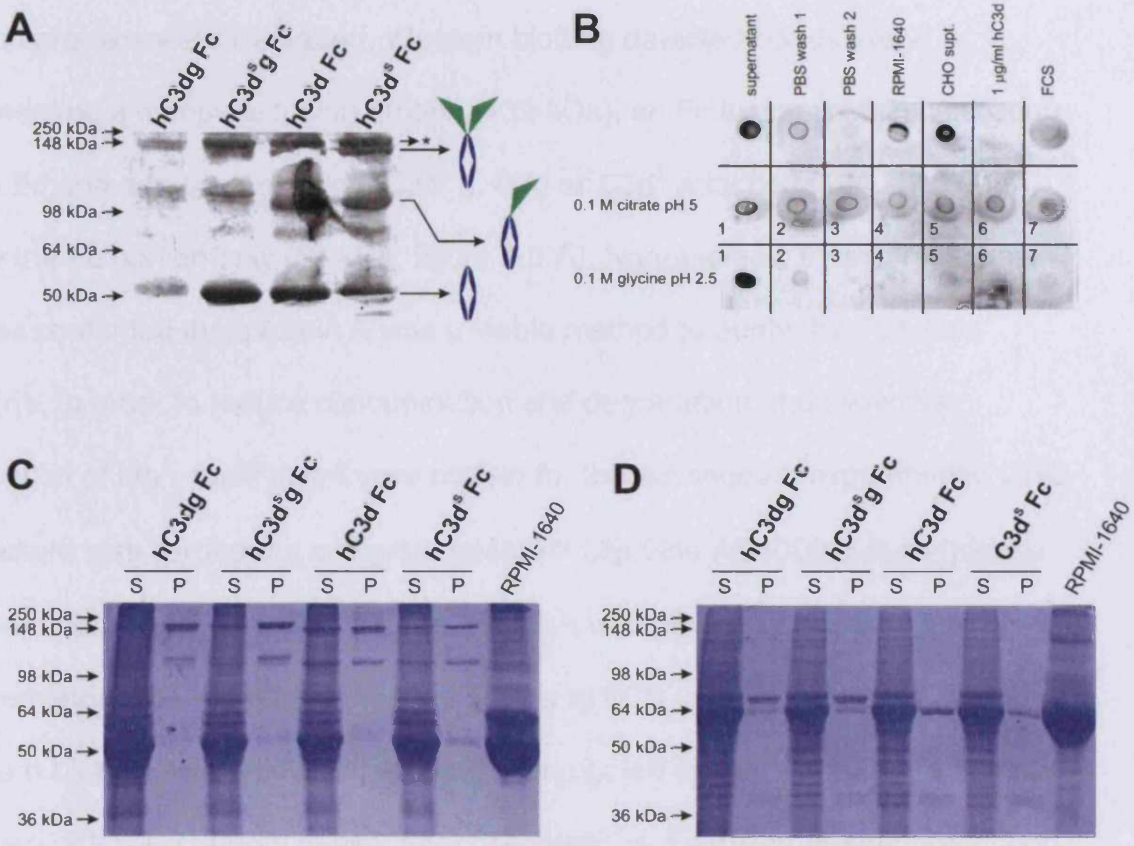
A
hC3dg Fc
hC3d^{s}g Fc
hC3d Fc
hC3d^{s} Fc
250 kDa
148 kDa
98 kDa
64 kDa
50 kDa
B
supernatant
PBS wash 1
PBS wash 2
RPMI-1640
CHO supt.
1 µg/ml hC3d
FCS
0.1 M citrate pH 5
0.1 M glycine pH 2.5
1 2 3 4 5 6 7
C
hC3dg Fc
hC3d^{s}g Fc
hC3d Fc
hC3d^{s} Fc
RPMI-1640
S P
250 kDa
148 kDa
98 kDa
64 kDa
50 kDa
36 kDa
D
hC3dg Fc
hC3d^{s}g Fc
hC3d Fc
C3d^{s} Fc
RPMI-1640
S P
250 kDa
148 kDa
98 kDa
64 kDa
50 kDa
36 kDa

the supernatants, 0.1 M citrate pH 5 elution buffer was applied prior to elution of the Fc fusion proteins in 0.1 M glycine HCl pH 2.5 (figure 4.3 B, glycine elution fraction 1). This procedure was largely successful but some bovine Ig remained. Unfortunately, these pilot studies also revealed that the majority of the purified fusions proteins were degraded. Western blotting detected bands likely representing a complete fusion protein (139 kDa), an Fc fusion protein consisting of the Fc and one copy of C3dg, C3d^{S}g, C3d or C3d^{S} attached (104 kDa) and finally the Fc portion only (50 kDa; figure 4.3 A). Nonetheless, these preliminary studies confirmed that protein A was a viable method to purify the Fc fusion proteins. In order to reduce contamination and degradation and allow the production of high quality/ultra pure protein for the subsequent experiments, CHO cell culture was carried out using the Integra™ CELLine AD1000 culture (please compare section 3.3.7) system. Contamination with bovine Ig was addressed by supplementing the media with 5% low bovine Ig FCS instead of 10% FCS. Western blotting with a bovine Ig-specific conjugated antibody confirmed complete absence of bovine Ig from subsequent preparations. Fc fusion protein production was scaled up and supernatant samples were purified with a 1 ml rProtein A HiTrap column using the Äkta Prime system. The concentration of fusion proteins was measured by spectrophotometry at 280 nm while coomassie stains served to assess quality and purity. Examples of C3dg/C3d^{S}g/C3d/C3d^{S} proteins purified in this manner are shown in figure 4.3 C (non-reduced) and D (reduced). These data confirmed that the optimised method improved the purity and quality of the products by decreasing levels of degradation. However hC3d^{S} Fc, whilst improved, was still slightly more degraded than the other fusions demonstrating that other factors influenced fusion protein stability.

Figure 4.4. Identification of Fc fusion breakdown products. 2.5%/7.5% gels were loaded with samples prepared in the same way as discussed in figure 4.3 D. Panel A shows a gel stained with silver nitrate of a three half-step dilution series of 1:25, 1:50 and 1:100. Panels B and C show the gels transferred to nitrocellulose membranes and probed with anti human C3d and anti human Fc respectively. Marker: SeeBlue Plus2

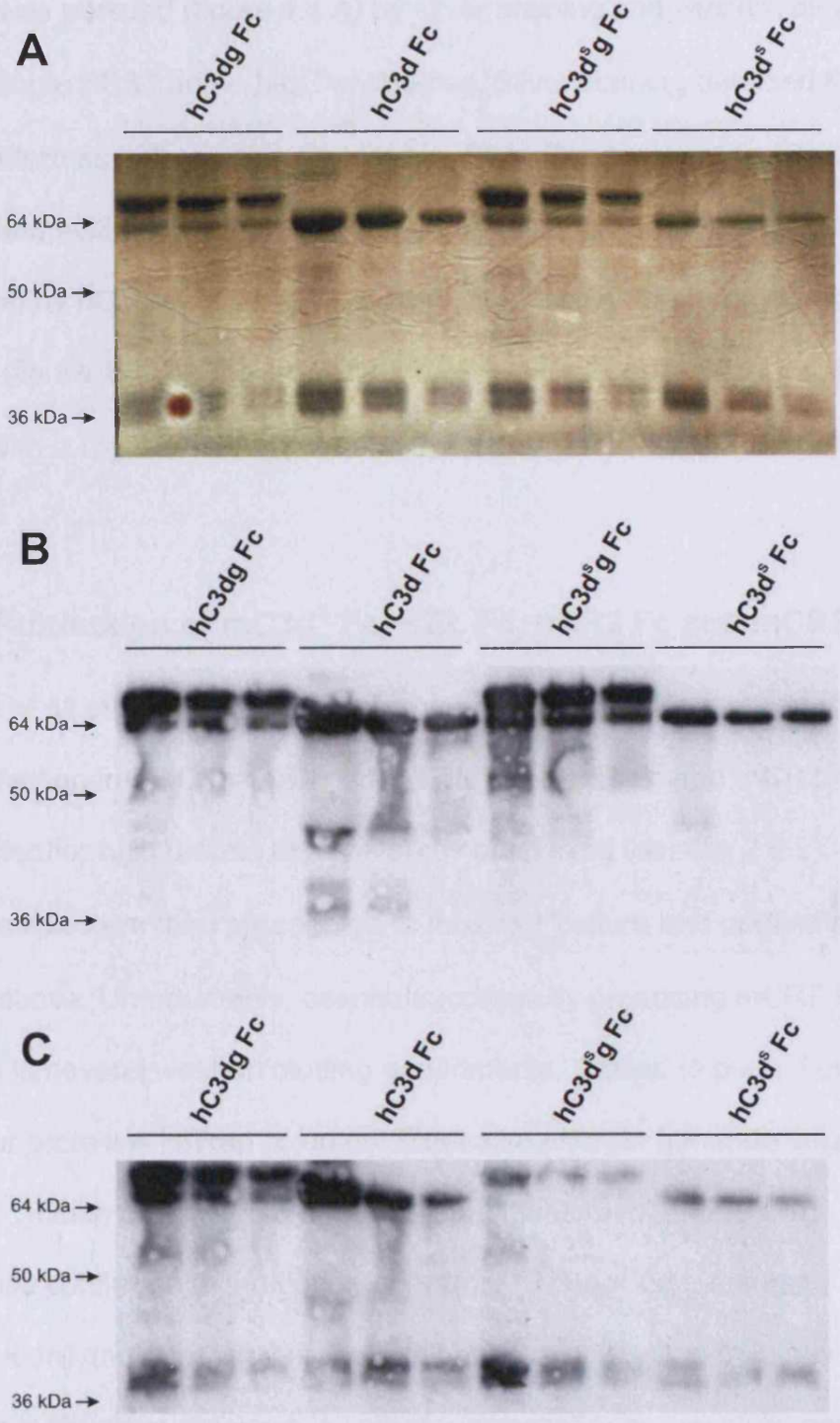
A
hC3dg Fc
hC3d Fc
hC3d^{s}g Fc
hC3d^{s} Fc
64 kDa
50 kDa
36 kDa
B
hC3dg Fc
hC3d Fc
hC3d^{s}g Fc
hC3d^{s} Fc
64 kDa
50 kDa
36 kDa
C
hC3dg Fc
hC3d Fc
hC3d^{s}g Fc
hC3d^{s} Fc
64 kDa
50 kDa
36 kDa

Furthermore, in the reducing gel, two smaller fusion protein species were detected in the hC3dg Fc and hC3d^{S}g Fc lanes (figure 4.3 D). The identification of these fragments was pursued (figure 4.4 A) by silver staining and western blotting analysis using α hC3d and α hIgG antibodies. Silver staining detected the same banding pattern as before using Coomassie Blue. The smaller two bands in the hC3dg Fc and hC3d^{S}g Fc lanes had the same apparent M.W. as hC3d and hC3d^{S}. Identification by hC3d-specific antibody indicated loss of the 'g' portion by unknown processes (figure 4.4 B). The lower molecular weight bands were identified as hIgG1 Fc with α hIgG HRPO (figure 4.4 C).

4.3.3 Production of mC3d^{S} Fc, HEL Fc, hCR2 Fc and mCR2 Fc

Production of all other Fc-fusion proteins was based on the optimised methods. After transfection in CHO the mC3d^{S} Fc, HEL Fc, hCR2 Fc and mCR2 Fc fusions were selected for high protein expression by outcloning (section 2.8.2). Clones with high expression were then propagated in Integra™ culture and purified as described above. Unfortunately, despite successfully producing mCR2 Fc and detecting it in several western blotting experiments, it failed to purify from either protein G or protein A HiTrap columns. Extensive effort to generate large quantities of mCR2 Fc fusion protein were unsuccessful, these results were also subsequently confirmed in the donor laboratory (S. Boackle, personal communication) and suggest that there might be an intrinsic problem with the mCR2 Fc construct we obtained. All other fusions were successfully generated and purified identically to those in the previous section. Concentration and purity were analysed as discussed above (figure 4.5). Coomassie blue staining of all Fc

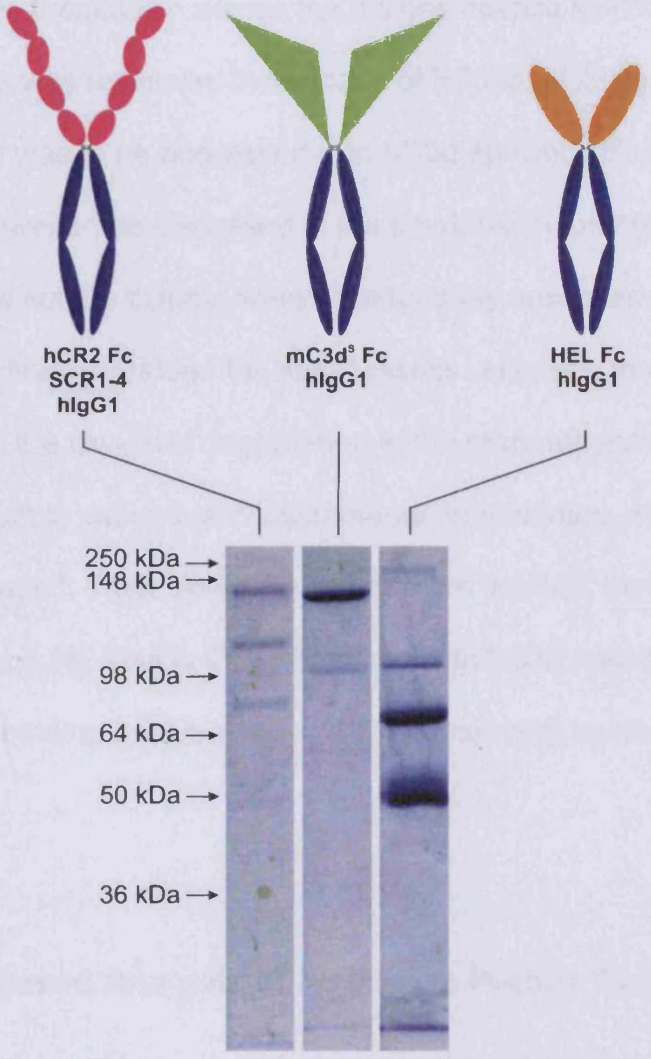

Figure 4.5. Murine C3d^S, hCR2 and HEL Fc fusion proteins structure and purity. Diagrams of the structures of the three fusion proteins and gel strips of 10% non-reducing SDS-PAGE gel(s) loaded with 10 µg/ml of each fusion followed by staining with coomassie blue (section 2.12.3). Major bands from top to bottom in the hCR2 Fc, mC3d^S Fc and HEL Fc lanes represent two-arm, one-arm and Fc only. Molecular weight marker: SeeBlue Plus2

fusions analysed on SDS-PAGE gels still indicated degradation and loss of the non-Fc portion although reduced compared to the previous analysis. The reason for the differences in breakdown across the fusions despite standardised production methods was unknown. In the case of hC3dg, hC3d^{S}g, hC3d and hC3d^{S} this problem was to be addressed with hC3d-specific affinity chromatography however, as discussed in the previous chapter (section 3.4), attempts to produce such a column were unfortunately unsuccessful. Repetition of production and purification yielded the same results. Although the majority of the fusions were intact, the low-level degradation in the preparations therefore had to be taken into account in subsequent experiments. In summary, seven Fc fusion proteins were produced. Their DNA sequences were verified, transfected and produced in CHO culture. This is the first time hC3dg/hC3d fusion proteins have been produced for binding analyses using both human and murine species ligands and receptors.

4.3.4 ELISA-Based Analysis of Fc Fusion Protein Function

The Fc fusion proteins had been detected successfully in western blotting using Fc-specific and hC3d-specific antibodies. In order to apply the immunosorbent assay from section 3.3.5 to the Fc fusion proteins, it was decided to ensure that hC3d could be detected in this assay. Hence, ELISA plate wells were treated with Gt α human Fc as capturing antibody. The human hC3dg/hC3d^{S}g/hC3d/hC3d^{S} Fc fusions were diluted, as before, in blocking buffer and loaded into the wells in triplicate at 2 μg/ml, 1 μg/ml, 0.5 μg/ml and 0.25 μg/ml. hCR2 Fc was used as a negative control at the same concentrations. The remainder of the assay was

carried out as described in section 2.12.6 using a monoclonal Ms α hC3d antibody and anti-mouse Ig-HRPO. As expected, all four human C3d versions were captured by the Fc-specific antibody and subsequently detected by the monoclonal anti-hC3d antibody (figure 4.6 A shows 1 µg/ml only). hCR2, the negative control, was not detected by the monoclonal antibody. With the confidence that hC3d could be detected in western blotting and ELISA the experimental design was changed to immobilisation of hCR2 Fc. hC3dg/hC3d^{S}g/hC3d/hC3d^{S} Fc fusions were loaded and detected with a polyclonal Rb α hC3d to conserve reagents. The antibody recognised monomeric hC3d in control wells but unexpectedly failed to detect the hC3dg/hC3d^{S}g/hC3d/hC3d^{S} Fc variants (figure 4.6 B). It is possible that the interaction between hC3d and CR2 prohibited access of the polyclonal antibody to the hC3d epitopes. This was probably caused by the presence of the Fc terminal protruding into the medium. Thus the conformation and the binding of these Fc fusions prohibited application of this assay in this particular case. Hence, this approach was not pursued any further. An alternative method was required to establish that the hC3d Fc proteins could bind directly to CR2 in a functional context, i.e. could hC3d bind CR2 expressed on the B-cell surface.

4.3.5 *In Vitro* Cell Binding Analysis Using the Human B-cell Lymphoma Cell Line Raji

In order to determine whether the fusion proteins would bind to hCR2 on the B-cell surface, hC3dg Fc, at concentrations ranging from 20 µg/ml to 0.3 µg/ml (7x 1:1) or the α CR2 monoclonal antibody, 171 (100) as control, were incubated with 1 x 10^{6} Raji cells (figure 4.7 A, B). Fc receptors were blocked prior to staining using

Figure 4.6. Analysis of hC3dg/hC3d^{S}g/hC3d/hC3d^{S} by immunosorbent assay. Gt α human Fc (panel A) was immobilised in ELISA plate wells at 100 ng/ml. Fc fusion proteins were loaded in blocking buffer and detected with a Ms α hC3d mAb and HRPO-conjugated anti-mouse Ig. hCR2 Fc was applied as negative control. Of the four concentrations 2.0, 1.0, 0.5 and 0.25 μg/ml only 1.0 μg/ml is shown for the sake of clarity. hCR2 Fc (panel B) was immobilised at 100 ng/ml and received hC3dg, hC3d^{S}g, hC3d or hC3d^{S} as described above. Monomeric hC3d served as positive control, CHO supernatant and RPMI-1640 were applied as negative controls. The strength of interaction was measured by spectrophotometry at 490 nm (y-axis). Interaction partners are indicated on the x-axis. The means from one of two independent experiments are shown. Error bars represent the standard error of the mean.

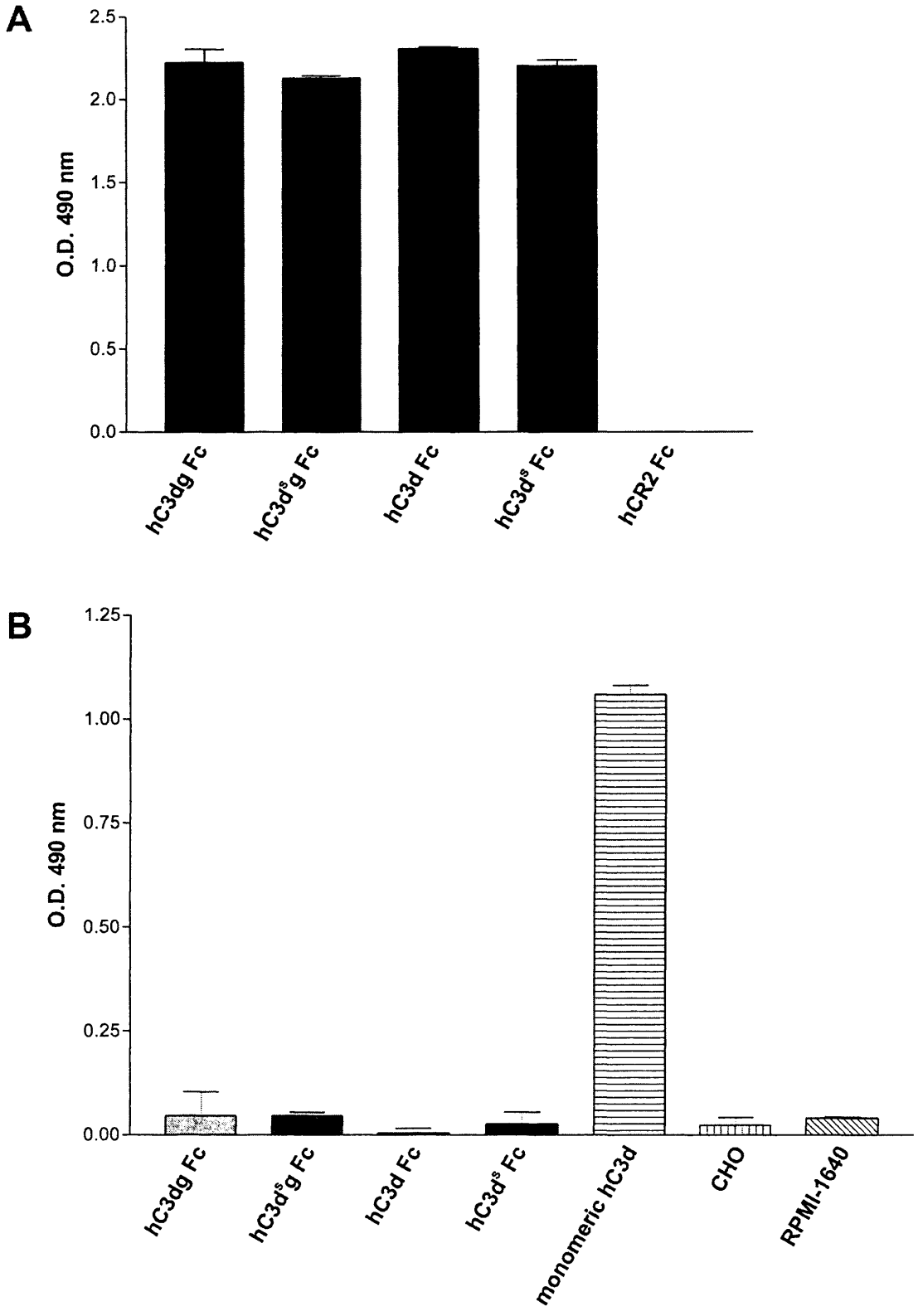
A
2.5
2.0
1.5
1.0
0.5
0.0
O.D. 490 nm
hC3dg Fc
hC3d^s g Fc
hC3d Fc
hC3d^s Fc
hCR2 Fc
B
1.25
1.00
0.75
0.50
0.25
0.00
O.D. 490 nm
hC3dg Fc
hC3d^s g Fc
hC3d Fc
hC3d^s Fc
monomeric hC3d
CHO
RPMI-1640

Figure 4.7. Fc fusion binding titration. Panel A shows a binding test of 10 μg/ml hC3dg Fc (thick line; detected with Dk α hIgG-RPE) compared to the binding of biotinylated 171 (1:1000, thin line, detected with 1:200 streptavidin PE), showing that C3dg Fc could bind to Raji cells (filled histogram: Dk α hIgG 2° only). Panel B shows a saturation curve derived from the FACS data. C3dg Fc was added at increasing concentration as indicated on the x-axis. The percentage of Raji cells with hC3dg Fc on the surface stained by Dk α hIgG-PE are plotted on the y-axis. Mean results from triplicate staining are shown and data is representative of two independent experiments. Error bars represent standard error of the mean.

A

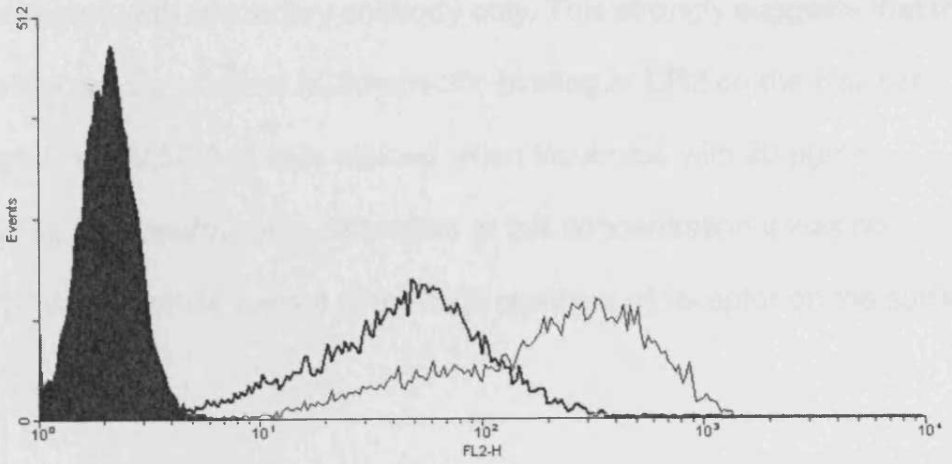
512
Events
0
10^0
10^1
10^2
10^3
10^4
FL2-H

B

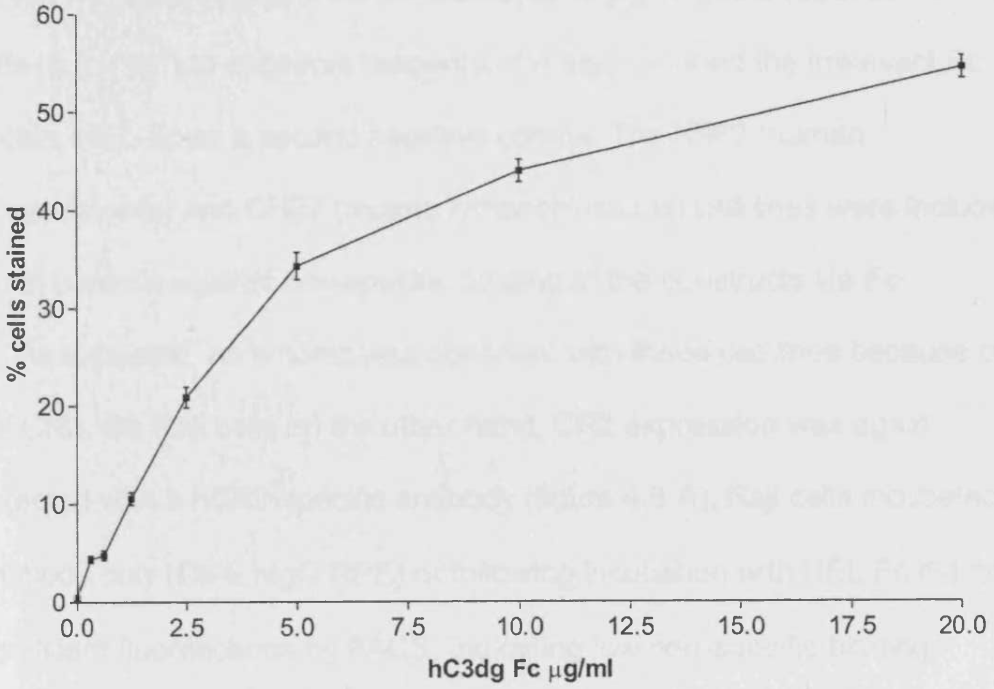
60
50
40
30
20
10
0
% cells stained
0.0
2.5
5.0
7.5
10.0
12.5
15.0
17.5
20.0
hC3dg Fc μg/ml

aggregated goat Ig and no above background fluorescence was detected after Raji cells were incubated with secondary antibody only. This strongly suggests that the observed staining was a result of hC3d-specific binding to CR2 on the Raji cell surface. Approximately 53% of cells stained when incubated with 20 µg/ml. Although binding was approaching saturation at this concentration it was not maximal, potentially a consequence of the high numbers of receptor on the surface (138, 350, 361).

The success of the hC3dg fusion encouraged us to extend this form of analysis to the remaining Fc fusions using a concentration of 10 µg/ml and a reduced number of Raji cells (0.5×10^6) to conserve reagents. We also included the irrelevant Fc fusion protein, HEL-Fc as a second negative control. The K562 (human erythroleukemia cells) and CH27 (murine lymphoblastoids) cell lines were included as additional controls against non-specific binding of the constructs via Fc-receptors. As expected, no binding was observed with these cell lines because of the lack of CR2. On Raji cells on the other hand, CR2 expression was again readily detected with a hCR2-specific antibody (figure 4.8 A). Raji cells incubated with 2° antibody only (Dk α hIgG RPE) or following incubation with HEL Fc did not exhibit significant fluorescence by FACS, indicating low non-specific binding. hC3dg, hC3d^{S}g, hC3d and hC3d^S displayed binding to Raji cells. Surprisingly, mC3d^S Fc fusion protein seemed to bind strongest to human CR2 and generated higher mean fluorescence intensity than any other fusion (as well as giving a significantly better signal than the directly conjugated commercial anti-human CR2 antibody (B-ly-4-PE, BD Biosciences)). Statistical analysis of mean fluorescence intensity data showed that all hC3dg Fc fusion proteins, apart from hC3d Fc, were

Figure 4.8. Mouse and human C3dg Fc fusion proteins binding to Raji. Panel A shows one representative histogram of three replicates for hC3dg, hC3d^{S}g, hC3d, hC3d^{S} and mC3d^{S} fusion proteins. Unstained cells, application of secondary antibody only and HEL Fc served as negative controls. The positive control, Ms α hCR2 PE (BD Pharmingen) confirmed the presence of CR2. The bottom row shows interaction of the fusion proteins with surface CR2. Bound Fc fusion proteins were detected as before with Dk α hIgG-RPE. Panel B shows a bar graph of the average mean fluorescence intensity from replicate analysis by FACS of each of the constructs. Data recorded from all murine and human fusion proteins were compared to the non-binding HEL-Fc. Standard error from the mean is shown, statistical significance was calculated by t test; ** $p < 0.01$, *** $p < 0.001$.

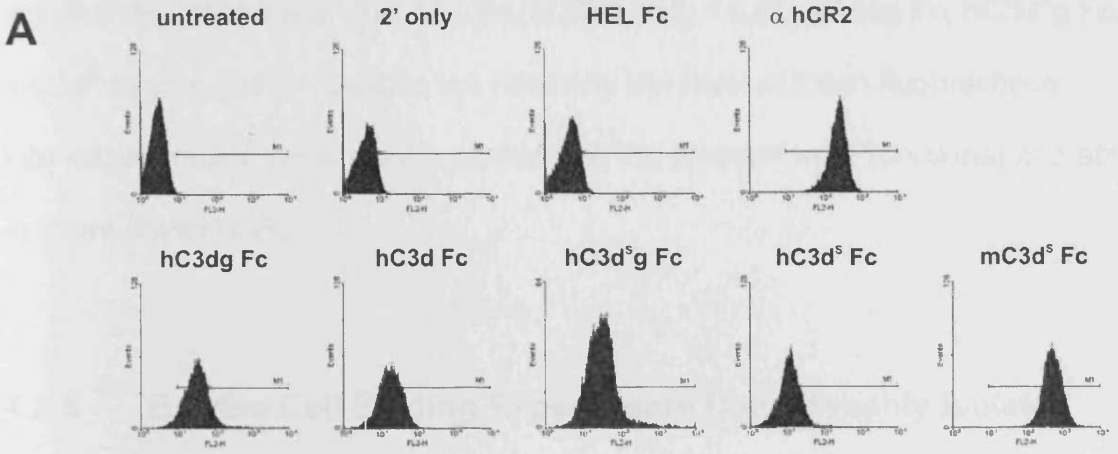
A
untreated
2' only
HEL Fc
α hCR2
hC3dg Fc
hC3d Fc
hC3d^{S}g Fc
hC3d^S Fc
mC3d^S Fc

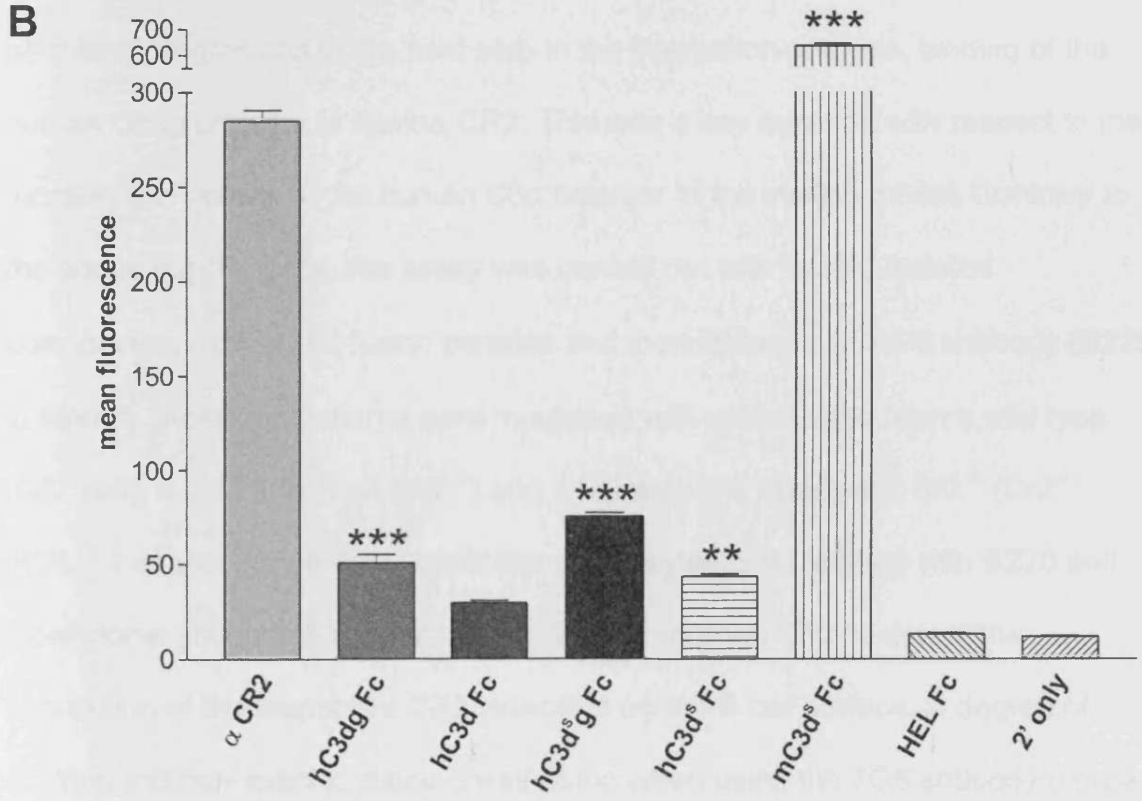
B
mean fluorescence
700
600
300
250
200
150
100
50
0
***
***
***
**
α CR2
hC3dg Fc
hC3d Fc
hC3d^{S}g Fc
hC3d^S Fc
mC3d^S Fc
HEL Fc
2' only

significantly greater than the HEL Fc ($hC3d^S$ Fc $p < 0.01$; hC3dg Fc, $hC3d^Sg$ Fc, $mC3d^S$ Fc $p < 0{,}001$). Despite the relatively low level of mean fluorescence intensity recorded these results proved that the proteins were functional and able to interact with hCR2.

4.3.6 *Ex Vivo* Cell Binding Experiments Using Freshly Isolated Murine Splenocytes

Successful binding experiments of these constructs with a human B-cell line permitted progression to the next step in the interaction analysis, binding of the human C3dg proteins to murine CR2. This was a key question with respect to the function and activity of the human C3d octamer in the murine model. Contrary to the above experiments, this assay was carried out with freshly isolated splenocytes, *ex vivo*. Fc fusion proteins and monoclonal α CD45R antibody (B220, to identify B-cell populations) were incubated with splenocytes from a wild type (C57Bl/6), a CR2 knockout ($Cr2^{-/-}$) and a human CR2 transgenic $Cr2^{-/-}$ ($Cr2^{-/-}$ $hCR2^{+/-}$) mouse (figure 4.9). Additional splenocytes were stained with B220 and monoclonal antibodies against mouse (7G6) or human CR2 to detect the expression of the respective CR2 receptors on the B cell surface. A degree of background non-specific staining was noted when using the 7G6 antibody (figure 4.9 A), this was potentially due to its biotin tag. Otherwise, CR2 expression was as predicted by original PCR genotype analysis previously established in the laboratory. As expected, only B220 bound to splenocytes isolated from $Cr2^{-/-}$ mice, which express neither mouse nor human CR2. Splenocytes isolated from wild type mice bound 7G6 and $mC3d^S$ Fc, indicated by a clear shift of the B220 positive (B cell) cell population into the upper right quadrant of the density plots shown

Figure 4.9. *Ex vivo* binding of the Fc fusions to murine splenocyte CR2.

Dot plot histograms from flow cytometry analysis of splenocytes isolated from three mice $Cr2^{-/-}$ (Panel A), $Cr2^{+/+}$ (Panel B) and $Cr2^{-/-}$ $hCR2^{+/-}$ (Panel C) are shown. 2 x 10^5 splenocytes were incubated with control antibodies (1 µg/ml mCR2-specific biotinylated 7G6 + streptavidin PE; pharmingen α hCR2 PE), a negative control (10 µg/ml HEL Fc) and the C3d-containing Fc fusions (10 µg/ml, refer to column title). B-lymphocytes were identified by forward and side scatter and then B220 FITC (FL1) staining. Fc fusion binding events were identified by the shift of cell populations from the lower right quadrant into the upper quadrant after detection using Dk α hIgG-RPE (FL2). Statistical analysis contained no fewer than 5,000 B220 positive events collected in a lymphocyte gate (according to forward and side scatter) and are representative of 3 experiments with similar results. The mean fluorescence of each replicate was used in one way analysis of variance and Tukey's multiple comparison as post test. *** $p < 0.001$

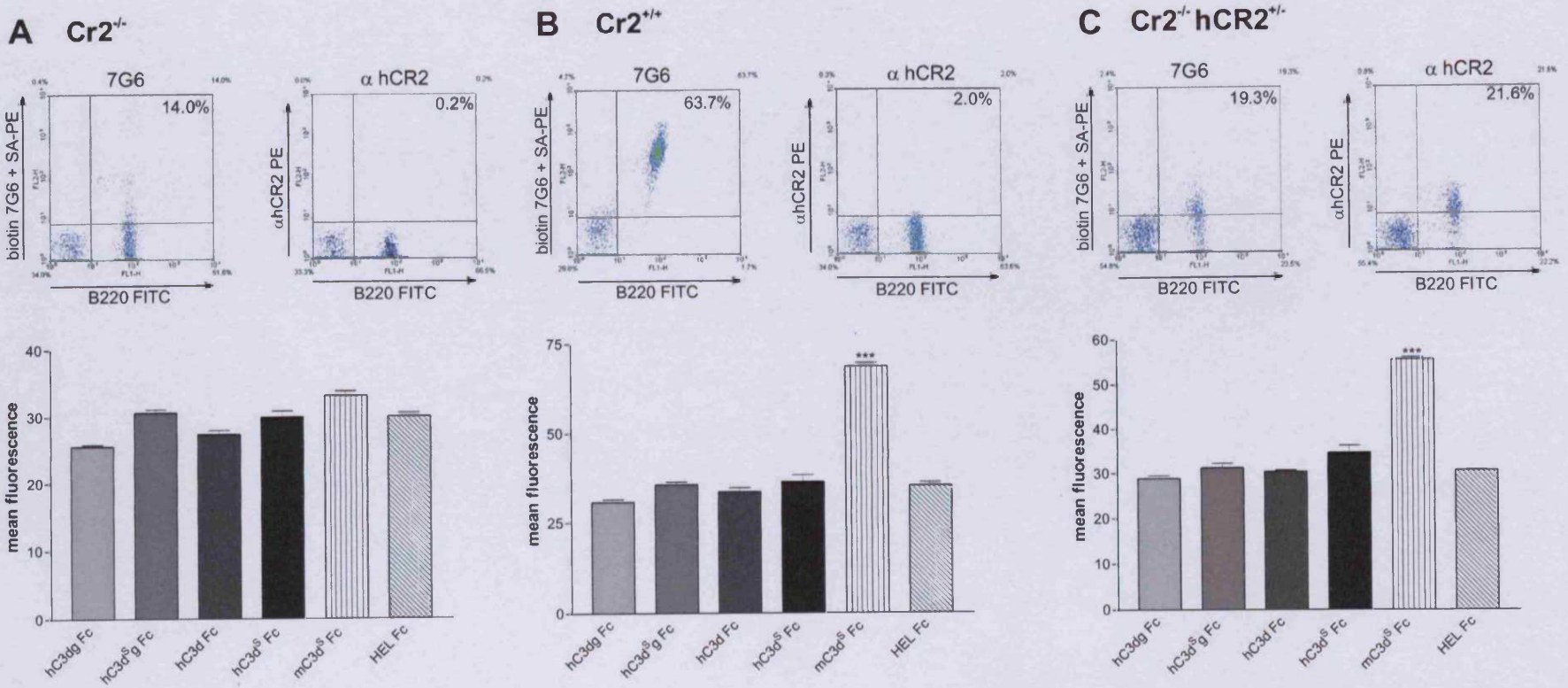
A Cr2-/-
7G6
14.0%
biotin 7G6 + SA-PE
B220 FITC
α hCR2
0.2%
αhCR2 PE
B220 FITC
B Cr2+/+
7G6
63.7%
biotin 7G6 + SA-PE
B220 FITC
α hCR2
2.0%
αhCR2 PE
B220 FITC
C Cr2-/- hCR2+/-
7G6
19.3%
biotin 7G6 + SA-PE
B220 FITC
α hCR2
21.6%
αhCR2 PE
B220 FITC
mean fluorescence
0
10
20
30
40
hC3dg Fc
hC3dSg Fc
hC3d Fc
hC3dS Fc
mC3dS Fc
HEL Fc
mean fluorescence
0
25
50
75
***
hC3dg Fc
hC3dSg Fc
hC3d Fc
hC3dS Fc
mC3dS Fc
HEL Fc
mean fluorescence
0
10
20
30
40
50
60
***
hC3dg Fc
hC3dSg Fc
hC3d Fc
hC3dS Fc
mC3dS Fc
HEL Fc

(figure 4.9). Indeed, mC3d^S Fc generated a significantly greater shift than the commercial anti-human CR2 antibody (Figure 4.9 B and C). Unfortunately, no shift was observed in the B cell population when incubated with any of the human C3dg/C3d Fc fusion proteins and possibly indicates that hC3d binding to mouse CR2 is not viable or was below the detection level of this assay. Notably and surprisingly, the human C3dg/C3d Fc fusions did not bind the hCR2 transgenic mouse splenocytes and raised the possibility that these fusion proteins were not functional or as concentrated as predicted. Overall, these data suggested that mC3d^S Fc could bind well to hCR2 but the converse was not proven.

4.3.7 Affinity Analysis by Surface Plasmon Resonance (SPR)

The previous analyses have provided strong evidence of the ability of the C3dg/ C3d Fc fusion proteins to interact with hCR2 and to some degree with mouse CR2. However, apparent failure to detect binding of hC3d to hCR2 in the *ex vivo* cell assays also suggested a more sensitive assay was required. Surface plasmon resonance (SPR) allows accurate real-time recording of interactions without the need for biomarkers or other secondary agents for detection, which can skew the relative intensity of an interaction. One side of the SPR chip consists of a thin gold and glass surface, which is used to reflect a beam of light at a specified angle. The other side of the chip is divided up into four flow cells with a dextran matrix on the surface, used to attach ligands covalently by amine coupling. SPR works by detecting binding events on the dextran side of the chip, which cause changes in the surface properties of the gold-coated surface. These potentially minute changes in the angle of the reflected light are recorded in real time and expressed as resonance units (RU) by the acquisition software. We used SPR to assess the

affinity of binding between m/h C3dg/C3d^{S}g/C3d/C3d^{S} and human CR2, identify changes in affinity due to the presence or absence of C3g, the presence or absence of the C3 thioester motif and to determine the strength of interaction between murine C3d and human CR2 proteins. The Biacore 3000 is fully automated allowing injection of µl-exact volumes of ligand and analyte. In preliminary experiments a CM5 Chip was coated with 6000 RU hCR2 Fc by standard amine coupling. In view of experiments carried out by others in this area (188, 204) one-third physiological salt concentration (50 mM) was used. Amounts of ligand and analytes, the C3dg/C3d Fc fusions, were set at high concentrations (10 µg/ml) and flowed over the surface to force a response. However, results were inconclusive and following failure to show binding of two monoclonal antibodies for hCR2 this approach was abandoned. Next, we tried amine-coupled protein A to capture hCR2 Fc and saturating free binding sites with Fc fragments but after several attempts background binding could not be resolved and this approach was also abandoned. Due to the failure of immobilised hCR2 Fc to produce meaningful results, ligand and analyte were reversed. A small amount of m/h C3dg/C3d^{S}g/ C3d/C3d^{S} Fc, HEL Fc or monomeric hC3d (100 RU) was immobilised on CM5 chips. Flow cells (1 or 3) preceding the ligand flow cells were left blank to subtract any secondary interactions with the dextran surface. Additional buffer effects were compensated by recording injections with HBS buffer. All reactions were run for sufficient time until equilibrium was reached and binding sites were saturated, allowing analysis with a steady state model. All kinetic analyses were carried out in buffer containing 150 mM NaCl as experiments with lower salt concentrations had been found to yield non-reproducible results. Moreover, optimisation of the salt concentrations showed that 75 mM and 50 mM increased non-specific interactions

with the dextran matrix (data not shown). Keeping the ionic strength at physiological levels was also considered to be most suitable to replicate or simulate natural conditions. hCR2 Fc was injected in triplicate at concentrations ranging from 0.19 nM to 50 nM in HBS buffer (figure 4.10). hCR2 bound to monomeric hC3d (figure 4.10 A) but not HEL Fc (figure 4.10 B), the interactions were therefore C3d- and not Fc-dependent. The reactions were repeated in the same manner with the Fc fusions. The first and most important observation made in the experiments was that in this configuration all C3d-containing Fc fusions were able to interact with hCR2. These observations confirmed that the fusions were indeed functional. Steady state equilibrium dissociation constants are shown in table 4.1, the value of χ^2 showed that the model described the data well.

Ligand	R_L^*	calc. R_{max}	K_D	χ^2
hC3dg Fc	94.7	55.23 ± 0.64	3.17 ± 0.11 nM	1.830
$hC3d^Sg$ Fc	95.7	60.37 ± 2.18	2.60 ± 0.22 nM	1.629
hC3d Fc	96.2	59.20 ± 2.91	5.18 ± 0.50 nM	1.677
$hC3d^S$ Fc	94.3	35.70 ± 0.72	7.66 ± 0.49 nM	2.890
$mC3d^S$ Fc	94.9	25.30 ± 0.06	1.47 ± 0.47 nM	1.527
hC3d	96.0	109.00 ± 1.53	10.63 ± 0.22 nM	3.650
HEL Fc	95.8	n.c.	n.c.	n.c.

Table 4.1. Steady state affinity dissociation constant. K_D represents the strength of the interaction, Rmax is an indicator for the activity of the surface. χ^2 is a measure of the goodness of fit. Values represent means and SEM of triplicate experiments. n.c. = not calculated by software
* amount of ligand immobilised on the surface in response units

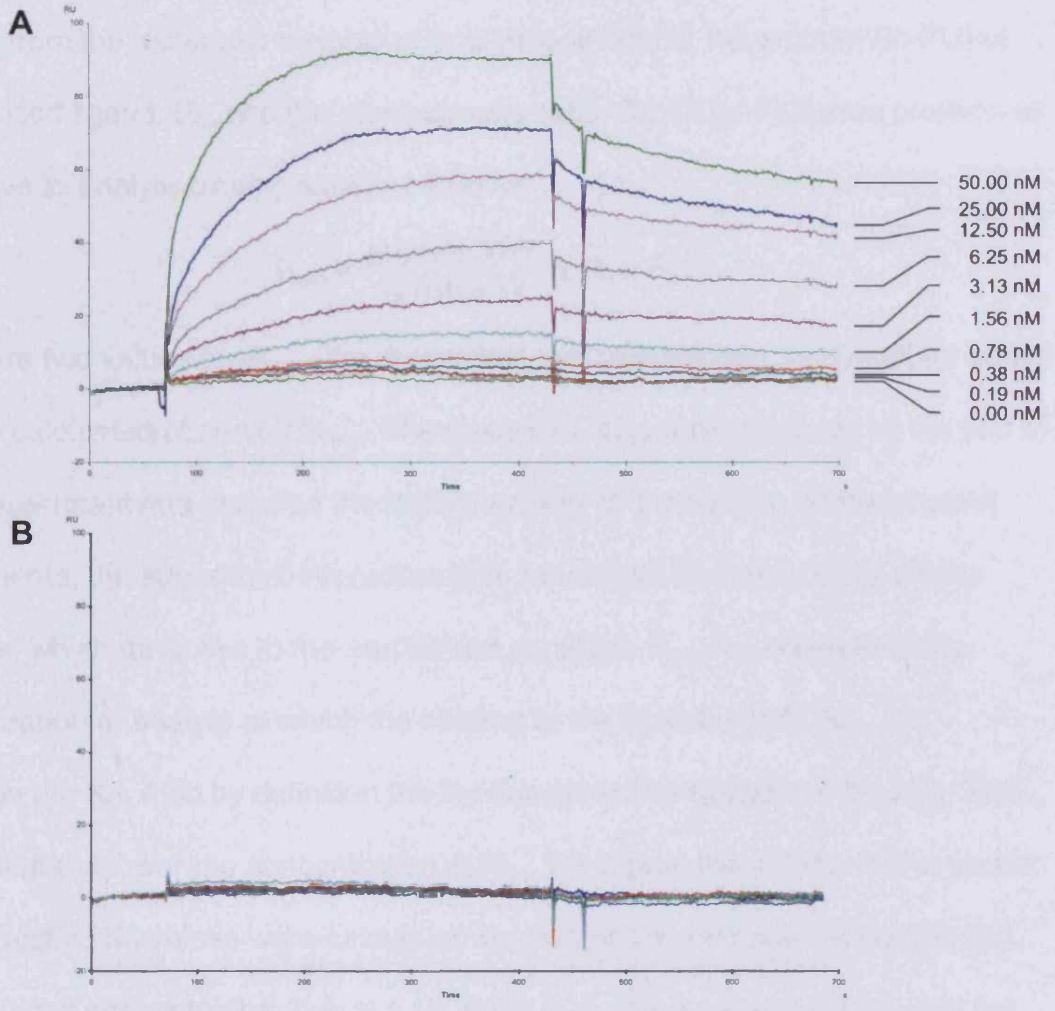

Figure 4.10. Control traces of surface plasmon resonance analysis. hCR2 Fc was flowed over CM5 chip surfaces with immobilised monomeric hC3d (A) or HEL Fc (B) at the concentrations indicated in panel A. Each line in the graph represents one of three replicates. Analyte was flowed over the surface at 30 µl/min and injected for 6 minutes followed by dissociation for 4 minutes.

The affinity or dissociation constant K_D was calculated as follows. The maximum binding capacity of a ligand immobilised on a surface is expressed as R_{max}. It is derived from the molecular weights of analyte and ligand, the amount (in RU) of immobilised ligand, R_L, and the stoichiometry ratio, S_m, (2 for Fc fusion proteins as they have to analyte binding sites) as follows:

$$R_{max} = \frac{\text{analyte MW}}{\text{ligand MW}} \times R_L \times S_m$$

There are two values for R_{max}, the theoretical, which is derived as described above and the calculated/observed R_{max}. The observed R_{max} was calculated at the end of each experiment and revealed the factual activity of the surface. In the present experiments, the strength of interaction was measured by steady state affinity analysis, which gave rise to the equilibrium constant, R_{eq}. R_{eq} represents the concentration of analyte at which the binding to the ligand is 50% R_{max}, by definition the K_D. Also by definition the K_D describes the strength of binding. This meant that the lower the concentration at R_{eq}, the higher the affinity. In this model, the respective K_D values were calculated by plotting the response at equilibrium against each concentration (figure 4.11, table 4.1). Steady state analysis did not provide data on kinetic interactions, i.e. the rate of association and dissociation but allowed comparison of affinity between ligand and analyte.

Values for the expected R_{max} took into account the bivalency of the analyte via S_m, however observed values were notably lower. The expected and calculated R_{max} of monomeric hC3d was higher due to the size of the protein. Immobilisation of 100 RU hC3d deposited approximately 2.5 times more protein on the surface compared to the fusions.

Figure 4.11. Steady state affinity graphs. One representative graph of three replicates is shown. The graphs were generated by plotting the concentrations of analyte flowed over the surface against the equilibrium response R_{eq} (in absorbance unites, AU). The slope of each curve indicates higher or lower affinity of the analyte to the ligand. Curves that flatten out rapidly reflect high affinity; more shallow slopes indicate lower affinity. χ^2 values derived from the curves showed that the model described the data well (see table 4.1).

monomeric hC3d

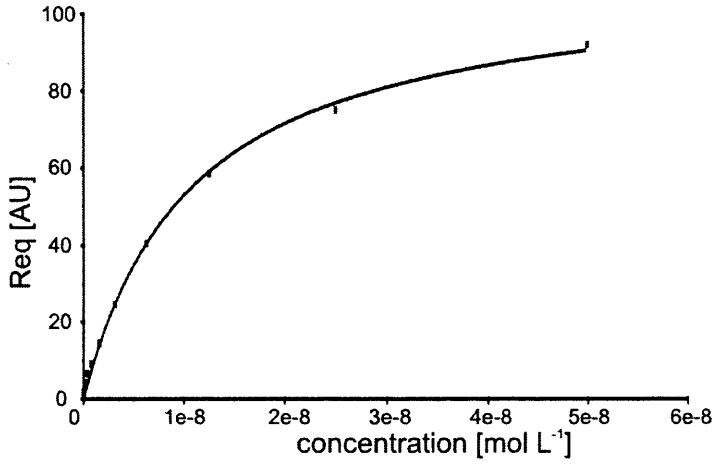

hC3dg Fc

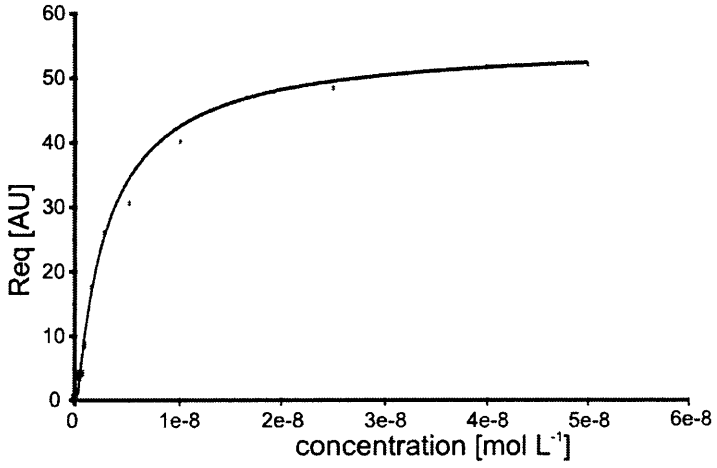

hC3d^{S}g Fc

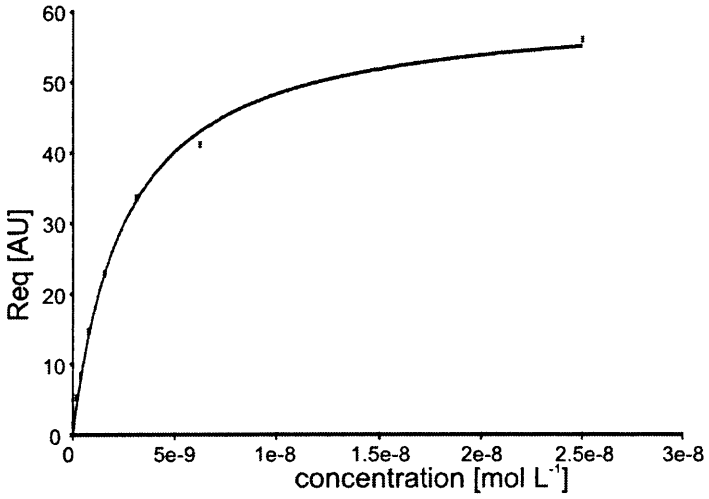

hC3d Fc

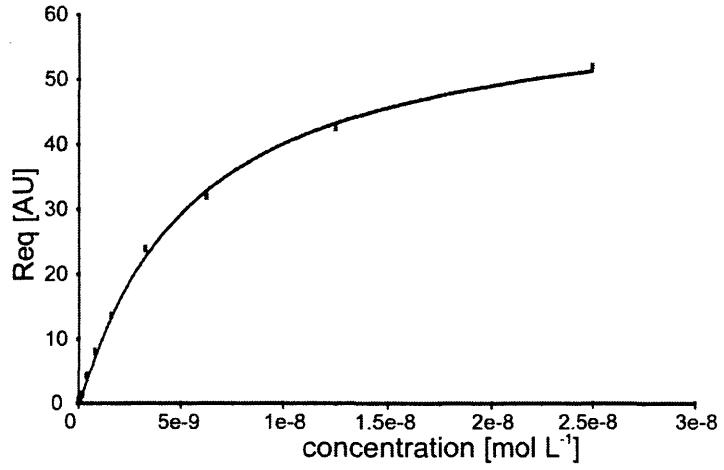

hC3d^{S} Fc

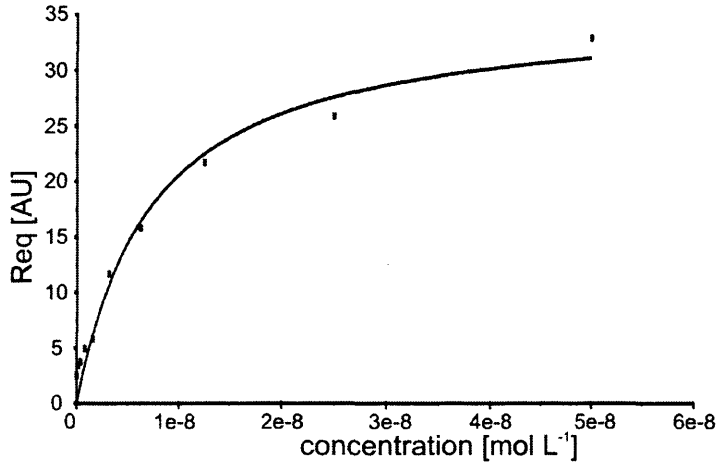

mC3d^{S} Fc

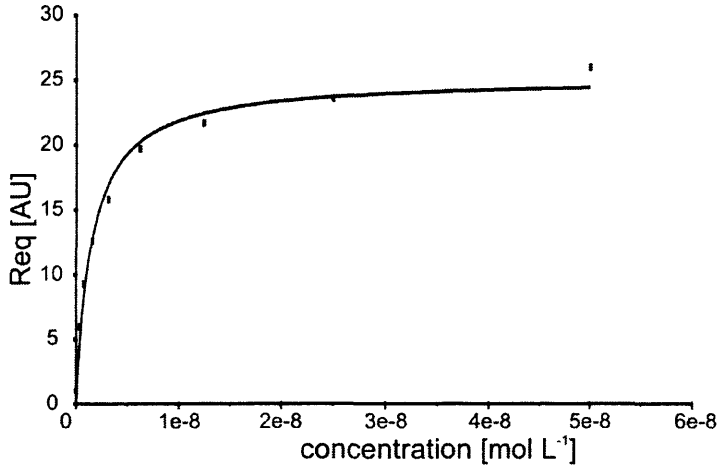

Despite higher immobilised amounts, hC3d bound hCR2 less efficiently (K_D = 10.63 ± 0.22 nM) than the Fc fusions (K_D ranged from 1.47 ± 0.47 nM to 7.66 ± 0.49 nM). Of all the fusion proteins $mC3d^S$ Fc exhibited highest affinity to hCR2 Fc (K_D = 1.47 ± 0.47 nM), which reflected results observed in the previous experiments. Affinity of the human versions to hCR2 Fc was slightly lower. hC3dg Fc and $hC3d^Sg$ Fc had seemingly higher affinity for hCR2 than hC3d Fc and $hC3d^S$ Fc. Analysis of the data with bivalent binding model indicated heterogeneous binding and is not shown here.

These experiments confirmed a difference in binding strengths between species. Murine $C3d^S$ has superior affinity to human CR2 SCR1-4 compared to its human homologues.

4.4 Discussion

The aim of this part of the study was to establish the functional relevance of CR2 interaction with C3d as a means to guide future testing of the octameric vaccine constructs. The laboratory had previously generated a hCR2 SCR1-4 and a mC3d^S Fc fusion protein. The first two SCRs had previously been identified as the C3d binding sites and therefore sufficient (128, 146, 188, 203, 349, 362). In conjunction with the availability of efficient purification systems and columns it was decided to use this format as a road map to develop a model to assess binding to CR2 and using the human C3d variants. Thus, five C3d-containing Fc fusions and an unrelated control protein (HEL Fc) were produced for testing. Murine CR2 Fc also consisted of the first 4 N-terminal SCRs, which contains the C3d binding site. This configuration reduced potential steric hindrance by SCRs 5-15 (339, 363). All except mCR2 Fc consisted of the protein of interest and the Fc fraction of human IgG1 (mCR2 Fc was fused to mouse IgG1 Fc). As the octameric proteins discussed in the previous chapter were destined to undergo testing in a murine as well as humanised ligand-receptor setting *in vivo*, both human and murine CR2 Fc fusions were generated in order to make predictions on *in vivo* effects.

Initially, binding was confirmed using the Raji cell line, a B-cell model that has proven to be a vital tool in the identification of CR2 and the interaction with C3 (section 1.7.2). The cells specifically express high numbers of CR2 on the surface (350) but lack CR1 and γ-isotype surface immunoglobulin (364) making them ideally suited for this type of analysis. The Fc tails allowed all CR2 binding partners to be detected with the same secondary antibody. This fundamentally reduced differences in specific secondary antibody binding by equalising staining across all

reagents. This approach was implemented after other detection methods had been explored. Direct C3d detection with secondary and tertiary antibodies had led to significant background signal problems. Signal amplification and secondary interaction with surface determinants caused interference in these assays, similar to the problematic detection in the immunosorbent assays using immobilised hCR2. To avoid the need for secondary reagents, two of the fusion proteins (hC3dg Fc and mC3d^S Fc) were directly labelled with FITC. Unfortunately, the FITC levels on each protein were variable despite the same labelling conditions. Furthermore, FITC interfered with cell binding. This precluded the use of these directly labelled molecules in any definitive analysis. Having optimised the conditions for the Raji binding assays, all C3d-containing reagents and controls were tested twice in triplicate. Murine and human C3dg/C3d^{S}g/C3d/C3d^S Fc fusions exhibited binding although hC3d Fc failed to reach significance. The most striking result was observed with mC3d^S Fc, which bound stronger than the commercial antibody (figure 4.8). Although these interactions were most likely between CR2 and the m/h C3dg/C3d^{S}g/C3d/C3d^S fusions, a competition assay using antibody 171, specific for the C3d binding site on hCR2 (100) should have substantiated these results and should be included in the future. Nevertheless, this experiment proved firstly that all m/h C3dg/C3d versions were capable of binding to the B-cell surface via CR2. Secondly, highly specific cross-species binding between mC3d^S and hCR2 was observed. Other investigators in the field have claimed in the past that murine C3d and human C3d bind CR2 of either species with equal affinity (128, 178) having used both species of C3d interchangeably in cell binding assays for more than two decades (158, 217, 221). In more recent work human C3d was able to activate murine splenocytes and release intracellular

calcium (165, 348, 365). However, the *in vitro* cell binding results presented herein demonstrated a notable difference in the strength of the interactions. This was somewhat surprising as such a major difference had not been anticipated especially in view of the wealth of studies gone before this. Indeed, the weaker binding observed especially in hC3d Fc was a cause for concern.

Although the cell binding data dispelled any initial doubts that the Fc constructs generated faulty, incorrectly folded or non-binding proteins, the notably lower activity of the human versions compared with the $mC3d^S$ Fc was unexpected (figure 4.8). One obvious reason for these differences could have been the varied levels of degradation observed across the Fc fusion preparations. Human antibodies of the IgG1 type are predominately purified with protein A affinity columns therefore this method was utilised in this study. The identity of all fusions was verified with specific antibodies, purity was confirmed by SDS-PAGE and coomassie blue as well as silver staining. Some preliminary purifications had shown considerable breakdown of the proteins. The exact reason for this was unclear although the hinge region of these fusion proteins is a common target site for proteolytic cleavage by papain, and the Fc fusion proteins have recombinant factor Xa, and prescission protease target sites engineered into their construction. Although none of these enzymes should have been present or were added here, degradation occurred at this site (figure 4.3 C). Breakdown was minimised by frequent exchange of medium, re-seeding of the cultures, immediate removal of cell debris by centrifugation and storage of the samples at –20°C. Further improvements in stability were achieved from changes in the medium composition and purification methods. Contamination with bovine serum Ig, originating from the

foetal calf serum used to supplement the growth medium was tackled by utilising commercially available low bovine Ig serum as alternative supplement. Production of Fc fusion proteins was moved from standard tissue culture flasks to the Integra™ system (section 3.3.8). Higher production levels were achieved whilst reduced volumes of supernatant were required for purification of sufficient amounts. Manually operated columns were changed for automated runs with the Äkta Prime system. The optimisation was a success as demonstrated by raised production levels, higher quality purified product and a significant overall reduction in processing time. Optimising the process in this way improved the stability of the fusions although some degradation was still visible (figure 4.3 C and D, figure 4.4, figure 4.5). hC3d^{S} Fc and more so HEL Fc were degraded to slightly higher degrees, shown by similar results following repetitions of production and purification. Protease inhibitors will be employed in future production of Fc fusion proteins to reduce breakdown to a minimum. Interestingly, closer inspection of hC3dg Fc and hC3d^{S}g Fc revealed some degradation to smaller species. The degraded products had the same apparent M.W. as C3d Fc and C3d^{S} Fc, implying removal of the 'g' segment from a minority of C3dg and C3d^{S}g (figure 4.4 A). It is possible that this was mediated by proteolytic enzymes in the supernatant removing the 'g' portions from a minority of C3dg and C3d^{S}g. This process is usually facilitated by non-complement proteolytic enzymes ((108) section 3.4), which may have been released into the growth medium by dying or dead cells. Under conventional culture conditions, the fusions could have been cleaved by commercial trypsin used to dislodge the CHO cells from the surface. CHO cells growing in the AD1000 flasks underwent trypsinisation only when cells were replenished, making this an unlikely source. Irrespectively, C3g could have been

removed enzymatically during production (compare section 3.4). Together with the findings from the previous chapter, this is a further indication that C3d is the physiological binding partner of CR2. Monomeric C3dg/C3d^{S}g/C3d/C3d^{S} was not detected, as it would not have bound to the protein A column. The absence of monomeric C3dg/C3d^{S}g/C3d/C3d^{S} also provided evidence that there was no degradation post purification. Lower molecular weight bands were identified as hIgG1 Fc by immunoprecipitation (figure 4.4 C).

Clearly, this degradation could partially be blamed for the lower interaction observed during the cell binding assays. The presence of single-arm species of the fusions and to some degree Fc portions present in the purified samples introduced disadvantageous variation into the experiments. Degradation of approximately 5% in mC3d Fc, 10% - 30% in the human C3dg/C3d^{S}g/C3d/C3d^{S} fusions and higher breakdown in HEL Fc could influence the results significantly independent of their affinity. Due to the progression of the work and the limited time left available in the project higher purity than presented here could unfortunately not be achieved. The matter should have been resolved by abolishing degradation completely, e.g. with a hC3d-specific affinity column. Unfortunately, as described in the previous chapter, several attempts to produce such a column of adequate quality for purification were unsuccessful. Another way of resolving these problems could be the integration of size exclusion chromatography as part of the purification process.

Despite the limitations introduced by the degradation, the Raji cell binding results provided the grounds for further more in-depth cell assays. A murine B-cell line equivalent to Raji, A20, was considered to test binding to the murine receptor.

However, screening for mouse CR2 expression following reconstitution of frozen stocks suggested contamination of the culture with a related cell line, which expressed hCR2. To avoid the risk of false positive interactions, an alternative more stringent approach was devised. Splenocytes were isolated from three mouse lines, WT, $CR2^{-/-}$ or $Cr2^{-/-}$ $hCR2^{+/-}$ (171, 172). CR2 levels on mouse B-cells are generally lower than the human counterparts (172) and although the amounts expressed on the surface roughly equal the normal murine levels, $hCR2^{high}$ cells used here possess only an equivalent of approximately 25 – 33% of human B-cell CR2 (221). Moreover, the $hCR2^{high}$ transgenic strain B-cells suffer from reduced cell numbers in the spleen due to altered B-cell ontogeny. Raji on the other hand express 4 – 5 times higher amounts of CR2 on the cell surface than human peripheral blood B-cells (138, 350, 361). Although interaction with Raji CR2 was almost certain, binding of the human C3dg/$C3d^{S}$g/C3d/$C3d^{S}$ variants was comparatively low. This confirmed past results that showed that low receptor numbers can influence binding and cell activation (48). It is therefore not surprising that human C3d – CR2 binding was below the detection level of the splenocyte assay. Conservative estimates from comparing the amount of CR2 present on the transgenic B-cells to the human B-cell line therefore suggest an up to 20-fold reduction in receptor numbers in the transgenic mice. In view of the octameric vaccine it had to be anticipated that the vaccine dose would have to be reasonably high to trigger a response. High-level protein production however is costly and time consuming; hence DNA vaccines were conceived to circumvent the problem. Constitutive *in vivo* production of the vaccine could provide sufficient concentrations. On the other hand, low target receptor numbers were the precise idea behind the vaccine design. An octamer was to provide enough binding sites

for antigen and adjuvant low receptor density situations. Experiments using the octameric vaccine and Raji cells were carried out but did not yield any useful results due to high background interference of secondary and tertiary reagents, justifying the Fc fusion binding model. Sufficient amounts of the octamers containing YFP produced by cell culture should yield the desired information on cell surface binding.

Because of the concerns raised in the previous analysis and to provide more in depth analysis surface plasmon resonance was utilised. SPR is a highly sensitive system that allowed simple alterations of conditions to be assessed much more rapidly. In particular the amounts of protein involved can be specified. There was one major setback in the execution of these studies. Several attempts at producing a vector expressing functional murine CR2 Fc by the laboratory were unsuccessful. Efforts were suspended when an Fc fusion protein was provided by Dr Susan Boackle's Group (University of Denver, CO, USA), based on murine IgG1. Despite successful cell culture production of the mCR2 Fc fusion (detected by western blot) and using a protein G column (mIgG1 has higher affinity for protein G than A) following the manufacturer's instructions, the protein did not purify and could not be salvaged. This situation was compounded by the fact that time and funding on this aspect of the project had run out and thus this key question of the exact hC3d binding affinity for mCR2 at this time remains unanswered.

Despite several attempts attaching hCR2 Fc to the chip surface, the experiments at first yielded inconclusive data. Furthermore, use of hCR2 monoclonal antibodies suggested that the hCR2 Fc fusion protein was not accessible when bound to the

chip surface (observed response ~5 RU). To orientate CR2 into the flowing medium, protein A was amine coupled to the surface. Initial readings were promising, however remaining protein A binding sites could not be saturated, which was vital to prevent false positive results through Fc portion-protein A interactions. Moreover, efficient regeneration in all above experiments could only be achieved with 50 mM NaOH, considered too harsh for repeated use. Hence ligand and analyte orientation were reversed. Approximately 100 RU of hC3dg/hC3d^{S}g/hC3d/ hC3d^{S}/mC3d^{S} Fc were immobilised on the chip surfaces. The manufacturer recommends low ligand surface concentrations of 100 – 200 RU because this allows high sensitivity measurements for affinity and kinetic studies and minimizes avidity effects and mass transfer. Moreover, this simplified saturation of the surface in the equilibrium binding model. Higher receptor densities could have proven difficult with bivalent interaction partners. Due to the degradation and non-specific orientation of the ligand during the immobilisation process the surface was more heterogeneous, reflected by calculated R_{max} values, which lay below the expected values.

Sarrias *et al.* made a critical discovery concerning assay design using CR2 and C3d in SPR (204). Although no direct explanation for differing on and off rates and K_D values was given in this particular study, initial association and dissociation phases occurred more rapidly when C3d was used as analyte. Such discrepancies cause difficulties when studies are to be compared. Here, it was decided to design the assay in the natural orientation, immobilising CR2 on the surface. However, several attempts did not yield any useful information and the reason for this specific orientation failing requires further investigation. It is possible that surface

bound CR2 suffered from steric hindrance via both arms of the molecule or through the surrounding dextran matrix. A more likely reason however was the orientation of the immobilised hCR2 Fc on the surface itself. Amine coupling is non-specific and depends on the charge of the molecule to be immobilised. If the CR2 portion had a stronger positive charge within the molecule than Fc it may have had a tendency to be coupled with the Fc tail protruding into the medium. This may explain why anti-hCR2 antibodies could not detect the protein even at immobilisation levels of 6000 RU because SCR 1-4 were buried in the matrix. Although monomeric C3d bound to hCR2 in the ELISA assay, similar problems may have hampered the binding of the Fc fusions. Epitope masking thus explains the failure to detect in both ELISA and SPR.

Notably, the results were highly reproducible at 150 mM NaCl (physiological concentration) where previous studies had experienced much decreased affinities (188, 204). In a recent study IFNα, monomeric C3d, EBV and CD23 binding to CR2 were assessed (339). As in previous studies, the proteins were produced in insect and bacterial cells (also see (188, 204)) and reactions were carried out at neutral pH and 50 mM NaCl, which had been claimed to yield strongest affinities. The present study was carried out in 150 mM salt because this reflected natural circumstances. Also, this had a particular role to play in the subsequent testing of the human $C3d^S$ vaccine *in vivo*. Comparing the set up of these and the present experiments, it is likely that the dimeric proteins used herein allowed experiments at 150 mM to be carried out in the first place, indicating synergistic binding when several copies of C3d were present.

The results from the experiments confirmed the findings from the cell-based assays that mC3d^S Fc interacted most efficiently with hCR2. The human versions performed less well although the differences were most remarkable between all Fc fusions and the monomeric control. However, monomeric and dimeric proteins could not be compared directly because the configurations were too different. Although higher amounts (~2.5x) of hC3d had been immobilised, the proteins were present at lower surface densities. In the case of the Fc fusions it was most likely for one molecule of hCR2 Fc to bind to one molecule of hC3d most resembling a 2:2 relationship. The different types of binding reactions are shown in figure 4.12. The fusions are more than likely to bind relatively freely to surface receptors during the B-cell experiments thanks to the receptor's mobility within the lipid rafts ((167, 168, 366); figure 4.12 A). Dextran surfaces did not allow this mobility and due to the low amounts of protein immobilised in the flow cell cross-linking was less likely (figure 4.12 B and C). In the meantime, SPR chips have been developed further and allow immobilisation of a wider range of ligands. The L1 chip, for instance, allows immobilisation of lipid bilayer-contained membrane proteins. This approach would provide the opportunity of incorporating the whole receptor into microsomal lipid bilayers, allowing highly sensitive lipid surface analysis *in vitro*. As well as characterising binding to the native receptor, the orientation issue could be resolved that way.

The discussed set up was required to prevent avidity effects and obtain conclusive affinity data. Although the configuration of the proteins in this study only allowed steady state analysis, the 2:2 relationship was analysed with a bivalent binding model. In general χ^2 values ranged from 2 – 5.1, indicating good quality data,

Figure 4.12. Proposed Fc binding to cell surfaces and Biacore flow cells. Panel A shows a binding schematic to B-cell surface CR2. Cross-linking was likely thanks to lipid raft mobility. Dextran-immobilised proteins shown in panels B and C were spaced much further apart, cross-linking was therefore a rare event. For the fusion proteins it was much more likely to undergo a 2:2 reaction (B). Monomers (C) were most likely to bind one molecule.

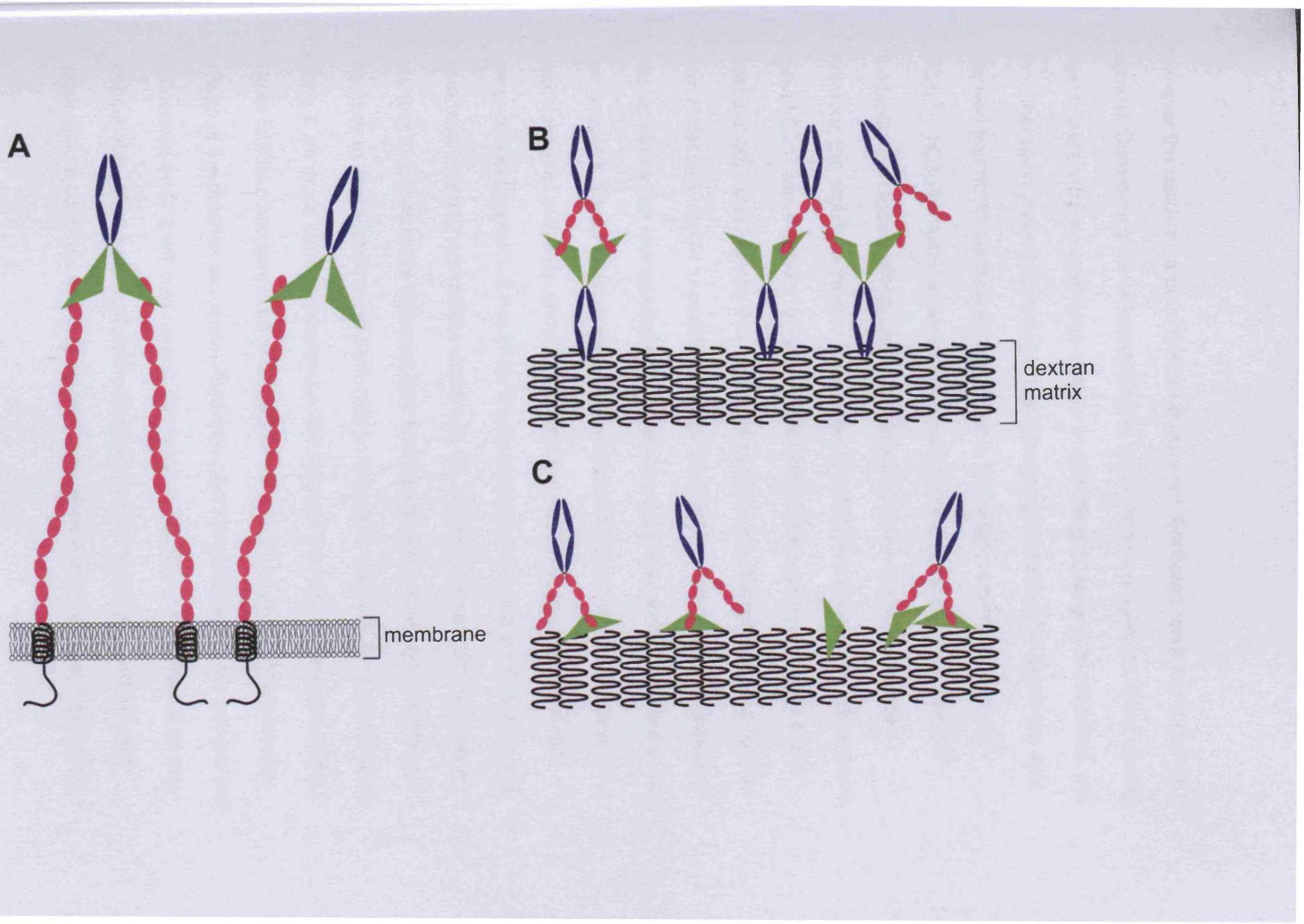
A
membrane
B
dextran
matrix
C

hC3d^{S}g. hC3d exhibited weaker affinity, slightly stronger than hC3d^{S}. mC3d^{S} evidently had highest affinity. Although the dissociation constants seemed different, the slightly increased breakdown of hC3d^{S} had to be taken into acco Less hC3d^{S} was available for binding relatively to the amount of protein in the preparation. Consequently this may have reduced the affinity influenced by or arm molecules unable to participate in the 2:2 binding reactions. It is because this and to further characterise these interactions that the above experiments be repeated. These findings, in particular the hCR2-mC3d interactions are fascinating but evidently, some of the data are not in keeping with the results presented in chapter 3. It has to be emphasized however that the Fc fusion ar octameric recombinant protein constructs are so fundamentally different that a number of factors could influence their binding strengths. Certainly the differe degrees of degradation could have had an impact on the data. Avidity effects likely to be much more pronounced in the octamer leading to improved bindin Other factors could simply be of a physical nature and caused by the size and shape of the octamer in solution. Intramolecular interactions with the antigen a influenced by C3g will also have to be resolved before these results will be tru comparable. Moreover, each experimental approach was optimised for each recombinant construct and they are not compatible with each other (figure 4.6

The experiments shown here add to previous work using recombinant CR2 consisting of SCR1-2, SCR1-4 and SCR 1-15 (188, 204, 339). All of these studies relied on single molecule interactions. As mentioned above, both orientations were tested resulting in specific affinity constants for each orientation. Asokan *et al.* recorded minimum K_D values of 0.314 µM for immobilised CR2 SCR1-4 (this study) and 0.179 µM for immobilised C3d (339). Shortening of the receptor in all studies increased the affinity between ligands and analytes. Experiments by Asokan *et al.*, who flowed CR2 1-2, CR2 1-4 and CR2 1-15 across immobilised C3d, highlighted the lowered affinity of the full-length version of CR2 (0.179 µM, 0.617 µM and 2.2 µM respectively; (339)). These findings were supported recently by work by Gilbert *et al.* who identified multiple interactions of CR2 with its ligands (363). Although the receptor is flexible and extended in solution (367), some weak inter-domain interactions in the µM to mM range appeared to be feasible. This would explain the lowered on and off rates (188) and higher K_D values with increased numbers of SCRs (339). Guthridge *et al.*, on the other hand, calculated affinity between the two proteins at 22.4 ± 2.4 nM for CR2 SCR 1-2 and 27.1 ± 1.1 nM for CR2 1-15 (188). These K_D values were considerably lower than claimed by the aforementioned closely related group. Experiments in both studies were carried out at 50 mM. The only difference lay in the instrument, Biacore 3000 and Biacore 2000 respectively; all other reaction conditions were equal. The reason for this variation is therefore unknown. A third study by another cooperating group analysed bivalent binding between single molecules (204). Their data indicated a two-step binding event of a low affinity interaction (2.8 µM/4.3 µM) and binding at lower K_D (231 nM/259 nM). These data were obtained at 50 mM and 75 mM NaCl respectively in the flow buffer utilising full-length CR2. However, yet again, these

results did not back up K_D values determined by Asokan *et al.* who estimated the high affinity interactions at 2.2 µM with the same ligand and analyte.

Despite the low reproducibility, all K_D values in this study were far below the previously published results. This is due to the presence of two binding sites of each ligand and analyte and shows a synergistic effect. Yet, differences in synergy between the variants of m/h C3dg/C3d^{S}g/C3d/C3d^S used here were clearly distinguishable. Obviously, the present study utilises bivalent proteins, which are significantly different to all past studies. The stronger affinities are a clear indication that bivalency has beneficial effects on the strength of binding as shown by Gilbert *et al.* using a CR2 Fc fusion protein (368). In the same study, however, it was shown that the conformation of such problems is subject to variation. Different conformations could have led to the lower calculated R_{max} due to unavailable binding sites. Despite this potential added complexity, the data support the choice of the present model. The inhibitory influence of monomeric C3d on B-cell activation (158, 218, 224) make this design more suitable to analyse C3d-CR2 interaction realistically.

Mouse and human complement receptors and ligands have been used interchangeably for more than 20 years, however the cross-species affinity was never evaluated accurately (158, 217, 221). The discussed experiments, carried out with dimeric proteins and murine and human protein species, do not contribute to the further characterisation of the single molecule C3d-CR2 interaction. On the contrary, the bivalency of the proteins adds a level of complexity, which resembles much more the natural situation. It has long been accepted that presence of a

single C3d molecule has inhibitory effects (218, 224). C3d oligomers (Fc and Oct) will therefore allow characterisation of binding events, although complex, between immune complexes and B-cells. Unfortunately, the experiments presented here remain incomplete without the murine CR2 SPR analysis. Another attempt at production and purification will hopefully provide the affinity data between hC3dg/ $hC3d^{S}g$/hC3d/$hC3d^{S}$/$mC3d^{S}$ and this receptor. The SPR experiments could also be optimised further utilising the above-mentioned protein A approach to immobilise the respective Fc fusions. Indeed, protein A and protein G coated analysis chips have recently become available from Biacore, which would simplify this approach greatly. Monomeric ligands, produced by cleaving the Fc fusion from the protein of interest could then produce results comparable to previous studies.

Finally, the data from the three different experimental approaches confirmed that murine $C3d^{S}$ had higher affinity for human CR2 than all four versions of human C3dg/C3d. These investigations will have to be completed with murine CR2 to provide information with the reciprocal set up. Although further experiments will be required, the data presented in this part of the study break with the commonly held assumption (178) of equal affinities of murine and human complement components.

The data presented in this chapter raised serious questions whether a human vaccine version was able to bind to murine B cells. Doubts that the fusions were not functional were dispelled by the SPR analyses, which demonstrated interactions of all C3dg/C3d variants with CR2. The cell binding assay's limitation was not failure to interact but rather lack of sensitivity. The low density of

complement receptor on the cell surface did not allow signal amplification via the secondary antibody. The octameric vaccine was designed to compensate for low receptor numbers on B-cells by being equipped with four times as many CR2 binding sites. *In vitro* cell binding studies using the octamer were unfortunately fraught by background interference and did not yield any results. The vaccine proteins were also not used in SPR analysis because they were unsuitable for the discussed design concerning ligand spacing and increased avidity effects. Although interaction of maximal C3d and CR2 molecules is desirable in the vaccine context, the aim was to identify differences in affinity among the m/h C3dg/C3d variants rather than recording avidity effects. The main limitation would have been the inability of the existing mathematical models to calculate affinity data from an immobilised octamer. The activity of the octamer could only have been tested appropriately with CR2 immobilised on the surface. Therefore the only viable means of testing functionality and cross-reactivity was *in vivo*, discussed in the following chapter.

Chapter 5

The Vaccine Octamer *In Vivo* – Protein and DNA Vaccine Administration

5.1 Introduction

It was shown in chapter 3 that the vaccine octamer hC3d^{S}-HEL-Oct could be produced and purified successfully from mammalian cell culture. In this part of the study, findings from the previous chapters were applied to plan a suitable vaccination strategy. CR2 could be targeted efficiently to maximise a response, however vaccine administration could be slowed down by production *in vitro*. In the first step, protein-based vaccine formulations were administered to experimental animals to prove that the octamers were functional *in vivo*. This would also provide a basis for comparison with downstream experiments. The constructs were subsequently inserted into DNA vaccine vectors. DNA vaccines are regarded by many as the future of vaccination thanks to their advantages over conventional protein vaccines ((231, 237, 369-372) section 1.10.1). The primary advantages of DNA vaccines are the ease of construction (373) and safety (231, 242, 269, 374). Pathogen attenuation or production of a recombinant protein vaccine can take years or weeks to months respectively. New genetic vaccines can in theory be produced within a week and be ready for testing. This potential has been harnessed for the design of genetic vaccines against a number of diseases, e.g. malaria (232, 249, 375), tuberculosis (270), HIV (271, 376), cancer (230) and allergy (377, 378). The other advantages are largely commercial considerations, i.e. large amounts of DNA can be produced, purified and stored with relative ease. In contrast to conventional vaccines, vaccine vectors are remarkably heat stable and benefit from a long shelf life without requiring cold storage (373). These are attractive traits for mass immunisation, especially in areas with difficult access and without electricity. Immunologically, DNA vaccines were found to elicit both specific antibodies as well as strong class I-restricted CTL responses (231, 374). DNA

vaccines have been administered most commonly by intramuscular injection into the leg muscle or transdermal (t.d.) delivery by gene gun into the abdominal skin, although various other routes have also been explored (227, 258, 261, 262). The DNA vaccines in the present study were administered by intramuscular injection or transdermal biolistic delivery via gene gun, which may transfect myocytes or APC keratinocytes and LC, respectively (369, 379).

C57Bl/6 WT mice were chosen in this first round of experiments as a model to test DNA vaccination with the C3d octamer constructs. They have been used extensively in immune response studies, both in our laboratory and in general. Additionally, future experiments with the available complement receptor transgenic and knockout mice on the C57Bl/6 background would allow direct comparison with these initial studies.

Additionally, with respect to judging the adjuvant potential of C3d as a molecular adjuvant, vectors containing CpG motifs (alternative adjuvant mechanism) were tested along side vectors lacking CpG motifs. The adjuvant potential of CpG motifs – as discussed in Section 1.11.5 – has been researched and reviewed in detail. As most DNA vaccine plasmids harbour them, the comparison whether the effects of C3d were lost in the effects of CpG promotion of a Th1 response was examined. C3d could also act synergistically with CpG-assisted vaccines (CpG^+) or override these effects. Thus, the true adjuvant potential of C3d in the DNA vaccine formulation could be assessed for vectors lacking CpG. This also allowed us to relate our data to previously published findings in which vaccine vectors encoding the linear C3d trimer had contained CpG sequences. The function of the vaccines

was assessed by collecting sera in regular intervals and analysing them with an in-house developed HEL-specific immunosorbent assay. This was the main method to establish functionality. The number of germinal centre B-cells, plasma and memory B-cells in the spleen at various times following vaccination, were also analysed. These key cell types drive the humoral immune response and study of their relative numbers in the sample tissues could provide vital clues about the effects of the vaccines.

5.2 Materials and Methods

5.2.1 Experimental Animals

Harlan (Surrey, UK) supplied 7 – 9 week old male C57Bl/6 mice, which were housed in conventional cages under the care of the staff at Biomedical Services (BMS) experimental animal facility. C57Bl/6 $Cr2^{-/-}hCR2^{+/-}$ were maintained in-house by BMS and Dr Kevin Marchbank. Mice were housed in specific pathogen-free conditions and handled according to Home Office guidelines.

5.2.2 Preparation and Administration of Protein Vaccines

Proteins for vaccination were made up in saline solution with or without CFA (Sigma, Poole, Dorset; 1:1, v/v). Groups of 5 – 6 anaesthetised mice received subcutaneous injections of antigen, listed in table 5.1 in 100 µl into the scruff of the neck. Booster vaccinations of 500 µg/ml native hen egg lysozyme (Sigma, Poole, UK) without adjuvant were administered at day 28.

Antigen	Concentration	Adjuvant
native hen egg lysozyme	500 µg/ml	CFA
HEL Fc	250 µg/ml	CFA
HEL Fc	250 µg/ml	-
$hC3d^{S}$-HEL-Oct	100 µg/ml	-
HEL-Oct	100 µg/ml	-

Table 5.1. Concentrations of antigen administered subcutaneously

5.2.3 Serum Sampling and Tissue Collection

Blood samples were taken prior to immunisation and weekly from day 14. Mice were held in a tube restrainer. The tips of their tails treated with ethylchloride (Dr Georg Friedrich Henning Chemische Fabrik Walldorf GmbH, Walldorf, Germany) followed by removal of the tip of the tail (< 1 mm) with a clean scalpel. Blood was collected in Microvette CB 300 blood collection tubes (Sarstedt, Leicester, UK) and left to clot at room temperature for 2 hours. Samples were stored at 4°C overnight. The clot was pelleted by centrifugation, serum was then removed and stored in a fresh container at –20°C. Experiments were terminated at day 42 (DNA) or day 35 (proteins). Mice were sacrificed humanely according to home office guidelines. A final blood sample was taken by cardiac puncture and spleens were removed. One half of the spleen was used for FACS analysis, the other half was snap frozen in isopentane on dry ice.

5.2.4 Vectors

5.2.4.1 CpG^- MCS

Lyopholised CpG^- MCS (containing a multiple cloning site) was provided by Invivogen (San Diego, USA, Figure 5.1). The vector and the vector-specific bacterial strain GT115 (section 2.5.) were reconstituted and handled according to the manufacturer's instructions. Vector and host had been modified to prevent formation of CpG dinucleotides, using the R6Kγ origin under control of GT115's *pir* gene. A CpG-free zeocin resistance gene facilitated bacterial selection. Mammalian expression was driven by a mouse CMV enhancer and human EF1α promoter and terminated by SV40.

5.2.4.2 CpG^+ HEL and CpG^+ $hC3d^S_3$-HEL

These vectors were originally supplied by Adprotech, now Inflazyme (actual names: pVK119-01 and pVK142-01 respectively). They were derived from the original C3d-containing DNA vaccine vectors ((218) also see (253, 337, 338)) and contained a CMV promoter and a kanamycin resistance gene. This group of vectors contained several CpG sequences, prokaryotic DNA adjuvant sequences (figure 5.2, table 5.2).

5.2.5 Introduction of a Multiple Cloning Site

A multiple cloning site (MCS) was designed consisting of Bts I, Not I, Xho I, HinD III, Bgl II, Eco R I, Eco RV, Xba I. 5'-phosphorylated oligonucleotides were supplied by MWG (Ebersberg, Germany) designed to create overhangs to fit into a Bts I and Bam HI-linearised vector. Equal amounts (10 pmol) of oligonucleotide were mixed, heated to 95°C and left to cool slowly to create the double stranded insert with overhangs. CpG^+ was digested with Bts I and Bam HI and mixed with the MCS fragment, 10 mM ATP, ligase and ligation buffer. The reactions were incubated at 16°C overnight and transformed by electroporation as described before (section 2.5).

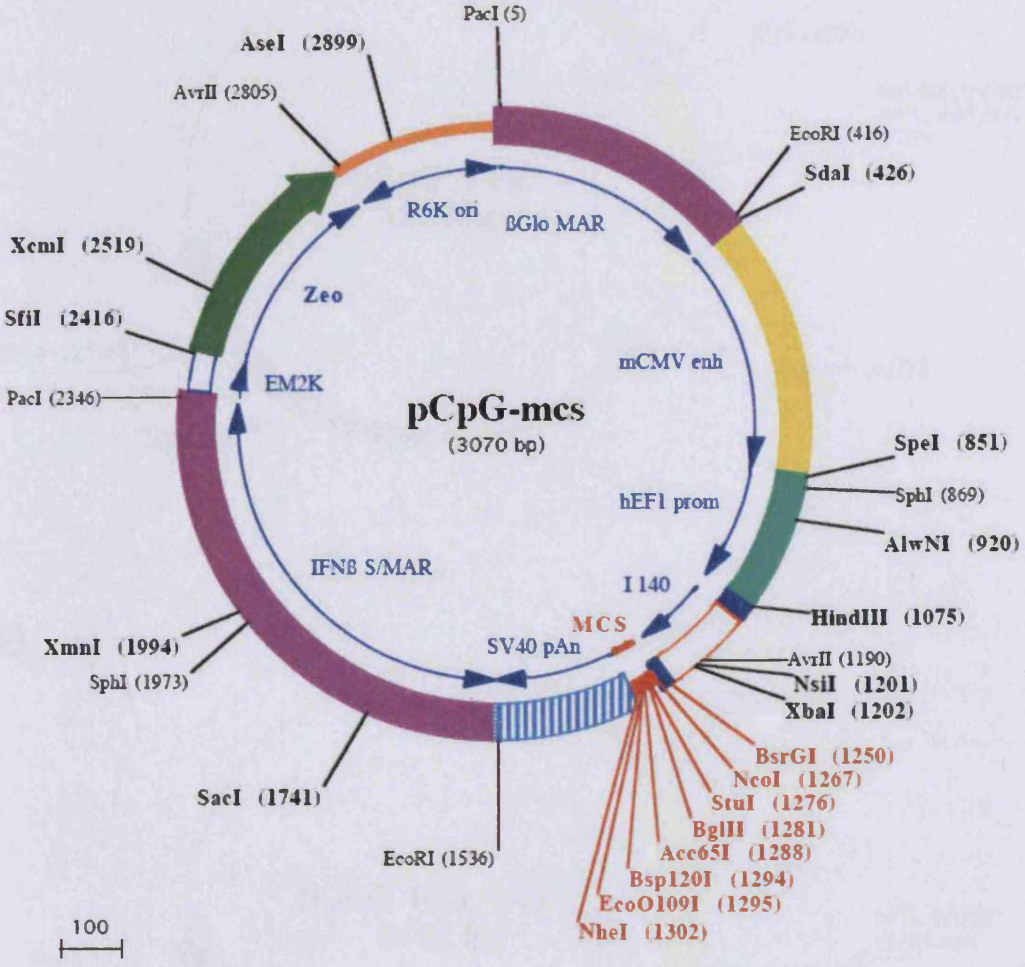

Figure 5.1. CpG⁻.

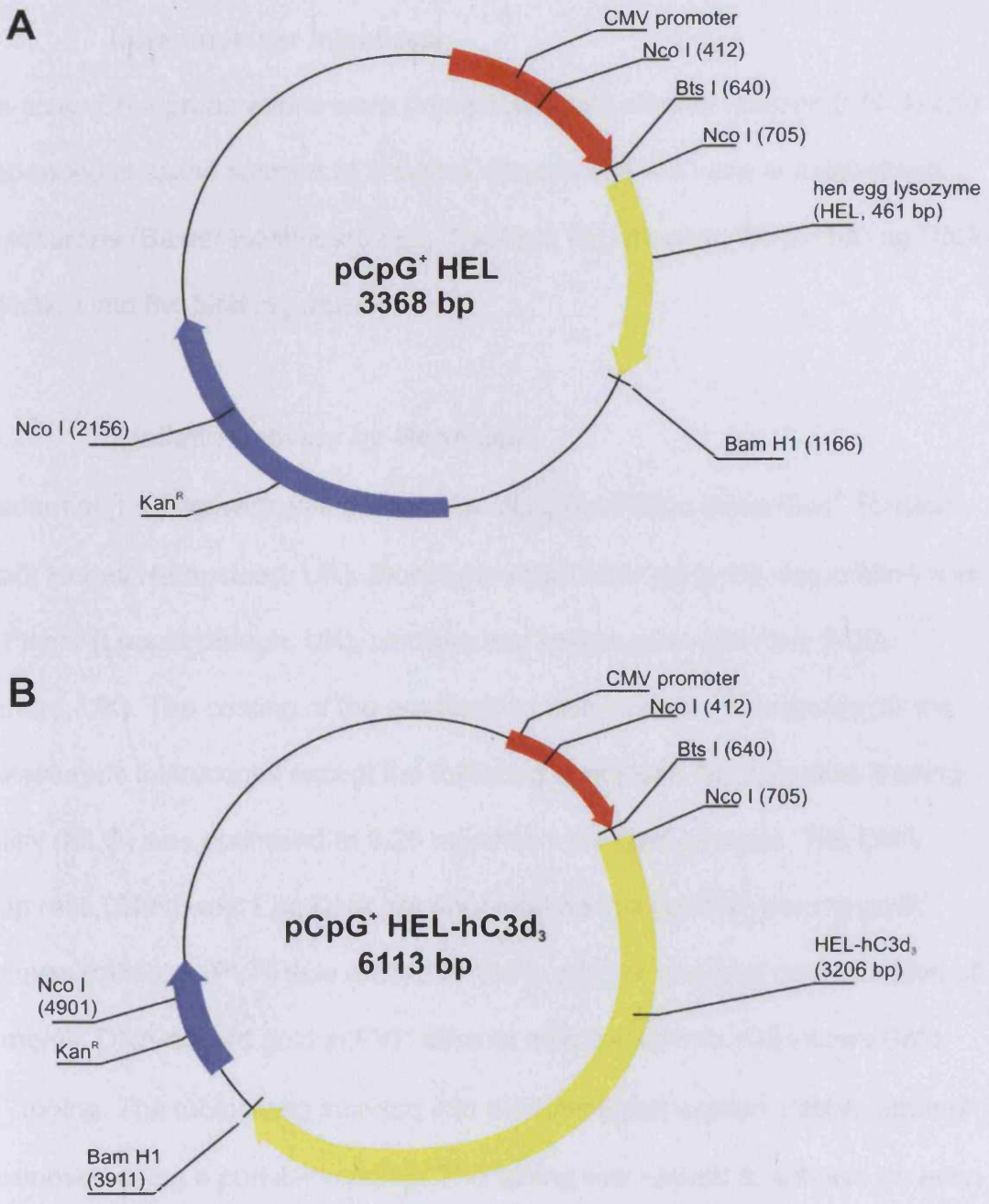

Figure 5.2. CpG+ vectors. Panel A: CpG+ HEL, panel B: CpG+ HEL-hC3d$^{S}_{3}$

5.2.6 Preparation and Administration of DNA Vaccine Formulations

5.2.6.1 Intramuscular Injections

Large-scale DNA preparations were precipitated with ethanol (section 2.10.3) and resuspended in saline solution at 2 mg/ml. Groups of 5 – 6 mice anaesthetised with isoflurane (Baxter Healthcare Ltd., Thetford, UK) received 50 µl (100 µg DNA) by injection into the hind leg muscle.

5.2.6.2 Biolistic Delivery by Gene Gun

Transdermal (t.d.) delivery was carried out using the Helios Gene Gun™ System (Biorad, Hemel Hampstead, UK). Biorad provided most reagents, spermidine was from Fisher (Loughborough, UK), nitrogen and helium gas were from BOC (Guildford, UK). The coating of the ammunition was carried out according to the manufacturer's instructions except the following conditions. Microparticle loading quantitiy (MLQ) was optimised to 0.25 mg/shot 1 µm gold particles. The DNA loading ratio (DLR) was 1 µg DNA per shot relating to 4 µg DNA per mg gold. Polyvinylpyrrolidone (PVP) was diluted in 100% ethanol to a final concentration of 0.15 mg/ml. DNA-coated gold in PVP ethanol was loaded into ~33 inches Gold-Coat™ tubing. The tubing was inserted into the tubing preparation station; ethanol was removed using a peristaltic pump. The tubing was rotated to achieve an even distribution of gold around the tubing followed by drying for 10 minutes with nitrogen. Gold-coated tube cuttings were stored at 4°C. Mice were anaesthetised for baseline blood sampling and to shave the abdominal area. Mice were allowed to awaken from anaesthesia prior to gold being fired into two non-overlapping skin sites using ultra-pure helium at 400 psi.

5.2.7 Statistical Analysis

Statistical analyses were conducted using the GraphPad software. Sets of data were compared by One-way ANOVA using the Tukey post-test and t-test. Where applicable, Kruskal-Wallis Test and Dunn's Multiple Comparison Test were used.

5.3 Results

5.3.1 Protein Vaccination

As administration of DNA into the skin or muscle does not guarantee equivalent production of the desired protein, which would influence the subsequent immune response, equimolar quantities of the recombinant octameric proteins (chapter 3) were injected into C57bl/6 mice to evaluate their ability to generate an immune response. This would confirm the vaccine was functionally active and yield information on the level of response that could be expected following DNA vaccination in later experiments. IgG as well as IgM titres were measured to profile the immune response in as much detail as possible. Four recombinant HEL-containing protein vaccine formulations (chapters 3 and 4) were prepared. HEL Fc (25 µg/mouse, ~22 pmol) was injected either in saline or in CFA. The two octamers, with and without C3d (each 10 µg/mouse, $C3d^+$ ~20 pmol, $C3d^-$ ~50 pmol), were injected in saline solution only. All mice were subsequently boosted 28 days later with 50 µg native HEL in saline. Sera were analysed with an in-house developed immunosorbent assay. 100 µg native HEL in bicarbonate buffer was immobilised in ELISA plate wells. Serum diluted in blocking buffer (sections 2.2 and 2.12.6) was applied to the wells in triplicate. Bound HEL-specific IgM or IgG was detected with mouse Ig HRPO-conjugated antibodies.

HEL+ CFA produced highest antibody levels of all protein vaccines examined here. Unexpectedly, injection of HEL Fc in CFA produced antibody responses lower than native HEL (50 µg/mouse; figure 5.3 A and B). However, as expected, HEL Fc in the presence of adjuvant (CFA) induced considerably higher anti-HEL antibody

production than in mice injected with HEL Fc in saline alone, which generated low levels of anti-HEL IgM production prior to boost and close to background levels of anti-HEL throughout. In this analysis, injection of HEL-Oct elicited no detectable anti-native HEL IgM or IgG responses (figure 5.3 C and D). Furthermore, boosting these mice with native HEL protein at day 28 did not result in any detectable anti-HEL antibody. IgM responses to hC3d^{S}-HEL-Oct mice were visibly higher than those noted in HEL-Oct and HEL Fc immunised mice throughout the experiment (figure 5.3 C). Unfortunately the difference in immune titre failed to reach significance. Analysis of anti-HEL IgG titre confirmed that hC3d^{S}-HEL-Oct had, on average, generated a greater response than HEL-Fc or HEL-Oct but titres between the six mice varied considerably (figure 5.4). Only two mice produced consistently high to medium levels of anti-HEL titre, a further two mice demonstrated a response after the boost and one exhibited low but detectable levels after boost. The remaining mouse showed no reaction following the primary immunisation and failed to develop a definitive response after the boost (figure 5.4). In conclusion, these results indicated that hC3d^{S}-HEL-Oct was superior to the control proteins (HEL Fc and HEL-Oct). This experiment confirmed that hC3d^{S}-HEL-Oct was functional encouraging us to investigate effects of the octamer construct applied in DNA vaccine form.

Figure 5.3. IgM and IgG antibody titres following subcutaneous injection of proteinaceous vaccines. The graphs show native HEL-specific antibody titres to each vaccine injected subcutaneously. Top row: HEL + CFA and HEL Fc + CFA; A: IgM, B: IgG. The two bottom graphs show the antibody titres in response to HEL Fc, hC3d^{S}-HEL-Oct and HEL-Oct all injected in saline solution: C: IgM, D: IgG. Mouse sera were collected at the indicated time points and analysed using native HEL in an immunosorbent assay. Mice were boosted with native HEL in saline at day 28 (indicated by arrow). Antibody titres are shown on the y-axis, calculated as the reciprocal of the dilution factor at absorbance at 490 nm; Data was derived from one experiment; HEL + CFA: n = 2, HEL Fc + CFA: n = 6, HEL Fc: n = 4, hC3d^{S}-HEL-Oct: n = 6, HEL-Oct: n = 6; Error bars: SEM.

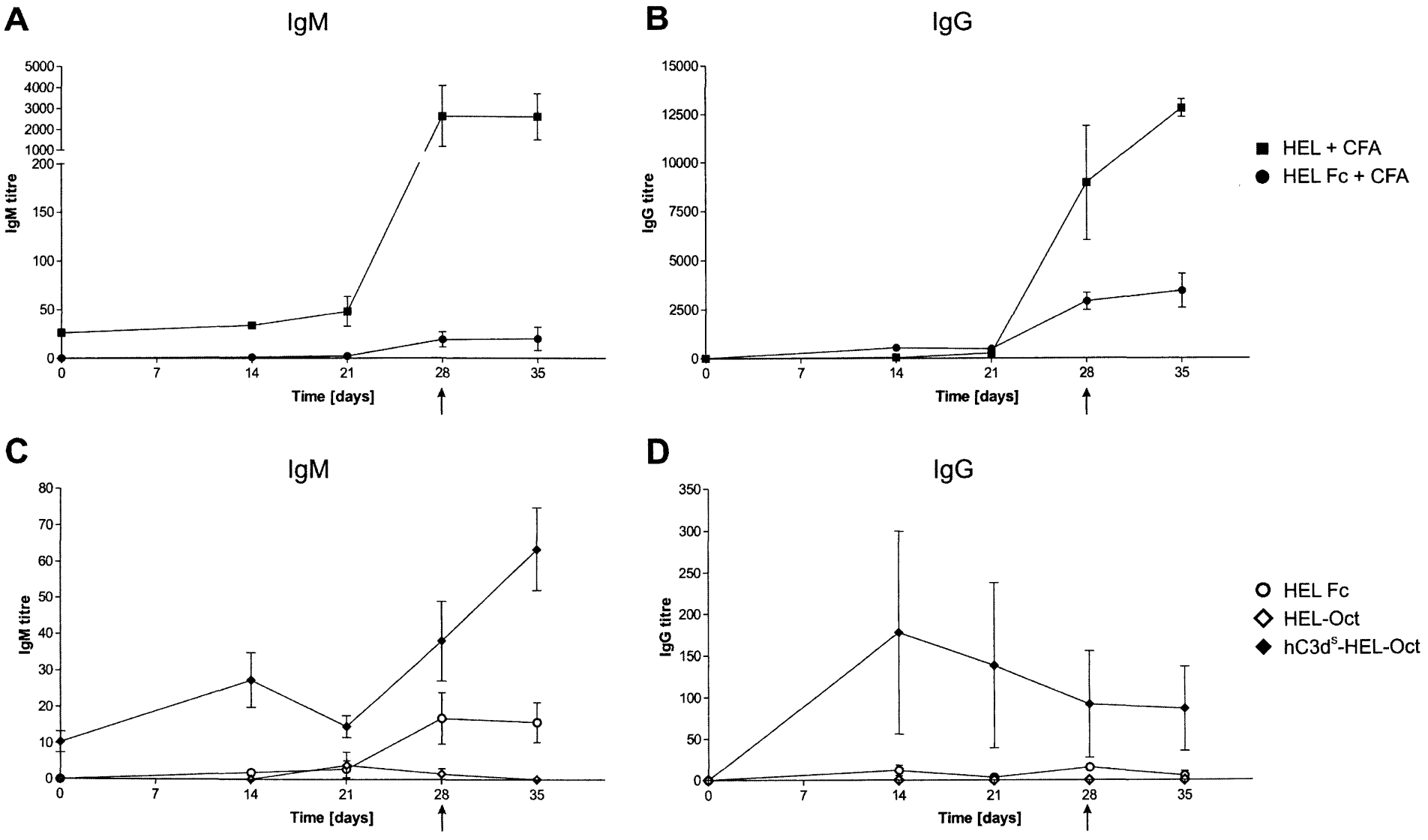
A
IgM
IgM titre
5000
4000
3000
2000
1000
200
150
100
50
0
0
7
14
21
28
35
Time [days]
B
IgG
IgG titre
15000
12500
10000
7500
5000
2500
0
Time [days]
HEL + CFA
HEL Fc + CFA
C
IgM
IgM titre
80
70
60
50
40
30
20
10
0
Time [days]
D
IgG
IgG titre
350
300
250
200
150
100
50
0
Time [days]
HEL Fc
HEL-Oct
hC3d^{s}-HEL-Oct

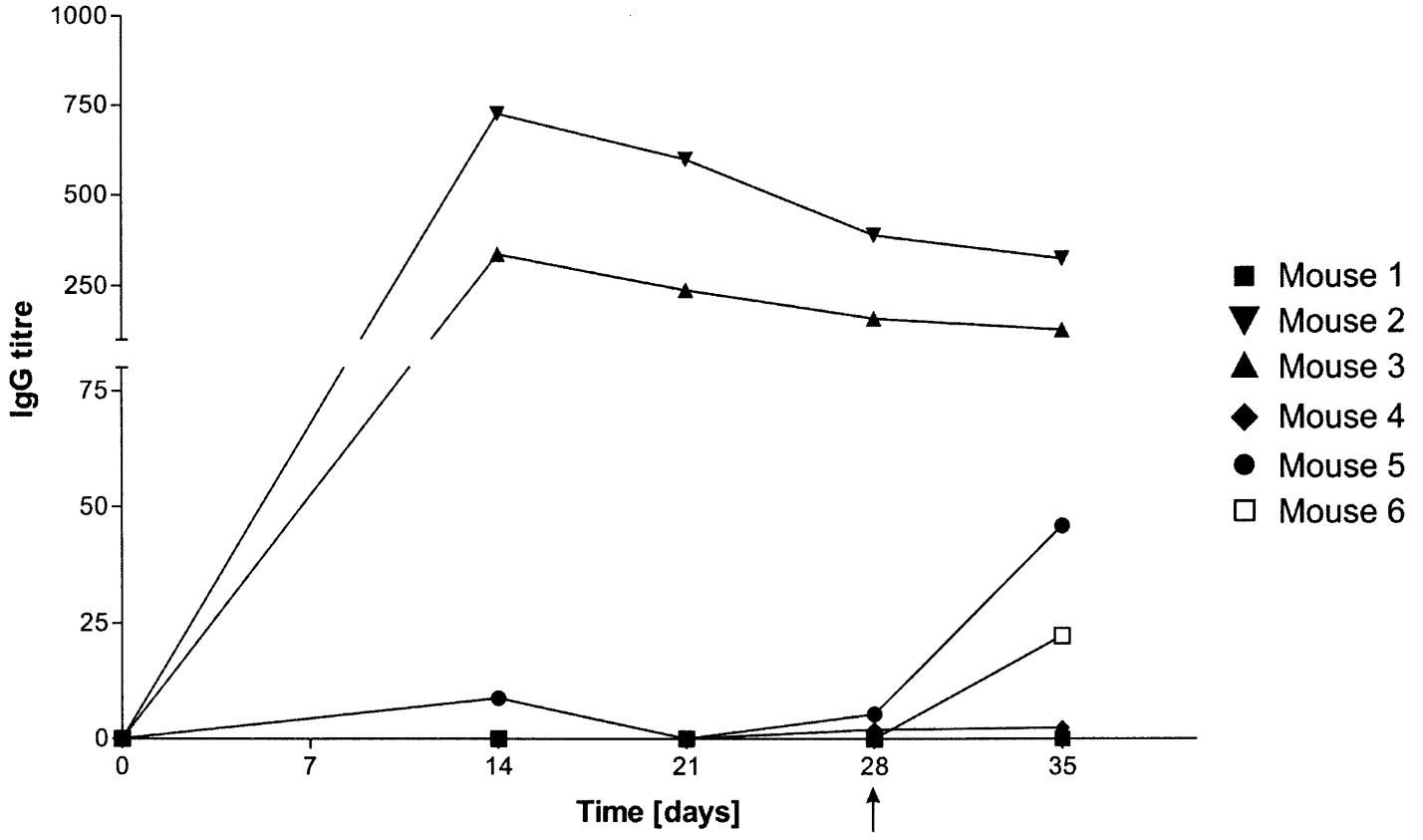

Figure 5.4. IgG antibody titres of mice injected with hC3d^{S}-HEL-Oct protein. Each line represents the IgG response from a single mouse following the C3d-adjuvant octamer. Mice were boosted with native HEL in saline at day 28 (arrow). Antibody titres are shown on the y-axis, calculated as the reciprocal of the dilution factor at absorbance at 490 nm

5.3.2 CpG analysis

DNA vaccines based on bacterial plasmids contain non-methylated CpG dinucleotides, which exert an immunostimulatory effect on mammalian immune cells. To exclude additional stimulatory effects and assess the true adjuvant activity of the vaccine, two vaccine vectors were included in the vaccination studies, one containing (CpG^-), one lacking CpG sequences (CpG^+). CpG presence or absence was analysed with the CpG plot tool on the European Bioinformatics Institute website (http://www.ebi.ac.uk/emboss/cpgplot). CpG^- did not contain any CpG sequences (figure 5.5, table 5.2) and was thus free of prokaryotic DNA adjuvant sequences. CpG removal included the zeocin resistance allele, which usually harbours a number of these dinucleotides. The CpG^+ vectors contained five and six putative CpG islands as shown in figure 5.5. The hen egg lysozyme DNA contained CpG sequences (750 – 970) but the human C3d sequences were CpG free.

Vector	Sequence start - stop	Length [bp]
CpG$^-$ MCS	No CpG sequences	
CpG$^+$ HEL	397 – 635	239
	753 – 971	219
	1534 – 1886	353
	1906 – 2384	479
	2913 – 3310	398
CpG$^+$ hC3d$^S{}_3$-HEL	397 – 635	239
	753 – 971	219
	1004 – 1206	203
	4279 – 4631	353
	4651 – 5129	479
	5658 – 6055	398

Table 5.2. CpG sequences in DNA vaccine vectors.

pCpG$^-$

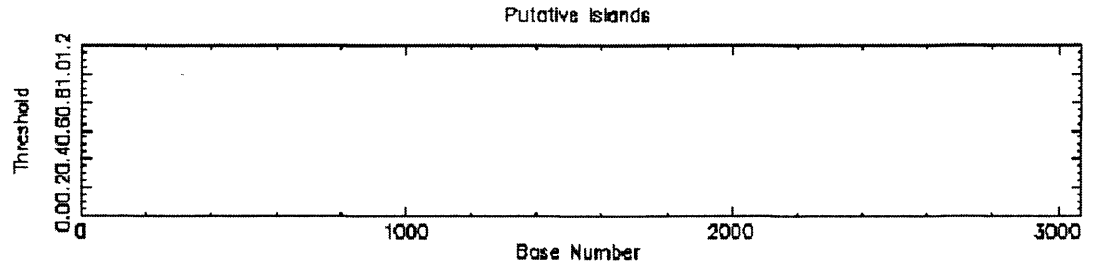

pCpG$^+$ HEL

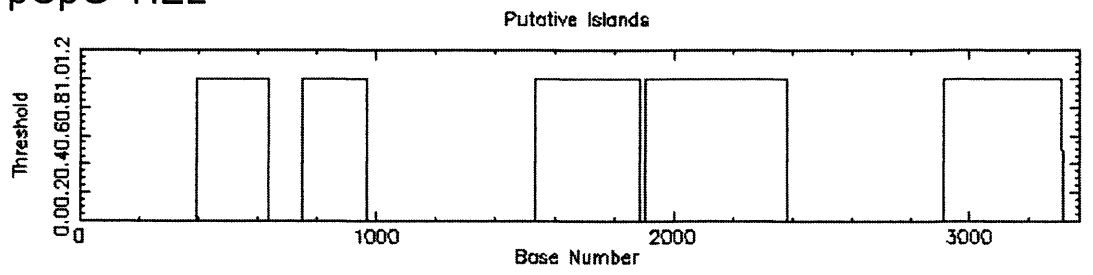

pCpG$^+$ HEL-hC3d$_3$

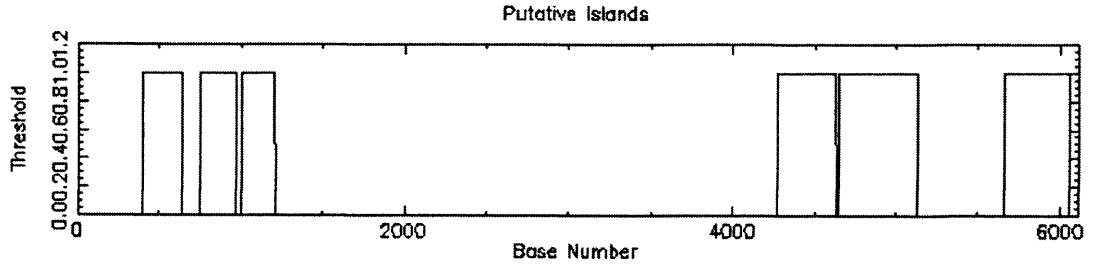

Figure 5.5. CpG content plots. Plots were generated using the European Bioinformatics Institute website. CpG-rich sequences are indicated by columns in the plots.

5.3.3 Generation of DNA vaccines

5.3.3.1 CpG^-

The DNA sequences of the octamers $C3d^S$-HEL-Oct and HEL-Oct were inserted into the CpG^- MCS vector by PCR amplification, restriction digest and ligation. Each construct was amplified from the pDR2EF1α vectors with primers containing an Nco I restriction site (Nco_CD33_F and Nco_8_R Appendix I). Positive colonies were screened by restriction digest, which confirmed the presence of the constructs in the CpG-free vector (figure 5.6). Each vector was cut with Nco I and Hind III. Digest of CpG-MCS produced bands representing the vector backbone (2878 bp) and a faint band representing an excised 192 bp vector fragment as predicted from analysis of the plasmid sequence. Digest of CpG^- $C3d^S$-HEL-Oct generated four expected bands, which were from top to bottom, the vector backbone, the recombinant sequence (1581 bp), the small vector fragment (192 bp) and the octameric sequence (180 bp). Due to their similar size these two bands are merged and not fully discernible using this analysis. Digest of CpG^- HEL-Oct revealed bands that represented, the vector and the octameric sequences as well as the HEL sequence (483 bp). Because the vector sequence obscured the existence of the 180bp Oct fragment and to confirm that no mutations had been accidentally introduced to these plasmids during their construction the DNA sequence of all constructs was verified to be identical to that predicted by dideoxysequencing.

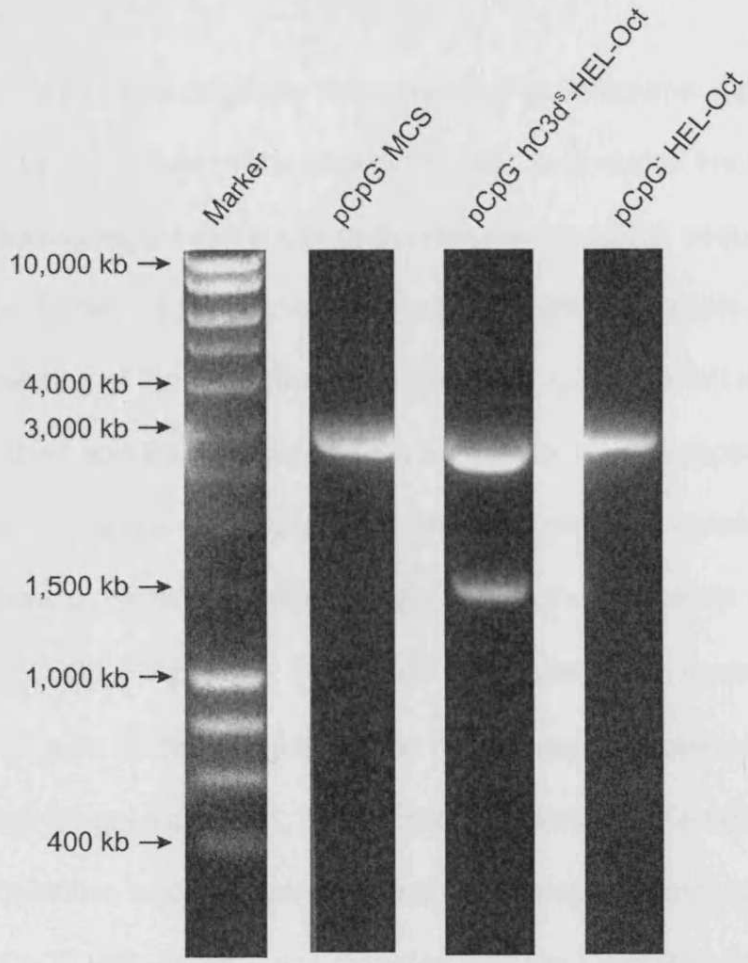

Figure 5.6. CpG⁻ vector restriction digests. Double digests of 2 µg of vector DNA were carried out with Nco I and Hind III in the appropriate buffers. Wells of a 0.8% agarose TAE gels were loaded with 50 µl DNA digest reaction containing 10% loading buffer. Ladder: Hyperladder I

5.3.3.2 CpG^+

Two DNA plasmid vectors had originally been supplied by Inflazyme, CpG^+ HEL and CpG^+ HEL-hC3d$^S_3$. Analysis of the plasmid sequence revealed the lack of a suitable multiple cloning region at the site of the recombinant DNA sequences. Therefore, prior to insertion of the recombinant octamer DNA a multiple cloning site was designed consisting of the restriction sites Bts I, Not I, Xho I, Hind III, Bgl II, Eco R I, Eco RV, Xba I and Bam HI yielding the vector CpG^+ MCS (Appendix I). The sequence was verified by dideoxysequencing. The octameric constructs were amplified with a forward primer annealing at the CD33 signal sequence containing an Xho I site (XhoI-CD33_F Appendix I). EF1α 3' was used as the reverse primer. The PCR product as well as the newly designed vector were digested with Xho I and Eco RV, purified by gel extraction, ligated and transformed by electroporation. The sequences of positive colonies were verified by dideoxysequencing and restriction digest. CpG^+ HEL-hC3d$^S_3$ was digested with Bts I and Bam HI (figure 5.7 left panel) resulting in the antigen-C3d trimer construct (3206 bp) and the vector backbone (2907 bp). The remaining constructs were digested with Nco I alone. In the original vectors, three Nco I sites had been present (figure 5.7). Restriction digests of CpG^+ HEL (figure 5.7) therefore resulted in three fragments (from top to bottom) of 1624 bp, 1451 bp and 293 bp. The restriction site at the 5' end of HEL was eliminated with the introduction of the MCS between Bts I and Bam HI. Consequently, the newly designed CpG^+ vectors were only cut in two positions. They yielded two fragments: a vector backbone fragment of 1624 bp common to all plasmids and a specific band containing the recombinant sequences or MCS.

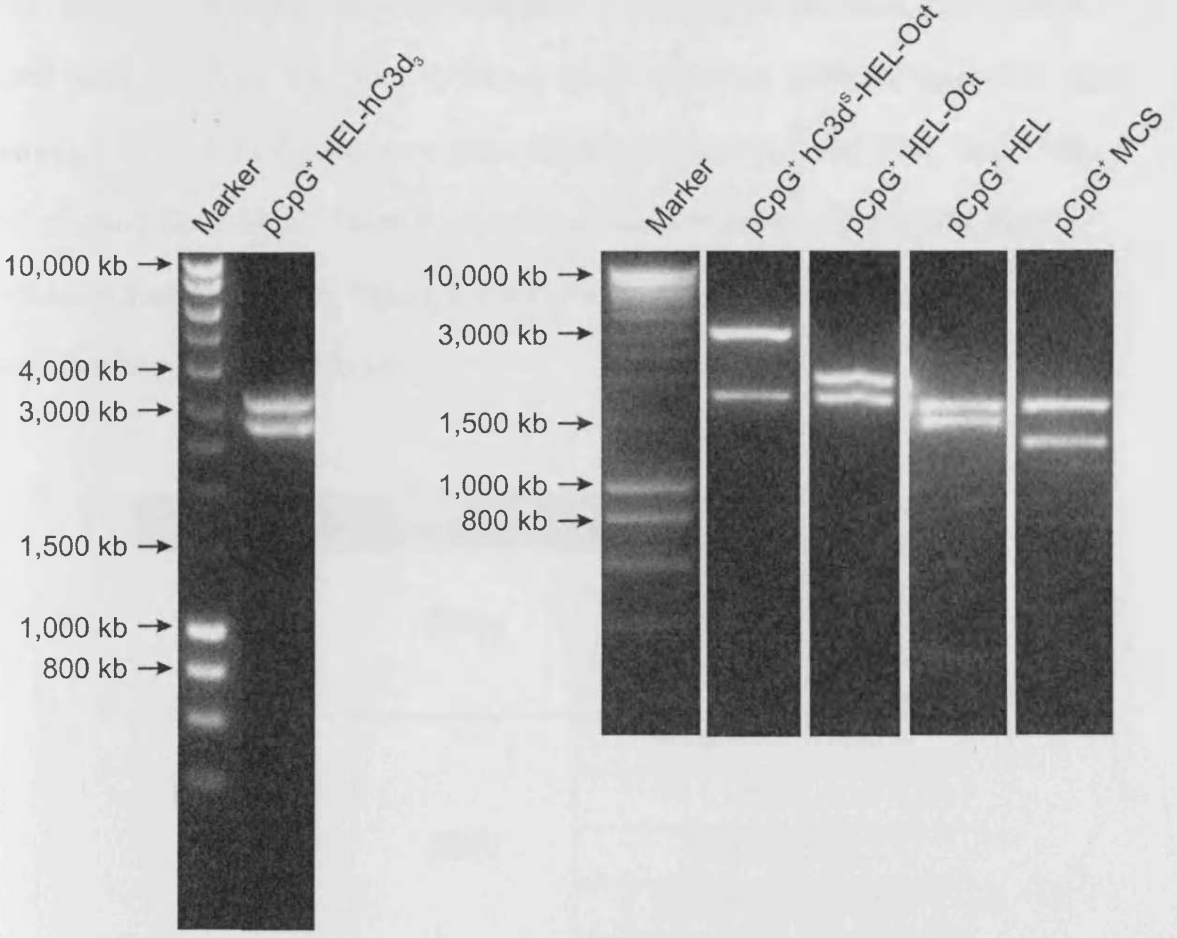

Figure 5.7. Restriction digests of CpG$^+$ vectors. Restriction digests were carried out with 2 µg DNA in appropriate buffers and loaded into wells of a 1% agarose (w/v) TAE gel. Left panel: CpG$^+$ HEL-hC3d$_3$ was digested with Bts I and Bam HI. Right panel: CpG$^+$ hC3d^S-HEL-Oct, CpG$^+$ HEL-Oct, CpG$^+$ HEL and CpG$^+$ MCS were digested with Nco I. Ladder: Hyperladder I

The detected fragment sizes corresponded to their expected sizes (CpG^+ MCS: 1333 bp, CpG^+ $C3d^S$-HEL-Oct: 2726 bp, CpG^+ HEL-Oct: 1826 bp, figure 5.7, right panel). Five vectors in total were generated in addition to CpG^+ HEL, CpG^+ HEL $hC3d^S{}_3$ and CpG^- MCS. Table 5.3 shows all vaccine constructs studied here including their promoters. Figure 5.8 shows the expected conformation of each protein when expressed *in vivo*.

Vector	Promoter	Inserted sequence
CpG^-	EF1α	MCS – no protein
		$hC3d^S$-HEL-Oct
		HEL-Oct
CpG^+	CMV	MCS – no protein
		HEL
		HEL-$hC3d^S{}_3$
		$hC3d^S$-HEL-Oct
		HEL-Oct

Table 5.3. DNA vaccine vectors

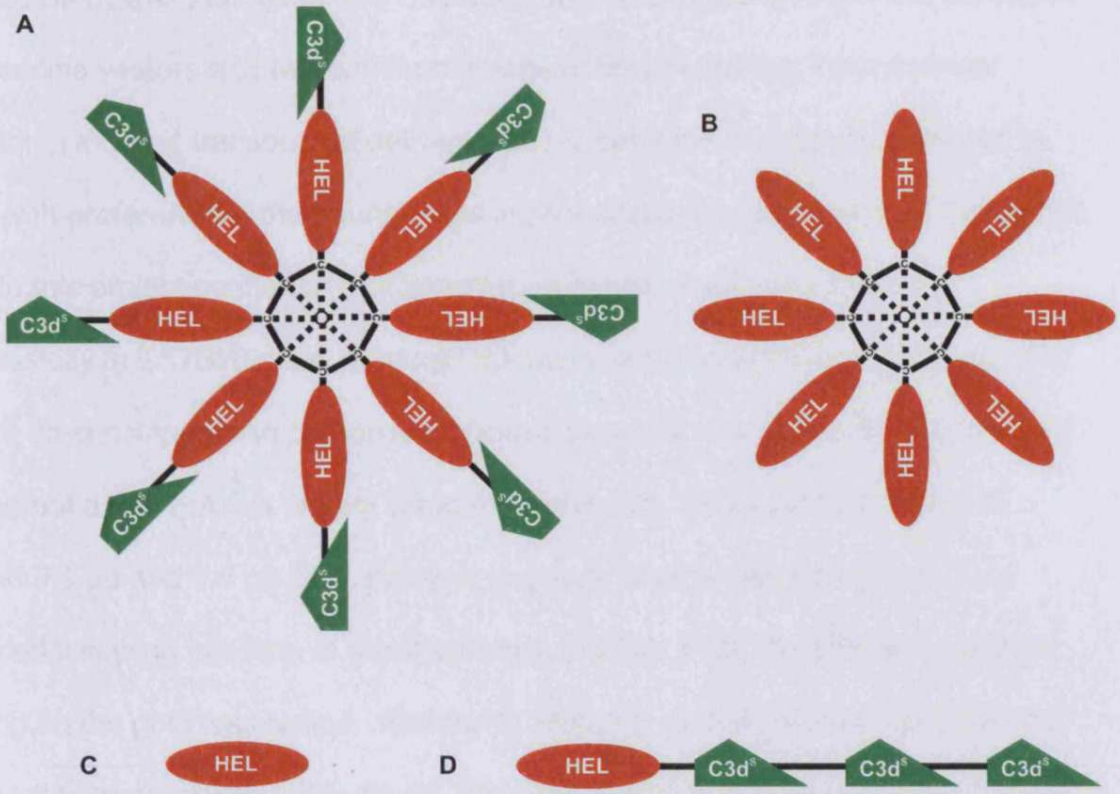

Figure 5.8. DNA vaccine constructs. Panels A through D show a diagrammatic representation of the four proteins to be expressed by the vaccine vectors. Panel A and B show the octameric proteins, one containing the human $C3d^S$ adjuvant, (A), the other lacking the molecular adjuvant. These were studied using DNA as well as purified proteins. The vaccine constructs HEL (C) and HEL-$hC3d_3$ (D) were used exclusively as DNA vaccines.

5.3.4 DNA Vaccination

Reassured by the finding that the C3d octamer could trigger a response, we tested two vaccine vectors and two common means of administration, intramuscular injection (i.m.) and transdermal delivery (t.d.) to determine which route should be used with preference in the future. Initial intramuscular injections with a DNA vector prior to this project confirmed that immune responses could be induced successfully in C57Bl/6 mice, although the response appeared to be delayed by at least 7 days compared to responses induced by protein injections. Trials were also carried out as part of this project using the gene gun. These pilot experiments utilised 0.1 µg and 0.5 µg DNA per shot to gauge whether antibodies could be detected following injection of small amounts of DNA. First, the efficiency of DNA coating on the gold was tested. Randomly selected cartridges from each vaccine preparation were washed with dH_2O. The supernatant was subsequently analysed by agarose gel electrophoresis. The vaccines could be readily detected in the gel at the respective concentrations (figure 5.9 A). Having confirmed the vaccines had been prepared successfully, the gold was fired into the skin of the mice. In comparison to past publications, responses in our experiments were near or below the detection level (figure 5.9 B). Dilution of the endpoint serum by 1:10 however revealed presence of HEL-specific IgG antibodies in animals injected with 0.5 µg and 0.1 µg DNA injected animals (figure 5.9 C). The low titres led to the decision to alter the conditions for the subsequent experiments (section 5.2.6). Adverse reactions due to the vaccines such as localised inflammation of the skin or symptoms otherwise affecting the mice were never observed. Unfortunately however, adverse effects were caused by hair removal using commercially available (Boots Gentle Hair Removal Cream) depilatory cream that was used

Figure 5.9. Trial gene gun vaccinations. Gold pellets were coated with CpG^+ HEL DNA corresponding to 0.1 µg and 0.5 µg DNA per shot and injected into the abdominal skin of two groups of C57Bl/6 mice (n = 3). Panel A shows the coating efficiency of DNA on gold. Ammunition cartridges were washed extensively in distilled water to release the DNA from the gold pellets. Gold was removed by centrifugation and the supernatant loaded into the wells of a 1% agarose gel. Panel B shows the course of the IgG response over three months. Sera collected by tail snip were diluted in blocking buffer 1:500 and analysed using the HEL ELISA. Panel C shows cardiac puncture serum samples. Antibody titres were measured by diluting sera in blocking buffer at the concentrations indicated on the x-axis.

A

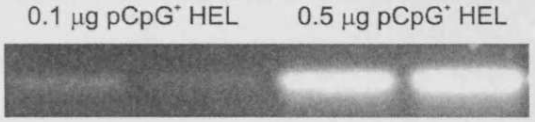
0.1 μg pCpG* HEL
0.5 μg pCpG* HEL

B

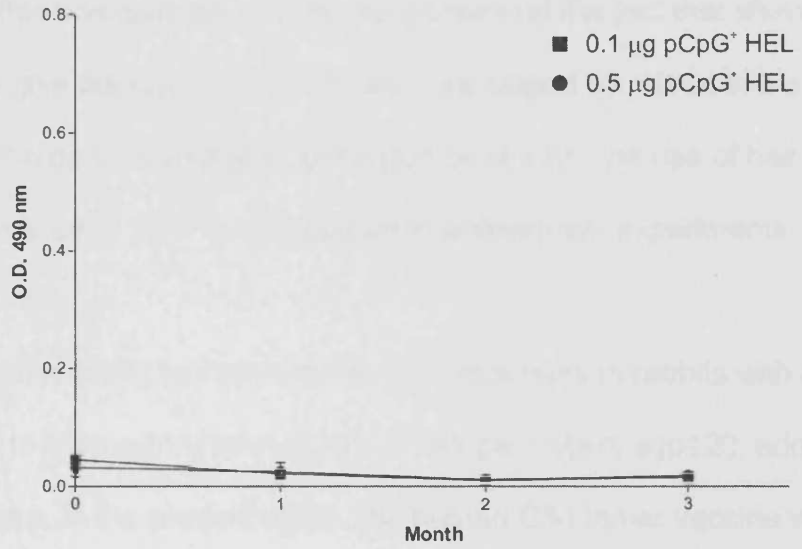
0.1 μg pCpG* HEL
0.5 μg pCpG* HEL
O.D. 490 nm
0.8
0.6
0.4
0.2
0.0
0
1
2
3
Month

C

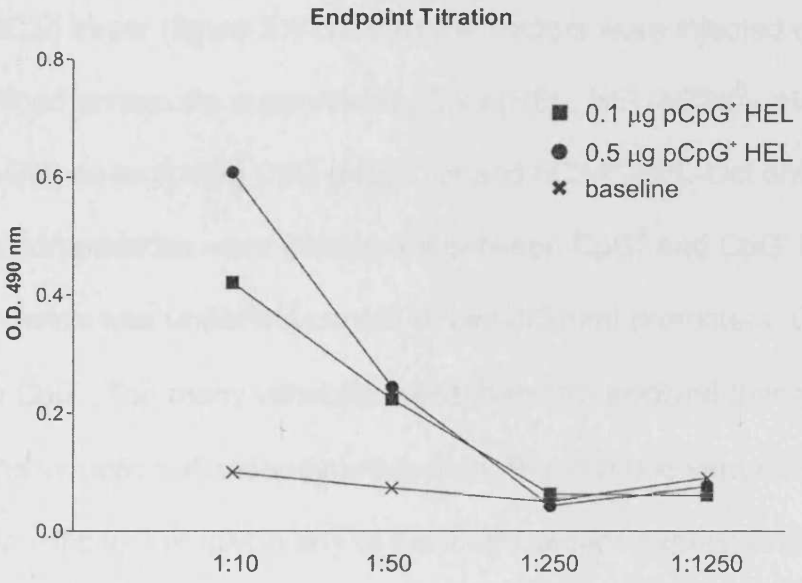
Endpoint Titration
0.1 μg pCpG* HEL
0.5 μg pCpG* HEL
baseline
O.D. 490 nm
0.8
0.6
0.4
0.2
0.0
1:10
1:50
1:250
1:1250

during the first vaccine trial. The use of the cream in this study resulted in an inflammatory reaction that resulted in scarring at the treated sites as well as the hind legs and feet and caused the mice considerable discomfort. Affected mice were immediately removed from the experiment and sacrificed humanely. Thus, because of this unexplained adverse response and the fact that shaving alone appeared to give adequate access to skin, as judged by reproducible "gold staining" of the dermal area after gene gun discharge, the use of hair removal cream was excluded from the procedure in subsequent experiments.

Previous studies (256) had shown immune responses in rabbits with a human C3d trimer fused to a secretory form of HIV envelope protein, sgp120, administered as a DNA vaccine. In the present study, the human C3d trimer vaccine was tested in mice using hen egg lysozyme (HEL-hC3d$^{S}_{3}$, figure 5.8 C). The control vaccine lacked the hC3d trimer (figure 5.8 D). Vaccine vectors were injected containing the above-described constructs supported by CpG (HEL, HEL-hC3d$^{S}_{3}$, HEL-Oct and hC3d^{S}-HEL-Oct) or excluding CpG (HEL-Oct and hC3d^{S}-HEL-Oct only). However no statistical comparisons were carried out between CpG^{+} and CpG^{-} because protein expression was under the control of two different promoters, CMV in CpG^{+} and EF1α in CpG^{-}. Too many variables were therefore involved that could have influenced the induction of antibody production. Pre-immune sera had no detectable specific IgG or IgM in any of the immunisation experiments.

Administration of CpG^{+} DNA into the anterior thigh muscle only elicited an IgM response following administration of hC3d^{S}-HEL-Oct compared to the other vaccine candidates (Figure 5.10 A, day 14 $p < 0.05$, day 42 $p < 0.001$). IgM titres

reached a plateau at day 28 but interestingly reached their peak at day 42 despite the lack of a second vaccine administration. HEL and HEL-hC3d$^{S}_{3}$ failed to induce significant titres and remained close to the baseline throughout the experiment. HEL-Oct produced modest amounts of IgM peaking at day 35. The general absence of IgG following CpG^{+} HEL administration throughout the monitored period (figure 5.10 B and D) indicated failure to induce Ig heavy chain class switch or seroconversion. Intramuscular injection of CpG^{+} HEL-hC3d$^{S}_{3}$ induced the strongest IgG response of all CpG^{+} vaccines within the first 14 days (figure 5.10 B). The octameric vaccines only raised modest IgG titres.

Gene gun vaccine application induced HEL-specific antibodies in all groups although the responses were relatively low (figure 5.10 C). Overall, IgM titres across the groups were not significantly different from each other. Average responses to HEL-Oct were higher in the gene gun method with titres peaking at day 42 but due to the variability of the response there was no significant difference between the administration methods in the CpG^{+} DNA vaccines. Anti-HEL antibodies in response to CpG^{+} HEL peaked at day 28. Injection of vector alone did not induce any detectable anti-HEL antibodies as would be expected. The other vaccines exhibited raised titres from day 21 and a continued upwards trend towards the end of the experiment, similar to i.m. injected hC3d^{S}-HEL-Oct DNA. HEL-hC3d$^{S}_{3}$ IgM levels were also consistently higher than levels observed in HEL-Oct ($p < 0.001$). This was achieved by hC3d^{S}-HEL-Oct only on day 21 ($p < 0.001$) after which the response faded again to near background levels. Generally, IgG and IgM levels in mice receiving vaccine via gene gun were low and highly variable across all groups causing statistical variation. For clarity, error bars were hence

Figure 5.10. Ig responses to CpG-assisted DNA vaccines administered by intramuscular injection or biolistic transfer. The diagrams show the change in Ig titres measured by absorbance at 490 nm (y axis) over time (x axis). C57Bl/6 WT mice received vaccine vector DNA by intramuscular injection (panels A and B) or biolistic transfer (panels C and D) at day 0. Sera were collected from three to six mice per group weekly from day 14 until day 42. IgM (panels A and C) and IgG (panels B and D) were screened against native HEL in an ELISA-based assay. Empty vector control responses have been subtracted from the traces on the graphs. Data shown from one experiment; each group consisted of 6 mice except t.d. CpG^{+} HEL-Oct (n = 5). Error bars are standard error of the mean but have been omitted in panels C and D for the purpose of clarity.

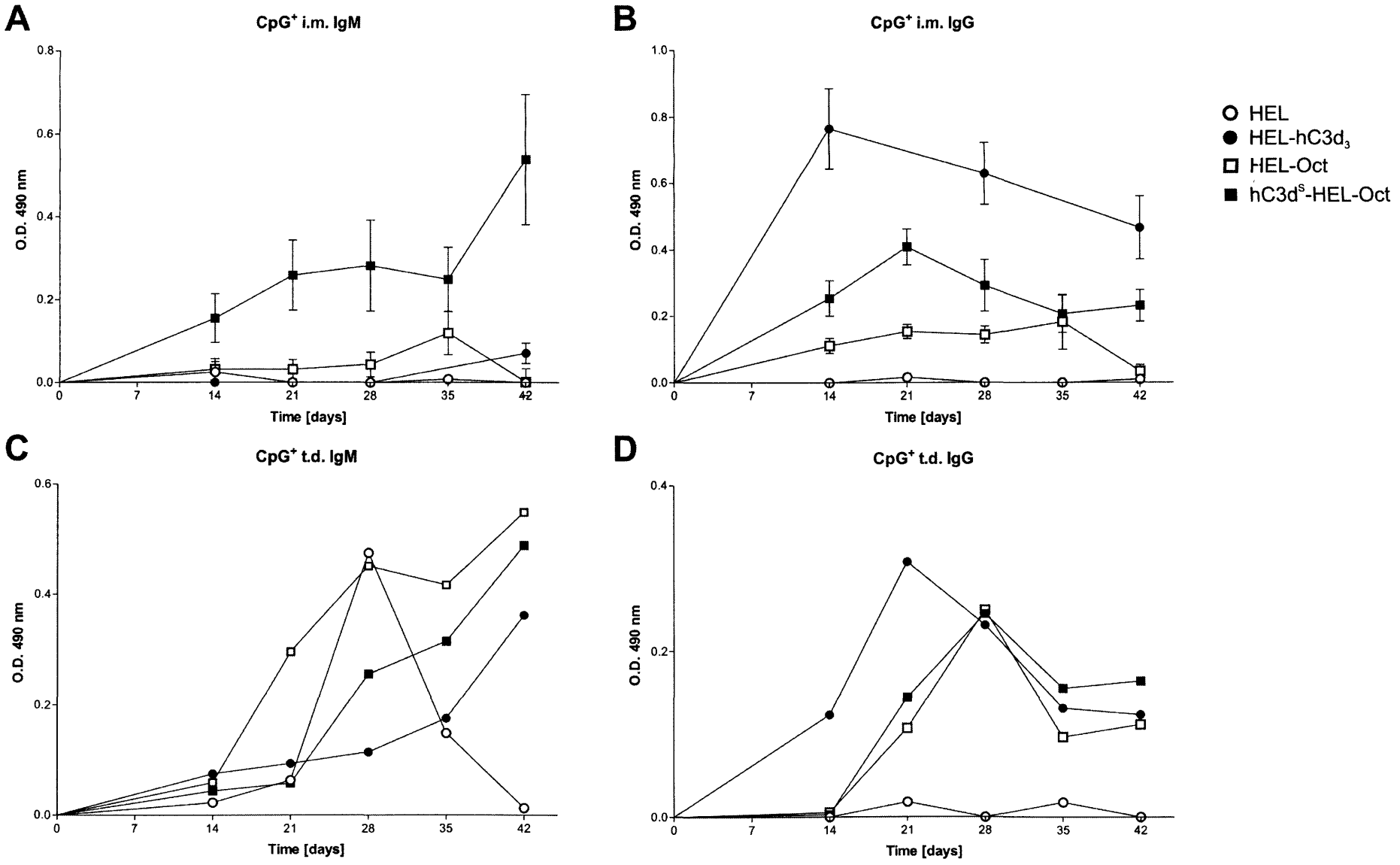
A
CpG+ i.m. IgM
O.D. 490 nm
Time [days]
B
CpG+ i.m. IgG
O.D. 490 nm
Time [days]
C
CpG+ t.d. IgM
O.D. 490 nm
Time [days]
D
CpG+ t.d. IgG
O.D. 490 nm
Time [days]
HEL
HEL-hC3d3
HEL-Oct
hC3ds-HEL-Oct

omitted from figures 5.10. C and D. The IgG response triggered by t.d. administration seemed to be delayed by one week compared to injection into the thigh muscle. Maximum titres were recorded at day 21 (HEL-hC3d$^{S}_{3}$) and day 28 (hC3d^{S}-HEL-Oct and HEL-Oct), respectively. However, responses were highly variable, especially among HEL-hC3d$^{S}_{3}$ injected mice. A single mouse exhibited highly elevated IgG levels while the others only started producing antibody from day 21. This reflected the protein injection-mediated responses. Both C3d-encoding vaccines rose above baseline. However, HEL-specific γ-type Ig levels raised by hC3d^{S}-HEL-Oct did not rise specifically above HEL-Oct-induced titres.

Comparison of the two administration routes did not reveal any differences in the IgM titres. IgG responses were similar in general, except that mice given intramuscular injections of HEL-hC3d$^{S}_{3}$, hC3d^{S}-HEL-Oct or HEL-Oct ($p < 0.05$) developed their responses earlier. A second experiment was carried out only utilising CpG^{+} hC3d^{S}-HEL-Oct. The aim was to substantiate and clarify the above results via both routes. Unfortunately, although neither the protocol nor materials used were altered, no responses were detected. At present, the reasons for this failed response are unknown and these findings require further investigation. In conclusion, DNA vaccination using these constructs was a less reliable or reproducible approach than had been first anticipated.

Mice were immunised with CpG-reduced DNA-vaccines to assess the effect on the octamer constructs' ability to generate a humoral immune response. As above, intramuscular injection and transdermal delivery as routes of administration were assessed. In general, the CpG^{-} vectors generated higher and less variable

responses for both routes of administration than the CpG containing vectors. The sera from empty-vector control injected mice were also analysed by ELISA, which showed that the control vector did not trigger an immune response against HEL. Native HEL-specific IgM responses following injection of HEL-Oct and hC3d^{S}-HEL-Oct into the thigh muscle were comparable (figure 5.11 A). Responses to both vaccines consistently rose above baseline levels ($p < 0.01$ and $p < 0.05$ respectively) throughout the duration of the experiment. Anti-HEL levels following intramuscular CpG^{-} HEL-Oct immunisation were slightly higher than hC3d^{S}-HEL-Oct in the IgM response throughout the experiment (figure 5.11 A). However, only low levels of γ-type anti-native HEL antibodies were produced. HEL-specific IgG titres rose until day 21 and waned slightly towards the end of the experiment (figure 5.11 B). Consequently, hC3d^{S}-HEL-Oct IgG titres were significantly different from the non-C3d counterpart throughout ($p < 0.001$).

Transdermal delivery successfully elicited IgM antibody specific for native HEL in the immunosorbent assay. However, the titres following administration of hC3d^{S}-HEL-Oct were higher than in response to HEL-Oct (e.g. $p < 0.05$ at day 14 and $p < 0.001$ at day 28, figure 5.11 C). For hC3d^{S}-HEL-Oct, IgM titres generally rose throughout the experiment, whilst anti-HEL levels post HEL-Oct injection rose until day 21, stagnated and rose again from day 28.

The IgG response to transdermal application of hC3d^{S}-HEL-Oct and HEL-Oct was almost exactly the same (figure 5.11 D). Contrary to the i.m. injections, HEL-Oct triggered production of IgG in conjunction with lower IgM titres (figure 5.11 C). The IgG titres of hC3d^{S}-HEL-Oct and HEL-Oct were almost identical until day 35.

Figure 5.11. Ig responses to CpG-reduced DNA vaccines administered by intramuscular injection or biolistic transfer. The diagrams show the change in Ig titres measured by absorbance at 490 nm (y axis) over time (x axis). C57Bl/6 WT mice received vaccine vector DNA by intramuscular injection (panels A and B) or biolistic transfer (panels C and D) at day 0. Sera were collected from three to six mice per group weekly from day 14 until day 42. IgM (panels A and C) and IgG (panels B and D) were screened against native HEL in an ELISA-based assay. Empty vector control responses have been subtracted from the traces on the graphs. Data shown from one experiment; each group consisted of 6 mice. Error bars: standard error of the mean.

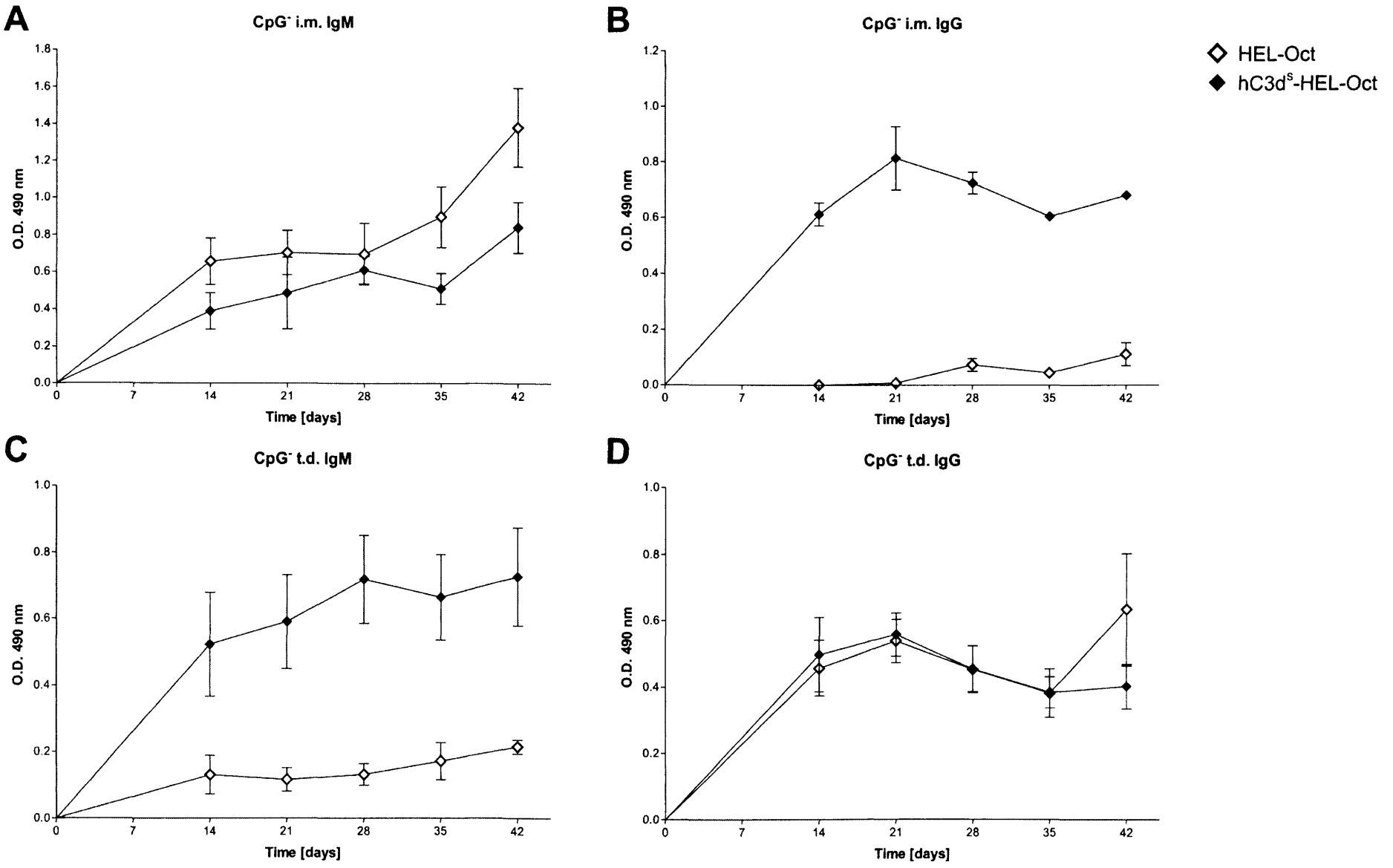
A
CpG⁻ i.m. IgM
O.D. 490 nm
Time [days]
B
CpG⁻ i.m. IgG
O.D. 490 nm
Time [days]
C
CpG⁻ t.d. IgM
O.D. 490 nm
Time [days]
D
CpG⁻ t.d. IgG
O.D. 490 nm
Time [days]
HEL-Oct
hC3d^s-HEL-Oct

Administration of CpG^+ $hC3d^S$-HEL-Oct revealed some distinguishable differences in the IgG concentration (i.e. the point at which responses reached there peak). In contrast, lack of CpG via both routes of administration led to almost congruent IgG profiles following $hC3d^S$-HEL-Oct administration (figure 5.11 B and D). Moreover, the responses generated by $hC3d^S$-HEL-Oct via either route were not significantly different from each other concerning both HEL-specific serum IgG or IgM. HEL-Oct only induced significant IgM titres following i.m. DNA injection but seroconversion failed in this experiment. IgM responses were low after biolistic transfer of CpG^- HEL-Oct. Therefore this was the more successful route of administration in respect of generation of IgG responses. These results suggest that CpG motifs could have an impact on the intensity of the response after delivery of the constructs via the two different routes.

Unfortunately, as with the CpG-assisted study a follow-up experiment failed to generate any measurable anti-HEL antibodies. In general, we found that the immune response after transdermal delivery of all vaccines suffered greatly from experiment to experiment and mouse to mouse variation. These experiments highlighted one draw back of DNA vaccination. Although DNA concentrations on gold pellets or in the syringe can be controlled, actual level of DNA uptake and subsequent protein produced *in vivo* can vary considerably.

5.3.5 Analysis of the Effects of the Vaccines on B-cell Populations in the Spleen

In order to analyse the cellular response to vaccination in more detail, spleens were removed following terminal bleeding for flow cytometric analysis. The relative amounts of germinal centre B-cells ($CD19^+$ $GL7^+$), plasma B-cells ($CD19^+$ $CD138^+$) and memory B-cells ($B220^+$ $CD38^{hi}$) present were established to provide evidence that the immune response to each construct was resulting in the generation of these key cells in humoral immune response.

GL7 is a glycoprotein expressed on the surface of germinal centre B-cells following activation and migration into the follicle. The presence of this surface antigen is an indicator for B-cells undergoing somatic hypermutation and affinity maturation as a result of antigen encounter and activation of the humoral immune response. As explained above, the protein vaccines were injected to gauge potential changes in cell numbers dependent on the recombinant vaccines. GC B-cells were identified as the $B220^+$ $GL7^+$ population (figure 5.12 A). Flow cytometric analysis showed that in the majority of the vaccine groups GC B-cell percentages did not differ from mice having received control only. The only difference was observed between mice injected with HEL Fc and mice receiving $hC3d^S$-HEL-Oct where $GL7^+$ B-cell percentages were slightly decreased (figure 5.12 B, $p < 0.05$). DNA vaccination had a more pronounced effect on $GL7^+$ populations. Mice injected intramuscularly with CpG-assisted HEL-Oct DNA and $hC3d^S$-HEL-Oct DNA vaccines exhibited stronger germinal centre activation at the end of the experiment (figure 5.12 C). 18.53 ± 0.5 % of B-cells expressed GL7 following HEL-Oct DNA 42 days after injection, significantly higher than baseline (empty vector control, $p < 0.05$).

Figure 5.12. Germinal centre B-cell analysis. Spleens were removed following the termination of the immunisation studies. Single cell suspensions were stained with the B-cell marker CD19 PE and GL7 FITC. Germinal centre B-cells were identified as $CD19^{+}$ $GL7^{+}$ cells in the top right quadrant of the FACS plot (panel A). Panels B through F show the proportion of these cells in relation to the total B-cell count for each individual mouse indicated by a single symbol group, means are indicated by a horizontal line in each column. Empty symbols refer to vaccines without adjuvant, filled symbols indicate their adjuvant counterparts (CFA in Panel B or C3d, panels C-F). Vaccine type and route of administration were as specified above each panel. Statistical analyses were carried out using the Kruskal-Wallis test followed by Dunns post analysis. Data derived from one experiment, saline: n = 1, HEL + CFA: n = 2, HEL Fc + CFA: n = 6, HEL Fc: n = 4, $hC3d^{S}$-HEL-Oct: n = 6, HEL-Oct: n = 6; DNA immunisations: n = 5 – 6; * $p < 0.05$; *** $p < 0.001$.

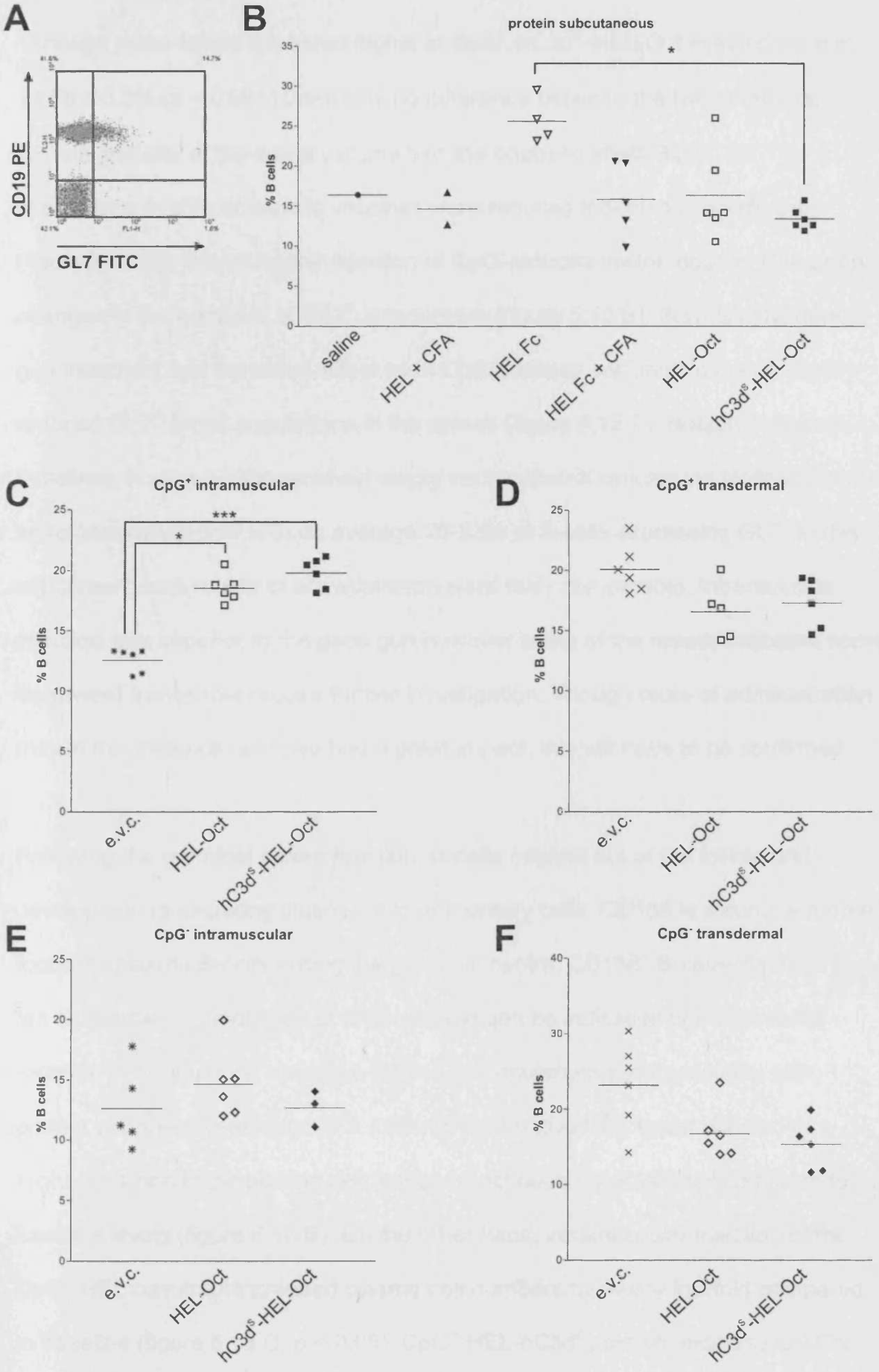
A
CD19 PE
GL7 FITC
B
protein subcutaneous
% B cells
saline
HEL + CFA
HEL Fc
HEL Fc + CFA
HEL-Oct
hC3d^{5}-HEL-Oct
C
CpG^{+} intramuscular
% B cells
e.v.c.
HEL-Oct
hC3d^{5}-HEL-Oct
D
CpG^{+} transdermal
% B cells
e.v.c.
HEL-Oct
hC3d^{5}-HEL-Oct
E
CpG^{-} intramuscular
% B cells
e.v.c.
HEL-Oct
hC3d^{5}-HEL-Oct
F
CpG^{-} transdermal
% B cells
e.v.c.
HEL-Oct
hC3d^{5}-HEL-Oct

Although these levels appeared higher in CpG^+ $hC3d^S$-HEL-Oct injected mice at 19.76 ± 0.5% ($p < 0.001$) there was no difference between the two octamers. Biolistic transfer of the same vaccine had the opposite effect $B220^+$ $GL7^+$ populations in both octameric vaccines were reduced though not significantly (figure 5.12 D). Intramuscular injection of CpG-reduced vector induced little or no changes in the numbers of $GL7^+$ splenocytes (figure 5.12 E). Surprisingly, gene gun treatment had the same effect as in CpG-assisted vaccines, causing slightly reduced $GL7^+$ B-cell populations in the spleen (figure 5.12 F). Notably however, baselines in mice having received empty vector control vaccine via biolistic transfer were generally higher with on average 20-23% of B-cells expressing GL7. In this experiment both routes of administration were fairly comparable. Intramuscular injection was superior to the gene gun however some of the results indicated some downward trends that require further investigation. Though route of administration may in this instance not have had a great impact, this will have to be confirmed.

Following the germinal centre reaction, B-cells migrate out of the follicle and develop into Ig-excreting plasma cells or memory cells. CD138 is a surface marker found on plasma B-cells exiting the germinal centre. $CD138^+$ B-cells (figure 5.13 A) are committed to production of antibody and can be indicative of a successful initiation of the humoral response (29, 45). Subcutaneous immunisation with protein vaccines in saline or CFA followed by a native HEL boost resulted in a slight reduction in the plasma cell numbers, although not statistically different to baseline levels (figure 5.13 B). On the other hand, intramuscular injection of the CpG^+ HEL construct increased plasma cell numbers by nearly fourfold compared to baseline (figure 5.13 C, $p < 0.05$). CpG^+ HEL-$hC3d^S{}_3$ did not increase $CD138^+$

Figure 5.13. Plasma B-cell analysis. Spleens were removed following the termination of the immunisation studies. Single cell suspensions were stained with the B-cell marker CD19 PE and biotinylated CD138. CD138 was detected with streptavidin-APC. Plasma B-cells were identified as $CD19^{+}$ $CD138^{+}$ cells in the top right quadrant of the FACS plot (panel A). Panels B through F show the proportion of these cells in relation to the total B-cell count for each individual mouse indicated by a single symbol group means are indicated by a horizontal line in each column. Empty symbols refer to vaccines without adjuvant, filled symbols indicate their adjuvant counterparts. Vaccine type and route of administration were as specified above each panel. Statistical analyses were carried out using the Kruskal-Wallis test followed by Dunns post analysis. Data derived from one experiment, saline: n = 5, HEL + CFA: n = 2, HEL Fc + CFA: n = 6 (staining of one failed), $hC3d^{S}$-HEL-Oct: n = 6, HEL-Oct: n = 6; DNA immunisations: n = 5 – 6; * $p < 0.05$; ** $p < 0.01$; *** $p < 0.001$.

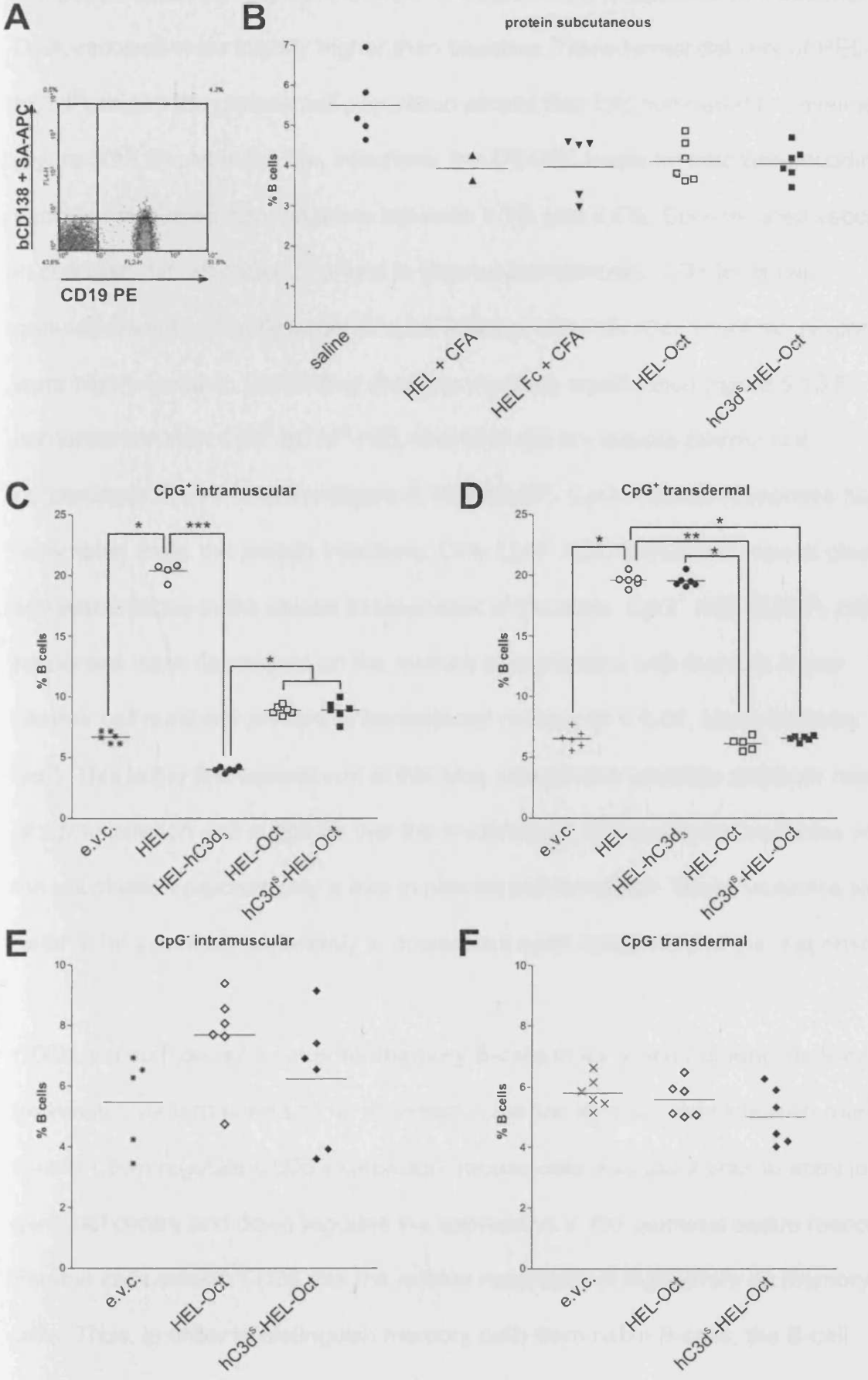
A
bCD138 + SA-APC
CD19 PE
B
protein subcutaneous
% B cells
saline
HEL + CFA
HEL Fc + CFA
HEL-Oct
hC3d^s-HEL-Oct
C
CpG$^+$ intramuscular
% B cells
e.v.c.
HEL
HEL-hC3d$_3$
HEL-Oct
hC3d^s-HEL-Oct
D
CpG$^+$ transdermal
% B cells
e.v.c.
HEL
HEL-hC3d$_3$
HEL-Oct
hC3d^s-HEL-Oct
E
CpG$^-$ intramuscular
% B cells
e.v.c.
HEL-Oct
hC3d^s-HEL-Oct
F
CpG$^-$ transdermal
% B cells
e.v.c.
HEL-Oct
hC3d^s-HEL-Oct

cell populations in the spleen. $CD138^+$ B-cells in mice immunised with octameric DNA vaccines were slightly higher than baseline. Transdermal delivery of HEL-$hC3d^S_3$ raised the plasma cell population almost four fold compared to baseline (figure 5.13 D). As in the i.m. injections, the $CD138^+$ levels for octamer-encoding vaccines remained near baseline between 6.1% and 6.5%. CpG-reduced vaccines, in contrast, did not cause changes in plasma cell numbers. $CD138^+$ B-cell populations were slightly larger in mice injected with HEL-Oct, however, responses were highly variable, preventing changes reaching significance (figure 5.13 E). Immunisation with CpG^- $hC3d^S$-HEL-Oct DNA did not elevate plasma cell percentages above baseline (figure 5.13 E and F). CpG-reduced responses hence resembled more the protein injections. Only CpG^+ HEL consistently raised plasma cell percentages in the spleen independent of the route. CpG^+ HEL-$hC3d^S_3$ cell responses were dependent on the method of application with five-fold higher plasma cell numbers present in transdermal delivery ($p < 0.01$, Mann-Whitney test). This is the first experiment of this kind using these vaccines and both routes of administration and suggests that the involvement of a number of variables within the vaccination process play a role in plasma cell formation. These variables will have to be assessed separately to dissect out each component of the response.

CD38 is a surface cell marker for memory B-cells in mice and humans. Its B-cell expression pattern seems to be reversed in the two species. While human memory B-cells down regulate CD38 expression, mouse cells express it prior to entry in the germinal centre and down regulate the expression in the germinal centre response. Plasma cells remain $CD38^-$ but the marker reappears at high levels on memory cells. Thus, in order to distinguish memory cells from naïve B-cells, the B-cell

population was counterstained with an IgM antibody (figure 5.14 A). IgM^- $CD38^{hi}$ B-cells were identified as memory B-cells (42, 45-47). Mice injected with HEL and HEL Fc in CFA had slightly elevated levels of memory B-cells compared with mice injected with saline alone or other constructs (figure 5.14 B). Disappointingly, memory B-cell percentages were relatively unchanged in the groups injected with proteins in saline compared to saline alone. Altogether, the protein vaccination indicated an interesting trend, which was also cause for some concern. Less memory cells were present following $hC3d^S$-HEL-Oct injection compared to HEL-Oct (figure 5.14 B). This result was recapitulated in the DNA vaccinated animals, in that none of the vaccine candidates caused a significant increase in $CD38^{hi}$ B-cells. In general, vaccination with CpG^+ constructs resulted in a reduction in memory B-cell populations (figure 5.14 C). Indeed, mice that received CpG^+ HEL and CpG^+ HEL-$hC3d^S{}_3$ by i.m. injection possessed about half the amount of memory cells compared with mice receiving empty vector ($p < 0.05$ and $p < 0.01$) and both octameric vaccines (not significant). The percentage of memory B cells in the spleens of mice immunised with CpG^+ HEL-Oct and CpG^+ $hC3d^S$-HEL-Oct were slightly reduced or remained at baseline level, respectively. The outcome was similar following transdermal delivery of the DNA constructs (figure 5.14 D). Interestingly, injection and biolistic delivery of CpG^+ $hC3d^S$-HEL-Oct resulted in a higher percentage of memory B-cells being present in the splenic compartment than seen in CpG^+ HEL-$hC3d^S{}_3$ immunised mice ($p < 0.01$ and $p < 0.05$ respectively). CpG^+ HEL seemed to induce higher memory cell percentages than CpG^+ HEL-$hC3d^S{}_3$. This effect was reversed in CpG^+ HEL-Oct and CpG^+ $hC3d^S$-HEL-Oct (figures 5.14 C and D). No such reductions were observed in intramuscular injected animals receiving CpG-reduced vaccines. There was also

Figure 5.14. Memory B-cell analysis. Spleens were removed following the termination of the immunisation studies. Single cell suspensions were stained with the murine B-cell marker B220 FITC, CD38 PE and biotinylated anti IgM. Anti IgM antibodies were detected with streptavidin APC. IgM^{-} $CD38^{hi}$ B-cells were gated from a B220 versus IgM plot (panel A, circle) and visualised as histogram. Relative cell percentages were derived from the cell population expressing high levels of CD38 as identified from naïve cells (M1, not shown). Panels B through F show the proportion of these cells in relation to the total B-cell count for each individual mouse indicated by a single symbol group means are indicated by a horizontal line in each column. Empty symbols refer to vaccines without adjuvant, filled symbols indicate their adjuvant counterparts. Vaccine type and route of administration were as specified above each panel. Statistical analyses were carried out using the Kruskal-Wallis test followed by Dunns post analysis. Data derived from one experiment, saline: n = 5, HEL + CFA: n = 2, HEL Fc + CFA: n = 6, HEL Fc: n = 4, $hC3d^{S}$-HEL-Oct: n = 6, HEL-Oct: n = 6; DNA immunisations: n = 5 – 6; * $p < 0.05$; $p < 0.01$; *** $p < 0.001$.

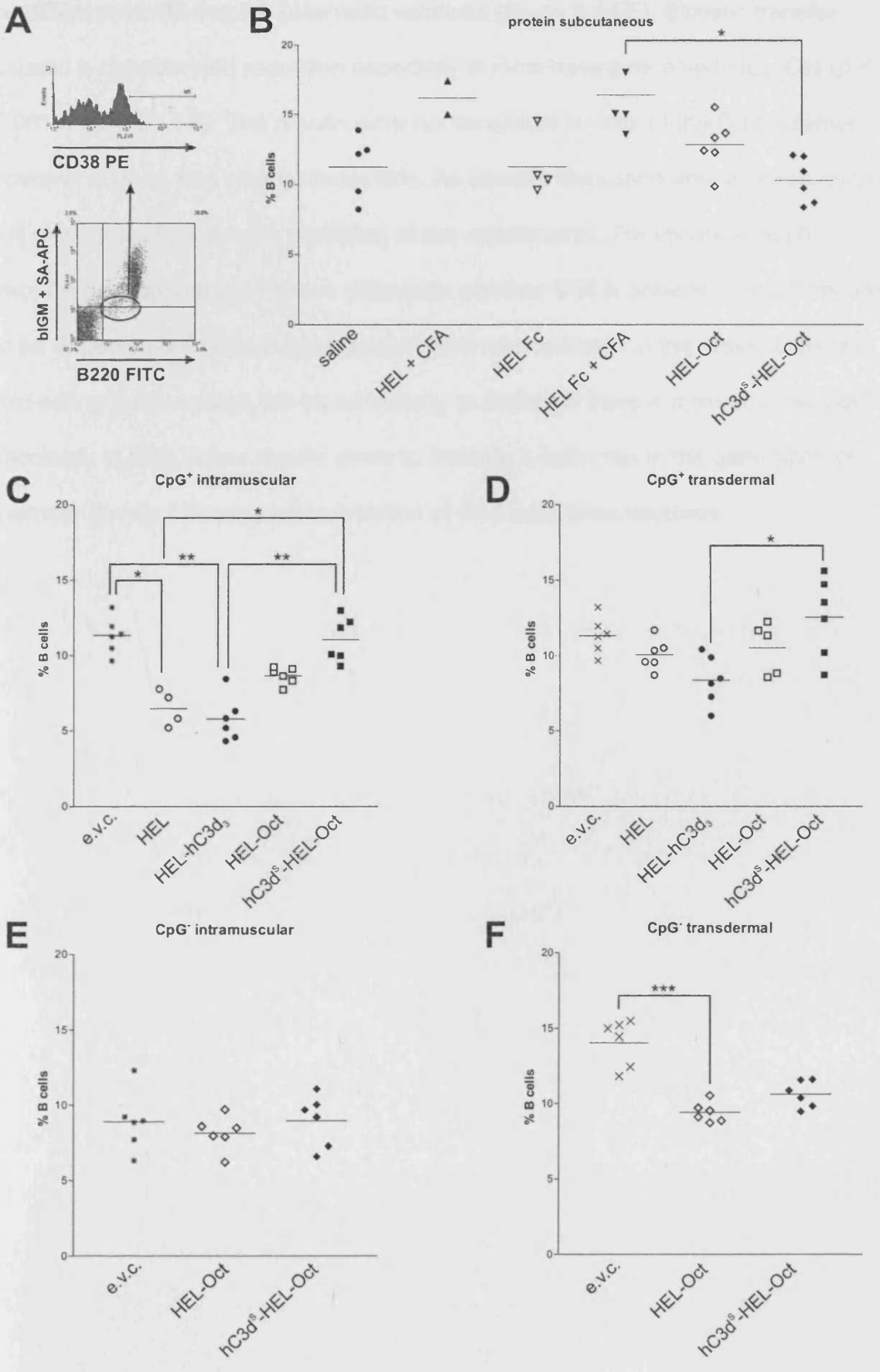
A
CD38 PE
bIGM + SA-APC
B220 FITC
B
protein subcutaneous
% B cells
saline
HEL + CFA
HEL Fc
HEL Fc + CFA
HEL-Oct
hC3d^s-HEL-Oct
C
CpG$^+$ intramuscular
% B cells
e.v.c.
HEL
HEL-hC3d$_3$
HEL-Oct
hC3d^s-HEL-Oct
D
CpG$^+$ transdermal
% B cells
e.v.c.
HEL
HEL-hC3d$_3$
HEL-Oct
hC3d^s-HEL-Oct
E
CpG$^-$ intramuscular
% B cells
e.v.c.
HEL-Oct
hC3d^s-HEL-Oct
F
CpG$^-$ transdermal
% B cells
e.v.c.
HEL-Oct
hC3d^s-HEL-Oct

no difference between the octameric vaccines (figure 5.14 E). Biolistic transfer caused a considerable reduction especially in mice having received HEL-Oct ($p < 0.001$, figure 5.14 F). The results were not as salient in case of the C3d octamer however a trend was clearly discernible. As already discussed above, these results will require confirmation by repetition of the experiments. For instance, each vaccine type appears to behave differently whether C3d is present or not. This was to be expected but not as unpredictable as it was recorded in the present studies. Repeating these assays will be necessary to discern if there is a trend in the CpG^- vaccines. In total, these results seem to indicate a reduction in the generation of memory B-cells following administration of C3d-supported vaccines.

5.4 Discussion

The first study utilising a recombinant vaccine containing murine $C3d^S$ as adjuvant was published by Dempsey and colleagues (218). Since 1996 this approach has not changed much. Murine C3d trimers are still used in vaccination studies in the same configuration although in some cases the arrangement has been altered slightly (380). Pathologically relevant antigens underwent *in vivo* testing in the last decade as recombinant protein vaccines as well as DNA vaccines (252-256, 299, 381-384). Experiments of this kind have conclusively proven that murine $C3d^S_3$ is a viable adjuvant approach in mice. To progress to human subjects, this study takes the next step by revising the original design using human $C3d^S$ and the oligomerising core sequence of C4BP. To assess the activity of this new model vaccine, HEL, the original model antigen, was inserted between the molecular adjuvant and the octamerising sequence.

The aim of this chapter was to test the optimised vaccine described in chapter 3 *in vivo*. The primary focus was whether the octamers would induce an immune response at all. Binding to CR2 had been verified during the optimisation process and interaction studies using Fc fusion proteins (chapter 4). The vaccine proteins were therefore injected first to estimate the magnitude of the immune response that could be expected. The protein vaccinations were administered following the prime-boost schedule as published by Dempsey *et al.* (218) although the native HEL boost was not administered in IFA. Also, as mentioned in section 4.4, the vaccine proteins were injected at much increased concentrations to force a response. Previous experiments with trimeric proteins induced responses at femtomolar concentrations (218). It was vital in this first step to gauge whether any

adjuvant was required in the boost at all. IgM as well as IgG responses were monitored to cover as many aspects of the immune response as possible (385). IgM responses precede the appearance of IgG-type immunoglobulins (13). Development of an IgM response but subsequent absence of IgG hence indicated failure to induce seroconversion. In addition, presence of raised IgM titres conveyed whether the vaccines interacted with the immune system at all.

As expected, CFA had a significant impact on vaccine activity as illustrated by HEL Fc + CFA compared to HEL Fc in PBS, which did not induce any significant antibody production. Titres induced by protein + CFA set the standard of achievable responses in experimental animals with traditional adjuvant formulations. HEL-mC3d$^{S}_{3}$ had achieved responses that far exceeded CFA-aided immune responses (218). It was therefore anticipated that similar or higher responses would result from a vaccine that employed eight copies of C3d. The medium to strong responses observed in three mice proved first and foremost that the vaccine was functional, that the experimental animals produced HEL-specific antibodies and that hC3d^{S} enhanced the immune response in mice. However, the antibody titres measured in the high responders were far below HEL + CFA levels. Reasons for the variations across the group are unclear and require further investigation. It is possible that, despite profuse mixing of the vaccine formulation and filtration prior to administration, precipitates formed in the syringe and needle, which led to heterogeneous amounts of protein administered to the mice. Neither blockage nor precipitation was observed during administration yet such complications have to be taken into account. Use of larger gauge needles or individual syringes could counteract such effects. Despite lower than anticipated

titres, the immune response was mounted more quickly in the hC3d^{S}-HEL-Oct-injected mice.

The cellular aspect of the humoral immune response was addressed by flow cytometry. The characterisation of proportional amounts of germinal centre cells (GL7^{+}), plasma cells (CD138^{+}) and memory cells (IgM^{-} CD38^{hi}) gave an insight into the impact of each vaccine on each cell type at the end of the experiments.

The germinal centre reaction is detectable in the spleen only for a limited period of time. GL7 can be detected – under optimised conditions – on splenocytes from 60 hours post stimulation (26) until 21 days after immunisation. At the time of the present experiments, day 42 after immunisation, the germinal centre reaction had taken place and levels should have normalised again. Significant rises in GL7^{+} cell populations were only recorded in mice that had received CpG^{+} HEL-Oct and CpG^{+} hC3d^{S}-HEL-Oct intramuscularly. In all other cases the levels observed in vaccinated animals remained near baseline. DNA vaccines can potentially remain in the host's tissue for an extended period of time being expressed constitutively, thus establishing a reservoir of antigen maintaining the immune response (386). Regardless, the detection of germinal centre B-cells was somewhat surprising. Germinal centres in the spleen tend to decrease in size and over time with each boost vaccination as immunological memory is established (29). Bona *et al.* analysed GL7^{+} cells following administration of a DNA vaccine containing influenza haemagglutinin (387). Relative GL7^{+} cell numbers peaked in the spleen at day 14, after which they diminished again. Despite the age of the experimental animals (7 days) and their therefore immature immune systems, the observations concurred

with the established course of events (29). This is interesting because responses to DNA vaccines may be delayed by some time, approximately one week, until the protein is expressed to sufficient levels to activate the immune system. The presence of germinal centres at this late stage will require further investigation. Analysis of the course and quantification of the specific immune response at each stage, prior to and subsequent of the GC reaction will shed more light on these observations.

The present measurements of GC cells were relatively high. Previous studies have determined relative numbers of these cells at approximately 4 – 8% of the $B220^{+}$ splenocyte population (26, 221, 388). The reason for this is unknown but could have been due to a secondary infection. It was discovered during these experiments that mice in the animal holding facility were infected with murine hepatitis virus (MHV). This was not visibly detrimental to their health and went largely unnoticed. Cellular stains used in these experiments could not discriminate between GC induced by a controlled injection or infection with an environmental pathogenic agent. Presumably, the primary effect of this was increased background staining in all mice. The different proportions of cell populations in each group therefore stemmed from the administered vaccine.

Memory B-cells are generated following the germinal centre response induced by an infection or administration of a vaccine. They can be activated upon re-encounter with a specific antigen allowing the immune system to respond faster and combat subsequent infections more efficiently. Several surface antigens are used to identify and distinguish the memory cell pool. As mature cells they are

characterised by absence of IgM and IgD but high numbers of CD38 as well as isotype-switched surface antibody isotypes, e.g. $IgG1^+$ (47). Here, memory B-cells were identified as $B220^+$ $sIgM^-$ $CD38^{hi}$ (45).

Some intriguing differences were observed as HEL-Oct injected mice had slightly raised cell populations but, surprisingly, presence of adjuvant ($hC3d^S$) suppressed the memory response. Smaller $CD38^{hi}$ populations in the spleen were observed in particular in the traditional vaccines administered as DNA. CpG^+ HEL and CpG^+ HEL-$hC3d^S{}_3$ administration i.m. and t.d. reduced $CD38^{hi}$ cells. These losses did not occur in the CpG-supported octameric vaccines. In the transdermally applied $hC3d^S$-HEL-Oct a slight increase in memory B-cell percentages compared to total B-cell numbers was observed. The presence of C3d in the octamer also led to a slightly larger $CD38^{hi}$ population in the CpG-free vaccines. Unfortunately, these differences were not significant enough to state with absolute certainty whether $hC3d^S$ caused this effect. In general, higher percentages of memory cells had been expected. At this stage in the immune response, however, most of the memory cells would have migrated to the bone marrow (389). Bone marrow was not examined in this study due to time constraints and it was expected that memory cells would be continually generated in the spleen. As this was clearly not the case, it will be vital to include bone marrow B-cells in further studies. The exact mechanisms of memory B-cell formation, dependent on vaccine/adjuvant formulation as well as method of administration, are still being unravelled (389).

Plasma cells represent the final step in the development of peripheral B-cells. They develop either during the germinal centre response or upon secondary challenge

(389-391). Estimation of their proportional amounts in the spleen yielded some information about the stage of the immune response. Relative plasma cell amounts in the spleen of mice that had received the protein vaccines did not change significantly. The DNA vaccines CpG^+ HEL and CpG^+ HEL-$hC3d^S_3$ had a more notable effect exhibiting high contents of plasma cells in the spleen following biolistic transfer (figure 5.13 C and D). The octameric vaccines, in contrast, did not cause a raise in $CD138^+$ splenocyte populations. In gene gun-treated mice, the $CD138^+$ cells were around baseline level (figure 5.13 F). Slightly larger $CD138^+$ cell populations were recorded in mice injected i.m. with $hC3d^S$-HEL-Oct and HEL-Oct with and without CpG at day 42 (figure 5.13 C and E). This, however, was no more than a trend. Plasma cells in splenic foci producing relatively low-affinity antibody are short-lived and undergo apoptosis from 7 – 14 days (63, 64, 390, 391). Plasma cells expressing high-affinity antibody develop from memory cells and settle in the bone marrow for antibody production (392, 393). There, they produce antibody, down-regulate CR2 expression and are, as long-lived as memory cells, detectable for up to one year post primary immunisation (391). In humans $CD138^+$ cells are not found in the spleen either but instead located in the bone marrow (394). Despite the short life of plasma cells in the spleen, the situation could be very different in DNA vaccines. Expression of the respective antigen can be sustained for a number of weeks after initiating the immune response up to seven days after the protein vaccine. Thus, antigen is provided to the secondary lymphoid tissue on a constant/regular basis. No clear relationship emerged when these key immune cell populations were compared to each other. Although the size of the GC decreases with repeated challenges, spleen plasma cells could have been present. This was clearly the case in mice that had received HEL and HEL-$hC3d^S_3$ by

needle and gene gun. As for the memory cells, analysis of the bone marrow may provide more clues on localisation of the antigen-specific plasma cell pool. Also, analysis of the immune cells at an earlier stage, i.e. 7, 14 and 21 days after primary immunisation should cast some more light on the mechanisms.

These immune cell studies have provided valuable information as well as generated more questions that require investigation. The effects exerted by the vaccines will have to be dissected further to pinpoint the components that play a part in the responses. Interestingly, CpG^+ could cause increases as well as reductions dependent on the route. CpG^- vaccines did not appear to be as reactive; often these mice only exhibited trends rather than real changes. Amounts of $CD38^{hi}$ cells on the other hand seemed to depend on route as well as vaccine type.

It is also possible that, especially in case of biolistic transfer, the antigen presenting cells (LC and dermal DC) migrated to the local draining lymph node and changes in cell populations were therefore not detected. Preliminary experiments examining presence of the above mentioned cell types in inguinal lymph nodes did not reveal any more conclusive data. Subsequent studies will include these tissues as well to ensure this facet of the immune response is investigated adequately.

DNA vaccinations represented an alternative to protein vaccinations due to the limitations of *in vitro* protein production. Initially, the linearly arranged tried-and-tested vaccines (i.e. CpG^+ HEL and CpG^+ HEL-$hC3d^S_3$, (218, 252)) were examined to assess *in vivo* activity. This established a standard response the new vaccines

could be compared to. None of these primary vaccinations were followed up by a booster immunisation. This allowed characterisation of the immune response to each vaccine over a six-week time frame. HEL-hC3d$^{S}_{3}$ was clearly superior to HEL as a vaccine but also induced more antibody than HEL-Oct and hC3d^{S}-HEL-Oct. These results were potentially influenced by unmethylated DNA sequences. CpG sequences can cause inflammation at the target sites, which can be particularly undesirable in gene therapy where long-term expression is required (395, 396). In addition it was discovered that elimination of CpG from the vectors could prolong expression *in vivo* (386). The octameric vaccines were therefore subsequently analysed without the influence of CpG vaccines. Interestingly, lack of CpG induced equal to higher IgM titres than CpG-assisted vaccines. HEL-Oct failed to produce any significant levels of anti-HEL IgG antibodies while hC3d^{S}-HEL-Oct, in contrast, induced similar levels to CpG^{+} HEL-hC3d$^{S}_{3}$. These results suggested that absence of CpG sequences could improve immune responses. This cannot be stated with absolute certainty as expression in the two vaccine vectors CpG^{+} and CpG^{-} was under control of CMV or EF1α promoters. Any differences in immune responses may have therefore been partially dependent on the expression levels.

Several publications have described administration of the C3d trimer vaccines by biolistic transfer using the gene gun. This method has become the primary choice for administration of many other researchers (238, 252, 256, 397). To allow broader comparison, biolistic transfer was incorporated in this study. Unfortunately, the results were not as clear-cut; therefore using this method for the CpG-assisted vaccines did not help determine an ideal vaccine type. Instead, the responses were highly variable and lower than expected for this method. Although

disappointing, these inconsistent titres within the immunised groups are not uncommon (254, 398). It could be argued that this was due to heterogeneity in the vaccine preparation. Such inconsistencies could be introduced at several stages during the preparative steps, i.e. gold pellet coating with DNA, gold pellet immobilisation on vaccine tubing walls or inadequate hair removal. More factors may have played a role, e.g. efficiency of cellular uptake and which cell types internalise the vaccine vectors. Another major factor was the immune system of each individual mouse. On the contrary, higher titres, low standard error and standard deviation especially in CpG^- injected mice did not support these arguments. Absence of CpG stabilised the activity of the vaccines. It is possible that this was due to lack of activation of the immune system until sufficient amounts of C3d-tagged antigen were present in circulation. On the other hand, these vaccines raised further issues as there was no difference between the two octameric vaccines (figure 5.11 D). This cast doubt whether C3d was at all active in the vaccines. Although some of the analyses had shown slight improvements of $hC3d^S$-HEL-Oct responses over HEL-Oct, they did not lead to the adjuvant effects that were originally expected (218, 252).

Comparison with other studies revealed similarities in the profile of the response. In a study examining the *in vivo* effects of haemagglutinin (HA)-$C3d^S_3$ by Ross *et al.* DNA was administered by gene gun (256). A single shot of vaccine sufficed to confer protective immunity. Also, the observed response resembled the immune titres observed in this study with increasing serum titres at day 42 ((256) also see (252, 399)). It is therefore likely that the octameric vaccine followed a similar pattern. In some studies, no measurable or only low immune titres were recorded

until 6 weeks into the experiment despite several boosts (398) This may have been due to the sensitivity of the assay or massively increased titres following the second boost. It was decided in this study to detect – for this first experiment – any immune responses irrespective of therapeutic or protective potential within the first six weeks. One of the acclaimed advantages of DNA vaccines has been the fast onset of immune responses. A response was therefore expected within this time. Several recent studies have also shortened the time taken for immunisation experiments (382, 383) and recorded very similar response patterns to the ones observed here.

All previous studies using the linear trimer arrangement were based on the same plasmids and constructs. As confirmed by CpG analysis, vaccine vectors provided by Adprotech/Inflazyme contained numerous CpG sequences. This is the first study to address the adjuvant potential of C3d in a DNA vaccine independent of CpG sequences. Since their recognition in the early 1980s (287), a number of studies have tested their adjuvant potential in conjunction with their intracellular receptor TLR9 (277). Among these, many have utilised CpG oligodeoxynucleotides (ODN) as isolated adjuvants successfully where they induced a strong Th1 response (275, 288, 400, 401). Some of these studies were carried out *in vitro* (400), others *in vivo* (275) where ODN were co-injected with HEL. Although DC in the skin contain TLR9 and have been implicated to contribute to cytokine release, no such strong effects were observed here. In fact, CpG-ODN have mainly been effective against intracellular pathogens by improving the capacity of DC to present antigen to T-cells (288). If this occurred in the present study, the lower antibody titres following CpG^+ administration could be explained by a response more biased

towards the cellular arm of the immune system. Analysis of specific T-cell populations should provide more clues on the immune bias caused by this vaccine. B-cells, the cell type that reacts strongest with CpG (277), could come in contact with CpG ODN, although this is unlikely following vaccination. The exact events following deposition in the skin remain to be elucidated. Skin samples were taken at the end of these experiments to analyse the tissue for presence of vector or vaccine protein. Unfortunately, time constraints did not allow these experiments to go ahead.

These initial studies are the first set in a series of experiments that will involve further in-depth optimisation of the vaccine organisation itself, species of the adjuvant, method of administration and prime/boost schedule. Vaccinated mice may receive a variety of secondary agents, e.g. repeated administration of the primary reagent, recombinant protein, DNA or native protein. Extension of the time frame of the vaccination studies may shed more light on the memory response and the duration of the primary response. Some of the immune titres were rising towards the end of the experiments, it is therefore vital to determine for how long this continues without boosting. Conversely, shortly after primary immunisation and the administration of the boosts, secondary lymphoid tissue, i.e. spleen, draining lymph nodes and bone marrow will be analysed. So far, clear connections between cell numbers and antibody titres have remained elusive. Analyses of cell types and serum titres in time course experiments will allow comparison of activity of the immune cells and emergence and diminution of specific immunoglobulins in the serum.

Due to the relatively low responses detected so far it had to be considered whether the octameric vaccines were as active as expected. The most convincing data in this respect was obtained from the protein immunisations. Although titres were not raised reliably in all the mice, the positive responses can be ascribed to C3d. Moreover, it is important to remember that all the experiments were carried out with human $C3d^S$. With the information on binding affinities calculated in the previous chapter, the affinity of $hC3d^S$ to mCR2 may be lower than to hCR2.

Therefore, activity of these proteins will be tested in transgenic human CR2 mice. Unfortunately, when the octameric protein became available, the $Cr2^{-/-}$ $hCR2^{+/-}$ C57Bl/6 colony was not reproducing as expected or required prohibiting these experiments. These experiments will be carried out as soon as a stable colony of sufficient size is established. In turn, experiments will be carried out using $mC3d^S$ in the octamer.

In summary, the novel vaccine $hC3d^S$-HEL-Oct was tested *in vivo* as protein and as DNA vaccine. In addition to the different methods of administration the influence of CpG sequences was assessed. These experiments represent a successful proof of concept. Advanced optimisation will be vital to develop this as a valid approach for human use. To achieve this, C3d will have to possess at least equivalent or better enhancing effects than other adjuvants in the field, e.g. CpG ODN or $C3d^S{}_3$. The basic concept discussed here provides a solid base for subsequent experiments and improvements. Thus, the main aim of this part of the study, verification of activity *in vivo*, has been achieved. Most importantly, these results confirmed the cross-reactivity between murine and human proteins that had been

taken for granted up to now. In conjunction with the previous chapter this work shows that cross-reactivity does exist but is far from equal.

Chapter 6

Conclusion and Further Experiments

6.1 Final Discussion

Since its conception a decade ago, the molecular adjuvant C3d has received considerable interest as a candidate adjuvant and recombinant vaccine component against a variety of viruses, bacteria and parasites. The linear trimer, especially delivered as DNA vaccine, has proven to be an ingenious means of cross-linking CR2 and BCR. However, the arrangement is not natural, as such linear C3d configurations do not form during complement activation. Furthermore, their mode of action is not fully understood (348, 402). The octameric proteins described herein, by design, should mimic a naturally formed immune complex more closely than the linear trimer and thus should provide more predictable responses. Although it is more likely that Ag and C3d on adjacent or opposing arms will engage their respective receptors, rather than Ag and C3d on the same arm.

I have shown that the octameric protein could be produced stably in cell culture, providing conclusive evidence that expression, assembly and excretion would occur with similar consistency in somatic cells following DNA vaccination. Optimisation of the C3 component revealed that there were notable differences dependent on the presence of C3g and the thioester moiety. Though expected, this effect was more pronounced than anticipated. Higher expression levels observed in the $C3d^{S}g$ octamer led to the conclusion that preceding vaccine designs may have been ill advised to use $C3d^{S}$, which yielded reduced levels. So far C3g lacks a specific role in the course of the immune response (chapter 3, discussion) but these findings and partial degradation of the C3dg/$C3d^{S}g$ Fc variants to C3d/$C3d^{S}$ Fc (chapter 4) may assign this 5 kDa fragment a novel role in C3d protein stability and binding strength *in vivo*. However, it does indicate a note of caution as if the

opposite orientation had been used, natural conversion of C3dg to C3d would have also released the antigen. Furthermore, receptor binding studies revealed that $C3d^{S}g$-YFP-Oct bound weakest to hCR2 SCR1-4 while $C3d^{S}$-YFP-Oct exhibited strongest binding. The increased binding of $C3d^{S}$ to CR2 thus illustrated that compromises in vaccine production levels and design have to be tolerated to achieve optimal interaction with the receptor.

Correct expression of the octameric products, their purity and interaction with CR2 was confirmed *in vitro* (chapter 3). The octamer function was then tested by *in vivo* injections of protein via the subcutaneous route. This preliminary data demonstrated that the octamer generated a significant immune response (chapter 5, figure 5.3). However, there remains considerable room for improvement. Having shown successfully that the octameric vaccine was functional, DNA vaccines were generated for *in vivo* testing. Induction of a HEL-specific immune response showed first and foremost that the vaccines were expressed in the tissue and triggered antibody production. The DNA vaccine encoding the octameric DNA vaccine worked well and was only just outperformed by the linear trimer HEL-$hC3d^{S}_{3}$. However, similar to the protein vaccine injections, the responses remained variable from animal to animal. In essence, the trends observed for most of the tested vaccines indicated long-term induction of an immune response though titres were in many cases low. The experiments suffered from poor reproducibility and failed to determine a clearly favourable administration method. DNA vaccination ultimately depends on a range of factors from vaccine preparation to administration, uptake, expression and the suitable immunological environment. Each one of these factors requires optimisation to minimalise interference.

One potentially confounding factor was excluded by inserting the octameric vaccine sequences into a CpG-reduced vector. This allowed exclusive assessment of the adjuvant potential of hC3d. Indeed, removal of CpG had a positive effect (higher Ig titres, diminished variability) on the immune response, although this could have been caused by the different plasmids themselves. CpG sequences have become a prominent candidate for use as adjuvants in animal models as well as in human vaccination (403-406). CpG sequences as a vaccine plasmid component are still a subject of debate. Some have argued that CpG as part of vaccine plasmids can have detrimental effects on the long-term expression of the introduced genes, others showed that immune responses can be induced without TLR9 present (395, 396, 407). The data presented herein also suggested that CpG within the plasmid vector can interfere with DNA vaccine function. Therefore, co-administration of CpG oligodeoxynucleotides (ODN), as shown by numerous studies by Krieg *et al.*, may be a more favourable adjuvant approach. The reason for the different intensities of the immune responses induced by CpG^+ and CpG^- remain to be determined. The use of CpG strongly depends on the nature of the antigen and should – as any other adjuvant – be considered carefully before being included or excluded from the vaccine design.

The cytometric analyses of the splenic immune cells carried out herein did not yield conclusive data. The presence of germinal centres six weeks after injection and potentially reduced memory cell populations gave a first insight that cellular processes may be somewhat different. However, due to the nature of these immune cells, i.e. appearance during the first three weeks of the adaptive immune

response followed by migration to the bone marrow, many of the cellular events were most likely missed. Cellular events in the secondary lymphoid tissue were measured with the aim of giving additional data from the experiments designed specifically to measure circulating antibody responses (chapter 5). Therefore, experiments designed specifically to analyse a particular cellular response or parameters will be planned for future studies and will include analyses at the appropriate/earlier time-points.

Closer inspection of the C3d-CR2 interaction using Fc fusion proteins generated one of the most surprising discoveries, in that, murine C3d had the strongest affinity for human CR2 compared to all other Fc fusion analysed (chapter 4). The Raji B-cell model as well as fresh splenocytes and eventually SPR analysis showed that murine $C3d^S$ Fc bound to hCR2 SCR1-4 some 2 – 3 times stronger than any of the human C3d versions. Unfortunately, the reciprocal arrangement (mCr2 Fc binding to hC3d variants) could not be analysed within the time limit of this study due to many technical problems in the generation and production of mCR2 Fc. Previous work and data derived from the vaccination studies suggest that an interaction between mCR2 and hC3d is highly likely (408). In summary, these results contradict the established view of equal affinities (128, 158, 178, 217, 221) and could have implications on interpretation of past as well as planning for future studies.

6.2 Future Directions and Experiments

The data presented herein describes the first crucial tests with a novel recombinant octameric C3d protein. However, in order to fully characterise the octamer, a range of experiments remain that unfortunately could not be carried out due to limited time.

For instance, the size of the octamer itself has made it difficult to confirm the number of $C3d^S$-HEL-Oct sub-units in each 'octamer construct' with absolute certainty. C4BP is found in the serum as hetero-octamer (7α chains/1β chain) or homo-heptamer (7α see section 1.12); it is therefore likely that such numerical variations may also arise here. In the future, Mass spectrometry could be used to determine the exact numbers of sub-units present in the protein although this will require careful electrophoretic separation of the largest species (316). Undoubtedly, further analysis and refinement of the vaccine protein will also be required. Herein, C3d and HEL were expressed next to each other without the use of spacers. Some preliminary attempts by F. Batista (Cancer Research UK, London Research Institute) to bind $hC3d^S$-HEL-Oct to splenocytes isolated from MD4 transgenic mice (326) have failed to yield an interaction (personal communication). This is despite the presence of the HyHEL-5 and HyHEL-10 epitopes in the octamer according to the sequence data (409-411). If epitope masking caused the lack of binding/interaction, remains to be fully examined. This preliminary finding suggests that a spacer between C3d and the antigen may be critical for full function of the octamer and although immune responses were detected in the injected mice herein, these responses could be improved

considerably by adding linker sequences between antigen and adjuvant to adjust flexibility or access to each component as required.

The original octameric plasmid was designed to allow rapid exchange of YFP cDNA with any antigenic cDNA using standard cloning methods. The multivalency provided by the C4BP core region acclaimed in previous studies has provided very sensitive reagents (314-316). In fact, one of the intended uses of the YFP-octamer was detection of B-cells with low CR2 density on the surface in fluorescence-based assay (e.g. microscopy, flow cytometry). Preliminary experiments on Raji cells were carried out but abandoned due to the lack of sufficient material and time for optimisation as well as the focus of this thesis being concentrated on the immunological function of the octamer. However, the octamer provides the option to use tags, receptors or antigens of virtually any protein to be used for "ligand fishing", being particularly useful in cases where elusive or low affinity interaction partners are involved (Timothy Hughes, personal communication). Similar reagents are available commercially although they do not offer the same degree of flexibility (412). Production methods will have to be reviewed to improve production yields of pure protein. If antigenicity is not an issue, e.g. for non-vaccine applications, a bacterial or insect culture system would be acceptable. Effective purification methods were established in this study; however, single step purification by affinity chromatography remains the method of choice and could be achieved in an antigen specific manner or using anti-C3d monoclonal antibodies.

A vital function of the vaccine, induction of an appropriate immune response, signified by the Th-bias, remains to be characterised. Each pathogen induces a

different type of immune response upon infection, depending on its lifecycle and tropism. Antigen preparations may only reflect a sample of those seen during the lifespan of a pathogen due to attenuation or supply of sub-units (see section 1.2 and 1.11). Each component, including antigen, adjuvant and method of administration, must therefore be considered carefully to sway the course in a favourable direction. For example, i.m. DNA vaccinations preferably induce Th1, while the gene gun causes Th2-biased responses (231). CpG as well as CFA are strong activators of a Th1 response, however this response can easily be overruled by the administration method (57, 293, 404, 413, 414). Assessment of the prevailing Ig-isotype as well as the signalling molecules, i.e. cytokines, excreted by the cells mounting the immune response should yield useful information on the target accuracy of the vaccine (252). If the correct Th-bias is not achieved, the formulation or administration method will need to be changed to combat the infecting agent appropriately (293, 383). Thus, future analyses should also include examination of T-cell populations, (to the octameric vaccines throughout the immune response) to evaluate whether a cytotoxic response is induced.

In the past, cross-linked C3d has been used in B-cell binding studies (158, 165, 217, 348, 365). The octamer provides this structure automatically by assembly within the cell but also offers additional potential applications. Thanks to its array-type conformation and multiple binding sites, the C3d octamer should be able to recruit several receptors to the same site on the membrane surface, in conjunction with YFP, the C3d octamer protein may provide further insights into processing, i.e. uptake and degradation of C3d-opsonised IC bound to CR2. Using the appropriate

equipment together with YFP or similar tags, this may allow documentation of such processes in real time or as a time course. Together with a specific antigen, it could be envisaged to engage BCR at the same time and trace the cellular localisation until breakdown and loss of fluorescence. Some of this has been attempted before in capping experiments with EBV bound to CR2 (366) and C3d-coated gold particles in uptake analysis (23).

The findings from the SPR studies have indicated a clear synergistic effect on affinity, which may be similar or stronger in the octamer. Murine C3d could, in this respect, strengthen the affinity of the octamer further. During the optimisation of the Fc fusion proteins, an attempt to label the Fc fusions directly with fluorescein isothiocyanate was undertaken. Although this approach failed in this instance, it remains a viable option. Thanks to their relatively high affinity compared to monomeric ligands, C3d Fc fusion proteins are a practicable alternative to monoclonal antibodies for surface CR2 detection and uptake studies. The Fc chain has proved vital in the present study as a "handle", i.e. antibody detection target during assays and purifications. Fc fusion proteins have for a long time proved to be a vital tool in the development of therapeutics and were instrumental in this study (356-360). So far, this is the first report to produce and utilise C3dg/C3d Fc fusion proteins and may generate some interest in the field. Aside from the analytical applications shown here, there are further potential uses in preparative steps such as purification of CR2 or immunoprecipitation. Their use can be extended to further assays thanks to their higher affinity to CR2 and may be used instead of antibodies in a similar fashion as the octamer (see above). As well as synergistic action, Fc fusion therapeutics benefit from extended half-life in

circulation (356), but also provide two receptor targets for use *in vivo*. Pathogens with specific immune evasion strategies such as Ig-binding protein A on *Staphylococcus aureus* (415) could be targeted in this way. This artificial opsonisation could promote phagocytosis and accelerate the clearance of that pathogen.

The physical nature, size and arrangement of the surface receptors and their interaction with the HEL C3d octamer will require further examination. CR2 is a 145 kDa rod-shaped protein that is flexible, but mostly extended, and protrudes into the surrounding medium (367). BCR, on the other hand, although of roughly the same size, is much more compact. As each SCR approximately equals the size of a single Ig domain there could be a misconception about the cross-linking processes and capabilities of IC. Due to the length of CR2 (and despite its flexibility while interacting with C3d-opsonised antigen) this could take place and remain far above the BCR. The antigen specific interaction with the surface bound Ig would occur closer to the cell surface. Thus, in reality a three-dimensional or a spatial problem may exist which could prevent cross-linking of CR2 to BCR. The B-cell surface is flexible and processes protrude into the medium, as shown during uptake experiments by Hess *et al.* (23). However, the involved receptors would at his point have been recruited to lipid rafts, which may have some effects on membrane fluidity due to their high cholesterol content (416). Equally, the recent discoveries that more than one C3d binding site may be present within CR2 (204, 363) may limit the ability of C3d tightly bound to antigen to interact with CR2 and BCR simultaneously. These spatial issues highlight the need for closer inspection of processes before, during and after capture by BCR/CR2. The octamer is a

compact protein and thus, it will be important to study MHC II presentation to confirm that uptake and processing of octameric proteins by B-cells is not dealt with differently from other tagged Ag. It is unlikely that any differences are present, as the C3d octamers size and conformation would roughly equal a typical immune complex, but this remains to be determined. Electron microscopy (see (23)) as well as cellular assays using fluorescence should shed more light on the receptor complex. Such spatial limitations are the most likely reason for the HEL-mC3d^{S} construct being found to be generally inhibitory (158, 217, 223, 224). This suggests that a certain distance has to be covered by a recombinant vaccine to effectively cross-link BCR and CR2. In the case of the octamer this could be further maximised by longer linkers or alternatively bi-cistronic vaccine vectors encoding hC3d^{S}-HEL-Oct and HEL-hC3d^{S}-Oct (417-421). Assembly in the cell should lead to a heterogeneous protein with HEL and C3d^{S} in random arrangements.

Murine C3d vaccines have been tried and tested extensively. This was one of the factors behind the choice of human C3d in the octamer design, which would provide a reagent ready for use in humanised models or clinical studies. It goes without saying that humans and mice are immunologically different, especially concerning CR2 (section 1.7.2). Therefore, the availability of *Cr2*$^{-/-}$ hCR2$^{+/-}$ transgenic mice (171) provides a useful *in vivo* model to study the immune response generated by human C3d vaccines prior to experiments in humans. The next generation of octameric vaccine will contain an antigen most likely derived from influenza due to the annual re-formulation of the vaccine and the recent threat from the avian variant. High amounts of protein will be required for efficient

vaccination; therefore the DNA vaccination route will be the most likely pursued. Obviously, it will be some time until any clinical trials can be envisaged. To date, no obviously detrimental effects have been reported, but there have been reports where C3d did not have the desired effect and caused inhibition rather than enhancement of the response (299, 380, 422-424). One reason for this outcome could be over-ligation of CR2, which has been shown to have an inhibitory effect although this is only observed *in vitro* (348, 425-428). The stimulatory and inhibitory concentrations were determined by Lee *et al.* (348) as above 1 µg/ml and 50 µg/ml respectively. Here, $hC3d^{S}$-HEL-Oct was administered at 10 µg/ml, which was within the stimulatory range. Moreover, the vaccine was naturally diluted and dispersed in the circulatory system following injection. The data also clearly indicated C3d-enhanced induction of the immune response in some of the mice. Whether eight binding sites each for BCR and CR2 could have inhibitory effects remains to be determined in detail. However, it is unlikely that all binding sites will in fact interact with a receptor. Despite its size, the octamer has to deal with some spatial issues, i.e. binding of one HEL molecule may block the binding sites of the two neighbouring ones. It has to be assumed that natural C3d-IC carry more than eight copies of C3d on their surface. Pathogens can also carry several hundred antigenic sites in a densely packed area, e.g. viruses. There may be an ideal number of BCR and CR2 that have to be cross-linked for the adjuvant effect. The factual causes for inhibition by C3d vaccines thus mainly remain unknown. This highlights the requirement to optimise each vaccine on a case-by case basis (422).

These concerns aside, the octamer in its current state would be suitable for human use and should be tolerated by the human immune system. The adjuvant species

is derived from human, as is the core of the protein, C4BP. Further complications can only be ruled out during further testing with available tools such as the use of high-affinity antibodies, and extensive *in vivo* testing in mice and eventually non-human primates prior to any considerations of a clinical trial. A number of C3d parameters that influence the immune response are still unknown. It has only recently been discovered that C3d appears in a weak dimer-monomer equilibrium during the immune response anyway (429). At this stage, the octamer is only about to undergo the first revision of arrangement, structure and antigen selection, thus, a considerable amount of optimisation remains. The next step will be the testing of the described octamer or an optimised version of it in the aforementioned $Cr2^{-/-}$ $hCR2^{+/-}$ transgenic mice. It is uncertain whether this octamer will eventually be turned into a vaccine for human use. Since the start of this study C3d as molecular adjuvant has received slightly less attention. This could be due to either the inhibitory effects discussed above or by further attempts by some investigators to optimise the CR2 binding site (430). Despite the success of the C3d trimer with certain antigens in mice, no clinical trials are on the horizon. One study in particular raised serious questions on the actual mode of action of C3d in the $Cr2^{-/-}$ model (402). However, if this approach were to be developed further for human use it would most likely be as a DNA vaccine thanks to the advantages in production and storage (231, 237, 369-372). The blueprint of the octamer is relatively simple compared to its complexity when expressed. This allows quick responses thanks to shortened development time to compensate for antigenic drift and shift, e.g. in HIV and influenza. Recent examples such as the threat from avian influenza, bioterrorism (e.g. attacks using smallpox, (431)) and the outbreak of severe acute respiratory syndrome virus (SARS) have shown that conventional production of

sufficient amounts of effective vaccine cannot be achieved in a short period of time. In case of SARS a DNA vaccine protective in animals had been found within 4 – 6 months (432, 433). However, if the octameric DNA vaccine is to be used in the future, the necessary safety requirements will have to be met before any trials are permitted (243). Despite a promising future, a wider range of tests than before, e.g. integration studies, biodistribution studies, concern over anti-nucleic acid antibody generation, duration of target antigen production after inoculation, will be required until considered safe (244). Guidelines on DNA vaccines' safety issues and testing procedures to get approval have to be strict and were put in place (245, 434, 435) after a hard lesson had been learned during an early trial in 1990 (246). Therefore the prime concern in current DNA vaccine development is safety as part of the design process as well as during preclinical studies (436).

Recent clinical trials with HIV DNA vaccines in human subjects have favoured heterologous prime-boost regimens ((437), also see (438)). Generally, they proved weakly immunogenic and elicited mainly weak or short-lived responses (439). It also appears that DNA dosages required to elicit an efficient response exceeded practical amounts. However, there have been some successes with small-scale trials, which showed some positive effects when more sensitive analyses were applied (436). Despite the thus-far unsatisfactory results in humans there are currently several hundred clinical trials involving DNA vaccines underway (440). Long-term effects of DNA vaccines in humans are unknown at present and it is likely to be many years before these findings emerge. However, the short and medium term effects have thus far been proven to be minor. A few clinical test subjects experienced some side effects such as local redness or skin damage but

the effects had disappeared two weeks into the trials (436). Whereas induction of an efficient immune response by a genetic vaccine has proved a struggle in humans, DNA vaccine trials in the veterinary setting have been successful. In 2005, the first DNA vaccine against West Nile virus in horses was licensed (441, 442)followed shortly after by a DNA vaccine against infectious hematopoietic necrosis virus in farmed salmon (443). It is generally recognised that vaccination as an immunopreventative measure is more cost effective than long-term treatment of disease or infection (436). This concerns man as well as the animals man keeps. Diseases affecting livestock cause suffering for the livestock but also considerable financial damage, which makes vaccine research and vaccination of farm animals economically as well as ethically important. The recent cases of avian influenza (H5N1 strain) have highlighted the need for such vaccines to also protect the human population. Veterinary science also explores novel routes and techniques (e.g. *in ovo* vaccination (441)or DNA vaccine tattooing (444). The substantial attention paid to veterinary vaccine research (445-448) and research findings (e.g. immune response induction and bias, vector optimisation, dosage, route, etc.) will have an impact on further development of human DNA vaccines. However, for future human use, only trials with non-human primates and human subjects will prove the true efficacy of a candidate vaccine (437).

6.3 Conclusion

This study set out to design and characterise the molecular adjuvant C3d as a novel octameric vaccine. Firstly, these studies provided insight why $C3d^S$ is the commonly used version in molecular adjuvant vaccines. The data also clearly indicated that much higher yields could be accomplished with an alternative variant, $C3d^Sg$, in the CHO cell based system. This highlighted the fact that frequently compromises have to be struck to achieve the set aims. In this case stronger binding was preferable to high expression levels. Secondly, production of the octamer in cell culture showed convincingly that whilst the protein products derived from clonal selection, high-yield production and purification were sufficient for few analyses and a limited number of *in vivo* experiments, this is probably not economically viable as a vaccine candidate either in the laboratory settings or in any clinical studies. The combination of *in vitro* characterisation, and production led to the conclusion that $hC3d^S$-HEL-Oct in a vaccine context should only be developed further as a DNA vaccine.

The decision to include $C3d^S$ rather than $C3d^Sg$ in the vaccine was based on a CR2 SCR1-4 Fc binding experiment as part of the comprehensive *in vitro* experiments. For the first time in complement research C3dg/$C3d^Sg$/C3d/$C3d^S$ Fc fusion proteins were generated utilising human and mouse proteins to examine these interactions in more detail. Up until now, binding has only been measured using monomeric C3dg/C3d (188, 204, 339), which as discussed above, causes inhibition of B-cell activation. Recent evidence suggests that even the single molecule interaction may be more complicated than anticipated and does not follow a 1:1 relationship (204, 429). A bivalent approach was therefore more

suitable for this type of analysis (compare (368)). Each of the CR2 interaction experiments using flow cytometry and the highly sensitive SPR analysis yielded the same surprising result. Contrary to a number of previous studies and the established view, murine C3d bound to human CR2 with much higher affinity than human C3d to human CR2. Although this does not devalue any previous work, it will require a re-evaluation of the results and a more careful design of experiments. This new aspect of cross-species activity demands closer investigation, especially in view of potential use in human vaccines. Aside from these striking results, some partial degradation of the C3dg/C3d^{S}g fusions to C3d/C3d^{S} may be an indicator that the major binding partner is C3d. C3g is cleaved off by proteolytic enzymes (e.g. plasmin, trypsin), present in abundance at sites of infection. Notably, the interaction data obtained from octamer and Fc fusion binding studies were apparently conflicting, but as these two constructs have a very different structure and organisation, it is difficult to directly compare them.

In vivo testing of the protein and DNA vaccines has yielded promising results: HEL-specific antibodies were raised by hC3d^{S}-HEL-Oct protein, but not HEL-Oct alone, provided tantalising evidence that hC3d^{S} did successfully enhance the immune response. The response was not as strong as the responses induced by CFA, but this may be resolved through further optimisation of these prototype vaccines. Importantly, the data clearly showed that this essentially human vaccine could induce antibody responses in mice, paving the way for future studies in both wild type and transgenic animals. In total, eight vaccine plasmids (5 x CpG^{+}, 3 x CpG^{-}) were administered via one of two routes (i.m. and t.d.) and their sera and splenocytes analysed. Unfortunately, no conclusive data was gained regarding the

performance of hC3d^{S}-HEL-Oct compared with the original linear trimer. The data generated did demonstrate convincingly that the C3d Octamer was a viable vaccine, but the experimental variation in these preliminary studies suggested that other factors were interfering with the immune response to hC3d^{S}-HEL-Oct. Removal of CpG from the formulation, i.e. the plasmid sequence, seemed to counteract some of the variations. On the whole, responses were higher to CpG reduced plasmids compared to the CpG^{+} vaccine plasmid responses. Flow cytometric analysis of germinal centre, plasma B-cells and memory B-cells after immunisation with hC3d^{S}-HEL-Oct demonstrated alterations in cell populations (e.g. memory cells) and indicated the persistence of germinal centres six weeks after injection. These provided useful additional data on the immune response generated by these vaccines, but will require sampling of cells at more time points (than exclusively at the end) in order to provide concrete data on the cellular mechanisms driven by these vaccines compared with the standard vaccines strategies currently employed.

In summary, this study has shown that the production and *in vivo* application of an octameric DNA vaccine with the in-built molecular adjuvant C3d^{S} is a viable method to enhance the specific antibody response to the respective antigen. Additionally, it was shown that the affinities of mouse and human C3d to human CR2 are not equal and murine is in fact the stronger interaction partner. These findings will allow further development of the octameric (and linear trimer) form of C3d adjuvant and clearly demonstrate the potential of C3d in Octamer form to act as a potent adjuvant, which will yield a novel, adaptable and efficient vaccine for human use in the foreseeable future.

Appendix I – Oligonucleotide PCR Primers

Name	Sequence 5' → 3'	Restriction sites	Length/ T_m	Application
C3dg_C58S_sense	CCCCTCGGGC**AGC** GG GGAACAGA	None	23 bp 71.3°C	Introduces thioester mutation cysteine → serine; forward primer
C3dg_C58S_anti	TCTGTTCCCC**GCT** GCCCGAGGGG	None	23 bp 71.3°C	Introduces thioester mutation cysteine → serine; reverse primer
C3g_deletion_F	CTGGCTATGGATA CTAGTCACCTCAT TGTGACCC	Spe I	34 bp 70.7°C	Deletion of 'g' portion; forward primer
C3g_deletion_R	GGGTCACAATGAG GTGACTAGTATCC ATAGCCAG	Spe I	34 bp 70.7°C	Deletion of 'g' portion; reverse primer
C3dgF	CGAACTAGTGAAG GAGTGCAGAAAGA GGACATC	Spe I	33 bp 72.7°C	Cloning, screening
C3dgR2	CCAGCGGCCGCGG TACCGCGGCTGGG CAGTTGGAGGGA	Not I	38 bp 76.3°C	Cloning, screening
nx-signal	CAAGCTAGCTCTA GATAACTAGAGAA CCCACTG	Nhe I	33 bp 67.1°C	Cloning, screening
nhe-C3dg-rev	CGAGCTAGCCGGC TGGGCAGTTGGAG GGA	Nhe I	29 bp 69.0°C	Cloning, screening
H3-shC4bp-F	CGAAAGCTTTAGA GTGGGAGACCCCC GAAGGCTGTG	HinD III	36 bp 83.1°C	Cloning, screening
EE-C4bp-End	CGAGAATTCGATA TCTTAATAGTTCT TTATCCAAAGTGG ATTG	Eco RI Eco RV	43 bp 74.6°C	Cloning, screening
C3d nog 5'	ACTAGTAAGCACC TCATTGTGACCCC	Spe I	26 bp 66.2°C	Cloning, screening
HEL_F_2	GCAGCGCTAGCAA GATCTAAAGTCTT TGGACGATG	Nhe I	35 bp 58.1°C	Cloning, screening
HEL-R	GCTGCGGCCGCTA AAGCTTGGGATCC CAGCCTGCAGCCT CTGATCC	Not I HinD III BamH I	46 bp 77.9°C	Cloning, screening
Nco_CD33_F	ATCCCATGGTAAC TAGAGAACCCACT GC	Nco I	37 bp 65.0°C	Cloning, screening

Name	Sequence 5' → 3'	Restriction sites	Length/ T_m	Application
Nco_8_R	AAACCATGGCTTG ATATCTTATAGTT CTTTATCCAAAGT GG	Nco I	41 bp 61.2°C	Cloning, screening
CpG_EF_F	TAGGGGTGACTAG TGGAGAAGAGCAT GC	Spe I	28 bp 69.3°C	sequencing primer $pCpG^-$ DNA vaccine vector
pvkseq_F	TTTGACTCACGGG GATTTCCAAGTCT CCACC	-	31 bp 76°C	sequencing primer $pCpG^+$ DNA vaccine vector
pvkseq_R	AAGGACAGTGGGA GTGGCACCTTCCA GG	-	28 bp 75.7°C	sequencing primer $pCpG^+$ DNA vaccine vector
XhoI-CD33_F	ATAACTCGAGATG CCGCTGCTGCTA CTGCTGCCC	Xho I	34 bp 75.8°C	Cloning, screening
pvk_mcs_F	CACTGCGCGGCCG CTCGAGAAGCTTA GATCTGAATTCGA TATCTCTAGAG	Bts I Not I Xho I Hind III Eco RI Eco RV Xba I	50 bp	multiple cloning site; 5' - phosphorylated
pvk_mcs_R	GATCCTCTAGAGA TATCGAATTCAGA TCTAAGCTTCTCG AGCGGCCGCGCAG TGGG		56 bp	

Bibliography

1. Jenner E. The Three Original Publications On Vaccination Against Smallpox: Kessinger Publishing; 1798.

2. Liu MA. Vaccine developments. Nature Medicine 1998;4(5 Suppl):515-9.

3. Makela PH. Vaccines, coming of age after 200 years. FEMS Microbiology Reviews 2000;24(1):9-20.

4. WHO. Smallpox. http://www.who.int/mediacentre/factsheets/smallpox/en/: World Health Organization; 2007.

5. WHO. Poliomyelitis. http://www.who.int/vaccine_research/diseases/poliomyelitis/en/index.html: World Health Organization; 2007.

6. FitzGerald D, Mrsny RJ. New approaches to antigen delivery. Critical Reviews in Therapeutic Drug Carrier Systems 2000;17(3):165-248.

7. Arnon R, Ben-Yedidia T. Old and new vaccine approaches. International Immunopharmacology 2003;3(8):1195-204.

8. Lydyard PM, Whelan A, W. FM. Immunology. 2nd ed. Abingdon: Taylor & Francis; 2004.

9. Pedersen AE. Immunity to Infection. Chichester: John Wiley & Sons Ltd; 2001.

10. James K. Immune Responses: Primary and Secondary. Chichester: John Wiley & Sons Ltd.; 2001.

11. Morgan BP. Complement - Clinical Aspects and Relevance to Disease. London: Academic Press Ltd.; 1990.

12. Eales L-J. Immunology for Life Scientists. 2nd ed. Chichester: John Wiley & Sons Ltd.; 2003.

13. Janeway AC, Travers P, Walport MJ, Shlomchik MJ. Immunobiology 5 - The Immunesystem in Health and Disease. 5 ed. New York: Garland Publishing; 2001.

14. Watts C. Capture and processing of exogenous antigens for presentation on MHC molecules. Annual Review of Immunology 1997;15:821-50.

15. Sandberg JK, Glas R. Antigen Processing. Chichester: John Wiley & sons Ltd.; 2005.

16. Banchereau J, Briere F, Caux C, Davoust J, Lebecque S, Liu Y-J, et al. Immunobiology of Dendritic Cells. Annual Review of Immunology 2000;18(1):767-811.

17. Swanson JA, Watts C. Macropinocytosis. Trends in Cell Biology 1995;5(11):424-8.

18. Nielsen CH, Leslie RG. Complement's participation in acquired immunity. Journal of Leukocyte Biology 2002;72(2):249-61.

19. Hess J, Laumen H, Muller KB, Wirth T. Molecular genetics of the germinal center reaction. Journal of Cellular Physiology 1998;177(4):525-34.

20. Mongini P, Vilensky M, Highet P, Inman J. The affinity threshold for human B cell activation via the antigen receptor complex is reduced upon co-ligation of the antigen receptor with CD21 (CR2). Journal of Immunology 1997;159(8):3782-91.

21. Kerekes K, Prechl J, Bajtay Z, Jozsi M, Erdei A. A further link between innate and adaptive immunity: C3 deposition on antigen-presenting cells enhances the proliferation of antigen-specific T cells. International Immunology 1998;10(12):1923-30.

22. Parker DC. The functions of antigen recognition in T cell-dependent B cell activation. Seminars in Immunology 1993;5(6):413-20.

23. Hess MW, Schwendinger MG, Eskelinen EL, Pfaller K, Pavelka M, Dierich MP, et al. Tracing uptake of C3dg-conjugated antigen into B cells via complement receptor type 2 (CR2, CD21). Blood 2000;95(8):2617-23.

24. Essen Dv, Kikutani H, Gray D. CD40 ligand-transduced co-stimulation of T cells in the development of helper function. Journal of Molecular Biology 1995;378(6557):620-3.

25. Toellner K-M, Scheel-Toellner D, Sprenger R, Duchrow M, Trumper LH, Ernst M, et al. The human germinal centre cells, follicular dendritic cells and germinal centre T cells produce B cell-stimulating cytokines. Cytokine 1995;7(4):344-54.

26. Laszlo G, Hathcock K, Dickler H, Hodes R. Characterization of a novel cell-surface molecule expressed on subpopulations of activated T and B cells. Journal of Immunology 1993;150(12):5252-62.

27. Cozine CL, Wolniak KL, Waldschmidt TJ. The primary germinal center response in mice. Current Opinion in Immunology 2005;17(3):298-302.

28. Wagner SD, Neuberger MS. Somatic Hypermutation of Immunoglobulin Genes. Annual Review of Immunology 1996;14(1):441-57.

29. Maclennan ICM. Germinal Centers. Annual Review of Immunology 1994;12(1):117-39.

30. Thorbecke G, Amin A, Tsiagbe V. Biology of germinal centers in lymphoid tissue. FASEB Journal 1994;8(11):832-40.

31. Wabl M, Cascalho M, Steinberg C. Hypermutation in antibody affinity maturation. Current Opinion in Immunology 1999;11(2):186-9.

32. Hollowood K, Goodlad J. Germinal centre cell kinetics. The Journal of Pathology 1998;185(3):229-33.

33. Bergmann-Leitner ES, Leitner WW. Danger, death and DNA vaccines. Microbes and Infection 2004;6(3):319-27.

34. Berek C, Berger A, Apel M. Maturation of the Immune Response in Germinal centres. Cell 1991;67(6):1121-9.

35. Liu Y-J, Arpin C. Germinal center development. Immunological Reviews 1997;156(1):111-26.

36. Lagresle C, Bella C, Defrance T, Maclennan I. Phenotypic and functional heterogeneity of the IgD- B cell compartment: identification of two major tonsillar B cell subsets. International Immunology 1993;5(10):1259-68.

37. Nielsen CH, Fischer EM, Leslie RG. The role of complement in the acquired immune response. Immunology 2000;100(1):4-12.

38. Mandel TE, Phipps RP, Abbot A, Tew JG. The follicular dendritic cell: long term antigen retention during immunity. Immunological Reviews 1980;53:29-59.

39. Vitetta ES, Berton MT, Burger C, Kepron M, Lee WT, Yin XM. Memory B and T Cells. Annual Review of Immunology 1991;9(1):193-217.

40. Fischer MB, Goerg S, Shen L, Prodeus AP, Goodnow CC, Kelsoe G, et al. Dependence of germinal center B cells on expression of CD21/CD35 for survival. Science 1998;280(5363):582-5.

41. Park CS, Choi YS. How do follicular dendritic cells interact intimately with B cells in the germinal centre? Immunology 2005;114(1):2-10.

42. McHeyzer-Williams MG, Ahmed R. B cell memory and the long-lived plasma cell. Current Opinion in Immunology 1999;11(2):172-9.

43. Guzman-Rojas L, Sims-Mourtada JC, Rangel R, Martinez-Valdez H. Life and death within germinal centres: a double-edged sword. Immunology 2002;107(2):167-75.

44. Jego G, Robillard N, Puthier D, Amiot M, Accard F, Pineau D, et al. Reactive Plasmacytoses Are Expansions of Plasmablasts Retaining the Capacity to Differentiate Into Plasma Cells. Blood 1999;94(2):701-12.

45. Ridderstad A, Tarlinton DM. Kinetics of establishing the memory B cell population as revealed by CD38 expression. Journal of Immunology 1998;160(10):4688-95.

46. Oliver A, Martin F, Kearney J. Mouse CD38 is down-regulated on germinal center B cells and mature plasma cells. Journal of Immunology 1997;158(3):1108-15.

47. Anderson SM, Tomayko MM, Shlomchik MJ. Intrinsic properties of human and murine memory B cells. Immunological Reviews 2006;211:280-94.

48. Boackle SA, Holers VM, Karp DR. CD21 augments antigen presentation in immune individuals. European Journal of Immunology 1997;27(1):122-9.

49. Mills JA, Cooperband SR. Lymphocyte Physiology. Annual Review of Medicine 1971;22(1):185-220.

50. Klaus GGB. B lymphocytes. 1 ed. Oxford: Oxford University Press; 1990.

51. Bondada S, Chelvarajan RL. B-Lymphocytes. Encyclopdia of Life Sciences 2001.

52. Haas KM, Hasegawa M, Steeber DA, Poe JC, Zabel MD, Bock CB, et al. Complement receptors CD21/35 link innate and protective immunity during Streptococcus pneumoniae infection by regulating IgG3 antibody responses. Immunity 2002;17(6):713-23.

53. Rolink A, Melchers F. B-cell development in the mouse. Immunology Letters Proceedings of the Symposium on Signals and Signal Processing in the Immune System 1996;54(2-3):157-61.

54. Krop I, deFougerolles AR, Hardy RR, Allison M, Schlissel MS, Fearon DT. Self-renewal of B-1 lymphocytes is dependent on CD19. European Journal of Immunology 1996;26(1):238-42.

55. Sato S, Ono N, Steeber DA, Pisetsky DS, Tedder TF. CD19 regulates B lymphocyte signaling thresholds critical for the development of B-1 lineage cells and autoimmunity. Journal of Immunology 1996;157(10):4371-8.

56. Fearon DT, Carter RH. The CD19/CR2/TAPA-1 Complex of B Lymphocytes: Linking Natural to Acquired Immunity. Annual Review of Immunology 1995;13(1):127-49.

57. Hardy RR, Hayakawa K. B cell development pathways. Annual Review of Immunology 2001;19:595-621.

58. Li YS, Hayakawa K, Hardy RR. The regulated expression of B lineage associated genes during B cell differentiation in bone marrow and fetal liver. Journal of Experimental Medicine 1993;178(3):951-60.

59. Carroll MC. The complement system in B cell regulation. Molecular Immunology XXth International Complement Workshop 2004;41(2-3):141-6.

60. Casola S, Otipoby KL, Alimzhanov M, Humme S, Uyttersprot N, Kutok JL, et al. B cell receptor signal strength determines B cell fate. Nature Immunology 2004;5(3):317-27.

61. Pillai S, Cariappa A, Moran ST. Marginal Zone B Cells. Annual Review of Immunology 2005;23(1):161-96.

62. Lopes-Carvalho T, Kearney JF. Development and selection of marginal zone B cells. Immunological Reviews 2004;197:192-205.

63. Martin F, Kearney JF. B-cell subsets and the mature preimmune repertoire. Marginal zone and B1 B cells as part of a "natural immune memory". Immunological Reviews 2000;175:70-9.

64. Martin F, Oliver AM, Kearney JF. Marginal zone and B1 B cells unite in the early response against T-independent blood-borne particulate antigens. Immunity 2001;14(5):617-29.

65. Carroll MC. The role of complement and complement receptors in induction and regulation of immunity. Annual Review of Immunology 1998;16:545-68.

66. Morley BJ, Walport MJ. The Complement Facts Book. 1 ed: Academic Press; 2000.

67. Ehrlich P, Morgenroth J. Zur Theorie der Lysinwirkung. Berliner Klinische Wochenschrift 1899;1:6 - 9.

68. Klein J, Horejší V. Immunology. 2nd ed. Oxford: Blackwell Science Ltd.; 1997.

69. Sunyer JO, Lambris JD. Complement. Encyclopdia of Life Sciences 2001.

70. Nonaka M, Yoshizaki F. Primitive complement system of invertebrates. Immunological Reviews 2004;198(1):203-15.

71. Fujita T, Endo Y, Nonaka M. Primitive complement system--recognition and activation. Molecular Immunology 2004;41(2-3):103-11.

72. Oliver AM, Martin F, Kearney JF. $IgM^{high}CD21^{high}$ Lymphocytes Enriched in the Splenic Marginal Zone Generate Effector Cells More Rapidly Than the Bulk of Follicular B Cells. Journal of Immunology 1999;162(12):7198-207.

73. Law SK, Reid KB. Complement. 2 ed. Oxford: IRL Press; 1995.

74. Sim RB, Tsiftsoglou SA. Proteases of the complement system. Biochemical Society Transactions 2004;32(Pt 1):21-7.

75. Müller-Eberhard HJ. Complement - Chemistry and Pathways. In: Gallin JI, Goldstein IM, Snyderman R, editors. Inflammation: Basic Principles and Clinical Correlates. 2nd ed. New York: Raven Press Ltd.; 1992.

76. Arlaud GJ, Colomb MG. Complement: Classical Pathway. Encyclopedia of Life Sciences 2005.

77. Morgan BP, Harris CL. Complement Regulatory Proteins. London: Academic Press Inc.; 1999.

78. Casanova JL, Abel L. Human Mannose-binding Lectin in Immunity: Friend, Foe, or Both? Journal of Experimental Medicine 2004;199(10):1295-9.

79. Matsushita M, Fujita T. The lectin pathway. Research in Immunology 1996;147(2):115-8.

80. Turner MW. The lectin pathway of complement activation. Research in Immunology 1996;147(2):110-5.

81. Epstein J, Eichbaum Q, Sheriff S, Ezekowitz RAB. The collectins in innate immunity. Current Opinion in Immunology 1996;8(1):29-35.

82. Presanis JS, Kojima M, Sim RB. Biochemistry and genetics of mannan-binding lectin (MBL). Biochemical Society Transactions 2003;31(Pt 4):748-52.

83. Kravitz MS, Pitashny M, Shoenfeld Y. Protective molecules--C-reactive protein (CRP), serum amyloid P (SAP), pentraxin3 (PTX3), mannose-binding lectin (MBL), and apolipoprotein A1 (Apo A1), and their autoantibodies: prevalence and clinical significance in autoimmunity. Journal of Clinical Immunology 2005;25(6):582-91.

84. Müller-Eberhard HJ. Molecular organization and function of the complement system. Annual Review of Biochemistry 1988;57:321-47.

85. Pillemer L, Blum L, Lepow IH, Ross OA, Todd EW, Wardlaw AC. The properdin system and immunity. I. Demonstration and isolation of a new serum protein, properdin, and its role in immune phenomena. Science 1954;120(3112):279-85.

86. Fearon DT, Austen KF. Properdin: Initiation of Alternative Complement Pathway. Proceedings of the National Academy of Sciences of the United States of America 1975;72(8):3220-4.

87. Fearon D, Austen K. Properdin: binding to C3b and stabilization of the C3b-dependent C3 convertase. Journal of Experimental Medicine 1975;142(4):856-63.

88. Lambris JD. The multifunctional role of C3, the third component of complement. Immunology Today 1988;9(12):387-93.

89. Müller-Eberhard HJ, Nilsson U, Aronsson T. Isolation and Characterization of Two {beta}1-Glycoproteins of Human Serum. Journal of Experimental Medicine 1960;111(2):201-15.

90. Müller-Eberhard HJ, Nilsson U. Relation of a {beta}1-Glycoprotein of Human Serum to the Complement System. Journal of Experimental Medicine 1960;111(2):217-34.

91. Sahu A, Lambris JD. Structure and biology of complement protein C3, a connecting link between innate and acquired immunity. Immunological Reviews 2001;180:35-48.

92. Al-Sharif WZ, Sunyer JO, Lambris JD, Smith LC. Sea Urchin Coelomocytes Specifically Express a Homologue of the Complement Component C3. Journal of Immunology 1998;160(6):2983-97.

93. Prahl JW, Lorenz PE, Schechter AN, Prah JW, Tack BF. Third component of human complement: appearance of a sulfhydryl group following chemical or enzymic inactivation. Biochemistry 1980;19(19):4471-78.

94. Janatova J, Tack BF, Prahl JW. Third component of human complement: structural requirements for its function. Biochemistry 1980;19(19):4479-85.

95. Tack BF, Prahl JW. 3rd Component of Human Complement - Purification from Plasma and Physicochemical Characterization. Biochemistry 1976;15(20):4513-21.

96. Bruijn MHLD, Fey GH. Human Complement Component C3: cDNA Coding Sequence and Derived Primary Structure. Proceedings of the National Academy of Sciences of the United States of America 1985;82(3):708-12.

97. Janssen BJC, Huizinga EG, Raaijmakers HCA, Roos A, Daha MR, Nilsson-Ekdahl K, et al. Structures of complement component C3 provide insights into the function and evolution of immunity. Nature 2005;437(7058):505-11.

98. Gadjeva M, Dodds AW, Taniguchi-Sidle A, Willis AC, Isenman DE, Law SK. The covalent binding reaction of complement component C3. Journal of Immunology 1998;161(2):985-90.

99. Szakonyi G, Guthridge JM, Li D, Young K, Holers VM, Chen XS. Structure of complement receptor 2 in complex with its C3d ligand. Science 2001;292(5522):1725-8.

100. Guthridge JM, Young K, Gipson MG, Sarrias MR, Szakonyi G, Chen XS, et al. Epitope mapping using the X-ray crystallographic structure of complement receptor type 2 (CR2)/CD21: identification of a highly inhibitory monoclonal antibody that directly recognizes the CR2-C3d interface. Journal of Immunology 2001;167(10):5758-66.

101. Hannan J, Young K, Szakonyi G, Overduin MJ, Perkins SJ, Chen X, et al. Structure of complement receptor (CR) 2 and CR2-C3d complexes. Biochemical Society Transactions 2002;30(Pt 6):983-9.

102. Nagar B, Jones RG, Diefenbach RJ, Isenman DE, Rini JM. X-ray Crystal Structure of C3d: A C3 Fragment and Ligand for Complement Receptor 2. Science 1998;280(5367):1277-81.

103. Morikis D, Lambris JD. The electrostatic nature of C3d-complement receptor 2 association. Journal of Immunology 2004;172(12):7537-47.

104. Prota AE, Sage DR, Stehle T, Fingeroth JD. The crystal structure of human CD21: Implications for Epstein-Barr virus and C3d binding. Proceedings of the National Academy of Sciences of the United States of America 2002;99(16):10641-46.

105. Lundwall A, Wetsel R, Domdey H, Tack B, Fey G. Structure of murine complement component C3. I. Nucleotide sequence of cloned complementary and genomic DNA coding for the beta chain. Journal of Biological Chemistry 1984;259(22):13851-6.

106. Wetsel R, Lundwall A, Davidson F, Gibson T, Tack B, Fey G. Structure of murine complement component C3. II. Nucleotide sequence of cloned complementary DNA coding for the alpha chain. Journal of Biological Chemistry 1984;259(22):13857-62.

107. Sahu A, Kozel TR, Pangburn MK. Specificity of the thioester-containing reactive site of human C3 and its significance to complement activation. Biochemical Journal 1994;302 (Pt 2):429-36.

108. Spiller OB, Blackbourn DJ, Mark L, Proctor DG, Blom AM. Functional activity of the complement regulator encoded by Kaposi's sarcoma-associated herpesvirus. Journal of Biological Chemistry 2003;278(11):9283-9.

109. Sim E, Wood AB, Hsiung LM, Sim RB. Pattern of degradation of human complement fragment, C3b. FEBS Letters 1981;132(1):55-60.

110. Fearon DT, Wong WW. Complement Ligand-Receptor Interactions that Mediate Biological Responses. Annual Review of Immunology 1983;1(1):243-71.

111. Law SK, Dodds AW. The internal thioester and the covalent binding properties of the complement proteins C3 and C4. Protein Science 1997;6(2):263-74.

112. Isenman DE, Cooper NR. The structure and function of the third component of human complement--I. The nature and extent of conformational changes accompanying C3 activation. Molecular Immunology 1981;18(4):331-9.

113. Dodds AW, Ren XD, Willis AC, Law SK. The reaction mechanism of the internal thioester in the human complement component C4. Nature 1996;379(6561):177-9.

114. Hack C, Paardekooper J, Smeenk R, Abbink J, Eerenberg A, Nuijens J. Disruption of the internal thioester bond in the third component of complement (C3) results in the exposure of neodeterminants also present on activation products of C3. An analysis with monoclonal antibodies. Journal of Immunology 1988;141(5):1602-1609.

115. Pepys MB, Dash AC, Fielder AH, Mirjah DD. Isolation and study of murine C3. Immunology 1977;33(4):491-9.

116. Dalmasso AP, Müller-Eberhard HJ. Hemolytic activity of lipoprotein-depleted serum and the effect of certain anions on complement. Journal of Immunology 1966;97(5):680-5.

117. Pangburn MK, Schreiber RD, Müller-Eberhard HJ. Formation of the initial C3 convertase of the alternative complement pathway. Acquisition of C3b-like activities by spontaneous hydrolysis of the putative thioester in native C3. Journal of Experimental Medicine 1981;154(3):856-67.

118. Clemenza L, Isenman DE. Structure-Guided Identification of C3d Residues Essential for Its Binding to Complement Receptor 2 (CD21). Journal of Immunology 2000;165(7):3839-48.

119. Hellwage J, Jokiranta TS, Friese MA, Wolk TU, Kampen E, Zipfel PF, et al. Complement C3b/C3d and Cell Surface Polyanions Are Recognized by Overlapping Binding Sites on the Most Carboxyl-Terminal Domain of Complement Factor H. Journal of Immunology 2002;169(12):6935-44.

120. Hellwage J, Jokiranta TS, Koistinen V, Vaarala O, Meri S, Zipfel PF. Functional properties of complement factor H-related proteins FHR-3 and FHR-4: binding to the C3d region of C3b and differential regulation by heparin. FEBS Letters 1999;462(3):345-52.

121. Walport MJ. Complement. Second of two parts. New England Journal of Medicine 2001;344(15):1140-4.

122. Cooper NR, Moore MD, Nemerow GR. Immunobiology of CR2, the B lymphocyte receptor for Epstein-Barr virus and the C3d complement fragment. Annual Review of Immunology 1988;6:85-113.

123. Hourcade D, Holers VM, Atkinson JP. The regulators of complement activation (RCA) gene cluster. Advances in Immunology 1989;45:381-416.

124. Leslie RG. Complement Receptors. Encyclopdia of Life Sciences 2001.

125. Reynes M, Aubert JP, Cohen JH, Audouin J, Tricottet V, Diebold J, et al. Human follicular dendritic cells express CR1, CR2, and CR3 complement receptor antigens. Journal of Immunology 1985;135(4):2687-94.

126. Ross GD, Polley MJ, Rabellino EM, Grey HM. Two Different Complement Receptors on Human Lymphocytes: One Specific for C3b and One Specific for C3b Inactivator-Cleaved C3b. Journal of Experimental Medicine 1973;138(4):798-811.

127. Fearon DT. Identification of the membrane glycoprotein that is the C3b receptor of the human erythrocyte, polymorphonuclear leukocyte, B lymphocyte, and monocyte. Journal of Experimental Medicine 1980;152(1):20-30.

128. Molina H, Kinoshita T, Webster CB, Holers VM. Analysis of C3b/C3d binding sites and factor I cofactor regions within mouse complement receptors 1 and 2. Journal of Immunology 1994;153(2):789-95.

129. Holers MV, Kinoshita T, Molina H. The evolution of mouse and human complement C3-binding proteins: divergence of form but conservation of function. Immunology Today 1992;13(6):231-6.

130. Kinoshita T, Takeda J, Hong K, Kozono H, Sakai H, Inoue K. Monoclonal antibodies to mouse complement receptor type 1 (CR1). Their use in a distribution study showing that mouse erythrocytes and platelets are CR1-negative. Journal of Immunology 1988;140(9):3066-72.

131. Gordon DL, Johnson GM, Hostetter MK. Characteristics of iC3b binding to human polymorphonuclear leucocytes. Immunology 1987;60(4):553-8.

132. Leslie RG, Nielsen CH. The classical and alternative pathways of complement activation play distinct roles in spontaneous C3 fragment deposition and membrane attack complex (MAC) formation on human B lymphocytes. Immunology 2004;111(1):86-90.

133. Leslie RG, Prodinger WM, Nielsen CH. Complement receptors type 1 (CR1, CD35) and 2 (CR2, CD21) cooperate in the binding of hydrolyzed complement factor 3 (C3i) to human B lymphocytes. European Journal of Immunology 2003;33(12):3311-21.

134. O'Shea JJ, Brown EJ, Seligmann BE, Metcalf JA, Frank MM, Gallin JI. Evidence for distinct intracellular pools of receptors for C3b and C3bi in human neutrophils. Journal of Immunology 1985;134(4):2580-7.

135. Iida K, Nadler L, Nussenzweig V. Identification of the membrane receptor for the complement fragment C3d by means of a monoclonal antibody. Journal of Experimental Medicine 1983;158(4):1021-33.

136. Lay WH, Nussenzweig V. Receptors for Complement on Leukocytes. Journal of Experimental Medicine 1968;128(5):991-1009.

137. Eden A, Miller GW, Nussenzweig V. Human lymphocytes bear membrane receptors for C3b and C3d. Journal of Clinical Investigation 1973;52(12):3239-42.

138. Tedder T, Clement L, Cooper M. Expression of C3d receptors during human B cell differentiation: immunofluorescence analysis with the HB-5 monoclonal antibody. Journal of Immunology 1984;133(2):678-83.

139. Weis JJ, Tedder TF, Fearon DT. Identification of a 145,000 Mr membrane protein as the C3d receptor (CR2) of human B lymphocytes. Proceedings of the National Academy of Sciences of the United States of America 1984;81(3):881-5.

140. Pulvertaft JV. Cytology of Burkitt's Tumour (African Lymphoma). Lancet 1964;39:238-40.

141. Epstein MA, Achong BG, Barr YM, Zajac B, Henle G, Henle W. Morphological and virological investigations on cultured Burkitt tumor lymphoblasts (strain Raji). Journal of the National Cancer Institute 1966;37(4):547-59.

142. Barel M, Charriaut C, Frade R. Isolation and characterization of a C3b receptor-like molecule from membranes of a human B lymphoblastoid cell line (Raji). FEBS Letters 1981;136(1):111-4.

143. Frade R, Barel M, Krikorian L, Charriaut C. Analysis of gp 140, a C3b-binding membrane component present on Raji cells: a comparison with factor H. European Journal of Immunology 1984;14(6):542-8.

144. Siaw M, Nemerow G, Cooper N. Biochemical and antigenic analysis of the Epstein Barr virus/C3d receptor (CR2). Journal of Immunology 1986;136(11):4146-51.

145. Barel M, Fiandino A, Delcayre A, Lyamani F, Frade R. Monoclonal and anti-idiotypic anti-EBV/C3d receptor antibodies detect two binding sites, one for EBV and one for C3d on glycoprotein 140, the EBV/C3dR, expressed on human B lymphocytes. Journal of Immunology 1988;141(5):1590-95.

146. Carel J, Myones B, Frazier B, Holers V. Structural requirements for C3d,g/Epstein-Barr virus receptor (CR2/CD21) ligand binding, internalization, and viral infection. Journal of Biological Chemistry 1990;265(21):12293-99.

147. Yefenof E, Klein G, Jondal M, Oldstone MB. Surface markers on human B and T-lymphocytes. IX. Two-color immunofluorescence studies on the association between ebv receptors and complement receptors on the surface of lymphoid cell lines. International Journal of Cancer 1976;17(6):693-700.

148. Fischer M, Ma M, Goerg S, Zhou X, Xia J, Finco O, et al. Regulation of the B cell response to T-dependent antigens by classical pathway complement. Journal of Immunology 1996;157(2):549-56.

149. Ahearn JM, Fischer MB, Croix D, Goerg S, Ma M, Xia J, et al. Disruption of the Cr2 locus results in a reduction in B-1a cells and in an impaired B cell response to T-dependent antigen. Immunity 1996;4(3):251-62.

150. Fearon DT, Carroll MC. Regulation of B lymphocyte responses to foreign and self-antigens by the CD19/CD21 complex. Annual Review of Immunology 2000;18:393-422.

151. Ahearn JM, Fearon DT. Structure and function of the complement receptors, CR1 (CD35) and CR2 (CD21). Advances in Immunology 1989;46:183-219.

152. Tsoukas CD, Lambris JD. Expression of CR2/EBV receptors on human thymocytes detected by monoclonal antibodies. European Journal of Immunology 1988;18(8):1299-302.

153. Fischer E, Delibrias C, Kazatchkine MD. Expression of CR2 (the C3dg/EBV receptor, CD21) on normal human peripheral blood T lymphocytes. Journal of Immunology 1991;146(3):865-9.

154. Andrasfalvy M, Prechl J, Hardy T, Erdei A, Bajtay Z. Mucosal type mast cells express complement receptor type 2 (CD21). Immunology Letters 2002;82(1-2):29-34.

155. Tolnay M, Vereshchagina LA, Tsokos GC. NF-kappa B regulates the expression of the human complement receptor 2 gene. Journal of Immunology 2002;169(11):6236-43.

156. Masilamani M, Kassahn D, Mikkat S, Glocker MO, Illges H. B cell activation leads to shedding of complement receptor type II (CR2/CD21). European Journal of Immunology 2003;33(9):2391-7.

157. Fujisaku A, Harley J, Frank M, Gruner B, Frazier B, Holers V. Genomic organization and polymorphisms of the human C3d/Epstein-Barr virus receptor. Journal of Biological Chemistry 1989;264(4):2118-25.

158. Melchers F, Erdei A, Schulz T, Dierich MP. Growth control of activated, synchronized murine B cells by the C3d fragment of human complement. Nature 1985;317(6034):264-7.

159. Barel M, Le Romancer M, Frade R. Activation of the EBV/C3d Receptor (CR2, CD21) on Human B Lymphocyte Surface Triggers Tyrosine Phosphorylation of the 95-kDa Nucleolin and Its Interaction with Phosphatidylinositol 3 Kinase. Journal of Immunology 2001;166(5):3167-73.

160. Bouillie S, Barel M, Frade R. Signaling Through the EBV/C3d Receptor (CR2, CD21) in Human B Lymphocytes: Activation of Phosphatidylinositol 3-Kinase via a CD19-Independent Pathway. Journal of Immunology 1999;162(1):136-43.

161. Frade R, Gauffre A, Hermann J, Barel M. EBV/C3d receptor (CR2) interacts by its intracytoplasmic carboxy- terminal domain and two distinct binding sites with the p53 anti- oncoprotein and the p68 calcium-binding protein. Journal of Immunology 1992;149(10):3232-8.

162. Barel M, Balbo M, Gauffre A, Frade R. Binding sites of the Epstein-Barr virus and C3d receptor (CR2, CD21) for its three intracellular ligands, the p53 anti-oncoprotein, the p68 calcium binding protein and the nuclear p120 ribonucleoprotein. Molecular Immunology 1995;32(6):389-97.

163. Bradbury LE, Kansas GS, Levy S, Evans RL, Tedder TF. The CD19/CD21 signal transducing complex of human B lymphocytes includes the target of antiproliferative antibody-1 and Leu-13 molecules. Journal of Immunology 1992;149(9):2841-50.

164. Bradbury LE, Goldmacher VS, Tedder TF. The CD19 signal transduction complex of B lymphocytes. Deletion of the CD19 cytoplasmic domain alters signal transduction but not complex formation with TAPA-1 and Leu 13. Journal of Immunology 1993;151(6):2915-27.

165. Henson SE, Smith D, Boackle SA, Holers VM, Karp DR. Generation of recombinant human C3dg tetramers for the analysis of CD21 binding and function. Journal of Immunological Methods 2001;258(1-2):97-109.

166. Rickert RC. Regulation of B lymphocyte activation by complement C3 and the B cell coreceptor complex. Current Opinion in Immunology 2005;17(3):237-43.

167. Cherukuri A, Cheng PC, Sohn HW, Pierce SK. The CD19/CD21 complex functions to prolong B cell antigen receptor signaling from lipid rafts. Immunity 2001;14(2):169-79.

168. Cambier JC, Pleiman CM, Clark MR. Signal Transduction by the B Cell Antigen Receptor and its Coreceptors. Annual Review of Immunology 1994;12(1):457-86.

169. Rickert RC, Rajewsky K, Roes J. Impairment of T-cell-dependent B-cell responses and B-l cell development in CD19-deficient mice. Nature 1995;376(6538):352-55.

170. Boackle SA. Complement and autoimmunity. Biomedicine & Pharmacotherapy 2003;57(7):269-73.

171. Marchbank KJ, Watson CC, Ritsema DF, Holers VM. Expression of human complement receptor 2 (CR2, CD21) in Cr2-/- mice restores humoral immune function. Journal of Immunology 2000;165(5):2354-61.

172. Marchbank KJ, Kulik L, Gipson MG, Morgan BP, Holers VM. Expression of human complement receptor type 2 (CD21) in mice during early B cell development results in a reduction in mature B cells and hypogammaglobulinemia. Journal of Immunology 2002;169(7):3526-35.

173. Sato S, Steeber DA, Jansen PJ, Tedder TF. CD19 expression levels regulate B lymphocyte development: human CD19 restores normal function in mice lacking endogenous CD19. Journal of Immunology 1997;158(10):4662-9.

174. Molina H, Kinoshita T, Inoue K, Carel J, Holers V. A molecular and immunochemical characterization of mouse CR2. Evidence for a single gene model of mouse complement receptors 1 and 2. Journal of Immunology 1990;145(9):2974-83.

175. Kurtz C, O'Toole E, Christensen S, Weis J. The murine complement receptor gene family. IV. Alternative splicing of Cr2 gene transcripts predicts two distinct gene products that share homologous domains with both human CR2 and CR1. Journal of Immunology 1990;144(9):3581-91.

176. Fingeroth JD, Benedict MA, Levy DN, Strominger JL. Identification of Murine Complement Receptor Type 2. Proceedings of the National Academy of Sciences of the United States of America 1989;86(1):242-6.

177. Krop I, Shaffer A, Fearon D, Schlissel M. The signaling activity of murine CD19 is regulated during cell development. Journal of Immunology 1996;157(1):48-56.

178. Molina H, Brenner C, Jacobi S, Gorka J, Carel J, Kinoshita T, et al. Analysis of Epstein-Barr virus-binding sites on complement receptor 2 (CR2/CD21) using human-mouse chimeras and peptides. At least two distinct sites are necessary for ligand-receptor interaction. Journal of Biological Chemistry 1991;266(19):12173-9.

179. Hebell T, Ahearn J, Fearon D. Suppression of the immune response by a soluble complement receptor of B lymphocytes. Science 1991;254(5028):102-5.

180. Molina H, Holers VM, Li B, Fung Y, Mariathasan S, Goellner J, et al. Markedly impaired humoral immune response in mice deficient in complement receptors 1 and 2. Proceedings of the National Academy of Sciences of the United States of America 1996;93(8):3357-61.

181. Fang Y, Xu C, Fu YX, Holers VM, Molina H. Expression of complement receptors 1 and 2 on follicular dendritic cells is necessary for the generation of a strong antigen-specific IgG response. Journal of Immunology 1998;160(11):5273-9.

182. Chen Z, Koralov SB, Gendelman M, Carroll MC, Kelsoe G. Humoral Immune Responses in Cr2-/- Mice: Enhanced Affinity Maturation but Impaired Antibody Persistence. Journal of Immunology 2000;164(9):4522-32.

183. Croix D, Ahearn J, Rosengard A, Han S, Kelsoe G, Ma M, et al. Antibody response to a T-dependent antigen requires B cell expression of complement receptors. Journal of Experimental Medicine 1996;183(4):1857-64.

184. Roberts T, Snow EC. Cutting edge: recruitment of the CD19/CD21 coreceptor to B cell antigen receptor is required for antigen-mediated expression of Bcl-2 by resting and cycling hen egg lysozyme transgenic B cells. Journal of Immunology 1999;162(8):4377-80.

185. Kozono Y, Duke RC, Schleicher MS, Holers VM. Co-ligation of mouse complement receptors 1 and 2 with surface IgM rescues splenic B cells and WEHI-231 cells from anti-surface IgM-induced apoptosis. European Journal of Immunology 1995;25(4):1013-7.

186. Klaus GG, Humphrey JH. The generation of memory cells. I. The role of C3 in the generation of B memory cells. Immunology 1977;33(1):31-40.

187. Schreiber RD, Pangburn MK, Müller-Eberhard HJ. C3 modified at the thiolester site: acquisition of reactivity with cellular C3b receptors. Bioscience Reports 1981;1(11):873-80.

188. Guthridge JM, Rakstang JK, Young KA, Hinshelwood J, Aslam M, Robertson A, et al. Structural studies in solution of the recombinant N-terminal pair of short consensus/complement repeat domains of complement receptor type 2 (CR2/CD21) and interactions with its ligand C3dg. Biochemistry 2001;40(20):5931-41.

189. Lambris JD, Ganu VS, Hirani S, Müller-Eberhard HJ. Mapping of the C3d receptor (CR2)-binding site and a neoantigenic site in the C3d domain of the third component of complement. Proceedings of the National Academy of Sciences of the United States of America 1985;82(12):4235-9.

190. Pepys MB, Taussig MJ. Complement-independence of tolerance induction. European Journal of Immunology 1974;4(5):349-52.

191. Pepys MB, Butterworth AE. Inhibition by C3 fragments of C3-dependent rosette formation and antigen-induced lymphocyte transformation. Clinical and Experimental Immunology 1974;18(2):273-82.

192. Pepys MB. Complement-mediated mixed aggregation of murine spleen cells. Nature 1974;249(452):51-3.

193. Pepys MB. Role of complement in induction of antibody production in vivo. Effect of cobra factor and other C3-reactive agents on thymus-dependent and thymus-independent antibody responses. Journal of Experimental Medicine 1974;140(1):126-45.

194. Feldmann M, Pepys MB. Role of C3 in in vitro lymphocyte cooperation. Nature 1974;249(453):159-61.

195. Papamichail M, Pepys MB. Lymphocyte binding of fluid phase mouse C3b. Immunology 1979;36(3):461-70.

196. Pepys MB. Studies in vivo of cobra factor and murine C3. Immunology 1975;28(2):369-77.

197. Walport MJ. Complement. First of two parts. New England Journal of Medicine 2001;344(14):1058-66.

198. Lamping N, Schumann RR, Burger R. Detection of two variants of complement component C3 in C3-deficient guinea pigs distinguished by the absence and presence of a thiolester. Molecular Immunology 2000;37(7):333-41.

199. O'Neil K, Ochs H, Heller S, Cork L, Morris J, Winkelstein J. Role of C3 in humoral immunity. Defective antibody production in C3- deficient dogs. Journal of Immunology 1988;140(6):1939-45.

200. Wessels M, Butko P, Ma M, Warren H, Lage A, Carroll M. Studies of Group B Streptococcal Infection in Mice Deficient in Complement Component C3 or C4 Demonstrate an Essential Role for Complement in both Innate and Acquired Immunity. Proceedings of the National Academy of Sciences of the United States of America 1995;92(25):11490-4.

201. Diefenbach RJ, Isenman DE. Mutation of residues in the C3dg region of human complement component C3 corresponding to a proposed binding site for complement receptor type 2 (CR2, CD21) does not abolish binding of iC3b or C3dg to CR2. Journal of Immunology 1995;154(5):2303-20.

202. Nemerow GR, Wolfert R, McNaughton ME, Cooper NR. Identification and characterization of the Epstein-Barr virus receptor on human B lymphocytes and its relationship to the C3d complement receptor (CR2). Journal of Virology 1985;55(2):347-51.

203. Molina H, Perkins SJ, Guthridge J, Gorka J, Kinoshita T, Holers VM. Characterization of a complement receptor 2 (CR2, CD21) ligand binding site for C3. An initial model of ligand interaction with two linked short consensus repeat modules. Journal of Immunology 1995;154(10):5426-35.

204. Sarrias MR, Franchini S, Canziani G, Argyropoulos E, Moore WT, Sahu A, et al. Kinetic Analysis of the Interactions of Complement Receptor 2 (CR2, CD21) with Its Ligands C3d, iC3b, and the EBV Glycoprotein gp350/220. Journal of Immunology 2001;167(3):1490-99.

205. Thornton BP, Vetvicka V, Ross GD. Function of C3 in a humoral response: iC3b/C3dg bound to an immune complex generated with natural antibody and a primary antigen promotes antigen uptake and the expression of co-stimulatory molecules by all B cells, but only stimulates immunoglobulin synthesis by antigen-specific B cells. Clinical and Experimental Immunology 1996;104(3):531-7.

206. Tedder T, Goldmacher V, Lambert J, Schlossman S. Epstein Barr virus binding induces internalization of the C3d receptor: a novel immunotoxin delivery system. Journal of Immunology 1986;137(4):1387-91.

207. Carter RH, Fearon DT. Polymeric C3dg primes human B lymphocytes for proliferation induced by anti-IgM. Journal of Immunology 1989;143(6):1755-60.

208. DeFranco AL. Structure and Function of the B Cell Antigen Receptor. Annual Review of Cell Biology 1993;9(1):377-410.

209. Prechl J, Baiu DC, Horvath A, Erdei A. Modeling the presentation of C3d-coated antigen by B lymphocytes: enhancement by CR1/2-BCR co-ligation is selective for the co-ligating antigen. International Immunology 2002;14(3):241-7.

210. Thornton B, Vetvicka V, Ross G. Natural antibody and complement-mediated antigen processing and presentation by B lymphocytes. Journal of Immunology 1994;152(4):1727-37.

211. Arvieux J, Yssel H, Colomb MG. Antigen-bound C3b and C4b enhance antigen-presenting cell function in activation of human T-cell clones. Immunology 1988;65(2):229-35.

212. Kozono Y, Abe R, Kozono H, Kelly RG, Azuma T, Holers VM. Cross-Linking CD21/CD35 or CD19 Increases Both B7-1 and B7-2 Expression on Murine Splenic B Cells. Journal of Immunology 1998;160(4):1565-72.

213. Cherukuri A, Cheng PC, Pierce SK. The Role of the CD19/CD21 Complex in B Cell Processing and Presentation of Complement-Tagged Antigens. Journal of Immunology 2001;167(1):163-72.

214. Santoro L, Drouet C, Reboul A, Mach JP, Colomb MG. Covalent binding of C3b to monoclonal antibodies selectively up-regulates heavy chain epitope recognition by T cells. European Journal of Immunology 1994;24(7):1620-6.

215. Pozdnyakova O, Guttormsen HK, Lalani FN, Carroll MC, Kasper DL. Impaired antibody response to group B streptococcal type III capsular polysaccharide in C3- and complement receptor 2-deficient mice. Journal of Immunology 2003;170(1):84-90.

216. Carter RH, Spycher MO, Ng YC, Hoffman R, Fearon DT. Synergistic interaction between complement receptor type 2 and membrane IgM on B lymphocytes. Journal of Immunology 1988;141(2):457-63.

217. Erdei A, Melchers F, Schulz T, Dierich M. The action of human C3 in soluble or cross-linked form with resting and activated murine B lymphocytes. European Journal of Immunology 1985;15(2):184-8.

218. Dempsey PW, Allison ME, Akkaraju S, Goodnow CC, Fearon DT. C3d of complement as a molecular adjuvant: bridging innate and acquired immunity. Science 1996;271(5247):348-50.

219. Tedder TF, Haas KM, Poe JC. CD19-CD21 complex regulates an intrinsic Src family kinase amplification loop that links innate immunity with B-lymphocyte intracellular calcium responses. Biochemical Society Transactions 2002;30:807-11.

220. Fearon DT. The complement system and adaptive immunity. Seminars in Immunology 1998;10(5):355-61.

221. Birrell L, Kulik L, Morgan BP, Holers VM, Marchbank KJ. B Cells from Mice Prematurely Expressing Human Complement Receptor Type 2 Are Unresponsive to T-Dependent Antigens. Journal of Immunology 2005;174(11):6974-82.

222. Griffioen AW, Rijkers GT, Janssens-Korpela P, Zegers BJ. Pneumococcal polysaccharides complexed with C3d bind to human B lymphocytes via complement receptor type 2. Infection and Immunity 1991;59(5):1839-45.

223. Bohnsack JF, Cooper NR. CR2 ligands modulate human B cell activation. Journal of Immunology 1988;141(8):2569-76.

224. Tsokos G, Lambris J, Finkelman F, Anastassiou E, June C. Monovalent ligands of complement receptor 2 inhibit whereas polyvalent ligands enhance anti-Ig-induced human B cell intracytoplasmic free calcium concentration. Journal of Immunology 1990;144(5):1640-45.

225. Hilleman MR. Six decades of vaccine development--a personal history. Nature Medicine 1998;4(5 Suppl):507-14.

226. McGhee JR, Mestecky J, Dertzbaugh MT, Eldridge JH, Hirasawa M, Kiyono H. The mucosal immune system: from fundamental concepts to vaccine development. Vaccine 1992;10(2):75-88.

227. Wang J, Murakami T, Yoshida S, Matsuoka H, Ishii A, Tanaka T, et al. Predominant cell-mediated immunity in the oral mucosa: gene gun-based vaccination against infectious diseases. Journal of Dermatological Science 2003;31(3):203-10.

228. Ban EM, van Ginkel FW, Simecka JW, Kiyono H, Robinson HL, McGhee JR. Mucosal immunization with DNA encoding influenza hemagglutinin. Vaccine. International Meeting on Nucleic Acid Vaccines for the Prevention of Infectious Diseases 1997;15(8):811-3.

229. Wang B, Dang K, Agadjanyan MG, Srikantans V, Li F, Ugen KE, et al. Mucosal immunization with a DNA vaccine induces immune responses against HIV-1 at a mucosal site. Vaccine. International Meeting on Nucleic Acid Vaccines for the Prevention of Infectious Diseases 1997;15(8):821-5.

230. Shedlock DJ, Weiner DB. DNA vaccination: antigen presentation and the induction of immunity. Journal of Leukocyte Biology 2000;68(6):793-806.

231. Donnelly JJ, Ulmer JB, Liu MA. DNA vaccines. Developments in Biological Standardization 1998;95:43-53.

232. Hedstrom RC, Doolan DL, Wang RB, Gardner MJ, Kumar A, Sedegah M, et al. The development of a multivalent DNA vaccine for malaria. Springer Seminars in Immunopathology 1997;19(2):147-59.

233. Stasney J, Cantarow A, Paschkis KE. Production of Neoplasms by Injection of Fractions of Mammalian Neoplasms. Cancer Research 1950;10(12):775-82.

234. Dubensky TW, Campbell BA, Villarreal LP. Direct Transfection of Viral and Plasmid DNA into the Liver or Spleen of Mice. Proceedings of the National Academy of Sciences of the United States of America 1984;81(23):7529-33.

235. Will H, Cattaneo R, Koch H-G, Darai G, Schaller H, Schellekens H, et al. Cloned HBV DNA causes hepatitis in chimpanzees. Nature 1982;299(5885):740-2.

236. Wolff JA, Malone RW, Williams P, Chong W, Acsadi G, Jani A, et al. Direct Gene-Transfer into Mouse Muscle Invivo. Science 1990;247(4949):1465-8.

237. Tang D-c, DeVit M, Johnston SA. Genetic immunization is a simple method for eliciting an immune response. Nature 1992;356(6365):152-4.

238. Fynan E, Webster R, Fuller D, Haynes J, Santoro J, Robinson H. DNA Vaccines: Protective Immunizations by Parenteral, Mucosal, and Gene-Gun Inoculations. Proceedings of the National Academy of Sciences of the United States of America 1993;90(24):11478-82.

239. Yang N, Burkholder J, Roberts B, Martinell B, McCabe D. In vivo and in vitro Gene Transfer to Mammalian Somatic Cells by Particle Bombardment. Proceedings of the National Academy of Sciences of the United States of America 1990;87(24):9568-72.

240. Williams R, Johnston S, Riedy M, DeVit M, McElligott S, Sanford J. Introduction of Foreign Genes into Tissues of Living Mice by DNA-Coated Microprojectiles. Proceedings of the National Academy of Sciences of the United States of America 1991;88(7):2726-30.

241. Gurunathan S, Klinman DM, Seder RA. DNA vaccines: immunology, application, and optimization. Annual Review of Immunology 2000;18:927-74.

242. Klinman DM, Takeno M, Ichino M, Gu ML, Yamshchikov G, Mor G, et al. DNA vaccines: safety and efficacy issues. Springer Seminars in Immunopathology 1997;19(2):245-56.

243. Donnelly J, Berry K, Ulmer JB. Technical and regulatory hurdles for DNA vaccines. International Journal for Parasitology 2003;33(5-6):457-67.

244. Smith HA, Klinman DM. The regulation of DNA vaccines. Current Opinion in Biotechnology 2001;12(3):299-303.

245. EMEA. Note for quality, preclinical, and clinical aspects of gene transfer mediated medicinal products. www.emea.europa.eu/pdfs/human/bwp/308899en.pdf: The European Agency for the Evaluation of Medicinal Products; 2001.

246. Thompson L. Human Gene Therapy - Harsh Lessons, High Hopes. FDA Consumer magazine 2000.

247. Corr M, Tighe H. Plasmid DNA vaccination: mechanism of antigen presentation. Springer Seminars in Immunopathology 1997;19(2):139-45.

248. Gilkeson GS, Pritchard AJ, Pisetsky DS. Specificity of anti-DNA antibodies induced in normal mice by immunization with bacterial DNA. Clinical Immunology and Immunopathology 1991;59(2):288-300.

249. Rainczuk A, Smooker PM, Kedzierski L, Black CG, Coppel RL, Spithill TW. The protective efficacy of MSP4/5 against lethal Plasmodium chabaudi adami challenge is dependent on the type of DNA vaccine vector and vaccination protocol. Vaccine 2003;21(21-22):3030-42.

250. Belperron AA, Feltquate D, Fox BA, Horii T, Bzik DJ. Immune responses induced by gene gun or intramuscular injection of DNA vaccines that express immunogenic regions of the serine repeat antigen from Plasmodium falciparum. Infection and Immunity 1999;67(10):5163-9.

251. Leitner WW, Seguin MC, Ballou WR, Seitz JP, Schultz AM, Sheehy MJ, et al. Immune responses induced by intramuscular or gene gun injection of protective deoxyribonucleic acid vaccines that express the circumsporozoite protein from Plasmodium berghei malaria parasites. Journal of Immunology 1997;159(12):6112-9.

252. Mitchell JA, Green TD, Bright RA, Ross TM. Induction of heterosubtypic immunity to influenza A virus using a DNA vaccine expressing hemagglutinin-C3d fusion proteins. Vaccine 2003;21(9-10):902-14.

253. Green TD, Montefiori DC, Ross TM. Enhancement of antibodies to the human immunodeficiency virus type 1 envelope by using the molecular adjuvant C3d. Journal of Virology 2003;77(3):2046-55.

254. Green TD, Newton BR, Rota PA, Xu Y, Robinson HL, Ross TM. C3d enhancement of neutralizing antibodies to measles hemagglutinin. Vaccine 2001;20(1-2):242-8.

255. Ross TM, Xu Y, Green TD, Montefiori DC, Robinson HL. Enhanced avidity maturation of antibody to human immunodeficiency virus envelope: DNA vaccination with gp120-C3d fusion proteins. AIDS Research and Human Retroviruses 2001;17(9):829-35.

256. Ross TM, Xu Y, Bright RA, Robinson HL. C3d enhancement of antibodies to hemagglutinin accelerates protection against influenza virus challenge. Nature Immunology 2000;1(2):127-31.

257. Scheiblhofer S, Chen D, Weiss R, Khan F, Mostbock S, Fegeding K, et al. Removal of the circumsporozoite protein (CSP) glycosylphosphatidylinositol signal sequence from a CSP DNA vaccine enhances induction of CSP-specific Th2 type immune responses and improvesprotection against malaria infection. European Journal of Immunology 2001;31(3):692-8.

258. Wang J, Murakami T, Hakamata Y, Ajiki T, Jinbu Y, Akasaka Y, et al. Gene gun-mediated oral mucosal transfer of interleukin 12 cDNA coupled with an irradiated melanoma vaccine in a hamster model: successful treatment of oral melanoma and distant skin lesion. Cancer Gene Therapy 2001;8(10):705-12.

259. Yoshida S, Kashiwamura SI, Hosoya Y, Luo E, Matsuoka H, Ishii A, et al. Direct immunization of malaria DNA vaccine into the liver by gene gun protects against lethal challenge of Plasmodium berghei sporozoite. Biochemical and Biophysical Research Communications 2000;271(1):107-15.

260. Wang L, Kedzierski L, Wesselingh SL, Coppel RL. Oral immunization with a recombinant malaria protein induces conformational antibodies and protects mice against lethal malaria. Infection and Immunity 2003;71(5):2356-64.

261. Peachman KK, Rao M, Alving CR. Immunization with DNA through the skin. Methods 2003;31(3):232-42.

262. Cui Z, Mumper RJ. Microparticles and nanoparticles as delivery systems for DNA vaccines. Critical Reviews in Therapeutic Drug Carrier Systems 2003;20(2-3):103-37.

263. Koide Y, Nagata T, Yoshida A, Uchijima M. DNA vaccines. Japanese Journal of Pharmacology 2000;83(3):167-74.

264. Torres C, Iwasaki A, Barber B, Robinson H. Differential dependence on target site tissue for gene gun and intramuscular DNA immunizations. Journal of Immunology 1997;158(10):4529-32.

265. Doria-Rose NA, Haigwood NL. DNA vaccine strategies: candidates for immune modulation and immunization regimens. Methods 2003;31(3):207-16.

266. Zhu M, Xu X, Liu H, Liu X, Wang S, Dong F, et al. Enhancement of DNA vaccine potency against herpes simplex virus 1 by co-administration of an interleukin-18 expression plasmid as a genetic adjuvant. Journal of Medical Microbiology 2003;52(Pt 3):223-8.

267. Siegrist CA. Neonatal and early life vaccinology. Vaccine 2001;19(25-26):3331-46.

268. Prather KJ, Sagar S, Murphy J, Chartrain M. Industrial scale production of plasmid DNA for vaccine and gene therapy: plasmid design, production, and purification. Enzyme and Microbial Technology 2003;33(7):865-83.

269. MacGregor RR, Boyer JD, Ugen KE, Lacy KE, Gluckman SJ, Bagarazzi ML, et al. First human trial of a DNA-based vaccine for treatment of human immunodeficiency virus type 1 infection: Safety and host response. Journal of Infectious Diseases 1998;178(1):92-100.

270. Lowrie DB, Silva CL, Tascon RE. Genetic vaccination against tuberculosis. Springer Seminars in Immunopathology 1997;19(2):161-73.

271. Kim JJ, Weiner DB. DNA gene vaccination for HIV. Springer Seminars in Immunopathology 1997;19(2):175-94.

272. Roman M, Spiegelberg HL, Broide D, Raz E. Gene immunization for allergic disorders. Springer Seminars in Immunopathology 1997;19(2):223-32.

273. Krieg AM. The role of CpG motifs in innate immunity. Current Opinion in Immunology 2000;12(1):35-43.

274. Krieg AM, Yi A-K, Hartmann G. Mechanisms and therapeutic applications of immune stimulatory CpG DNA. Pharmacology & Therapeutics 1999;84(2):113-20.

275. Chu RS, Targoni OS, Krieg AM, Lehmann PV, Harding CV. CpG oligodeoxynucleotides act as adjuvants that switch on T helper 1 (Th1) immunity. Journal of Experimental Medicine 1997;186(10):1623-31.

276. Krieg AM, Yi A-K, Matson S, Waldschmidt TJ, Bishop GA, Teasdale R, et al. CpG motifs in bacterial DNA trigger direct B-cell activation. Nature 1995;374(6522):546-9.

277. Hemmi H, Takeuchi O, Kawai T, Kaisho T, Sato S, Sanjo H, et al. A Toll-like receptor recognizes bacterial DNA. Nature 2000;408(6813):740-5.

278. Vogel FR. Improving vaccine performance with adjuvants. Clinical Infectious Diseases 2000;30 Suppl 3:S266-70.

279. O'Hagan DT, MacKichan ML, Singh M. Recent developments in adjuvants for vaccines against infectious diseases. Biomolecular Engineering 2001;18(3):69-85.

280. Marciani DJ. Vaccine adjuvants: role and mechanisms of action in vaccine immunogenicity. Drug Discovery Today 2003;8(20):934-43.

281. Chang JCC, Diveley JP, Savary JR, Jensen FC. Adjuvant activity of incomplete Freund's adjuvant. Advanced Drug Delivery Reviews 1998;32(3):173-86.

282. Baylor NW, Egan W, Richman P. Aluminum salts in vaccines--US perspective. Vaccine 2002;20 Suppl 3:S18-23.

283. Allison AC. The mode of action of immunological adjuvants. In: Modulation of the Immune Response to Vaccine Antigens; 1998. p. 3-11.

284. Alving CR. Design and selection of vaccine adjuvants: animal models and human trials. Vaccine 2002;20:S56-S64.

285. Vogel FR, Powell MF, Alving CR. A Compendium of Vaccine Adjuvants and Excipients (2nd Edition).

286. Cox JC, Coulter AR. Adjuvants--a classification and review of their modes of action. Vaccine 1997;15(3):248-56.

287. Bird AP. DNA methylation and the frequency of CpG in animal DNA. Nucleic Acids Research 1980;8(7):1499-504.

288. Dittmer U, Olbrich AR. Treatment of infectious diseases with immunostimulatory oligodeoxynucleotides containing CpG motifs. Current Opinion in Microbiology 2003;6(5):472-7.

289. Messina J, Gilkeson G, Pisetsky D. Stimulation of in vitro murine lymphocyte proliferation by bacterial DNA. Journal of Immunology 1991;147(6):1759-1764.

290. Krieg AM, Yi AK, Schorr J, Davis HL. The role of CpG dinucleotides in DNA vaccines. Trends in Microbiology 1998;6(1):23-7.

291. Takeda K, Akira S. Toll-like receptors in innate immunity. International Immunology 2005;17(1):1-14.

292. Ahmad-Nejad P, Hacker H, Rutz M, Bauer S, Vabulas RM, Wagner H. Bacterial CpG-DNA and lipopolysaccharides activate Toll-like receptors at distinct cellular compartments. European Journal of Immunology 2002;32(7):1958-68.

293. Zimmermann S, Egeter O, Hausmann S, Lipford GB, Rocken M, Wagner H, et al. CpG oligodeoxynucleotides trigger protective and curative Th1 responses in lethal murine leishmaniasis. Journal of Immunology 1998;160(8):3627-30.

294. Su Z, Tam MF, Jankovic D, Stevenson MM. Vaccination with novel immunostimulatory adjuvants against blood-stage malaria in mice. Infection and Immunity 2003;71(9):5178-87.

295. Jones TR, Obaldia N, 3rd, Gramzinski RA, Charoenvit Y, Kolodny N, Kitov S, et al. Synthetic oligodeoxynucleotides containing CpG motifs enhance immunogenicity of a peptide malaria vaccine in Aotus monkeys. Vaccine 1999;17(23-24):3065-71.

296. Watanabe I, Ross TM, Tamura S, Ichinohe T, Ito S, Takahashi H, et al. Protection against influenza virus infection by intranasal administration of C3d-fused hemagglutinin. Vaccine 2003;21(31):4532-8.

297. Test ST, Mitsuyoshi J, Connolly CC, Lucas AH. Increased immunogenicity and induction of class switching by conjugation of complement C3d to pneumococcal serotype 14 capsular polysaccharide. Infection and Immunity 2001;69(5):3031-40.

298. Lou D, Kohler H. Enhanced molecular mimicry of CEA using photoaffinity crosslinked C3d peptide. Nature Biotechnology 1998;16(5):458-62.

299. Suradhat S, Braun RP, Lewis PJ, Babiuk LA, van Drunen Littel-van den Hurk S, Griebel PJ, et al. Fusion of C3d molecule with bovine rotavirus VP7 or bovine herpesvirus type 1 glycoprotein D inhibits immune responses following DNA immunization. Veterinary Immunology and Immunopathology 2001;83(1-2):79-92.

300. Wang L, Sunyer JO, Bello LJ. Fusion to C3d enhances the immunogenicity of the E2 glycoprotein of type 2 bovine viral diarrhea virus. Journal of Virology 2004;78(4):1616-22.

301. Newman J, Rice JS, Wang C, Harris SL, Diamond B. Identification of an antigen-specific B cell population. Journal of Immunological Methods 2003;272(1-2):177-87.

302. Villiers MB, Marche PN, Villiers CL. Improvement of long-lasting response and antibody affinity by the complexation of antigen with complement C3b. International Immunology 2003;15(1):91-5.

303. Pihlgren M, Fulurija A, Villiers M-B, Tougne C, Lambert P-H, Villiers CL, et al. Influence of complement C3 amount on IgG responses in early life: immunization with C3b-conjugated antigen increases murine neonatal antibody responses. Vaccine 2004;23(3):329-35.

304. Chatellier J, Hill F, Fersht AR. From minichaperone to GroEL 2: Importance of avidity of the multisite ring structure. Journal of Molecular Biology 2000;304(5):883-96.

305. Scharfstein J, Ferreira A, Gigli I, Nussenzweig V. Human C4-binding protein. I. Isolation and characterization. Journal of Experimental Medicine 1978;148(1):207-22.

306. Fujita T, Gigli I, Nussenzweig V. Human C4-binding protein. II. Role in proteolysis of C4b by C3b-inactivator. Journal of Experimental Medicine 1978;148(4):1044-51.

307. Criado-Garcia O, Fernaud-Espinosa I, Bovolenta P, Sainz de la Cuesta R, Rodriguez de Cordoba S. Expression of the beta-chain of the complement regulator C4b-binding protein in human ovary. European Journal of Cell Biology 1999;78(9):657-64.

308. Gigli I, Fujita T, Nussenzweig V. Modulation of the Classical Pathway C3 Convertase by Plasma Proteins C4 Binding Protein and C3b Inactivator. Proceedings of the National Academy of Sciences of the United States of America 1979;76(12):6596-600.

309. Dahlback B, Muller-Eberhard HJ. Ultrastructure of C4b-binding protein fragments formed by limited proteolysis using chymotrypsin. Journal of Biological Chemistry 1984;259(19):11631-4.

310. Villoutreix BO, Hardig Y, Wallqvist A, Covell DG, Garcia de Frutos P, Dahlback B. Structural investigation of C4b-binding protein by molecular modeling: localization of putative binding sites. Proteins 1998;31(4):391-405.

311. Kask L, Hillarp A, Ramesh B, Dahlback B, Blom AM. Structural requirements for the intracellular subunit polymerization of the complement inhibitor C4b-binding protein. Biochemistry 2002;41(30):9349-57.

312. Villoutreix BO, Blom AM, Webb J, Dahlback B. The complement regulator C4b-binding protein analyzed by molecular modeling, bioinformatics and computer-aided experimental design. Immunopharmacology 1999;42(1-3):121-34.

313. Hillarp A, Dahlback B. Novel subunit in C4b-binding protein required for protein S binding. Journal of Biological Chemistry 1988;263(25):12759-12764.

314. Libyh MT, Goossens D, Oudin S, Gupta N, Dervillez X, Juszczak G, et al. A recombinant human scFv anti-Rh(D) antibody with multiple valences using a C-terminal fragment of C4-binding protein. Blood 1997;90(10):3978-83.

315. Oudin S, Libyh MT, Goossens D, Dervillez X, Philbert F, Reveil B, et al. A soluble recombinant multimeric anti-Rh(D) single-chain Fv/CR1 molecule restores the immune complex binding ability of CR1-deficient erythrocytes. Journal of Immunology 2000;164(3):1505-13.

316. Christiansen D, Devaux P, Reveil B, Evlashev A, Horvat B, Lamy J, et al. Octamerization enables soluble CD46 receptor to neutralize measles virus in vitro and in vivo. Journal of Virology 2000;74(10):4672-8.

317. Phillips DC. The Hen Egg-White Lysozyme Molecule. Proceedings of the National Academy of Sciences of the United States of America 1967;57(3):484-93.

318. Atassi MZ, Lee CL. The precise and entire antigenic structure of native lysozyme. Biochemical Journal 1978;171(2):429-34.

319. Davies DR, Cohen GH. Interactions of protein antigens with antibodies. Proceedings of the National Academy of Sciences of the United States of America 1996;93(1):7-12.

320. Ibrahimi IM, Prager EM, White TJ, Wilson AC. Amino acid sequence of California quail lysozyme. Effect of evolutionary substitutions on the antigenic structure of lysozyme. Biochemistry 1979;18(13):2736-44.

321. Kumagai I, Sunada F, Takeda S, Miura K. Redesign of the substrate-binding site of hen egg white lysozyme based on the molecular evolution of C-type lysozymes. Journal of Biological Chemistry 1992;267(7):4608-12.

322. Schwalbe H, Grimshaw SB, Spencer A, Buck M, Boyd J, Dobson CM, et al. A refined solution structure of hen lysozyme determined using residual dipolar coupling data. Protein Science 2001;10(4):677-88.

323. Gengoux C, Leclerc C. In vivo induction of CD4+ T cell responses by antigens covalently linked to synthetic microspheres does not require adjuvant. International Immunology 1995;7(1):45-53.

324. Baca-Estrada ME, Ewen C, Mahony D, Babiuk LA, Wilkie D, Foldvari M. The haemopoietic growth factor, Flt3L, alters the immune response induced by transcutaneous immunization. Immunology 2002;107(1):69-76.

325. Unanue ER. Perspective on antigen processing and presentation. Immunological Reviews 2002;185:86-102.

326. Goodnow CC, Crosbie J, Adelstein S, Lavoie TB, Smith-Gill SJ, Brink RA, et al. Altered immunoglobulin expression and functional silencing of self-reactive B lymphocytes in transgenic mice. Nature 1988;334(6184):676-82.

327. Wang YQ, Krieg AM. Induction of autoantibody production but not autoimmune disease in HEL transgenic mice vaccinated with HEL in combination with CpG or control oligodeoxynucleotides. Vaccine 2004;22(20):2641-50.

328. Boussif O, Lezoualc'h F, Zanta MA, Mergny MD, Scherman D, Demeneix B, et al. A versatile vector for gene and oligonucleotide transfer into cells in culture and in vivo: polyethylenimine. Proceedings of the National Academy of Sciences of the United States of America 1995;92(16):7297-301.

329. Lambert RC, Maulet Y, Dupont JL, Mykita S, Craig P, Volsen S, et al. Polyethylenimine-mediated DNA transfection of peripheral and central neurons in primary culture: probing Ca2+ channel structure and function with antisense oligonucleotides. Molecular and Cellular Neurosciences 1996;7(3):239-46.

330. Laemmli UK. Cleavage of structural proteins during the assembly of the head of bacteriophage T4. Nature 1970;227(259):680-5.

331. Dunn SD. Effects of the modification of transfer buffer composition and the renaturation of proteins in gels on the recognition of proteins on Western blots by monoclonal antibodies. Analytical Biochemistry 1986;157(1):144-53.

332. Morrissey JH. Silver stain for proteins in polyacrylamide gels: a modified procedure with enhanced uniform sensitivity. Analytical Biochemistry 1981;117(2):307-10.

333. Isaac L, Aivazian D, Taniguchi-Sidle A, Ebanks RO, Farah CS, Florido MP, et al. Native conformations of human complement components C3 and C4 show different dependencies on thioester formation. Biochemical Journal 1998;329 (Pt 3):705-12.

334. Charreau B, Cassard A, Tesson L, Le Mauff B, Navenot JM, Blanchard D, et al. Protection of rat endothelial cells from primate complement-mediated lysis by expression of human CD59 and/or decay-accelerating factor. Transplantation 1994;58(11):1222-9.

335. Powell MB, Marchbank KJ, Rushmere NK, van den Berg CW, Morgan BP. Molecular cloning, chromosomal localization, expression, and functional characterization of the mouse analogue of human CD59. Journal of Immunology 1997;158(4):1692-702.

336. Meng YG, Liang J, Wong WL, Chisholm V. Green fluorescent protein as a second selectable marker for selection of high producing clones from transfected CHO cells. Gene 2000;242(1-2):201-207.

337. Barrault DV, Knight AM. Distinct Sequences in the Cytoplasmic Domain of Complement Receptor 2 Are Involved in Antigen Internalization and Presentation. Journal of Immunology 2004;172(6):3509-17.

338. Barrault DV, Steward M, Cox VF, Smith RAG, Knight AM. Efficient production of complement (C3d)3 fusion proteins using the baculovirus expression vector system. Journal of Immunological Methods 2005;304(1-2):158-73.

339. Asokan R, Hua J, Young KA, Gould HJ, Hannan JP, Kraus DM, et al. Characterization of Human Complement Receptor Type 2 (CR2/CD21) as a Receptor for IFN-{alpha}: A Potential Role in Systemic Lupus Erythematosus. Journal of Immunology 2006;177(1):383-94.

340. Fest S, Huebener N, Weixler S, Bleeke M, Zeng Y, Strandsby A, et al. Characterization of GD2 peptide mimotope DNA vaccines effective against spontaneous neuroblastoma metastases. Cancer Research 2006;66(21):10567-75.

341. Wang ZQ, Cui J, Wei HY, Han HM, Zhang HW, Li YL. Vaccination of mice with DNA vaccine induces the immune response and partial protection against T. spiralis infection. Vaccine 2006;24(8):1205-12.

342. Guo H, Wang X, Jiang G, Yang P. Construction of a sIgA-enhancing anti-Porphyromonas gingivalis FimA vaccine and nasal immunization in mice. Immunology Letters 2006;107(1):71-5.

343. Li DJ, Wang HM, Li L, Zhao XR, Wang MY, Zhu Y, et al. Gene fusion of molecular adjuvant C3d to hCGbeta enhances the anti-hCGbeta antibody response in DNA immunization. Journal of Reproductive Immunology 2003;60(2):129-41.

344. Puck TT, Cieciura SJ, Robinson A. Genetics of Somatic Mammalian Cells: III. Long-Term Cultivation of Euploid Cells from Human and Animal Subjects. Journal of Experimental Medicine 1958;108(6):945-56.

345. Hillarp A, Hessing M, Dahlback B. Protein S binding in relation to the subunit composition of human C4b-binding protein. FEBS Letters 1989;259(1):53-6.

346. Hillarp A, Dahlback B. Cloning of cDNA Coding for the {beta} Chain of Human Complement Component C4b-Binding Protein: Sequence Homology with the {alpha}-Chain. Proceedings of the National Academy of Sciences of the United States of America 1990;87(3):1183-7.

347. Dahlback B, Smith CA, Muller-Eberhard HJ. Visualization of Human C4b-Binding Protein and Its Complexes with Vitamin K-Dependent Protein S and Complement Protein C4b. Proceedings of the National Academy of Sciences of the United States of America 1983;80(11):3461-5.

348. Lee Y, Haas KM, Gor DO, Ding X, Karp DR, Greenspan NS, et al. Complement Component C3d-Antigen Complexes Can Either Augment or Inhibit B Lymphocyte Activation and Humoral Immunity in Mice Depending on the Degree of CD21/CD19 Complex Engagement. Journal of Immunology 2005;175(12):8011-23.

349. Prodinger WM, Schwendinger MG, Schoch J, Kochle M, Larcher C, Dierich MP. Characterization of C3dg binding to a recess formed between short consensus repeats 1 and 2 of complement receptor type 2 (CR2; CD21). Journal of Immunology 1998;161(9):4604-10.

350. Marquart HV, Olesen EH, Johnson AA, Damgaard G, Leslie RG. A comparative study of normal B cells and the EBV-positive Burkitt's lymphoma cell line, Raji, as activators of the complement system. Scandinavian Journal of Immunology 1997;46(3):246-53.

351. Becherer JD, Lambris JD. Identification of the C3b receptor-binding domain in third component of complement. Journal of Biological Chemistry 1988;263(28):14586-91.

352. Dodds AW, Sim RB. Complement - A Practical Approach. Oxford: IRL Press; 1997.

353. Lachmann PJ, Pangburn MK, Oldroyd RG. Breakdown of C3 after complement activation. Identification of a new fragment C3g, using monoclonal antibodies. Journal of Experimental Medicine 1982;156(1):205-16.

354. Davis AE, 3rd, Harrison RA, Lachmann PJ. Physiologic inactivation of fluid phase C3b: isolation and structural analysis of C3c, C3d,g (alpha 2D), and C3g. Journal of Immunology 1984;132(4):1960-6.

355. Henwick S, Hetherington SV, Hostetter MK. Specificity of three anti-complement factor 3 monoclonal antibodies. Journal of Immunological Methods 1992;153(1-2):173-84.

356. Harris CL, Williams AS, Linton SM, Morgan BP. Coupling complement regulators to immunoglobulin domains generates effective anti-complement reagents with extended half-life in vivo. Clinical & Experimental Immunology 2002;129(2):198-207.

357. Quigg RJ, Kozono Y, Berthiaume D, Lim A, Salant DJ, Weinfeld A, et al. Blockade of Antibody-Induced Glomerulonephritis with Crry-Ig, a Soluble Murine Complement Inhibitor. Journal of Immunology 1998;160(9):4553-60.

358. Harris CL, Hughes CE, Williams AS, Goodfellow I, Evans DJ, Caterson B, et al. Generation of Anti-complement "Prodrugs": Cleavable Reagents for Specific Delivery of Complement Regulators to Disease Sites. Journal of Biological Chemistry 2003;278(38):36068-76.

359. Harris CL, Spiller OB, Morgan BP. Human and rodent decay-accelerating factors (CD55) are not species restricted in their complement-inhibiting activities. Immunology 2000;100(4):462-70.

360. Atkinson C, Song H, Lu B, Qiao F, Burns TA, Holers VM, et al. Targeted complement inhibition by C3d recognition ameliorates tissue injury without apparent increase in susceptibility to infection. Journal of Clinical Investigation 2005;115(9):2444-53.

361. Mold C, Cooper N, Nemerow G. Incorporation of the purified Epstein Barr virus/C3d receptor (CR2) into liposomes and demonstration of its dual ligand binding functions. Journal of Immunology 1986;136(11):4140-5.

362. Lowell CA, Klickstein LB, Carter RH, Mitchell JA, Fearon DT, Ahearn JM. Mapping of the Epstein-Barr virus and C3dg binding sites to a common domain on complement receptor type 2. Journal of Experimental Medicine 1989;170(6):1931-46.

363. Gilbert HE, Asokan R, Holers VM, Perkins SJ. The 15 SCR flexible extracellular domains of human complement receptor type 2 can mediate multiple ligand and antigen interactions. Journal of Molecular Biology 2006;362(5):1132-47.

364. Epstein AL, Henle W, Henle G, Hewetson JF, Kaplan HS. Surface Marker Characteristics and Epstein-Barr Virus Studies of Two Established North American Burkitt's Lymphoma Cell Lines. Proceedings of the National Academy of Sciences of the United States of America 1976;73(1):228-32.

365. Lyubchenko T, Dal Porto J, Cambier JC, Holers VM. Coligation of the B Cell Receptor with Complement Receptor Type 2 (CR2/CD21) Using Its Natural Ligand C3dg: Activation without Engagement of an Inhibitory Signaling Pathway. Journal of Immunology 2005;174(6):3264-72.

366. Tanner J, Weis J, Fearon D, Whang Y, Kieff E. Epstein-Barr virus gp350/220 binding to the B lymphocyte C3d receptor mediates adsorption, capping, and endocytosis. Cell 1987;50(2):203-13.

367. Moore MD, DiScipio RG, Cooper NR, Nemerow GR. Hydrodynamic, electron microscopic, and ligand-binding analysis of the Epstein-Barr virus/C3dg receptor (CR2). Journal of Biological Chemistry 1989;264(34):20576-82.

368. Gilbert HE, Aslam M, Guthridge JM, Holers VM, Perkins SJ. Extended flexible linker structures in the complement chimaeric conjugate CR2-Ig by scattering, analytical ultracentrifugation and constrained modelling: implications for function and therapy. Journal of Molecular Biology 2006;356(2):397-412.

369. Tighe H, Corr M, Roman M, Raz E. Gene vaccination: plasmid DNA is more than just a blueprint. Immunology Today 1998;19(2):89-97.

370. Gregersen JP. DNA vaccines. Naturwissenschaften 2001;88(12):504-13.

371. Wang R, Doolan DL, Le TP, Hedstrom RC, Coonan KM, Charoenvit Y, et al. Induction of antigen-specific cytotoxic T lymphocytes in humans by a malaria DNA vaccine. Science 1998;282(5388):476-80.

372. Liu MA, Fu TM, Donnelly JJ, Caulfield MJ, Ulmer JB. DNA vaccines. Mechanisms for generation of immune responses. Advances in Experimental Medicine and Biology 1998;452:187-91.

373. Xiang ZQ, Pasquini S, He Z, Deng H, Wang Y, BlaszczykThurin MA, et al. Genetic vaccines - a revolution in vaccinology? Springer Seminars in Immunopathology 1997;19(2):257-68.

374. Liu MA. DNA vaccines: a review. Journal of Internal Medicine 2003;253(4):402-10.

375. Tuteja R. DNA vaccine against malaria: a long way to go. Critical Reviews Biochemistry and Molecular Biology 2002;37(1):29-54.

376. Fomsgaard A. HIV-1 DNA vaccines. Immunology Letters 1999;65(1-2):127-31.

377. Hartl A, Weiss R, Hochreiter R, Scheiblhofer S, Thalhamer J. DNA vaccines for allergy treatment. Methods 2004;32(3):328-39.

378. Roman M, Spiegelberg HL, Broide D, Raz E. Gene immunization for allergic disorders. Springer Seminars in Immunopathology 1997;19(2):223-32.

379. van de Poel RH, Meijers JC, Dahlb inverted question markck B, Bouma BN. C4b-binding protein (C4BP) beta-chain Short Consensus Repeat-2 specifically contributes to the interaction of C4BP with protein S. Blood Cells, Molecules and Diseases 1999;25(5-6):279-86.

380. Bower JF, Yang XZ, Sodroski J, Ross TM. Elicitation of neutralizing antibodies with DNA vaccines expressing soluble stabilized human immunodeficiency virus type 1 envelope glycoprotein trimers conjugated to C3d. Journal of Virology 2004;78(9):4710-19.

381. Steward M, Cox V, Oldroyd R, Gallagher S, Kareclas P, Ragnauth C, et al. Towards a human C3d-based vaccine for malaria. Molecular Immunology 2001;38(2-3):118.

382. Fan H, Tong T, Chen H, Guo A. Immunization of DNA vaccine encoding C3d-VP1 fusion enhanced protective immune response against foot-and-mouth disease virus. Virus Genes 2007.

383. Wang XL, Zhao XR, Yu M, Yuan MM, Yao XY, Li DJ. Gene conjugation of molecular adjuvant C3d3 to hCGbeta increased the anti-hCGbeta Th2 and humoral immune response in DNA immunization. Journal of Gene Medicine 2006;8(4):498-505.

384. Bower JF, Green TD, Ross TM. DNA vaccines expressing soluble CD4-envelope proteins fused to C3d elicit cross-reactive neutralizing antibodies to HIV-1. Virology 2004;328(2):292-300.

385. Mitsuyoshi JK, Hu Y, Test ST. Role of Complement Receptor Type 2 and Endogenous Complement in the Humoral Immune Response to Conjugates of Complement C3d and Pneumococcal Serotype 14 Capsular Polysaccharide. Infection and Immunity 2005;73(11):7311-6.

386. Yew NS, Przybylska M, Ziegler RJ, Liu D, Cheng SH. High and sustained transgene expression in vivo from plasmid vectors containing a hybrid ubiquitin promoter. Molecular Therapy 2001;4(1):75-82.

387. Bona C, Radu D, Kodera T. Molecular studies on the diversification of hemagglutinin--specific human neonatal repertoire subsequent to immunization with naked DNA. Vaccine 2004;22(13-14):1624-30.

388. Han S, Dillon SR, Zheng B, Shimoda M, Schlissel MS, Kelsoe G. V(D)J recombinase activity in a subset of germinal center B lymphocytes. Science 1997;278(5336):301-5.

389. McHeyzer-Williams LJ, Malherbe LP, McHeyzer-Williams MG. Checkpoints in memory B-cell evolution. Immunological Reviews 2006;211:255-68.

390. Smith KG, Hewitson TD, Nossal GJ, Tarlinton DM. The phenotype and fate of the antibody-forming cells of the splenic foci. European Journal of Immunology 1996;26(2):444-8.

391. Manz RA, Thiel A, Radbruch A. Lifetime of plasma cells in the bone marrow. Nature 1997;388(6638):133-4.

392. Slifka MK, Matloubian M, Ahmed R. Bone marrow is a major site of long-term antibody production after acute viral infection. Journal of Virology 1995;69(3):1895-902.

393. McHeyzer-Williams LJ, Cool M, McHeyzer-Williams MG. Antigen-specific B cell memory: expression and replenishment of a novel B220(-) memory b cell compartment. Journal of Experimental Medicine 2000;191(7):1149-66.

394. Ellyard JI, Avery DT, Phan TG, Hare NJ, Hodgkin PD, Tangye SG. Antigen-selected, immunoglobulin-secreting cells persist in human spleen and bone marrow. Blood 2004;103(10):3805-12.

395. Sawamura D, Abe R, Goto M, Akiyama M, Hemmi H, Akira S, et al. Direct injection of plasmid DNA into the skin induces dermatitis by activation of monocytes through toll-like receptor 9. Journal of Gene Medicine 2005;7(5):664-71.

396. Hodges BL, Taylor KM, Joseph MF, Bourgeois SA, Scheule RK. Long-term transgene expression from plasmid DNA gene therapy vectors is negatively affected by CpG dinucleotides. Molecular Therapy 2004;10(2):269-78.

397. Zarozinski CC, Fynan EF, Selin LK, Robinson HL, Welsh RM. Protective CTL-dependent immunity and enhanced immunopathology in mice immunized by particle bombardment with DNA encoding an internal virion protein. Journal of Immunology 1995;154(8):4010-7.

398. Toapanta FR, Ross TM. Mouse strain-dependent differences in enhancement of immune responses by C3d. Vaccine 2004;22(13-14):1773-81.

399. Tong T, Fan H, Tan Y, Xiao S, Ling J, Chen H, et al. C3d enhanced DNA vaccination induced humoral immune response to glycoprotein C of pseudorabies virus. Biochemical and Biophysical Research Communications 2006;347(4):845-51.

400. Moseman EA, Liang X, Dawson AJ, Panoskaltsis-Mortari A, Krieg AM, Liu Y-J, et al. Human Plasmacytoid Dendritic Cells Activated by CpG Oligodeoxynucleotides Induce the Generation of CD4+CD25+ Regulatory T Cells. Journal of Immunology 2004;173(7):4433-42.

401. Jakob T, Walker PS, Krieg AM, Udey MC, Vogel JC. Activation of cutaneous dendritic cells by CpG-containing oligodeoxynucleotides: a role for dendritic cells in the augmentation of Th1 responses by immunostimulatory DNA. Journal of Immunology 1998;161(6):3042-9.

402. Haas KM, Toapanta FR, Oliver JA, Poe JC, Weis JH, Karp DR, et al. Cutting Edge: C3d Functions as a Molecular Adjuvant in the Absence of CD21/35 Expression. Journal of Immunology 2004;172(10):5833-7.

403. Krieg AM. Therapeutic potential of Toll-like receptor 9 activation. Nature Reviews Drug Discovery 2006;5(6):471-84.

404. Liu L, Zhou X, Liu H, Xiang L, Yuan Z. CpG motif acts as a 'danger signal' and provides a T helper type 1-biased microenvironment for DNA vaccination. Immunology 2005;115(2):223-30.

405. Coban C, Ishii KJ, Gursel M, Klinman DM, Kumar N. Effect of plasmid backbone modification by different human CpG motifs on the immunogenicity of DNA vaccine vectors. Journal of Leukocyte Biology 2005;78(3):647-55.

406. Krieg AM. CpG oligonucleotides as immune adjuvants. Ernst Schering Res Found Workshop 2000(30):105-18.

407. Tudor D, Dubuquoy C, Gaboriau V, Lefevre F, Charley B, Riffault S. TLR9 pathway is involved in adjuvant effects of plasmid DNA-based vaccines. Vaccine 2005;23(10):1258-64.

408. Martin DR, Yuryev A, Kalli KR, Fearon DT, Ahearn JM. Determination of the structural basis for selective binding of Epstein-Barr virus to human complement receptor type 2. Journal of Experimental Medicine 1991;174(6):1299-311.

409. Padlan EA, Silverton EW, Sheriff S, Cohen GH, Smith-Gill SJ, Davies DR. Structure of an antibody-antigen complex: crystal structure of the HyHEL-10 Fab-lysozyme complex. Proceedings of the National Academy of Sciences of the United States of America 1989;86(15):5938-42.

410. Smith-Gill SJ, Wilson AC, Potter M, Prager EM, Feldmann RJ, Mainhart CR. Mapping the antigenic epitope for a monoclonal antibody against lysozyme. Journal of Immunology 1982;128(1):314-22.

411. Smith-Gill SJ, Mainhart C, Lavoie TB, Feldmann RJ, Drohan W, Brooks BR. A three-dimensional model of an anti-lysozyme antibody. Journal of Molecular Biology 1987;194(4):713-24.

412. ProImmune. MHC Class II Ultimers™ for detecting single antigen-specific CD4+ T cell responses. http://www.proimmune.com/ecommerce/page.php?page=class2; 2006.

413. Kumar S, Jones TR, Oakley MS, Zheng H, Kuppusamy SP, Taye A, et al. CpG oligodeoxynucleotide and Montanide ISA 51 adjuvant combination enhanced the protective efficacy of a subunit malaria vaccine. Infection and Immunity 2004;72(2):949-57.

414. Weiss R, Scheiblhofer S, Freund J, Ferreira F, Livey I, Thalhamer J. Gene gun bombardment with gold particles displays a particular Th2-promoting signal that over-rules the Th1-inducing effect of immunostimulatory CpG motifs in DNA vaccines. Vaccine 2002;20(25-26):3148-54.

415. Iwatsuki K, Yamasaki O, Morizane S, Oono T. Staphylococcal cutaneous infections: invasion, evasion and aggression. Journal of Dermatological Science 2006;42(3):203-14.

416. Hanzal-Bayer MF, Hancock JF. Lipid rafts and membrane traffic. FEBS Letters 2007;581(11):2098-104.

417. Bagley KC, Shata MT, Onyabe DY, DeVico AL, Fouts TR, Lewis GK, et al. Immunogenicity of DNA vaccines that direct the coincident expression of the 120 kDa glycoprotein of human immunodeficiency virus and the catalytic domain of cholera toxin. Vaccine 2003;21(23):3335-41.

418. Barouch DH, Santra S, Steenbeke TD, Zheng XX, Perry HC, Davies ME, et al. Augmentation and suppression of immune responses to an HIV-1 DNA vaccine by plasmid cytokine/Ig administration. Journal of Immunology 1998;161(4):1875-82.

419. Barouch DH, Santra S, Tenner-Racz K, Racz P, Kuroda MJ, Schmitz JE, et al. Potent CD4+ T cell responses elicited by a bicistronic HIV-1 DNA vaccine expressing gp120 and GM-CSF. Journal of Immunology 2002;168(2):562-8.

420. Rainczuk A, Scorza T, Spithill TW, Smooker PM. A bicistronic DNA vaccine containing apical membrane antigen 1 and merozoite surface protein 4/5 can prime humoral and cellular immune responses and partially protect mice against virulent Plasmodium chabaudi adami DS malaria. Infection and Immunity 2004;72(10):5565-73.

421. Wild J, Gruner B, Metzger K, Kuhrober A, Pudollek HP, Hauser H, et al. Polyvalent vaccination against hepatitis B surface and core antigen using a dicistronic expression plasmid. Vaccine 1998;16(4):353-60.

422. Bergmann-Leitner ES, Leitner WW, Tsokos GC. Complement 3d: From molecular adjuvant to target of immune escape mechanisms. Clinical Immunology 2006;121(2):177-85.

423. Gor DO, Ding X, Li Q, Greenspan NS. Genetic fusion of three tandem copies of murine C3d sequences to diphtheria toxin fragment B elicits a decreased fragment B-specific antibody response. Immunology Letters 2006;102(1).

424. Bergmann-Leitner ES, Scheiblhofer S, Weiss R, Duncan EH, Leitner WW, Chen D, et al. C3d binding to the circumsporozoite protein carboxy-terminus deviates immunity against malaria. International Immunology 2005;17(3):245-255.

425. Heyman B, Wiersma EJ, Kinoshita T. In vivo inhibition of the antibody response by a complement receptor-specific monoclonal antibody. Journal of Experimental Medicine 1990;172(2):665-8.

426. Gustavsson S, Kinoshita T, Heyman B. Antibodies to murine complement receptor 1 and 2 can inhibit the antibody response in vivo without inhibiting T helper cell induction. Journal of Immunology 1995;154(12):6524-8.

427. Chakravarty L, Zabel MD, Weis JJ, Weis JH. Depletion of Lyn kinase from the BCR complex and inhibition of B cell activation by excess CD21 ligation. International Immunology 2002;14(2):139-46.

428. Bennett M, Leanderson T. Was it there all the time? Scandinavian Journal of Immunology 2003;57(6):499-505.

429. Gilbert HE, Eaton JT, Hannan JP, Holers VM, Perkins SJ. Solution structure of the complex between CR2 SCR 1-2 and C3d of human complement: an X-ray scattering and sedimentation modelling study. Journal of Molecular Biology 2005;346(3):859-73.

430. Bower JF, Ross TM. A minimum CR2 binding domain of C3d enhances immunity following vaccination. Advances in Experimental Medicine and Biology 2006;586:249-64.

431. Moore ZS, Seward JF, Lane JM. Smallpox. The Lancet 2006;367(9508):425-435.

432. O'Hagan DT, Rappuoli R. The safety of vaccines. Drug Discovery Today 2004;9(19):846-54.

433. Yang ZY, Kong WP, Huang Y, Roberts A, Murphy BR, Subbarao K, et al. A DNA vaccine induces SARS coronavirus neutralization and protective immunity in mice. Nature 2004;428(6982):561-4.

434. WHO. DNA vaccines. http://www.who.int/biologicals/areas/vaccines/dna/en/; 2007.

435. WHO. Guidelines for assuring the quality and nonclinical safety evaluation of DNA vaccines, Annex 1. http://www.who.int/entity/biologicals/publications/ECBS%202005%20Annex%201%20DNA.pdf; 2005.

436. Hanke T, McMichael AJ, Dorrell L. Clinical experience with plasmid DNA- and modified vaccinia virus Ankara-vectored human immunodeficiency virus type 1 clade A vaccine focusing on T-cell induction. Journal of General Virology 2007;88:1-12.

437. Hokey DA, Weiner DB. DNA vaccines for HIV: challenges and opportunities. Springer Seminars in Immunopathology 2006;28(3):267-79.

438. Orme IM. Preclinical testing of new vaccines for tuberculosis: A comprehensive review. Vaccine 2006;24(1):2-19.

439. McMichael AJ. HIV vaccines. Annual Review of Immunology 2006;24:227-55.

440. NIH. Clinicaltrials.gov - Information on Clinical Trials and Human Research Studies. In: US National Institutes of Health.

441. Ulmer JB, Wahren B, Liu MA. Gene-based vaccines: recent technical and clinical advances. Trends in Molecular Medicine 2006;12(5):216-22.

442. Powell K. DNA vaccines - back in the saddle again? Nature Biotechnology 2004;22(7):799-801.

443. Lorenzen N, LaPatra SE. DNA vaccines for aquacultured fish. Revue Scientifique Et Technique-Office International Des Epizooties 2005;24(1):201-13.

444. Bins AD, Jorritsma A, Wolkers MC, Hung C-F, Wu T-C, Schumacher TNM, et al. A rapid and potent DNA vaccination strategy defined by in vivo monitoring of antigen expression. Nature Medicine 2005;11(8):899-904.

445. Soboll G, Hussey SB, Whalley JM, Allen GP, Koen MT, Santucci N, et al. Antibody and cellular immune responses following DNA vaccination and EHV-1 infection of ponies. Veterinary Immunology and Immunopathology 2006;111(1-2):81-95.

446. Dong XN, Chen YH. Marker vaccine strategies and candidate CSFV marker vaccines. Vaccine 2007;25(2):205-30.

447. Dumonteil E. DNA vaccines against protozoan parasites: Advances and challenges. Journal of Biomedicine and Biotechnology 2007:-.

448. Talbot BG, Lacasse P. Progress in the development of mastitis vaccines. Livestock Production Science 2005;98(1-2):101-13.

Epilogue

Faust. Habe nun, ach! Philosophie,
Juristerei und Medizin,
Und leider auch Theologie
Durchaus studiert, mit heißem Bemühn.
Da steh ich nun, ich armer Tor!
Und bin so klug als wie zuvor;
Heiße Magister, heiße Doktor gar
Und ziehe schon an die zehen Jahr
Herauf, herab und quer und krumm
Meine Schüler an der Nase herum-
Und sehe, daß wir nichts wissen können!
Das will mir schier das Herz verbrennen.
Zwar bin ich gescheiter als all die Laffen,
Doktoren, Magister, Schreiber und Pfaffen;
Mich plagen keine Skrupel noch Zweifel,
Fürchte mich weder vor Hölle noch Teufel-
Dafür ist mir auch alle Freud entrissen,
Bilde mir nicht ein, was Rechts zu wissen,
Bilde mir nicht ein, ich könnte was lehren,
Die Menschen zu bessern und zu bekehren.
Auch hab ich weder Gut noch Geld,
Noch Ehr und Herrlichkeit der Welt;
Es möchte kein Hund so länger leben!
Drum hab ich mich der Magie ergeben,
Ob mir durch Geistes Kraft und Mund
Nicht manch Geheimnis würde kund;
Daß ich nicht mehr mit saurem Schweiß
Zu sagen brauche, was ich nicht weiß;
Daß ich erkenne, was die Welt
Im Innersten zusammenhält,
Schau alle Wirkenskraft und Samen,
Und tu nicht mehr in Worten kramen.

O sähst du, voller Mondenschein,
Zum letzenmal auf meine Pein,
Den ich so manche Mitternacht
An diesem Pult herangewacht:
Dann über Büchern und Papier,
Trübsel'ger Freund, erschienst du mir!
Ach! könnt ich doch auf Bergeshöhn
In deinem lieben Lichte gehn,
Um Bergeshöhle mit Geistern schweben,
Auf Wiesen in deinem Dämmer weben,
Von allem Wissensqualm entladen,
In deinem Tau gesund mich baden!

Weh! steck ich in dem Kerker noch?
Verfluchtes dumpfes Mauerloch,
Wo selbst das liebe Himmelslicht
Trüb durch gemalte Scheiben bricht!
Beschränkt mit diesem Bücherhauf,
den Würme nagen, Staub bedeckt,
Den bis ans hohe Gewölb hinauf
Ein angeraucht Papier umsteckt;
Mit Gläsern, Büchsen rings umstellt,
Mit Instrumenten vollgepfropft,
Urväter Hausrat drein gestopft-
Das ist deine Welt! das heißt eine Welt!

Faust, Johann Wolfgang von Goethe